INL/CRADA-04-10

CRADA FINAL REPORT

Final Report: Development of Renewable Microbial Polyesters for Cost Effective and Energy-Efficient Wood-Plastic Composites

Idaho National Laboratory

and

ECO:LOGIC Engineering, Inc.; P. H. Glatfelter; Strandex Corporation; and Washington State University

Completed: April 8, 2010

Prepared by
Idaho National Laboratory
Idaho Falls, Idaho 83415
http://www.inl.gov
Under DOE Idaho Operations Office
Contract No. DE-AC07-05ID14517

Defer Release Until April 8, 2015

EXECUTIVE SUMMARY

Purpose and Scope

The forestry, wood and paper industries in the United States provide thousands of productive well-paying jobs; however, in the face of the recent economic downturn it faces significant challenges in remaining economically viable and competitive. To compete successfully on a global market that is increasingly driven by the need for sustainable products and practices, the industry must improve margins and diversify product lines while continuing to produce the staple products. One approach that can help to accomplish this goal sustainably is the forest biorefinery. In the forest biorefinery, traditional waste streams are utilized singly or in combination to manufacture additional products in a profitable and environmentally sustainable manner.

In this project, we proposed to produce wood fiber reinforced thermoplastic composites (WFRTCs) using microbial thermoplastic polyesters in place of petroleum-derived plastic. WFRTCs are a rapidly growing product area, averaging a 38% growth rate since 1997. Their production is dependent on substantial quantities of petroleum based thermoplastics, increasing their overall energy costs by over 230% when compared to traditional Engineered Wood Products (EWP). Utilizing bio-based thermoplastics for these materials can reduce our dependence on foreign petroleum.

Renewable microbial polyesters are not currently used in WFRTCs primarily because their production costs are several times higher than those of conventional petrochemical-derived plastics, limiting their use to small specialty markets. The strategy for this project was to economically produce WFRTCs using microbial polyesters by reducing or eliminating the most costly steps in the bio-plastic production. This would be achieved by producing them in and from waste effluents from the municipal and forest products sectors, and by eliminating the costly purification steps. After production the plastic-laden biosolids would be dried and used directly to replace petroleum-derived plastics in WFRTCs. Using this strategy, we could greatly reduce the cost of producing and utilizing these renewable plastics in WFRTCs.

This was a collaborative project among the Idaho National Laboratory, Washington State University, the University of California-Davis, Glatfelter Corporation, Strandex Corporation, and ECO:LOGIC Engineering, Inc. The project was comprised of five tasks. The first four tasks addressed PHA production, extrusion, and composite properties. Feedstock performance and compositional properties were determined in the laboratory by WSU. Both pure commercial PHAs (Task 1) and unpurified effluent-derived PHAs (Task 4) were used. Results were used to define appropriate effluent feedstocks (Task 2) and optimize supplements (Task 3) to produce biosolids for the preferred composite formulations. Task 5 included a pilot-scale extrusion of wood-PHA-biosolids composites.

KEY RESULTS

Production of PHA-laden Biosolids from Waste Sources

Effect of Feedstock on PHA Type/Amount

Efficient utilization of carbon inputs is critical to the economic viability of the current forest products sector. Input carbon losses occur at various locations within a pulp mill, including losses as volatile organics and wastewater. Opportunities exist to capture this carbon in the form of value-added products such as biodegradable polymers. Waste activated sludge from a pulp mill wastewater treatment module was enriched for 80 days to produce a methanol-utilizing consortium with the goal of using this consortium to produce biopolymers from methanol-rich pulp mill waste streams. Five enrichment conditions were utilized: three high-methanol streams from the kraft mill foul condensate system, one methanol-amended stream from the mill wastewater plant, and one methanol-only enrichment. Enrichment reactors were operated aerobically in sequencing batch mode at neutral pH and 25°C with a hydraulic residence time (HRT) and a solids retention time (SRT) of four days. Non-enriched waste activated sludge did not consume methanol or reduce chemical oxygen demand. With enrichment, however, the chemical oxygen demand reduction over 24 hour feed/decant cycles ranged from 79 to 89 %, and methanol concentrations dropped below method detection limits. Neither the non-enriched waste activated sludge nor any of the enrichment cultures accumulated polyhydroxyalkanoates (PHAs) under enrichment conditions. Similarly, the non-enriched waste activated sludge did not accumulate PHAs under nitrogen limited conditions, which have been used to induce PHA accumulation in other mixed microbial cultures. By contrast, enriched cultures accumulated PHAs to nearly 14% on a dry weight basis under nitrogen limited conditions. This indicates that selectively-enriched pulp mill waste activated sludge can serve as an inoculum for PHA production from methanol-rich pulp mill effluents. Further, besides being a source of high strength chemical oxygen demand (COD), the foul condensates were also a significant source of ammonium nitrogen. This makes it unnecessary to add nitrogen during either growth (N-sufficient) or PHA production (N-limited) phases when using the foul condensates as the carbon source.

Supplementation of Waste Effluents for Production of PHA

Tests were conducted to assess the effect of carbon to nitrogen ratio on polyhydroxyalkanoate production by pulp mill activated sludge. In reactors fed methanol as the sole carbon source, results confirmed that both nitrogen limitation and a feast-famine regime were necessary to induce PHA storage and maximize PHA yield. The conditions in the methanol-only reactors operated within the C/N 20-60 range allowed a balance between cell growth, to maintain high mixed liquor volatile suspended solids (MLVSS) concentrations, and PHA storage, thereby maximizing production of PHA in the reactor. The results suggest optimal PHA storage in the methanol-only reactors required both a feast-famine regime and a nitrogen-limited environment. Nitrogen limitation alone allowed for PHA storage, but did not support high PHA yields. Finally, a feast-famine environment by itself was insufficient to induce PHA storage. In contrast, reactors fed diluted foul condensate were driven by a different set of limiting factors. Cell growth in the diluted foul condensate reactors was not directly affected by the amount of nitrogen present because none of the reactors were nitrogen limited, a result of the ammonium present in the foul condensate. The greater fraction of non-methanol carbon provided to the C/N 3 and 15 reactors likely affected the metabolic state or composition of the consortium that had been selectively enriched for methanol consumption. Feast-famine conditions in the absence of nitrogen limitation were sufficient to induce PHA storage above a C/N of 30. However, neither feast-famine nor nitrogen-limited conditions existed in the C/N 3 and 15 reactors. PHA storage below C/N 15 was likely stimulated by some other macro- or micro-nutrient deficiency. It is possible that the smaller proportion of primary clarifier effluent in the C/N 3 and 15 reactors resulted in a nutritional deficiency in the daily feed medium, which induced PHA storage by the consortia.

Experiments were conducted to determine the effects of selected reactor conditions on polyhydroxyalkanoate production from pulp mill activated sludge using foul condensates. The goal of this study was to evaluate the relationship between the food:microorganism ratio (F:M), the solids retention time (SRT), the hydraulic retention time (HRT) and PHA production in sequencing batch reactors (SBRs) inoculated with mixed consortia enriched from pulp mill activated sludge and fed pulp mill effluents. A face-centered cube central composite design experiment was used simultaneously assess the effects of SRT, HRT, and F:M on PHA %, PHA concentration, total biomass, methanol and COD degradation, and ammonium degradation. The ability of the consortia to produce PHA, whether on a concentration basis or on a fraction of the total dry organic matter basis (PHA %), was predominantly affected by the F:M ratio. In addition, F:M overwhelmingly affected the amount of carbon source degradation that occurred in each reactor. Therefore, the amount of carbon entering the system played the dominant role in determining how much PHA the consortia were able to store and how much of the carbon source the consortia were able to degrade. The ability to support cell growth in the reactors was mainly controlled by the combined effects of SRT and HRT. Biomass concentrations increased with increased SRT and decreased HRT, which gave a selective advantage to slower growing cells. Ammonium degradation was similarly affected by SRT. However, F:M also played a role in ammonium degradation as the nitrogen source used in this work was also the carbon source (foul condensate). Total PHA concentration in the reactors is a function of the biomass concentration in the media and the PHA concentration within the cells. To maximize PHA production using pulp mill effluents and consortia enriched from pulp mill activated sludge a PHA-producing SBR system must be operated at an intermediate F:M of 3, at the high SRT value of 12 days, and at the intermediate HRT value of 2 days. If a PHA-producing SBR is operated under these conditions, a maximum PHA concentration of 0.11 g/L can be achieved.

Composite Processing & Material Properties of WFRTCs Substituting PHA for HDPE

Purified PHA ± Cell Debris Composite Processing & Material Properties

Biopolymers have been limited in use to packaging applications since their introduction into consumer products. In an effort to develop polyhydroxybutyrate (PHB) for competition in the wood plastics industry with applications such as decking, siding, and fencing, composites of PHB and wood fiber (WF) were produced with wood levels comparable to those used for wood-plastic composite (WPC) applications. These were compared with composites prepared using polypropylene (PP) and high density polyethylene (HDPE). The composites were processed through injection molding to conserve raw materials and produce uniform test specimens. Tensile testing of the unmodified PHB/WF composites resulted in an average Young's modulus of 8.1-GPa, and Ultimate strength of 21.9-MPa. Interpretation of these results suggests that PHB/WF composites have high stiffness compared to PP/WF composites, and are more comparable in stiffness with PS/WF composites. The strength of PHB/WF composites was comparable with that of PP/WF. The addition of interfacial modifiers had a positive influence on both stiffness and strength. The most promising interfacial modifier was pMDI. At concentrations of 0, 1, 2, and 4%, pMDI improved tensile properties more effectively than Uralac, D.E.R., and MA-PHB. The addition of 4% pMDI coincided with a 57% increase in ultimate strength, and a 21% increase in Young's modulus. Similarly, water absorption tests indicated increased resistance to water uptake with the addition of interfacial modifiers; pMDI produced the greatest improvements. Improved fiber adhesion was observed with the addition of pMDI, and seen in SEM micrographs. Micrographs of the control showed a large degree of fiber pull-out, and fully exposed fibers. Composites modified with D.E.R. and Uralac showed signs of improved fiber adhesion, however pMDI exhibited complete fiber-matrix coherency.

Investigations into the effect of pMDI on the polymer morphology of PHB/WF composites showed signs of increased T_m, T_g, and decreased ΔH_m and ΔH_c in the control composite (which included

lubricant). Interpretation of these results suggests improved fiber adhesion and possible crosslinking within the PHB-lubricant-pMDI system.

To further investigate the viability of PHB/WF composites for use in commercial WPC applications, PHB/WF composites were extruded with the modifiers shown to significantly improve mechanical properties of the final composite. Additionally, the effects of processing PHB/WF composites through injection molding and extrusion processes were compared. Raw formulations were prepared similarly for both processes with various interfacial modifiers, and resulting mechanical and physical differences examined. Tensile testing of composites showed higher values of Young's modulus and ultimate tensile strength for injection molded specimens relative to extruded specimens. Similar composite specimens showed higher density from injection molding processes than from extrusion processing. The variation in mechanical properties was compared using statistical analysis of density as a covariate in an ANCOVA using processing methods and interfacial modifier types as main effects. Further differences in mechanical properties were attributed to fiber dispersion within the matrix. Micrographs of the composite surfaces from SEM suggested decreased size in fiber bundles with injection molded composites. Regardless of processing method, the type of interfacial modifier added to the composite formulations affected fiber dispersion, likely through better fiber wetting.

Mechanical properties of PHB/WF composites processed through extrusion were shown to be competitive with coupled PP/WF composites. PHB/WF composites modified with pMDI exhibited higher stiffness, and comparable strength to MAPP coupled PP/WF composites at the same percentage of modifiers. Water absorption of the composites processed by different methods displayed considerable differences in behavior. Cracking of the injection molded specimens was observed and was suggested to be a result of the higher composite density. Extruded specimens displayed differences relative to only water uptake and saturation. Prior to cracking, moisture transport was more limited in injection molded specimens than that in extruded specimens.

Interpretation of DSC traces suggested differences in crystal perfection between injection molded and extruded specimens. The degree of crystallization, as measured through the heat of fusion and the heat of crystallization was unchanged respective to processing method.

Waste Effluents PHA Composite Processing & Material Properties

Injection molding tests were conducted to develop formulations for PHB/wood flour/cell debris ternary composites. Purified PHB and PHB-free cell debris were successfully compounded with wood flour by twin screw extrusion and molded into test samples by injection molding. Because of the cell debris' large size, irregular shape, poor interfacial bonding, and thermal degradation during processing, the mechanical properties and water resistance of the composites were found to decrease with increasing cell debris content. Improving interfacial bonding between PHB and cell debris, and reducing cell debris particle size are expected to improve composite properties due to better bonding and larger contact area. Improvements would allow the plastic-laden cell debris to be successfully applied in WPCs. Subsequent tests were performed using extrusion to develop improved formulations. Via extrusion testing, we successfully developed extruded PHB/wood flour/cell debris products. Torque rheometry was used to determine extrusion temperature profiles for the formulations with different cell debris contents. A suitable temperature profile was set for each formulation so that a high packing pressure in the die occurred. All the products extruded at high die pressure were free of sample defects even at high cell debris contents. The composites prepared by direct extrusion showed a property trend similar to those prepared by extrusion compounding and injection molding; the mechanical properties and water resistance of the composites decreased with the increasing content of the cell debris. The PHB/wood flour/cell debris composites with a cell debris/wood flour ratio of 3:2 showed mechanical properties and water resistance similar to the commercial HDPE WPC. Therefore, the cell debris laden biodegradable PHB/wood flour composites could potentially replace some of current fossil oil derived WPCs.

Pilot Testing of PHA Production and Composite Extrusion

Pilot-scale production of PHA using waste feedstock and biosolids from a wastewater treatment system.

A feasibility study of PHA production utilizing mixed cultures and industrial waste streams at pilot-scale was conducted at the Chillicothe mill with foul condensates, and at UC-Davis with brewery waste. The pulp and paper mill pilot unit satisfied the first objective of this study. PHA-laden biomass was not produced because the SBR was not stable at the C/N of 30. The following conclusions were drawn from this test: (1) the pilot-scale unit did not perform in a manner similar to the bench scale work under similar process conditions. Hence, further optimization of this process at the pilot-scale will be necessary for process success. (2) The successful startups used an enriched culture and Methanol-Utilizing Bacteria Medium B. Future work should investigate the necessity of Methanol-Utilizing Bacteria Medium B. And, (3) in contrast to the laboratory tests, the pilot unit became overloaded at a C/N of 30; future work should investigate the causes of this result.

Brewery waste runs were conducted to ensure the production of PHA-laden biomass at the 700 L scale for the project. This was necessary to ensure the feasibility of producing PHA-laden biosolids at larger scale utilizing waste feedstock and biosolids from a wastewater treatment system. The following conclusions were drawn for this follow-up study: (1) PHA production at the 700L scale using waste feedstock and biosolids from a wastewater treatment system is feasible. (2) PHA content is variable between cycles and future work should investigate the causes. And, (3) reactor design and operational conditions produced useful quantities of PHA laden biomass, which were subsequently dried and stabilized for extrusion runs of natural fiber reinforced composite thermoplastics.

Developing PHB/Wood Four/Cell Debris Ternary Composites through Pilot-scale Extrusion

It was demonstrated in Task 4 that the PHB/wood flour/cell debris composites could be successfully prepared by both injection molding and extrusion. The composites with the cell debris/wood flour ratio of 3:2 (PWC60) exhibited properties comparable to commercial WPCs. In this study, PWC60 deck boards were prepared using an industrial scale extrusion line. Flexural properties, density profile, and nail/screw withdrawal strength of the deck boards were investigated. Industrial scale extrusion of PWC60 deck boards was successfully performed. HDPE/wood flour (HW) and PHB/wood flour (PW) deck boards were also extruded and examined for comparison. The whole-cell composite (PWC60) boards were more prone to sample defects than the cell debris-free boards (HW and PW) due to thermal degradation of the cell debris during extrusion. The PWC60 boards showed flexural properties comparable to the HW and PW boards and the screw withdrawal strength was higher than both the HW and PW boards (1.39 vs.1.23-kgf/mm). However, the PWC60 boards were too hard for nailing using general purpose nails; a problem that could easily be solved by pre-drilling holes before nailing or screwing.

CONCLUSIONS & RECOMMENDATIONS

In keeping with ITP's focus on energy savings, waste reduction and environmental benefits, the production of WFRTCs from forest product waste streams has the potential for significant impacts on all three categories. Our original energy savings and waste reduction analysis in 2004 estimated significant annual energy savings of over 42 trillion BTU by 2020, and if the proposed technology deployed across only the building/construction thermoplastics industry, the potential for 310 trillion BTU annually. As early as 2010, projected reductions in NO_X, CO, and SO_2 represented an estimated 8.6, 1.9, and 16% of the total emissions of these pollutants in the Polymer & Resin Manufacturing sector of Chemical and Applied Product Manufacture, according to the 2001 US EPA emission inventories. The inclusion of additional biorefinery waste streams in the carbon feedstock pool offers an even larger source of high strength waste effluents for the production of WFRTCs. Improved economic competitiveness of the

domestic forest products industry is expected, since the plastic is the highest cost component in WFRTC formulations, comprising on average 52% of formulation costs and 30% of total product costs.

We have demonstrated that biopolymers (polyhydroxyalkanoates, PHA) can be successfully produced from wood pulping waste streams and that viable wood fiber reinforced thermoplastic composite products can be produced from these materials. The results show that microbial polyester (PHB in this study) can be extruded together with wastewater-derived cell mass and wood flour into deck products having performance properties comparable to existing commercial HDPE/WF composite products. This study has thus proven the underlying concept that the microbial polyesters produced from waste effluents can be used to make cost-effective and energy-efficient wood-plastic composites. The cost of purified microbial polyesters is about 5-20 times that of HDPE depending on the cost of crude oil, due to high purification (40%), carbon substrate (40%) and sterilized fermentation (20%) costs for the PHB. Hence, the ability to produce competitive and functional composites with unpurified PHA-biomass mixtures from waste carbon sources in unsterile systems—without cell debris removal—is a significant step forward in producing competitive value-added structural composites from forest products residuals using a biorefinery approach. As demonstrated in the energy and waste analysis for the project, significant energy savings and waste reductions can also be realized using this approach.

In the technology developed under this project, three different byproducts have been used as the feed stocks for the biopolymer reactors: (1) methanol-rich foul condensates from the pulping operation, (2) primary clarifier effluent and (3) activated sludge from the mill's wastewater treatment plant. In the reactor, natural consortia of bacteria accumulated polyesters that can substitute for oil-derived plastics. The biosolids were subsequently recovered, dried, and used in the manufacture of natural fiber composites that exhibited properties comparable to commercially available structural composite materials. Depending on the formulations utilized, these products may be engineered to exhibit different levels of biodegradability, lending them to a variety of applications. Of particular interest for future work is a family of construction materials where biodegradability will actually enhance the product performance. One example of such a product is erosion control materials that are used to retain soil on construction sites while simultaneously establishing vegetation. Here, biopolymers and natural composites with enhanced biodegradation properties will provide value to a market dominated by petroleum-based plastics.

We recommend that the next step for development of useful products using this technology is to scale the technology from the 700-L pilot reactor to a small-scale production facility, with dedicated operation staff and engineering controls. In addition, we recommend that a market study be conducted as well as further product development for construction products that will utilize the unique properties of this bio-based material.

CONTENTS

FIGURES

TABLES

Final Report: Development of Renewable Microbial Polyesters for Cost Effective and Energy-Efficient Wood-Plastic Composites

PROJECT SUMMARY

Introduction

In 2000, annual worldwide fossil fuel use for all thermoplastics was ca. 270 million tons of oil and gas. Approximately 151 million tons of this was used as a feedstock for the thermoplastic, while the remainder was utilized as the energy required to perform various steps in the manufacturing process. In 2002, the combined sales of thermoplastic used in the building/ construction and furniture/furnishings industries totaled 16.9 billion lb (8.5 million tons). Since typical wood-plastic composites contain 30-50% plastic, and because the improved mechanical and processing properties facilitate an overall removal of material through reducing product size, as much as 0.310 quads of annual energy savings could be realized by 2020 in the building and furniture markets by replacing petroleum-derived plastic with renewable plastic.

Renewable polyhydroxyalkanoates (PHAs) are not currently used in wood fiber reinforced thermoplastic composites (WFRTCs) – not because their material properties are inferior – but because their production costs are several times higher than those of conventional petrochemical-derived plastics. In fact, many PHAs have properties very similar to petroleum-derived plastics, but their high production costs have limited their use to small specialty markets. Production costs in the late 1990s were $4/lb, compared to less than $0.50/lb for polyethylene. The culprits are high feedstock, extraction, and purification costs, required because these specialty markets, as well as the current market for WFRTCs, demand pure plastic feedstocks. But are purified plastics really necessary to produce WFRTCs?

Prior to this project in an unpublished study, the proposal team showed that WFRTCs with properties approaching those of traditional composites could be produced using crude poly-3-hydroxybutyrate (P3HB, a bacterial PHA), without removing the cell debris. What was striking about this result was that it was obtained without optimizing the composite formulation and with less than 40% plastic in the formulation. This innovative approach challenged the paradigm that pure plastics are required for WFRTCs, and promised to minimize or eliminate PHA purification costs. Because extraction and purification of PHAs comprise nearly 40% of their production costs, it is exciting that these costs can potentially be so easily eliminated.

To further lower PHA production costs, feedstock costs could also be reduced. It has been generally recognized that municipal wastewater treatment effluents (WTE) naturally contain PHA-producing bacteria, and that WTE could potentially replace costly PHA feedstocks. Bacterial species that are known PHA-producers have also been observed in pulp & paper effluents, and pulp & paper effluents that do not naturally contain them could be augmented with effluents that do. We performed an assessment of P3HB in several WTE sources and found P3HB concentrations ranging from 25 to 50% of the cell mass. Unfortunately, these effluents are 1000-times less concentrated than typical commercial PHA fermentations, which greatly increases extraction and purification costs. Producing WFRTCs using unpurified PHA-laden bacteria circumvents this issue, reducing processing steps to simply dewatering – which wastewater treatment facilities do anyway – and drying. This provides the critical innovation necessary to economically produce WFRTCs using PHAs.

A three-phased approach was utilized for the project described in this report:

Phase 1: This phase determined the PHA compositions, amounts, composite formulations, and material properties that can be achieved from these effluents. In Task 1, we determined the required PHA compositions and formulations for production of competitive WFRTCs, using commercially available purified PHAs. In Task 2, we determined the PHA compositions produced in and from various municipal wastewater effluents and pulp & paper mill effluents originating from various processing steps.

Phase 2: This phase defined commercially important parameters. In Task 3, we determined necessary process modifications or feedstock supplements required to stimulate the naturally present bacteria in the chosen effluents to produce maximal amounts of PHAs. In Task 4, WFRTCs were produced from commercially available PHAs together with PHA-devoid cell debris harvested from a municipal wastewater treatment facility. Processing parameters, composite formulations, and product performance criteria were established as production guidelines to define a system that could be implemented in an industrial WFRTC production facility.

Phase 3: This phase proved the concept that these WFRTCs could be produced commercially in large scale extruders. In Task 5, the operation of a 700-L pilot PHA production system utilizing brewery wastewater/biosolids and pulp mill foul condensates/biosolids was demonstrated, and potential issues with operation onsite at an operating mill were identified. WFRTCs were produced from commercial PHB and PHA-devoid biosolids in a commercial pilot-scale extruder facility to estimate ease of processing at the commercial scale, and to provide board for testing of the material properties.

The results of this work are described in the following sections. Because of the breadth of the work, the results are presented in manuscript form in sections presenting discrete elements of the project. Because of the wide scope covered and the cross-disciplinary nature of the components of the project, the tasks are not presented in numerical order, but are presented together with their like components. The PHA production work is presented first (Tasks 2 and 3), followed by the composites work (Tasks 1 and 4). The Task 5 work is presented together following these. Finally, two short studies addressing measurement of the performance properties of the pilot composites are presented and the appendices.

Results – Production of PHA-laden Biosolids from Waste Sources

Task 2 – Effect of Feedstock on PHA Type/Amount

Investigators: Frank J. Loge[1], David N. Thompson[2], Hsin-Ying Liu[1], Gregory R. Mockos[1], William A. Smith[2]

Performing Institutions: [1]The University of California-Davis; [2]Idaho National Laboratory

Selective Enrichment of a Methanol-Utilizing Consortium using Pulp & Paper Mill Waste Streams

Summary

Efficient utilization of carbon inputs is critical to the economic viability of the current forest products sector. Input carbon losses occur in various locations within a pulp mill, including losses as volatile organics and wastewater. Opportunities exist to capture this carbon in the form of value-added products such as biodegradable polymers. Waste activated sludge from a pulp mill wastewater facility was enriched for 80 days for a methanol-utilizing consortium with the goal of using this consortium to produce biopolymers from methanol-rich pulp mill waste streams. Five enrichment conditions were

utilized: three high-methanol streams from the kraft mill foul condensate system, one methanol-amended stream from the mill wastewater plant, and one methanol-only enrichment. Enrichment reactors were operated aerobically in sequencing batch mode at neutral pH and 25°C with a hydraulic residence time and a solids retention time of four days. Non-enriched waste activated sludge did not consume methanol or reduce chemical oxygen demand. With enrichment, however, the chemical oxygen demand reduction over 24 hour feed/decant cycles ranged from 79 to 89 %, and methanol concentrations dropped below method detection limits. Neither the non-enriched waste activated sludge nor any of the enrichment cultures accumulated polyhydroxyalkanoates (PHAs) under conditions of nitrogen sufficiency. Similarly, the non-enriched waste activated sludge did not accumulate PHAs under nitrogen limited conditions. By contrast, enriched cultures accumulated PHAs to nearly 14% on a dry weight basis under nitrogen limited conditions. This indicates that selectively-enriched pulp mill waste activated sludge can serve as an inoculum for PHA production from methanol-rich pulp mill effluents.

Introduction

The ability to efficiently use waste streams and renewable resources is essential for the development of a sustainable and profitable forest products industry. The pulp and paper industry is continuously evolving to meet the demand for products that are manufactured efficiently, cost-effectively, and in an environmentally friendly manner. In striving to meet increasingly stringent environmental regulations and the socio-political pressure for sustainability, the pulp & paper industry has made process improvements resulting in an increase in the quality and diversity of its products and a decrease in its energy use and environmental impact (Miller 2005). However, opportunities exist to further reduce the environmental footprint of pulp and paper mills. Currently, several input carbon losses occur in various locations within pulp mills, including losses as volatile organic carbon (VOC) compounds such as methanol in kraft mill condensate collection systems. The kraft pulping process uses a hot sodium sulfide-hydroxide solution to digest wood chips and liberate the cellulose fibers, which are subsequently used to manufacture a wide range of paper products (Dufresne 2001). Condensed gases from the digesters are collected to reduce the discharge of volatile organic and reduced sulfur compounds from the mill. These contaminated condensates or “foul condensates” contain such compounds as hydrogen sulfide, methyl mercaptan, ethanol, methanol, acetone, and terpenes. Methanol is the primary hazardous air pollutant of concern and constitutes up to 80% of the organic matter and most of the chemical oxygen demand (COD) from foul condensates (Springer 2000). Condensates can either be reused (typically for pulp or chip washing) or can be treated prior to discharge to the wastewater treatment system. Conventional treatment methods rely upon energy-intensive technologies such as incinerators and scrubbers, which ultimately produce VOC, SO_x, NO_x, and particulate emissions (Smook 1992).

A sustainable alternative treatment of COD from foul condensates can be achieved through a biological conversion of the methanol into commercially useful biopolymers, such as polyhydroxyalkanoates (PHAs). Polyhydroxyalkanoates are polyesters composed of 3-hydroxy fatty acid monomers in which the carboxyl group of one monomer forms an ester bond with the hydroxyl group of the neighboring monomer (Madison 1999). Numerous bacteria are able to synthesize and store PHAs as intracellular carbon and energy reserves (Anderson 1990). Bacteria accumulate PHAs under one or a combination of the following environmental conditions: macronutrient (nitrogen or phosphorous) or micronutrient (potassium, magnesium, or sulfate) limitation in the presence of excess carbon; electron donor/acceptor variability (aerobic/anaerobic cycling); or a feast-famine regime (Dionisi 2004b).

Polyhydroxyalkanoates exhibit material properties similar, in part, to conventional petroleum-based thermoplastics with the added benefit of being entirely biodegradable (Braunegg 1998). PHAs can serve as an alternative to petroleum-based thermoplastics in selected applications such as natural fiber reinforced thermoplastic composites. These composites are produced by co-extruding mixtures of natural fibers such as wood together with plastics such as high density polyethylene to produce strong materials for durable applications (Smith 2006). By replacing the petroleum-derived plastics with thermoplastic bacterial polyesters such as PHAs, the composite products sector could serve as a future market for

unpurified PHAs (Coats 2007). However, the integration of PHAs with natural fiber reinforced thermoplastic composites faces both technical and economic challenges that need to be met for the end product to be commercially viable. Currently, PHAs are not economically competitive with petroleum-based thermoplastics (Philip 2007). The most influential factors driving PHA production costs are extraction, purification, and carbon substrate cost. By minimizing or eliminating extraction and purification steps and by using an inexpensive substrate, the cost of PHAs can potentially be reduced to a competitive level. In applications such as natural fiber composites, PHA extraction from the cell mass may not be required (Coats 2007). In addition, the use of pulp mill effluents such as foul condensates as an inexpensive carbon source can provide a cost-effective means by which PHA is produced using pulp mill effluents. An illustration of this approach can be seen in Figure 1. This approach would also allow for reduced waste production and potentially create an additional profit stream within pulp and paper mills.

Extensive work has been performed using activated sludge from domestic wastewater to produce PHAs from readily degradable carbon sources such as mixed fatty acids and undefined fermentation products from anaerobic sludge digestion (Satoh 1998; Satoh 1999; Reis 2003). In the case of pulp mills, the raw wastewater is less conducive to PHA production because of the recalcitrant nature of the carbon and its low concentration (Dufresne 2001). Therefore, it is necessary to amend the wastewater with an additional carbon source to facilitate PHA production. In this instance, methanol from the foul condensates provides both an available and inexpensive biologically degradable carbon source for PHA production. Since the bacteria in the pulp mill waste activated sludge are not accustomed to methanol as a primary carbon and energy source in the wastewater treatment system, the activated sludge consortium must undergo enrichment to acclimate to the foul condensates. A selective enrichment of the waste activated sludge is required to select for a microbial consortium capable of simultaneously utilizing the methanol in foul condensates while synthesizing PHAs.

The goal of this study was to enrich a culture from pulp and paper secondary waste activated sludge that can grow aerobically using methanol-rich pulp and paper mill foul condensate streams originating from a kraft chemical recovery process. The enrichments will be used in future experiments to explore the range of environmental conditions necessary to produce and accumulate PHAs using pulp and paper effluents with the ultimate goal of incorporating the PHA-rich biomass into natural fiber reinforced thermoplastic composite materials.

Materials and Methods

Source of Microorganisms

A mixed microbial consortium was obtained from the return waste activated sludge line within the wastewater treatment facility at the P.H. Glatfelter pulp & paper mill in Chillicothe, OH. Activated sludge was shipped overnight at 4°C and used within 48 hours of receipt. The activated sludge had a mixed liquor volatile suspended solids (MLVSS) concentration of 3200 mg L^{-1}, a pH of 7.43, and a COD of 180 mg L^{-1}. The activated sludge was used to inoculate sequencing batch reactors used in enrichment experiments at one-fourth of the total volume of the reactors.

Pulp & Paper Mill Waste Streams

Five conditions were chosen for the enrichment of the original waste activated sludge. Three foul condensate effluents from the pulp mill kraft chemical recovery process were selected based on their high COD: 1) the combined evaporator condensates (3200 tank foul condensate or FC 3200), 2) blow heat accumulator overflow foul condensate (FC BHAO), and 3) evaporator foul condensate (FC EVAP). The remaining two media used for enrichment consisted of primary clarifier effluent (primary out abbreviated as "1° OUT") supplemented with methanol, and waste activated sludge supplemented with methanol (WAS-only).

The COD of the foul condensates were highly variable (see Table 1). In the FC BHAO the COD ranged from 4600 to 46300 mg L^{-1}. In the FC 3200 the COD ranged from 810 mg L^{-1} to 47400 mg L^{-1}. In the FC EVAP the COD ranged from 4800 mg L^{-1} to 17400 mg L^{-1}. On the other hand, the 1° OUT

received had a reasonably consistent COD between 300 and 400 mg L^{-1}. The primary carbon source in the foul condensates was methanol, which accounted for 51-72% of the COD, depending on the date sampled. This large variability demonstrates the changing compositions of the materials received, and is assumed to be a result of the variability of the wood species used as feedstocks for the pulp mill. The primary carbon source in the 1° OUT was not identified.

The foul condensates were not a significant source of total suspended solids (TSS). The average values for TSS were consistently an order of magnitude less than the TSS of the waste activated sludge that was used as the source of inoculum. The average values for foul condensate COD, pH, and TSS are in Table 1. When samples were received from the pulp mill, pH, COD, and TSS were immediately measured. Foul condensates were adjusted to neutral pH using 1 N HCl (Fisher Scientific, Fair Lawn, NJ) and the materials were stored at 4°C to minimize biological activity and COD degradation. In some cases, the foul condensates contained a non-aqueous phase liquid that was removed by decanting and disposed prior to using the foul condensates.

Nutrient Media

To ensure the presence of the necessary macronutrients and micronutrients to select for a community capable of consuming methanol as the main carbon source, Methanol-Utilizing Bacteria Medium B (Atlas 1997) was utilized as a nutrient addition. The nutrient media was supplied to all enrichment reactors to ensure balanced growth conditions. The nutrient medium was used without methanol addition for the FC 3200, FC BHAO, and FC EVAP enrichments, since the foul condensates contained sufficient concentrations of methanol. Methanol (99.9%; Fisher Scientific, Fair Lawn, NJ) was added to the nutrient media supplied to the 1° OUT and WAS-only enrichment reactors.

System Design and Operation

Fifteen sequencing batch reactors, each with a working volume 160 mL, were run at a hydraulic retention time (HRT) equal to the solids retention time (SRT) of four days. Air was supplied (200 mL min^{-1} or 1.24 vvm) to provide oxygen and mixing. Each enrichment condition was prepared in triplicate. The reactors were operated on a 24 hour feed/decant cycle with one quarter of the reactor volume (40mL) being replaced with fresh feed. In the FC 3200, FC BHAO, and FC EVAP reactors the feed consisted of a mixture of the nutrient media and the respective foul condensate. The 1° OUT reactors were fed a mixture of the nutrient medium supplemented with methanol and the 1° OUT from the pulp mill. Finally, the WAS-only reactors were simply fed the nutrient media supplemented with methanol. The ratio of nutrient media to the waste being fed was determined by reaching a final total COD in the feed of 2500 mg L^{-1}. This value was chosen as the ceiling for COD/methanol concentration as it is within the range of methanol concentrations demonstrated to be optimal for PHA production in pure culture (Suzuki 1986; Bourque 1992; Kim 1996) yet minimize any potential toxic effects on the microbial community (Bormann 1997). The reactors were supplied continuously with oil-free instrument air, which was humidified to reduce evaporation from the reactors. Thereafter, the airflow was separated using a gang valve and then regulated using a flow meter (Cole-Parmer Vernon Hills, IL).

The reactors were constructed using 2" × 6" ($d \times h$) glass process pipe, closed at both ends with Teflon® end caps, and sealed with rubber gaskets and stainless steel clamps (Ace Glass, Vineland, NJ). Reactors were sealed to contain the hydrogen sulfide, methyl mercaptan, and other malodorous and hazardous compounds present in the foul condensates. Reactors were vented through a series of two granular activated carbon beds (CC601 and Midas OCM; USFilter, Los Angeles, CA) that effectively removed hydrogen sulfide and methyl mercaptan from the effluent gases. The experimental process flow diagram is shown in Figure 2.

Prior to initiating the enrichments, a nonsteady-state mass balance was performed to account for methanol stripping due to aeration. The amount of methanol stripped over a 24 hour period was calculated according to Equations 1 and 2:

$$\%\ Methanol\ \ Stripped = \left(\frac{C_i - C_f}{C_i} \right) \times 100 \quad (1)$$

$$C_f = C_i \exp\left[-\left(\frac{Q_{air} \Delta t H_{methanol}}{V_{reactor}} \right) \right] \quad (2)$$

where C_i is the methanol concentration at time zero, C_f is the methanol concentration in reactor after 24 hours, Q_{air} is the air flow rate, Δt is the time interval, $V_{reactor}$ is the reactor volume, and $H_{methanol}$ is the dimensionless Henry's constant for methanol ($1.858*10^{-4}$ for methanol at 25°C (Weast 1984)).

The mass balance model predicted that 28% of the methanol would be stripped over a 24 hour period (one feed/decant cycle). This was verified by an average methanol decrease of 26% over a 24 hour period in five replicate stripping columns constructed and operated identically to the enrichment reactors (data not shown). Based on these results, an additional 36 µL of 99.99% methanol was added daily to the reactors along with the feed to compensate for methanol loss due to stripping.

Sampling and Analysis

Samples were collected from the daily decants immediately before feeding and analyzed for MLVSS, COD, methanol, and ammonium (NH_4^+) concentration. A 40 mL sample was recovered from each reactor every 3rd and 4th day of an HRT period. The unfiltered samples from the 3rd day were stored at -80°C for future microbial community analysis. The unfiltered samples conserved on the 4th day were initially used to measure MLVSS according to ASTM Standard Method 2540 E (APHA 1992) using Millipore TCLP AP40 glass fiber filters. The samples were then filtered through a Millex GP 0.22 µm Express PES Membrane filter unit (Millipore Corporation, Billerica, MA) and analyzed for soluble COD, methanol, and NH_4^+.

COD

COD was measured according to ASTM Standard Method 5220 D (APHA 1992) using Hach high–range ampoules with a Hach DRB 200 digestion block and Hach DR 2010 portable data logging spectrophotometer (Hach Company, Loveland, CO) set at a 620 nm wavelength.

Methanol

Methanol was analyzed by high performance liquid chromatography (HPLC) using a Hitachi HPLC D-6000 Series HPLC system (Tokyo, Japan) consisting of a Hewlett Packard 1047A RI Detector (Agilent Technologies, Palo Alto, CA), a Hitachi L6200A Gradient Pump (Tokyo, Japan), and a Hitachi AS-4000 autosampler (Tokyo, Japan). The mobile phase consisted of 0.01% H_2SO_4 at 0.6 ml min^{-1}. Twenty microliter samples were prepared at 1:1 dilution and injected into a Bio Rad Aminex HPX-87H (300mm x 7.8mm ID) column (Hercules, CA) with a Bio Rad Micro-Guard cartridge (Cat. No. 125-0131). Methanol standards were prepared at 0.01 – 0.1% by volume using 99.99% methanol. Samples were run at 60°C, with the detector set at 50°C. The method detection limit (MDL) for the methanol analysis was 100 mg L^{-1}.

Ammonium

Soluble ammonium ion concentrations were measured by ion chromatography using a system consisting of a Dionex ED40 conductivity detector with a GP50 gradient pump, an AS50 autosampler, an AD20 absorbance detector, and an EG40 eluent generator (Dionex Corporation, Sunnyvale, CA). Samples were analyzed using 5 µL injections at a flow rate of 1 mL min^{-1}. Samples were injected into a Dionex IonPac CS12A (250mm x 4mm ID) for cations with the Dionex ECG-MSA cartridge in the eluent generator system. Data were collected using Peaknet v. 5.21 (Dionex Corporation, Sunnyvale, CA). Cation standards were prepared using the Dionex 6 Cation Standard II #46070. A seven level cation

standardization was performed (DI water, 5 standards, and the non-dilute Cation Standard II solution). The MDL for the NH_4^+ analysis was 0.5 mg L^{-1}.

Polyhydroxyalkanoates

PHA analysis was conducted as described by Braunegg (Braunegg 1978), with the following modifications. Upon completion of the 20th HRT, the reactors were fed their respective substrate media and four 40 mL samples were taken for PHA analysis per reactor over a 24 hour period. The unfiltered 40 mL biomass samples were bleached by adding 2 mL of commercial grade bleach (5% NaClO) (Clorox, Oakland, CA) and centrifuged at 4300 x g for 15 minutes. The pellet was then dried at 60°C for 24 hours. Between 20-40 mg of the dried biomass was weighed and suspended in a mixture of 2 mL acidified methanol (3% H_2SO_4, v/v) and 2 mL chloroform. The chloroform contained 0.5 mg mL^{-1} benzoic acid as an internal standard. The mixture was then digested at 100°C for 4 hours in a Hach DRB 200 digestion block (Hach Company, Loveland, CO).

Once the digestion was completed, 1 mL of deionized water was added and the mixture was vortexed for 30 seconds. After allowing the organic phase to separate from the aqueous phase, Pasteur pipettes were used to remove the organic phase. The organic phase was then filtered through another Pasteur pipette packed with a cotton plug and 1 g of sodium sulfate (Fisher Scientific, Fair Lawn, NJ) to remove any remaining water. The organic phase, which contained the methyl ester monomers of the PHA molecules, was analyzed by gas chromatography using an Agilent Technologies 6850 Network GC System with a Thermal Couple Detector system (Agilent Technologies, Palo Alto, CA). The samples were run at 60°C and at 1 ml min^{-1} with 1 µL injections using a Zebron ZB-624 column (250mm x 1.4mm ID) (Phenomenex Inc., Torrance, CA). The GC Chemstation 2001 software (Agilent Technologies, Palo Alto, CA) was utilized for data analysis. The concentration of PHA was quantified against standards of PHB and PHV (Poly(3-hydroxybutyric acid-co-3-hydroxyvaleric acid) standard) (Sigma-Aldrich, St. Louis, MO) as derivatized methyl esters and extraction efficiency was calculated based on the benzoic acid internal standard.

Results and Discussion

The enrichments were run for a total of 20 HRTs, or 80 days, to allow the selective enrichment of a consortium capable of utilizing methanol in the various media as their main carbon source. The data shown in Figures 3 – 6 are the averages of the three replicate reactors run for each medium, and represent the end point values for each HRT (40 mL 4th day samples; see above). Error bars shown indicate one standard deviation.

MLVSS

MLVSS in all reactors declined as a result of washout during enrichment of the culture for methanol-utilizing bacteria. The MLVSS, which is representative of the total microbial biomass in the cultures, stabilized in all reactors between approximately HRT 8 and 12. Because stabilization of MLVSS is not necessarily indicative of stability of the microbial community, it was decided to continue the enrichment feedings until either rebound of the MLVSS was observed (indicating growth of the selected community), or until the MLVSS was stable for an extended period (indicating steady state cell concentration for the carbon loads supplied). The FC 3200 and FC BHAO reactors required the longest amount of time to stabilize the MLVSS (Figure 3A-B), whereas, the WAS-only enrichments required the least amount of time (Figure 3E). In the FC EVAP and 1°OUT reactors, the MLVSS rebounded before stabilizing (Figure 3C-D).

Soluble COD

Soluble COD present in the reactors at the end of the 24 hour feeding cycle initially varied widely for both the FC 3200 and FC BHAO reactors (Figure 4A-B). This variability mirrored the larger than expected variability in the COD of these foul condensates. The large increase in COD between HRT 2 and 6 for the FC BHAO reactors was likely due to the unexpected increase in the FC BHAO foul

condensate COD from 4600 to 46300 mg L^{-1} (Figure 4B). The other enrichments began COD degradation immediately (Figure 4C-E). In all reactors the COD was degraded an average of 79-89% after enrichment for 20 HRTs. In the enrichments that were fed foul condensates, 11-21% of the input COD was found to be non-biodegradable.

Methanol

Methanol was the main contributor to COD in the enrichment reactors. Methanol comprised 51-72% of the COD in the foul condensate wastes. This wide range was due to the varying nature of the foul condensates, and ultimately, to the composition of the wood feedstocks entering the mill. The enriched consortia in all of the reactors consumed methanol to levels below the 100 mg L^{-1} methanol (HPLC) detection limit by HRT 8 (Figure 5A-E). This indicates functional stability in the system by HRT 8 with respect to methanol consumption. To ensure community stability in the reactors, as well as to assess the long-term functional stability of the consortia, the reactors were further run to HRT 20. The resulting communities were capable of degrading added methanol and methanol present in the pulp mill effluents.

Ammonium (NH_4^+)

All reactors were fed a balanced growth medium containing 300 mg L^{-1} NH_4^+ as the primary source of nitrogen. Nutrient conditions were chosen to foster balanced microbial growth—no nutrient limitations were anticipated or observed. Figure 6A-E clearly demonstrates that the organisms in each enrichment condition were not lacking in nitrogen. The concentration in the balanced growth medium was asymptotically reached after the community had stabilized in both the 1°OUT and WAS-only enrichments. Notably, the foul condensates from the Chillicothe mill proved to be a source of additional NH_4^+ (Figure 6A-C), which resulted in nitrogen sufficiency reflected as C:N ratios as low as 3 in the FC 3200 enrichments. Peak COD and NH_4^+ concentrations occurred simultaneously in the FC 3200 and FC BHAO reactors (Figure 6A-B and Figure 4A-B).

The objective of this work was to selectively enrich methanol-utilizing organisms from the original pulp mill waste activated sludge. Secondary waste activated sludge from the P. H. Glatfelter wastewater treatment plant was tested for its ability to degrade methanol and produce PHA. It was found that without enrichment, the bacteria within the waste activated sludge from the pulp mill wastewater facility did not degrade methanol or accumulate PHA over a 24 hour period (data not shown). Thus, the selective enrichment of the activated sludge microbial community on methanol was necessary to obtain a culture that could aerobically degrade methanol and accumulate PHA derived from methanol carbon. After a period of 20 HRTs, the pulp mill waste activated sludge was enriched for consortia capable of using the methanol from foul condensates and the methanol added to the WAS-only and 1°OUT enrichments.

As a consequence of the selection process, the MLVSS of the activated sludge initially decreased in all of the enrichment reactors due to washout of members of the microbial community. This was expected since the organisms present in the pulp mill activated sludge were not accustomed to methanol as a primary carbon source since significant methanol does not reach the wastewater treatment facility but is accumulated in the foul condensates, which are combusted during disposal. After initially decreasing, the MLVSS in all reactors stabilized—FC EVAP and 1° OUT eventually showed a rebound in MLVSS, indicative of the selection for an altered microbial community. The decrease in MLVSS was evidence of the washout of non-methanol-utilizing bacteria during the enrichments, as well as washout of methanol-utilizing bacteria having doubling times longer than the SRT (4 days). Nonetheless, the underlying microbial community structure, dynamics, and functional stability and how they are related in mixed consortia are poorly understood (Gentile 2007). Despite the potential structural and functional changes during the enrichment process, the mixed microbial communities were continuously capable of degrading methanol, which was their intended function. It is believed that functional stability observed in engineered systems such as sequencing batch reactors is a result of the functional redundancy within the system (Briones 2003), especially with respect to microbial carbon assimilation pathways. Therefore, despite

process upsets or influent changes, the dynamic changes within a biological reactor utilizing a diverse microbial community are overshadowed by functional stability when the microbial community is faced with a consistent set of operating conditions over a long period of time (Kaewpipat 2002). Based on this knowledge, the enrichment reactors were run for 20 HRTs to attempt to assess long-term functional stability and attain microbial community stability. Future work will characterize the microbial population throughout the enrichment process using t-RFLP.

The COD, pH, and TSS of the foul condensates used in the enrichments were highly variable resulting at least in part from the transient nature of the wood species used at the pulp mill. However, while COD variability was expected in the foul condensates because of varying throughput at the facility, seasonal variations, and quality of wood being processed, the magnitude of COD variation observed was not expected. The pulp mill effluents used were taken directly from pre-existing sample points within the facility. It is believed that the sampling lines may not have been allowed to fully purge before sample collection due to the extensive presence of toxic and/or odorous compounds including hydrogen sulfide, methyl mercaptan, ethanol, methanol, acetone, terpenes, and various other VOCs in the foul condensates. This may have contributed to added variability in the foul condensates. This is supported by the case of the 1°OUT, as it was sampled from a well-purged sampling line and had consistent COD, pH, and TSS throughout the enrichment process. Unless improved foul condensate collection procedures are employed, the variability of the foul condensates will present a challenge in the design of a biological treatment system to synthesize PHA from pulp mill waste effluents. Such fluctuations in waste quality can negatively impact biological treatment systems if the fluctuations are not attenuated prior to treatment. A potential improvement to the collection procedure would be the use of feedstock mixing and dilution tank in which the condensates would be diluted to a pre-determined COD using another lower carbon concentration effluent prior to biological treatment. Monitoring and controlling effluent carbon and nitrogen concentrations will be vital for the successful operation of a biological process that degrades methanol and produces biopolymers from pulp mill effluents.

Foul condensates were a significant source of ammonium nitrogen. Ammonia is produced in the pulping process due to the caustic digestion of proteins in the wood fed to the mill. The feedstock wood species has a significant impact on the concentration of ammonia present in the pulping process streams since it dictates the amount of wood nitrogen present (Kymäläinen 2001). Once the wood and pulp are digested, the primary exit point for ammonia in a pulp mill within a kraft chemical recovery process is in the foul condensates (Kymäläinen 1999). Foul condensates are a condensed caustic waste stream in which the ammonia either remains in the gas phase or is dissolved in the foul condensate as aqueous ammonia. In the present work, once the foul condensates were received for the enrichment experiment, they were neutralized and ammonia was converted into the soluble ammonium ion. The combination of the nitrogen in the foul condensates and ammonium present in the nutrient media provided conditions of nitrogen sufficiency for all of the enrichments (C:N of 3).

The three main environmental conditions that stimulate PHA storage in a mixed consortium are nutrient limitation, variation in electron donor/acceptor availability, or the presence of a feast-famine environment (Dionisi 2005b). In this study, the enrichment reactors were operated with the intent of enriching the original pulp mill activated sludge for consortia capable of utilizing methanol in pulp mill effluents while synthesizing PHA in a nutrient-sufficient feast-famine environment. Therefore, it was expected that PHA production could be stimulated solely by a feast-famine regime in the presence of excess nutrients (Salehizadeh 2004). However, the enrichment reactors did not produce PHA under the nutrient-sufficient enrichment conditions, even though feast-famine conditions were maintained. Although a low C:N ratio condition was more advantageous for cell growth, it did not favor PHA accumulation. Based on these observations, it was hypothesized that it would be necessary to combine a feast-famine regime with nutrient limitation (by increasing the C:N) to stimulate PHA storage using the enriched cultures. With a lower nitrogen concentration with respect to available carbon, it has been shown that a higher proportion of the carbon can be directed toward PHA synthesis (Chua 1999; Ma 2000; Serafim 2004). Cultures from the WAS-only enrichments were subsequently tested for PHA production

under a combined feast-famine and N-limited environment, resulting in the production of up to 13.9% PHA on a dry cell weight basis. By contrast, the original non-enriched waste activated sludge did not yield any PHA under N-limited conditions.

The results of this study indicate that the enrichment process altered the original activated sludge community – which was originally unable to degrade methanol or produce PHA – and produced a consortium capable of degrading methanol under both N-sufficient and N-limited conditions. Alterations to the community will be studied in future experiments using molecular methods. While we expected the enriched community to produce PHA from methanol under feast-famine conditions, both N-limitation and feast famine conditions were ultimately required to stimulate PHA production. This indicates that nutrient limitation, variation in electron donor/acceptor availability, and feast-famine may not each be singly sufficient in all cases for stimulating PHA accumulation by bacteria.

Conclusion and Future Work

Activated sludge obtained from the pulp mill's wastewater treatment plant was successfully enriched for consortia capable of aerobically degrading methanol from high-strength carbon pulp mill waste streams. The COD in all of the enrichments was reduced by 79 to 89 %. Foul condensates were found to be a suitable feedstock, although their variability must be mitigated to avoid process design challenges. Besides being a source of high strength COD, the foul condensates were also a significant source of ammonium nitrogen. This makes it unnecessary to add nitrogen during either growth (N-sufficient) or PHA production (N-limited) phases when using the foul condensates as the carbon source.

References

Anderson, A.J. and E.A. Dawes (1990) Occurrence, Metabolism, Metabolic Role, and Industrial Uses of Bacterial Polyhydroxyalkanoates. Microbiological Reviews, 54(4): 450-472.

APHA (1992) Standard Methods for the Examination of Water and Wastewater, 20th ed., American Public Health Association, Washington D.C.

Atlas, R.M. (1997) Handbook of Microbiological Media, 2nd ed., CRC Press, Boca Raton, FL, p. 891.

Bormann, E.J., M. Leissner, and B. Beer (1997) Growth and Formation of PoIy(hydroxybutyric acid) by Methylobacterium rhodesianum at Methanol Concentrations of above 25 g/l. Acta Biotechnologica, 17(4): 279-289.

Bourque, D., B. Ouellette, G. Andre, and D. Groleau (1992) Production of poly-β-hydroxybutyrate from methanol: Characterization of a new isolate of Methylobacterium extorquens. Applied Microbiology and Biotechnology, 37(1): 7-12.

Braunegg, G., B. Sonnleitner, and R.M. Lafferty (1978) A rapid gas chromatographic method for the determination of poly-β-hydroxybutyric acid in microbial biomass. European Journal of Applied Microbiology and Biotechnology, 6(1): 29-37.

Braunegg, G., G. Lefebvre, and K.F. Genser (1998) Polyhydroxyalkanoates, biopolyesters from renewable resources: Physiological and engineering aspects. Journal of Biotechnology, 65(2-3): 127-161.

Briones, A. and L. Raskin. (2003) Diversity and dynamics of microbial communities in engineered environments and their implications for process stability. Current Opinions in Biotechnology, 14:270–276.

Chua, H., P.H.F. Yu, and C.K. Ma (1999) Accumulation of Biopolymers in Activated Sludge Biomass. Applied Biochemistry and Biotechnology, 77-79(1-3): 389-399.

Coats, E.R., F.J. Loge, K. Englund, and M.P. Wolcott (2007) Production of natural fiber reinforced thermoplastic composites through the use of PHB-rich biomass. Bioresource Technology, in press.

Dionisi, D., M, Beccari, S. Di Gregorio, M. Majone, M.P. Papini, and G. Vallini (2005) Storage of biodegradable polymers by an enriched microbial community in a sequencing batch reactor operated at high organic load rate. Journal of Chemical Technology and Biotechnology, 80: 1306-1318.

Dionisi, D., M. Majone, V. Papa, and M. Beccari (2004) Biodegradable Polymers From Organic Acids by Using Activated Sludge Enriched by Aerobic Periodic Feeding. Biotechnology and Bioengineering, 85(6): 569-579.

Dufresne, R., A. Liard, and M.S. Blum (2001) Anaerobic Treatment of Condensates: Trial at a Kraft Pulp and Paper Mill. Water Environment Research 73(1): 103-109.

Gentile, M.E., C.M. Jessup, J.L. Nyman, and C.S. Criddle (2007) Correlation of Functional Instability and Community Dynamics in Denitrifying Dispersed-Growth Reactors. Applied and Environmental Microbiology, 73(3): 680-690.

Kaewpipat, K. and J. C.P.L. Grady (2002) Microbial population dynamics in laboratory-scale activated sludge reactors. Water Science & Technology, 46(1-2): 19-27.

Kim, S.W., P. Kim, Hyun S. Lee, and Jung H. Kim (1996) High Production of Poly-β-hydroxybutyrate (PHB) from Methylobacterium organophilum under Potassium Limitation. Biotechnology Letters, 18(1): 25-30.

Kymäläinen, M., M. Forssén, and M. Hupa (1999) The Fate of Nitrogen in the Chemical Recovery Process in a Kraft Pulp Mill. Part I. A General View. Journal of Pulp and Paper Science, 25(12): 410-417.

Kymäläinen, M., M. Holmström, M. Forssén, and M. Hupa (2001) The Fate of Nitrogen in the Chemical Recovery Process in a Kraft Pulp Mill. Part III: The Effect of Some Process Variables. Journal of Pulp and Paper Science, 27(9): 317-324.

Ma, C.K., H. Chua, P.H.F. Yu, and K. Hong (2000) Optimal Production of Polyhydroxyalkanoates in Activated Sludge Biomass. Applied Biochemistry and Biotechnology, 84(1-9): 981-990.

Madison, L.L. and G.W. Huisman (1999) Metabolic Engineering of Poly(3-hydroxyalkanoates): From DNA to Plastic. Microbiology and Molecular Biology Reviews, 63(1): 21-53.

Miller, M., M. Justiniano, and S. McQueen (2005) Energy and Environmental Profile of the U.S. Pulp and Paper Industry. U.S. Department of Energy, Office of Energy Efficiency and Renewable Energy, Industrial Technologies Program, Washington, DC.

Philip, S., T. Keshavarz, and I. Roy (2007) Polyhydroxyalkanoates: Biodegradable polymers with a range of applications. Journal of Chemical Technology and Biotechnology, 82(3): 233-247.

Reis, M.A.M., L.S. Serafim, P.C. Lemos, A.M. Ramos, F.R. Aguiar, and M.C.M. Van Loosdrecht (2003) Production of polyhydroxyalkanoates by mixed microbial cultures. Bioprocess and Biosystems Engineering, 25(6): 377-385.

Salehizadeh, H. and M.C.M.V. Loosdrecht (2004) Production of polyhydroxyalkanoates by mixed culture: recent trends and biotechnological importance. Biotechnology Advances, 22(3): 261-279.

Satoh, H., T. Mino, and T. Matsuo (1999) PHA production by activated sludge. International Journal of Biological Macromolecules, 25: 105-199.

Satoh, H., Y. Iwamoto, T. Mino, and T. Matsuo (1998) Activated sludge as a possible source of biodegradable plastic. Water Science & Technology, 38(2): 103-109.

Serafim, L.S., P.C. Lemos, R. Oliveira, and M.A.M. Reis (2004) Optimization of Polyhydroxybutyrate Production by Mixed Cultures Submitted to Aerobic Dynamic Feeding Conditions. Biotechnology and Bioengineering, 87(2): 145-160.

Smith, P.M. and M.P. Wolcott (2006) Opportunities for Wood/Natural Fiber-Plastic Composites in Residential and Industrial Applications. Forest Products Journal, 56(3): 4-11.

Smook, G.A. (1992) Handbook for Pulp & Paper Technologists, 2nd ed., Angus Wilde Publications, Bellingham, WA, p. 382.

Springer, A.M. (2000) Industrial Environmental Control Pulp and Paper Industry, 3rd ed., Tappi Press, Atlanta, GA, pp. 238-239.

Suzuki, T., T. Yamane, and S. Shimizu (1986) Mass production of poly-β-hydroxybutyric acid by fully automatic fed-batch culture of methylotroph. Applied Microbiology and Biotechnology, 23(5): 322-329.

Weast, R.C. (1984) Handbook of Chemistry and Physics, 64th ed., CRC Press, Boca Raton, FL.

Figures

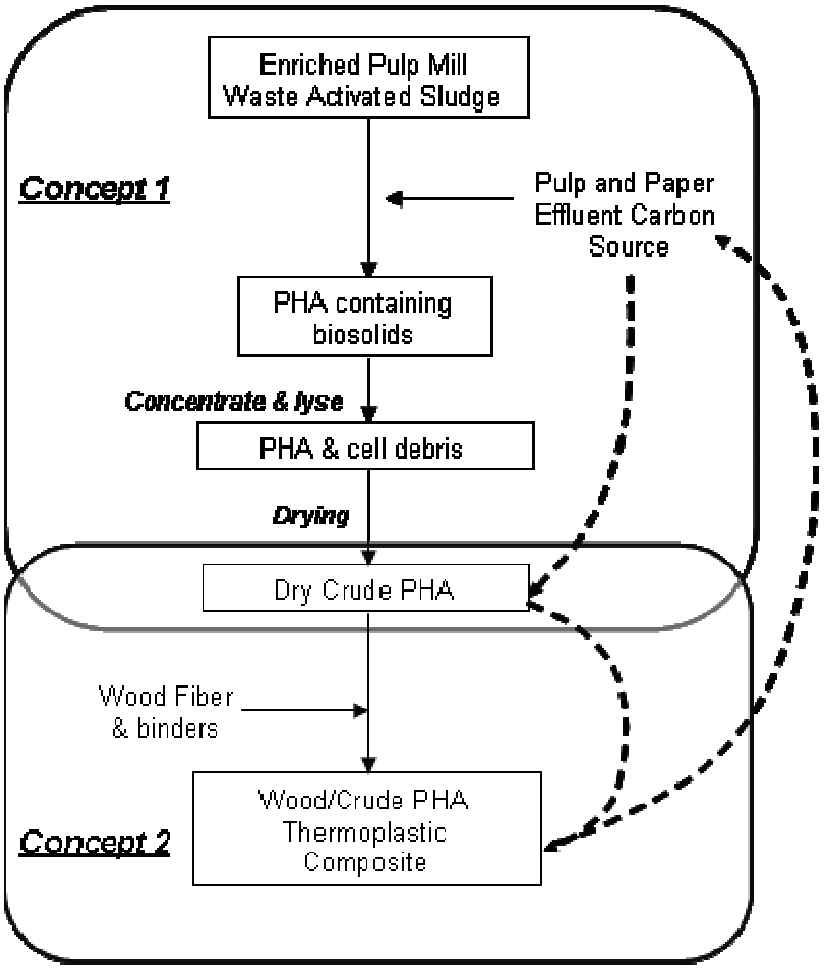

Figure 1. Approach for minimizing costs associated with the manufacture of natural fiber reinforced thermoplastic composites using unpurified PHAs

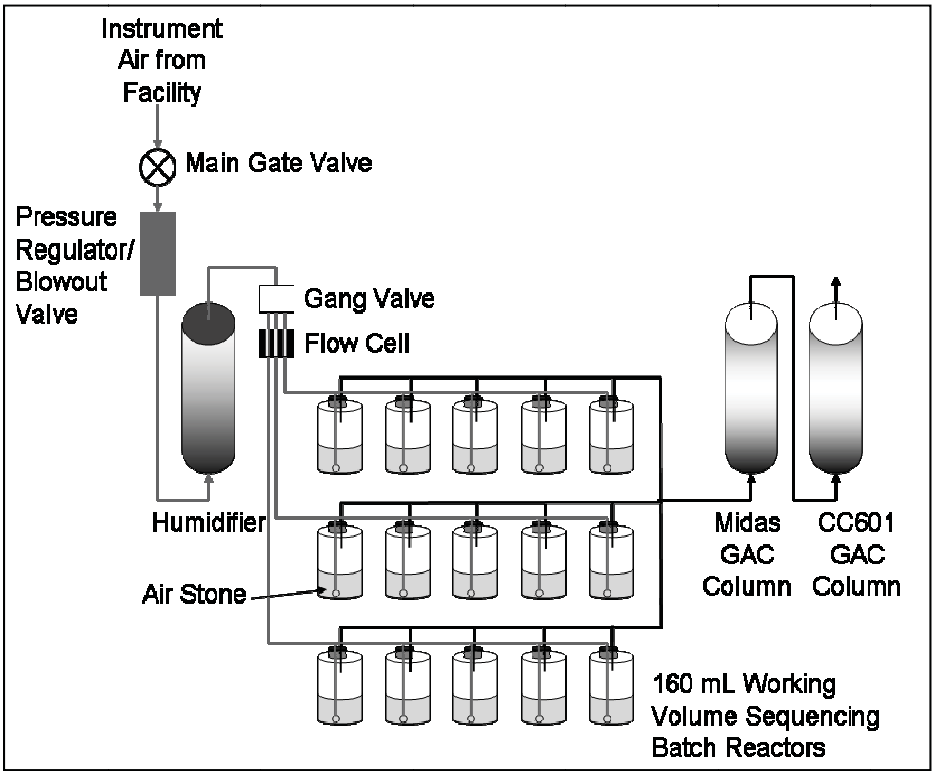

Figure 2. Enrichment experiment process flow diagram

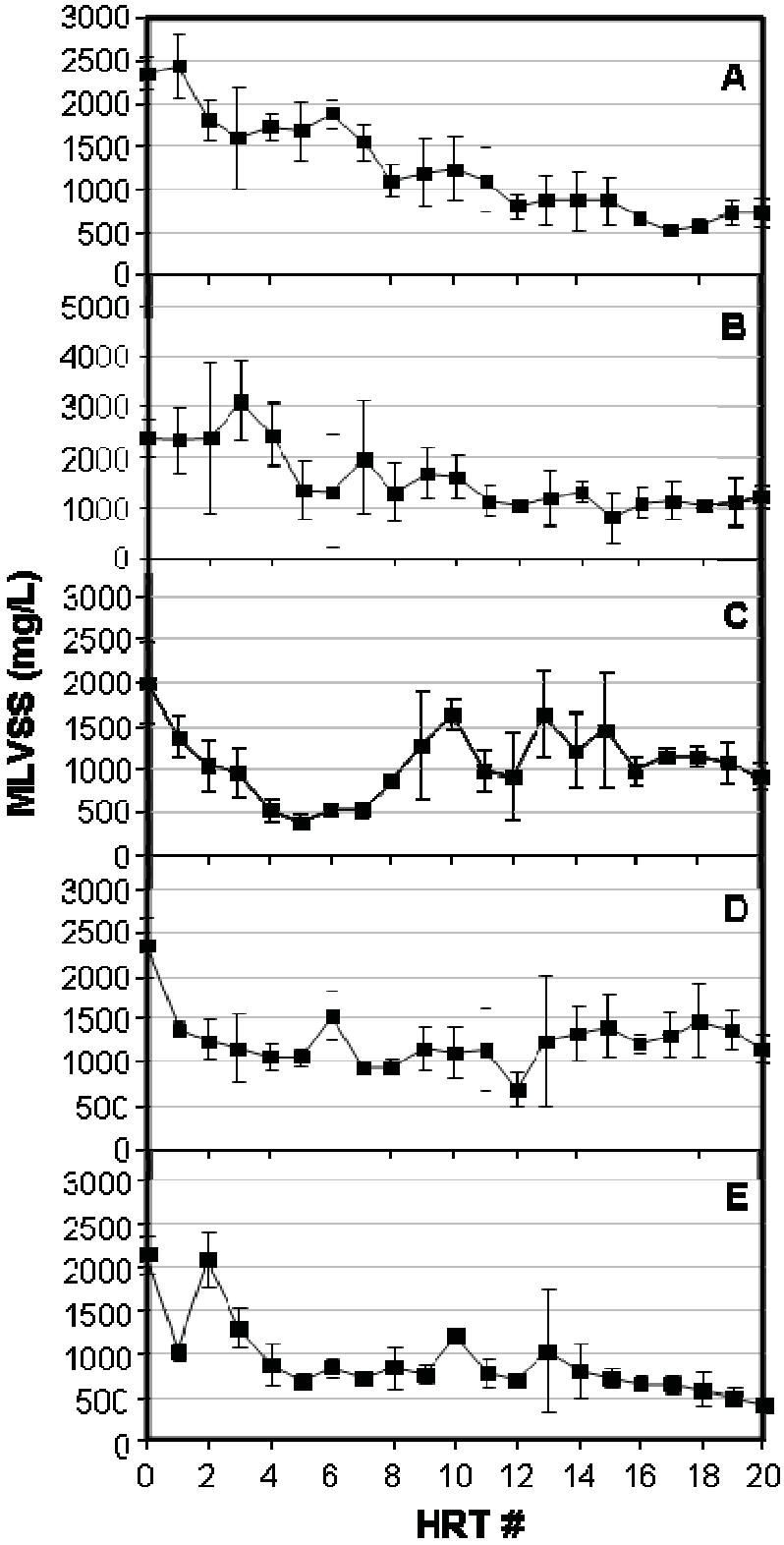

Figure 3A-E. Variation of MLVSS with HRT. Data shown are from samples taken at the end of the 24 hour feed period, and are the average of three replicate reactors. A FC 3200. B FC BHAO. C FC EVAP. D 1°OUT. E WAS-only.

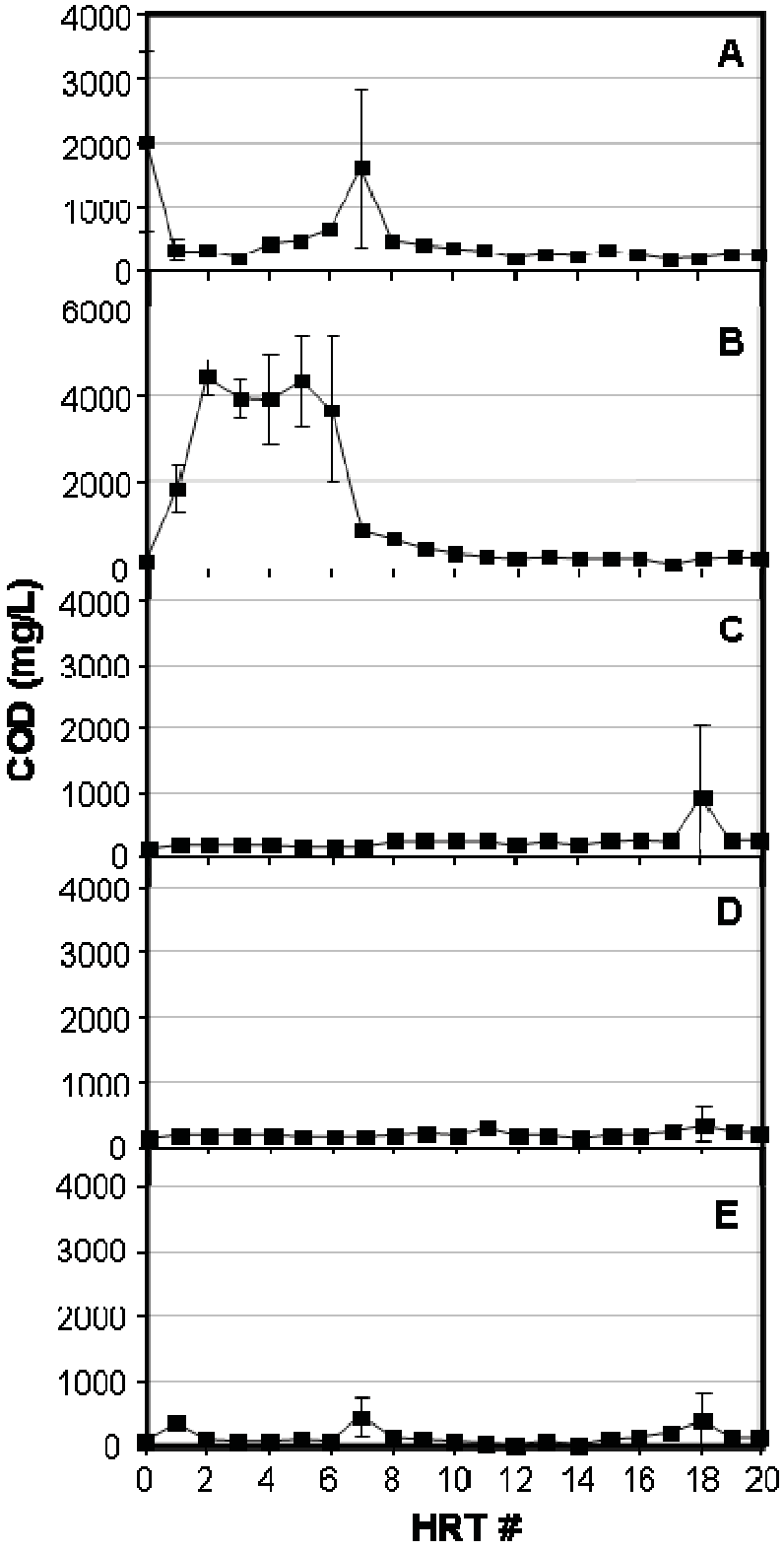

Figure 4A-E. Variation of COD with HRT. Data shown are from samples taken at the end of the 24 hour feed period, and are the average of three replicate reactors. A FC 3200. B FC BHAO. C FC EVAP. D 1°OUT. E WAS-only.

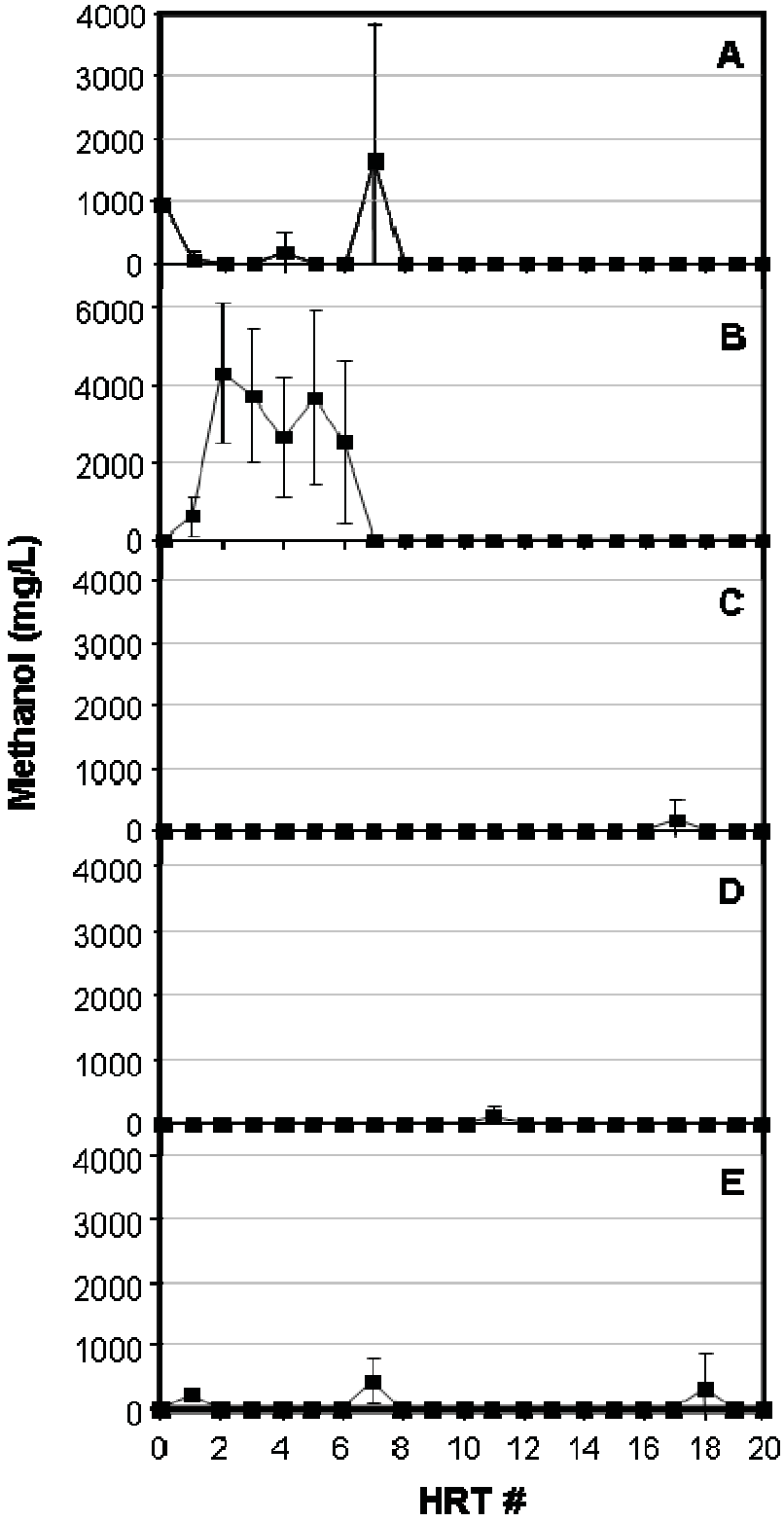

Figure 5A-E. Variation of Methanol with HRT. Data shown are from samples taken at the end of the 24 hour feed period, and are the average of three replicate reactors. A FC 3200. B FC BHAO. C FC EVAP. D 1°OUT. E WAS-only.

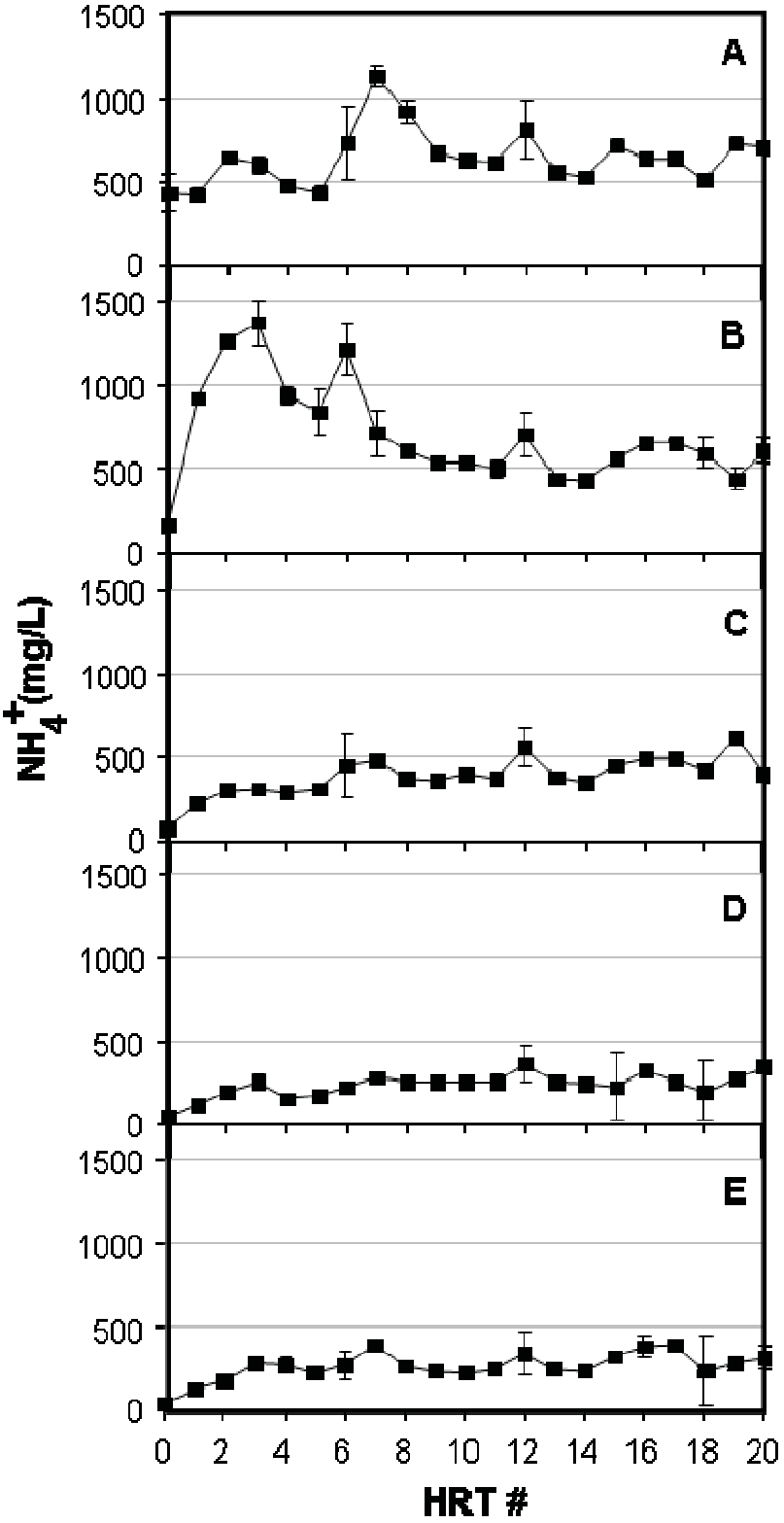

Figure 6A-E. Variation of NH4+ with HRT. Data shown are from samples taken at the end of the 24 hour feed period, and are the average of three replicate reactors. A FC 3200. B FC BHAO. C FC EVAP. D 1°OUT. E WAS-only.

Tables

Table 1. Average COD, TSS, and pH for the foul condensates and 1°OUT as received

Waste Stream ID	COD[1] (mg/L)	TSS[2] (mg/L)	pH
FC 3200	30200 ± 13545	47 ± 23	9.66 ± 0.84
FC BHAO	13314 ± 16433	976 ± 1537	9.39 ± 0.99
FC EVAP	5487 ± 4247	116 ± 29	9.48 ± 1.11
1° Out	480 ± 286	600 ± 303	7.48 ± 0.45
[1]Chemical Oxygen Demand ± one standard deviation [2]Total Suspended Solids ± one standard deviation			

Task 3 – Supplementation of Waste Effluents for Production of PHA

Investigators: David N. Thompson[1], Frank J. Loge[2], Gregory R. Mockos[2], William A. Smith[1]

Performing Institutions: [1]Idaho National Laboratory; [2]The University of California-Davis

Effect of Carbon to Nitrogen Ratio on Polyhydroxyalkanoate Production by Pulp Mill Activated Sludge

Summary

The impact of nitrogen limitation on polyhydroxyalkanoate (PHA) storage was investigated in methylotrophic consortia enriched from pulp mill activated sludge subjected to a feast-famine regime. Ten sequencing batch reactors were operated aerobically at neutral pH and 25°C with a hydraulic residence time and a solids retention time of four days. PHA storage was first evaluated at carbon to nitrogen (C/N) ratios of 3, 20, 60, 100, and 140 using a consortium fed only methanol as the primary carbon source (designated "methanol-only"). At a C/N of 60 this consortium produced a peak PHA concentration of about 16 % on a total dry suspended organic material basis. PHA storage was then evaluated at C/N ratios of 3, 15, 30, 45, and 60 in reactors (designated "diluted foul condensate" reactors) fed a separately-enriched consortium fed foul condensate, condensed organic waste recovered from kraft pulping, diluted with primary clarifier effluent. These reactors yielded a peak PHA concentration of about 15% on a total dry suspended organic material basis at a C/N of 60. In the methanol-only reactors, a combination of feast-famine and nitrogen limitation was required for induction of PHA storage and necessary to produce robust cultures capable of efficiently storing PHA in high yield. This is in contrast to studies that have shown these factors to be independently sufficient to stimulate PHA storage. In the diluted foul condensate reactors PHA storage was not induced by feast-famine conditions alone at very low C/N, suggesting that nitrogen availability would also affect PHA storage for these reactors. However, at higher C/N values, nitrogen was not completely consumed, indicating that nitrogen was not a limiting nutrient at any of the C/N values tested.

Introduction

Polyhydroxyalkanoates (PHAs) are biologically synthesized polyesters that exhibit mechanical properties similar to polypropylene with the added benefit of biodegradability (Lenz 2005). The ability to store excess carbon in the form of intracellular PHA granules gives PHA-accumulating bacteria a competitive advantage in environments that are subject to frequent change (Lee 1999). Several environmental conditions have been shown to be independently sufficient to promote the growth of PHA-accumulating bacteria and subsequent polymer storage: (i) a nutrient limitation (e.g., either macro- or micro-) in the presence of excess carbon (Suzuki 1986; Suzuki 1986; Daniel 1992; Kim 1996; Chua 1999; Ma 2000); (ii) cycling between an oxic and anoxic environment (Dionisi 2004a; Serafim 2004) or (iii) cyclic periods of feast and famine (Loosdrecht 1997; Carta 2001; Dircks 2001a; Dionisi 2004b). The first condition occurs when carbon utilization for cell growth is limited by a lack of a macro- or micro-nutrient (Braunegg 2004). High carbon to nitrogen (C/N) ratios have been shown to favor PHA synthesis at the expense of cell growth (Chua 1999; Ma 2000). Additionally, intracellular PHA accumulation has been observed to be proportional to the C/N ratio (Serafim 2004). The second condition (e.g., anoxic-oxic cycling) favors cells that can assimilate organic compounds in an anoxic environment while growing under oxic conditions at the expense of the stored carbon (Dionisi 2004a; Dionisi 2004b). The third condition (feast-famine cycling) is a result of successive alternating periods of external substrate availability (feast period) and unavailability (famine period). The alternating cycles cause unbalanced growth conditions in which cells that are capable of quickly assimilating available carbon and storing it as

PHA have a selective advantage over cells that can only assimilate carbon concurrent with biosynthesis (Beun 2000; Salehizadeh 2004).

The three environmental conditions described above have been used independently to induce PHA production by a variety of bacteria from numerous carbon-rich waste streams (Anderson 1990; Braunegg 1998; Madison 1999; Khanna 2005). In this study, PHA production from "foul condensates," condensed organics recovered as wastes from kraft pulping (Miller 2005), was investigated. Foul condensates contain methanol, a regulated volatile organic compound (VOC) present at up to 80% of the organic matter in the waste stream (Springer 2000). The kraft pulping process liberates cellulose fibers, later used in papermaking, from wood chips using a hot sodium sulfide-hydroxide digestion (Dufresne 2001). Foul condensates are a regulated effluent from the kraft chemical recovery process and constitute a malodorous high-strength carbon waste stream that is either recycled within the pulp mill or incinerated. Biological conversion of foul condensate-derived methanol into renewable value-added products such as PHAs could provide a sustainable alternative to current foul condensate management strategies, as well as an additional revenue stream for the mills.

In a prior study conducted by our research group, sequencing batch reactors (SBRs) were operated to produce microbial enrichments of pulp mill activated sludge that (i) consumed methanol and (ii) had the potential to synthesize PHA in a feast-famine environment without a macronutrient (nitrogen) limitation (Mockos et al. 2008). However, the enrichments did not produce PHA under the nitrogen-sufficient enrichment conditions, despite 80 days of operation under a feast-famine regime. The low or nonexistent amounts of PHA found in these reactors when run under nitrogen-sufficient feast-famine conditions indicated that the enrichments might require the combination of nitrogen limitation and feast-famine environment to induce PHA storage.

The goal of this study was to test the effects of nitrogen limitation on methanol consumption, biomass formation and PHA accumulation using two different methanol-respiring enrichment cultures (Mockos 2008) to inoculate ten SBRs. The first consortium, enriched using a nutrient medium with methanol as the sole carbon source in our previous study, was inoculated into five SBRs, fed a fixed methanol concentration, and operated at C/N ratios of 3, 20, 60, 100, and 140. The second consortium, comprised of a mixture of two separately-enriched consortia from the previous study (enriched using foul condensate or primary clarifier effluent), was inoculated into five SBRs fed foul condensate diluted with primary clarifier effluent, and operated at C/N ratios of 3, 15, 30 , 45, and 60. After stabilization of the cultures in the SBRs, a 24-hour feed and decant cycle was performed in each of the reactors and the PHA content was measured in each reactor to determine the impact of C/N on PHA production for each enrichment/feedstock combination.

Materials and Methods

Ten bench-scale SBRs, each with a working volume of four liters, were constructed from a 20.32 cm tall clear acrylic cylinder with a 20.32 cm inside diameter and 1.27 cm wall thickness. The acrylic shell was mounted on a 20.32 cm diameter Sanitaire® Silver Series II fine bubble disc diffuser membrane (ITT Industries, Brown Deer, WI). Air was supplied at 1500 mL min^{-1} (0.375 vvm) to provide both oxygen and mixing. Reactors were vented through two granular activated carbon columns (CC601 and Midas OCM; USFilter, Los Angeles, CA) to minimize exposure to the malodorous foul condensates. The reactors were operated at hydraulic and solids residence times (HRT and SRT, respectively) of four days with a 24-hour feed/decant cycle in which one quarter of the reactor volume was replaced daily with 1 L of new feed (i.e., 0.25 dilution ratio). The experimental setup is shown in Figure 7.

Pulp Mill Effluents

Two waste streams from a kraft pulp and paper mill facility (P.H. Glatfelter, Chillicothe, OH) were used as sources of carbon and nitrogen in this study. The first waste stream was obtained from the pulping process and contained condensed organics ("foul condensates"). The second waste stream was obtained from the non-sterile effluent of the primary clarifier in the industrial wastewater treatment

system at the mill. The compositions of the foul condensate and primary clarifier effluent are shown in Table 2. The pulp mill effluent compositions in Table 2 are the averages from analyses performed for each waste stream received from the mill over the course of the experiment. The large variability in the data in Table 2 demonstrates the changing compositions of the materials received, and is assumed to be a result of the variability of the wood species used as feedstocks for the pulp mill. Less than 0.5 mg L^{-1} nitrate and nitrite were present in these effluents. Both waste streams are described in detail elsewhere (Mockos 2008).

Microorganisms

The microbial consortia used in this study were obtained from a previous study (Mockos 2008) in which we enriched activated sludge collected from the return activated sludge line at the P.H. Glatfelter pulp mill wastewater treatment facility (Chillicothe, OH). The consortia were enriched using SBRs operated aerobically with an HRT and SRT of 4 days. One consortium (designated "methanol-only") was enriched using Methanol-Utilizing Bacteria Medium B (Atlas 1997) amended with methanol (99.9%; Fisher Scientific, Fair Lawn, NJ) to a final COD in the feed of 2.5 g L^{-1}. The other consortium used in this study (used to inoculate the designated "diluted foul condensate" reactors) was comprised of a mixture of two separately-enriched consortia (Mockos 2008). The first of these was enriched on foul condensate; the second was enriched on primary clarifier effluent amended with methanol. The volumetric mix ratio of the two enrichments was set at 9:1 (foul condensate enrichment:primary clarifier/methanol enrichment), which was the approximate ratio of COD present in the diluted foul condensate used for the enrichment to the COD in the primary clarifier effluent.

The inocula for the C/N experiments were produced by culturing the enrichments in SBRs at HRT=SRT=4 days and a C/N of 3. The methanol-only enrichment was fed methanol at 2.5 g L^{-1}, and stabilized with respect to MLVSS and COD removal after 5 HRTs. The diluted foul condensate reactor inoculum was fed a mixture of foul condensate diluted with primary clarifier effluent to a final total COD concentration of 5 g L^{-1}. This SBR stabilized with respect to MLVSS and COD removal after 14 HRTs. Following stabilization, the daily decants from the methanol-only and diluted foul condensate SBRs were stored at -80°C in 40% (v/v) glycerol (Fisher Scientific, Fair Lawn, NJ) for use as inocula in the C/N experiments. When sufficient seed for the C/N experiments had been stored, the separately frozen stocks were thawed, mixed together, and re-suspended in phosphate-saline buffer solution at neutral pH containing 1.2 g L^{-1} anhydrous Na_2HPO_4, 0.18 g L^{-1} $NaH_2PO_4 \cdot H_2O$, and 8.5 g L^{-1} reagent grade NaCl (Fisher Scientific, Fair Lawn, NJ).

Reactor Operation

All reactors were inoculated by re-suspending 2 L of each respective inoculum into 2 L of the desired feed. The reactors were continuously air-sparged and run with HRT = SRT = 4 days for 20 days to allow the consortia to acclimate and stabilize prior to detailed PHA analyses. Temperature in the reactors was not controlled; however, the reactors were operated at an average temperature of 21˚C with a standard deviation of 2˚C. For each of the two feed sources, the total COD in each reactor was kept constant at 5 g L^{-1}; this value was selected as a conservative upper bound to limit potential toxic effects of methanol on the microbial population (Bormann 1997), and because it was within the reported range of methanol concentration for optimal PHA production (Bourque 1992).

The feed for the methanol-only reactors was prepared by amending Methanol-Utilizing Bacteria Medium B (Atlas 1997) with pure methanol (99.9%; Fisher Scientific, Fair Lawn, NJ) added to a final COD of 5 g L^{-1}. C/N ratios of 3, 20, 60, 100, and 140 were attained in five 2 L aliquots of this medium by varying the quantity of ammonium sulfate (Fisher Scientific, Fair Lawn, NJ) added to the feedstock. For this study, C/N was calculated by dividing the total COD concentration by the ammonium concentration (both in mg L^{-1}). The C/N ratio was calculated using this method due to the lack of information regarding the exact carbon source and nitrogen source composition of the waste streams used in this work. Notably, during the original enrichment cultures using foul condensate 11-21% of the total COD in the foul

condensates was non-biodegradable (Mockos 2008), suggesting that the biological oxygen demand (BOD) may have been only 79-89% of the total COD.

The diluted foul condensate reactors were fed a mixture comprised of the pulp mill foul condensate from the kraft chemical recovery process diluted with primary clarifier effluent from the pulp mill wastewater treatment facility. The COD in the reactors' feedstock was fixed at 5 g L^{-1}. As a result of the COD and ammonium concentrations in the two feed components this resulted in a C/N of approximately 30. Ammonium sulfate was added to the feedstock to achieve C/N of 3 and 15; methanol was added to achieve C/N of 45 and 60. Because the total COD in the reactors was fixed, the highest C/N ratio attainable was 60.

Volatile compounds, including the feedstock methanol, were stripped from the medium to some degree because the reactors were aerated. The amount of methanol stripped (26 %) was estimated as previously described (Mockos 2008) and the feed concentrations were adjusted by adding reagent grade methanol (99.9%; Fisher Scientific, Fair Lawn, NJ) at the time of each feeding to account for this loss. The amount of methanol added to the feed mixture to account for loss due to stripping was included in the overall COD concentration when calculating the different C/N ratios.

Sampling and Analyses

Reactor performance over the 20-day acclimation phase was monitored by sampling at the beginning and end of the last 24 hour feed/decant cycle of each SRT. The samples were analyzed for Mixed Liquor Volatile Suspended Solids (MLVSS), Mixed Liquor Suspended Solids (MLSS), and COD. MLVSS and MLSS were measured according to ASTM Standard Method 2540 A-G (APHA 20051992) using Millipore TCLP AP40 glass fiber filters. MLSS was used to track the amount of total suspended solids present in the reactors, while MLVSS was used as a surrogate measure of the fraction of suspended solids considered biomass. During operation, varying degrees of growth was observed adhered to the reactor walls; this biomass was not resuspended before sampling and thus was not included in the MLVSS measurements. Soluble COD was measured according to ASTM Standard Method 5220 A (APHA 20051992) using Hach high–range ampoules with a Hach DRB 200 digestion block and Hach DR 2010 portable data logging spectrophotometer (Hach Company, Loveland, CO) set at a 620 nm wavelength.

Immediately after being fed at the conclusion of the 20-day acclimation phase, a single 48 mL aliquot was withdrawn from each reactor for measurement of the organic fraction of the total suspended solids. The 48 mL aliquot was mixed with 2 mL of commercial grade bleach (5% NaClO) (Clorox, Oakland, CA) and centrifuged at 4,300 ×*g* for 15 minutes. The pellets were dried at 60°C for 24 hours, weighed to determine the total suspended solids, ashed at 550°C, and reweighed to determine the non-volatile and volatile fractions. The organic fraction, which included cellular biomass and short cellulose fibers present in the primary clarifier effluent, was calculated by difference.

Reactor performance immediately after the 20-day acclimation phase was then monitored by sampling every two hours over a single 24-hour feed and decant cycle. The samples were analyzed for pH, temperature, dissolved oxygen (DO), COD, methanol, ammonium, and PHA. Each parameter was measured once over the course of a single 24-hour feed cycle per reactor. The lack of replication prevented a complete statistical interpretation of the data. However, despite the lack of replication, the analytical procedures performed allowed important trends in the measured parameters to be assessed. The samples were filtered through a Millex GP 0.22 μm Express PES Membrane filter unit (Millipore Corporation, Billerica, MA) prior to analyses of COD, ammonium, and methanol. Temperature, pH, and DO were measured directly in the reactors. Dissolved oxygen and temperature were measured using an Orion® 1230 DO Meter with an Orion® 083010 DO Probe (Orion Research, Beverly, MA), while pH was measured using an Accumet® AP61 Portable pH Meter with an Accumet® Gel-Filled Pencil-Thin pH electrode (Fisher Scientific, Fair Lawn, NJ).

Methanol was analyzed by high performance liquid chromatography (HPLC) using a Hitachi HPLC D-6000 Series HPLC system (Tokyo, Japan) consisting of a Hewlett Packard 1047A refractive

index detector (Agilent Technologies, Palo Alto, CA), a Hitachi L6200A gradient pump (Tokyo, Japan), and a Hitachi AS-4000 autosampler (Tokyo, Japan). The mobile phase consisted of 0.1% H_3PO_4 at 0.5 mL min^{-1}. Samples (120 µL) were prepared at 1:1 dilution and injected into a Supelcogel C-610-H (300mm x 7.8mm ID) column (Bellefonte, PA) with a Supelcogel H guard column (Cat. No. 59304-U). Methanol standards were prepared at 5-1000 mg L^{-1} using 99.99% methanol (Fisher Scientific, Fair Lawn, NJ). Samples were run at a column temperature of 30°C and a detector temperature of 35°C. The method detection limit (MDL) for the methanol analysis was 5 mg L^{-1}.

Ammonium concentrations were measured by ion chromatography using a Dionex ED40 conductivity detector with a GP50 gradient pump, an AS50 autosampler, an AD20 absorbance detector, and an EG40 eluent generator (Dionex Corporation, Sunnyvale, CA). Samples were analyzed using 5 µL injections at a flow rate of 1 mL min^{-1}. Analytes were separated using a Dionex IonPac CS12A (250mm x 4mm ID) with a Dionex ECG-MSA eluent generator cartridge. Data were collected and analyzed using Peaknet v. 5.21 (Dionex Corporation, Sunnyvale, CA). Cation standards were prepared using the Dionex 6 Cation Standard II #46070. A seven-level cation standardization was performed (DI water, 5 standards, and the non-dilute Cation Standard II solution). The MDL for the ammonium analysis was 0.5 mg L^{-1} NH_4^+.

PHA concentrations are reported in this study on a total suspended organic matter basis as measured by MLVSS; because there were short cellulose fibers present in the primary clarifier effluent, the diluted foul condensate reactors include the cellulose fibers in the MLVSS measurement. Analysis of PHAs was conducted according to the procedure described by Braunegg et al. (1978), with the following modifications. Unfiltered 48 mL biomass samples were mixed with 2 mL of commercial grade bleach (5% NaClO) (Clorox, Oakland, CA) and centrifuged at 4,300 ×*g* for 15 minutes to harvest the solids. The pellet was then dried at 60°C for 24 hours. Between 20-40 mg of the dried reactor solids were quantitatively suspended in a mixture of 2 mL acidified methanol (3% H_2SO_4, v/v) and 2 mL chloroform. The mixture was spiked with 0.5 mg mL^{-1} benzoic acid as an internal standard to quantify recovery. The mixture was then digested at 100°C for 4 hours in a Hach DRB 200 digestion block (Hach Company, Loveland, CO). Once the digestion was completed, 1 mL of deionized water was added and the mixture was vortexed for 30 seconds. After phase separation, the organic phase was removed using a Pasteur pipette, and then filtered through a second Pasteur pipette packed with a cotton plug and 1 g of sodium sulfate (Fisher Scientific, Fair Lawn, NJ) to remove any remaining water. The organic phase, which contained the esterified monomers from the depolymerized PHA molecules, was analyzed by gas chromatography using a Hewlett Packard 5890 Series II GC System with a Flame Ionization Detector (Agilent Technologies, Palo Alto, CA). Samples were run at 40°C for 2 minutes at 1 mL min^{-1} with 1 µL injections using a Rtx-1 column (30m x 0.25µm x 0.25 stationary film thickness) (Restek, Bellefonte, PA). Injector temperature was 225°C and detector temperature was 250°C. Data were analyzed using GC Chemstation 1990-2000 Rev.A.08.01 software (Agilent Technologies, Palo Alto, CA). The concentration of PHA was quantified against standards of PHB and PHV (Poly(3-hydroxybutyric acid-co-3-hydroxyvaleric acid) standard) (Sigma-Aldrich, St. Louis, MO) as derivatized methyl esters and extraction efficiency was calculated based on the benzoic acid internal standard. PHA concentrations were then multiplied by the total suspended solids and divided by the organic fraction of the initial total suspended solids measured for each reactor to compensate for the inorganic portion of the harvested pellet.

Results

All of the reactors reached functionally-stable operation by the end of the fifth SRT (20 days) prior to periodic sampling over one 24-hour feed and decant cycle. It is not known whether the consortium in each reactor had reached community stability after 20 days; samples were taken at this time point and stored for future community analysis. During the acclimation period, MLVSS, MLSS, and COD degradation were measured at the end of each SRT (i.e., every 4 days) to assess reactor stability. Reactor stability was arbitrarily defined as the point at which the MLVSS and MLSS concentrations and

COD degradation values were within ±10% for three consecutive SRTs. At this point, the reactors were sampled every two hours over a single 24-hour feed and decant cycle to assess trends in pH, temperature, DO, COD, methanol, ammonium, and PHA.

Methanol-Only Reactors

The consortia in the reactors operated at C/N ratios of 3, 20, and 60 degraded between 98 and 100% of COD over the 24-hour feed and decant cycle, while the reactors at C/N ratios of 100 and 140 degraded only 26 and 18% of the COD, respectively (Figure 8). Similar trends were seen with the methanol consumption data, for which the reactors at C/N ratios of 3, 20, and 60 consumed 97, 86, and 85% of the methanol, respectively, over the 24-hour feed and decant cycle, and the reactors at C/N ratios of 100 and 140 reactors each consumed 32% of the methanol (Figure 8).

The dissolved oxygen concentrations in the C/N 3 and 20 reactors dropped quickly to 18-30 % of the DO saturation concentration after addition of the feed followed by a return to near-saturation once the available carbon had been consumed (the maximum DO concentration during a feed/decant cycle was used as the experimentally- attained DO saturation concentration) (Figure 8). There was no significant change in DO over the 24-hour feed and decant cycle in the C/N 60, 100, and 140 reactors (Figure 8).

Ammonium was detected in the C/N 3 reactor throughout the 24-hour feed cycle. In contrast, the consumption of ammonium nitrogen in the reactors run at C/N ratios of 20, 60, 100, and 140 was nearly immediate as indicated by the rapid drop at the beginning of the 24-hour feed and decant cycle (Figure 9). The C/N 60 reactor produced a peak PHA content of 16% on a total suspended organic material basis. In contrast to the reactors operated at higher C/N ratios, essentially no PHA accumulation was observed in the C/N 3 reactor (Figure 8 and Figure 10). The C/N 20 reactor yielded 10% PHA on a total suspended organic material basis. The C/N 100 and 140 reactors yielded peak PHA concentrations of 11 and 10%, respectively, on a total suspended organic matter basis (Figure 10). An average of 4% PHA was present at the beginning of the feed cycle in all reactors except for the C/N 3 reactor, indicating incomplete metabolism of PHA stored during the previous 24-hour feed and decant cycle (the final 24 hour period of SRT 5) in these reactors (Figure 8).

Diluted Foul Condensate Reactors

In the diluted foul condensate reactors, the observed COD consumption was similar for all of the C/N values, ranging from 88 to 92% over the 24-hour feed and decant cycle (Figure 11). In contrast, methanol consumption increased with increasing C/N; the methanol consumption rate also increased with C/N up to C/N 45, and then decreased at C/N 60. The C/N 3 and 15 reactors degraded methanol by 97 and 92%, respectively, at approximately linear rates over the 24-hour feed and decant cycle (Figure 11). Methanol was removed after 16 hours in the C/N 30 and 45 reactors, dropping below the detection limit at 18 hours. In the C/N 60 reactor, methanol was nearly depleted after 18 hours, dropping below the detection limit at 24 hours.

The observed trends in DO were also similar over the range of C/N values tested. After the reactors were fed, the DO concentrations dropped to 45-55 % of the DO saturation concentration and remained below saturation until the methanol was entirely consumed (Figure 11).

In contrast to the methanol-only reactors, very little nitrogen consumption was observed in the diluted foul condensate reactors over the course of the 24-hour feed and decant cycle, regardless of the C/N (Figure 12). Thus, there was no nitrogen limitation imposed upon these cultures at any point over the daily feed and decant cycle.

A peak PHA concentration of 15% was observed in the C/N 60 reactor, on a total suspended organic material basis. The C/N 3, 15, 30, and 45 reactors yielded peak PHA concentrations of 8, 14, 14, and 9%, respectively, on a total suspended organic material basis (Figure 13). PHA carry-over of 3% or less was observed from the previous feed cycle in all of the diluted foul condensate reactors (Figure 11).

Discussion

The consortia used in this study were enriched previously (Mockos et al. 2008) using the same feedstock sources. In the previous study, the enrichments were intentionally conducted using nitrogen-sufficient conditions to assure balanced growth, however, it was observed that no PHA accumulated in the bacteria under these conditions even when they were operated in a feast-famine environment. Waste activated sludge collected from the mill's industrial wastewater treatment system, which served as the source of the inoculum for the enrichments, did not accumulate PHA under N-limited conditions. Hence, the influence of C/N on PHA storage by the enriched consortia was investigated further.

Methanol-Only Reactor Performance

The results confirm the expected link between nitrogen limitation and cell growth (Serafim 2004). Nitrogen limitation was observed in all of the methanol-only reactors except the C/N 3 reactor (Figure 9). There was evidence of microbial activity in the C/N 3 and 20 reactors, observed as a rapid drop in DO at the onset of substrate addition. A rapid decrease in DO immediately after substrate addition followed by a quick return to saturation levels after the carbon source is consumed is an indication of rapid cell respiration within a reactor (Braunegg 1998; Beun 2002). Stable, but relatively low (~500 to 600 mg L^{-1}) MLVSS concentrations indicated that some portion of the respired carbon contributed to cell growth (Table 3). In contrast, the DO did not drop in the C/N 60, 100, and 140 reactors, indicating that consumption of oxygen for metabolic processes was greatly reduced (Figure 8). MLVSS concentrations were lower for these reactors relative to the C/N 3 and 20 reactors indicating decreased cell growth rates and subsequent washout of cells during decant. Taken together with the DO data in Figure 8, the relative rates of methanol consumption indicate that robust cellular activity was supported in reactors operated at C/N ratios of 3 and 20 and that some portion of carbon was used for growth. More carbon is required to support the anabolic metabolism and the associated high energy requirements for cell growth, leading to higher and more rapid uptake of available carbon. When nitrogen (or another essential nutrient) is limited, cell growth is limited resulting in suppressed carbon consumption for growth (Serafim 2004).

Above C/N 20, the methanol carbon was not used primarily for growth. At C/N 60, the methanol was depleted over the 24-hour period; however, the DO and MLVSS data suggest that little of the methanol was used for high oxygen-consuming anabolic reactions (Figure 8). As the nitrogen was further limited, the C/N 100 and 140 reactors demonstrated severely reduced methanol consumption over the 24-hour sampling period, leading to carry-over of methanol from one cycle to the next. Thus there was no feast-famine condition present in these cultures. There was also evidence that the cells were severely stressed with the MLVSS in these reactors being 30 – 40 % of that observed in the lower C/N reactors (Table 3). COD degradation was also suppressed in these reactors with little to no COD degradation over the course of a feed cycle (Table 3). Hence, the severe nitrogen limitation imposed in these cultures was the driving force behind the limited activity in these cultures.

These observations indicate that the operational conditions created a continuum of environmental stressors beginning at C/N 3 with solely feast-famine conditions, and ending at C/N 140 with solely nitrogen-limited metabolism (Table 4). The C/N 3 reactor was clearly in feast-famine but not nitrogen limited environment as evidenced by the rapid growth and consumption of the COD and methanol. In contrast, the C/N 100 and 140 reactors were clearly in nitrogen limitation but not a feast-famine environment, as evidenced by the carry-over of methanol and the lower MLVSS. The C/N 20 reactor was in both a feast-famine (drop in DO, rapid methanol depletion) and a nitrogen limited (rapid ammonium depletion) environment. The C/N 60 reactor did not show a dip in DO and showed reduced rates of COD and methanol consumption and never reached a feast-famine condition; however, it was clearly nitrogen-limited (Table 4).

Consistent with the previous study (Mockos 2008), PHA storage in the present work was not observed in the nitrogen sufficient feast-famine C/N 3 reactor (Figure 8). A feast-famine environment was thus by itself insufficient to induce PHA storage in this consortium; nitrogen limitation was also required (Figure 8 and Figure 9). This is in contrast to prior studies (Loosdrecht 1997; Carta 2001; Dircks

2001; Beun 2002; Dionisi 2004a) that have shown PHA storage to be induced by feast-famine conditions, independent of other environmental variables.

In the present study PHA storage was observed when nitrogen limitation was introduced at C/N 20 and greater (Figure 8 and Figure 9). Interestingly, PHA carry-over was observed in all of the C/N values from 20 to 140, suggesting either the ability to metabolize the stored carbon was limited, or there was no need to use the stored carbon. Therefore, we assert that nitrogen limitation was the dominant environmental factor affecting PHA production. It has been shown that the C/N ratio in a SBR system influences the proportion of carbon that is used for cellular growth or directed to intracellular PHA storage (Chua 1999). When balanced nutrient conditions exist, growth is favored (Ma 2000); conversely, when nitrogen or another nutrient is limiting, the majority of the available carbon is stored as PHA or other bio-polymers (Lee 1996). However, in the present study, nitrogen limitation by itself did not produce a robust culture capable of depleting the substrate and maintaining high biomass concentrations, and thus offering the opportunity to maximize PHA accumulation. Increasingly severe nitrogen limitation had detrimental effects on cellular growth and carbon metabolism as evidenced in the DO and methanol consumption profiles seen in Figure 8 and the lower MLVSS values seen in Table 3.

The best combination of growth and PHA storage occurred in the range C/N 20–60. The C/N 20 reactor supported growth even though nitrogen was limited and feast-famine conditions were achieved (Figure 8). In this culture, PHA storage followed established trends for a feast-famine environment. In such systems intracellular levels of PHA gradually increase until the carbon source is depleted (Salehizadeh et al. 2004). The stored PHA is then used by the cell as a sequestered carbon and energy source, giving it a competitive advantage over other cells in the environment (Reis 2003; Serafim 2004). In the C/N 60 reactor, which was also nitrogen limited, rapid growth did not occur and feast-famine conditions were not achieved. PHA was accumulated in this culture early in the 24-hour period while methanol was still present in high levels, indicating nitrogen limitation alone was responsible for PHA accumulation. However, methanol was depleted in the culture showing that sufficient biomass was present to store a portion of the methanol as PHA. The combination of conditions within the C/N 20-60 range was necessary to promote sufficient cell growth in order to maintain high MLVSS but still provide nutrient-limiting conditions that promote PHA storage.

Diluted Foul Condensate Reactor Performance

There was evidence of microbial activity in all the diluted foul condensate reactors as DO concentrations dropped when carbon substrate was added (Figure 11). The decrease in DO immediately after substrate addition followed by a rebound to saturation levels after the carbon source was consumed indicated metabolic activity within the reactors (Braunegg 1998; Beun 2002). There was no discernable difference in the magnitude of the initial DO drop among the different C/N ratios in the diluted foul condensate reactors; DO concentrations dropped to an average of 50% of the DO saturation concentration (Figure 11). The MLVSS values over the course of several 24-hour feed cycles remained relatively constant once the reactors completed the five-SRT/HRT stabilization process (data not shown), which indicates some portion of the respired carbon contributed to cell growth and reproduction. However, MLVSS concentrations (Table 5) remained relatively low (~500 mg L^{-1}) compared to typical wastewater treatment reactors. When the reactors had stabilized with respect to MLVSS, MLSS, and COD removal, the consortia were able to consume the majority of the carbon substrate by the end of the feed cycle, at which point, microbial activity either ceased or was severely reduced as demonstrated by the return of DO to the saturation concentration. The DO concentrations in the diluted foul condensate reactors required almost the entirety of the feed cycle to rebound to saturation levels. The time at which methanol was depleted corresponded with the time at which the DO returned to saturation for all of the reactors, indicating that the methanol was used for aerobic activity. The slower rebound with respect to the methanol-only reactors indicated that lowered cellular activity occurred for a much longer period of time over the course of the 24-hour feed cycle (Figure 11).

Nutrient limitations affect microbial growth rates and soluble carbon substrate removal (Ma 2000). Macronutrients that affect growth rate and COD removal include nitrogen and phosphorus; micronutrients include potassium, sodium, iron, magnesium, sulfur, and copper as well as others. When nutrients other than carbon are limiting, the total quantity and rate of carbon consumption is decreased. Our results indicate that the foul condensate reactors received sufficient carbon and nitrogen as indicated by the COD and ammonium carryover observed in Figure 11 and Figure 12. If nitrogen were a limiting nutrient, then one would expect rapid ammonium depletion (as was observed in the methanol-only reactors described above) or expect MLVSS to increase as C/N decreased. However, each of the diluted foul condensate reactors had ammonium carryover and had similar MLVSS concentrations (Table 5) making it clear that nitrogen was not the limiting nutrient.

Unlike the methanol-only reactors, the dilute foul condensate reactors received no micronutrient amendments (Methanol Medium B), but were diluted using primary effluent from the pulp mill wastewater treatment facility. Analyses indicated the mill's primary effluent to be high in total dissolved solids, predominately sodium, chloride, carbonate (non-speciated), and phosphate. It also contained bromide, calcium, potassium, magnesium, sulfate and trace amounts of iron (data not shown). Some other nutrient—such as copper, cobalt or zinc, which were not detected in our analyses—may have controlled the growth rates and COD removal in these reactors. Alternatively, some of the foul condensate's COD may have been unavailable to the consortia, resulting in effective carbon limitation despite COD carryover. Finally, some component of either the foul condensate or the primary effluent may have been toxic to the cells. Attempts to assess foul condensate toxicity during growth of a related consortium on solid media did not indicate a significant effect, however these tests were inconclusive (data not shown) and cannot be extrapolated to the present consortium.

The reactors operated at C/N ratios of 3 and 15 degraded the methanol at a slower rate than the reactors operated at C/N ratios greater than 30, however the total COD consumption remained essentially constant in all of the reactors. This is demonstrated by the fact that neither the C/N 3, nor the C/N 15 reactors was capable of entirely removing the methanol by the end of the feed cycle. As a consequence, these two reactors were never under a feast-famine regime with respect to methanol or total COD. Conversely, the reactors operated at C/N ratios above 30 were under a feast-famine regime with respect to methanol as it was degraded 16 to 18 hours after feeding (Figure 11). The type of COD in the reactors varied with the C/N ratio (see Table **6**). COD concentrations decreased in all reactors, however, not all of the available COD was exhausted (Figure 11). This may indicate that the foul condensate contained a recalcitrant fraction of carbon that the cells were unable to use as a substrate (Dufresne 2001). COD concentrations stabilized after the methanol had been consumed implying that methanol was the main COD-contributing substrate that was used by the consortia.

The discrepancy between the methanol and COD degradation rates between the C/N 3 and 15 reactors and the C/N 30, 45, and 60 reactors may be explained by the carbon source in the daily reactor feed. The daily feed for the C/N 3 and 15 reactors was not amended with methanol, as methanol concentrations already present in the foul condensates were sufficient to obtain the desired C/N ratios while keeping the total COD concentration at 5 g L^{-1}. Nitrogen, in the form of ammonium sulfate was also added to these reactors to obtain the lower C/N ratios. Conversely, above a C/N of 30, neither methanol nor ammonium sulfate was amended to the daily feed as the ratio of foul condensate to wastewater (obtained as primary clarifier effluent) in the daily feed decreased as the C/N increased (Table **6**). As a result, as the C/N ratio increased, the total fraction of COD that was methanol from foul condensate increased and the fraction of COD that was non-methanol decreased. Hence, from the perspective of the carbon source being fed to the reactors, the C/N 3 and 15 reactors had a higher fraction of non-methanol COD present. Given that the cells predominately used methanol as the carbon source, a lower initial concentration of substrate (e.g., methanol) would likely lead to a lower consumption rate given that substrate utilization rate is proportional to the cell growth rate, which in turn is dependent on the substrate concentration (Tchobanoglous et al. 2003; Grady et al. 1999).

PHA storage occurred at all C/N ratios, with polymer storage improving with increasing C/N above 30. At C/N ratios of 15 and 30, PHA followed established trends for a feast-famine culture in which PHA concentration gradually increases until the carbon source is depleted (Salehizadeh 2004). The stored PHA was then internally used by the cell as an energy and carbon reserve when external carbon substrate was no longer available in the system (Reis et al. 2003). PHA was stored and then rapidly consumed after the peak PHA concentration above C/N 30, indicating that the cultures in the reactors operated at a C/N above 30 were under a severe feast-famine regime which favored almost immediate intracellular PHA consumption (Figure 5). All of the diluted foul condensate reactors had excess nitrogen, PHA storage, and a dip in DO concentration initially after feeding (Table 7). The reactors operated in the C/N 30-60 range performed similarly with respect to these four parameters. The C/N 30-60 reactors produced PHA and were capable of growth in a feast-famine and non nitrogen-limited environment, as evidenced by the carry-over of ammonium and lack of methanol carry-over. Hence, it can be inferred that the feast-famine regime was sufficient to induce PHA storage in the C/N 30-60 range (Table 5).

Nitrogen availability did not appear to influence PHA storage in these reactors. This was inconsistent with the results in the previous study (Mockos 2008) in which a feast-famine regime alone was insufficient to induce PHA storage. However, these results were consistent with prior studies (Loosdrecht 1997; Dircks 2001; Beun 2002; Dionisi 2004a) that have shown PHA storage can be induced under feast-famine conditions alone. The C/N 3 and 15 reactors, due to the reduced methanol consumption over the 24-hour sampling period, had methanol carry-over from one cycle to the next; thus, there was no feast-famine in these cultures. Nonetheless, the C/N 3 and 15 reactors stored PHA and were capable of growth (Table 5). This would imply that neither the feast-famine regime nor the availability of nitrogen played a determining role in intracellular polymer storage below a C/N of 15.

The specific mechanisms for stimulating PHA storage in C/N ratios less than 15 are unclear; however, it is most likely that PHA storage resulted from a macro- or micro-nutrient deficiency. In addition, the PHA storage in the reactors operated below a C/N of 15 was likely not the result of toxicity exerted by the elevated ammonium concentrations as such concentrations were well below toxic ammonium concentrations reported in the literature (Miller 2005). The diluted foul condensate reactors were fed mixtures of the foul condensate and primary clarifier effluent in ratios designed to attain the desired C/N ratios while keeping the total COD in the feed constant at 5 g L^{-1}. Besides being the primary source of COD in the feed, the foul condensates were also the primary nitrogen source. Because of the overwhelming amount of both carbon substrate and nitrogen in the foul condensate, it was necessary to extensively dilute it with primary clarifier effluent to attain the higher C/N ratios (Table 8). The primary clarifier effluent was more likely to be a significant source of non-carbon and non-nitrogen micronutrients as it is an intermediary step within the pulp mill wastewater facility. As the C/N increased in the diluted foul condensate reactors, the relative amount of primary clarifier effluent used in the feed mixture increased (Table 8). Hence, the low C/N ratio (below C/N 15) reactors had less primary clarifier effluent used in the preparation of the feed than did the high C/N ratio (above C/N 30) reactors. It is, therefore, possible that the consortia in the diluted foul condensate reactors operated at a C/N below 15, which were not nitrogen limited or under a feast-famine condition, may have been limited by a nutrient other than nitrogen because of a smaller portion of the reactor feed being composed of primary clarifier effluent, the likely source of non-carbon and non-nitrogen nutrients as described above. Such a limitation would have induced PHA storage irrespective of a nitrogen limitation or the imposition of a feast-famine regime.

Conclusions and Future Work

In the methanol-only reactors, the results confirmed that both nitrogen limitation and a feast-famine regime were necessary to induce PHA storage and maximize PHA yield. The conditions in the methanol-only reactors operated within the C/N 20-60 range allowed a balance between cell growth, to maintain high MLVSS concentrations, and PHA storage, thereby maximizing production of PHA in the reactor. Therefore, the results from this study suggest optimal PHA storage in the methanol-only reactors required both a feast-famine regime and a nitrogen-limited environment. Nitrogen limitation alone

allowed for PHA storage, but did not support high PHA yields. Finally, a feast-famine environment by itself was insufficient to induce PHA storage.

The diluted foul condensate reactors were driven by a different set of limiting factors than the methanol-only reactors. Cell growth in the diluted foul condensate reactors was not directly affected by the amount of nitrogen present because none of the reactors were nitrogen limited. The greater fraction of non-methanol carbon C/N 3 and 15 reactors likely affected the metabolic state of the consortia that had been selectively enriched for methanol consumption. A feast-famine and non nitrogen-limited environment was sufficient to induce PHA storage above a C/N of 30, while neither the feast-famine regime nor the availability of nitrogen were responsible for PHA storage below a C/N of 15. PHA storage below C/N 15 was likely stimulated by a macro- or micro-nutrient deficiency. The smaller proportion of primary clarifier effluent in the C/N 3 and 15 reactors likely resulted in a micronutrient deficiency in the daily feed medium, resulting in PHA storage.

References

Anderson, A.J. and E.A. Dawes (1990) Occurrence, Metabolism, Metabolic Role, and Industrial Uses of Bacterial Polyhydroxyalkanoates. Microbiological Reviews, 54(4): p. 450-472.

APHA (2005) Standard Methods for the Examination of Water and Wastewater, 21st ed., American Public Health Association, Washington D.C.

Atlas, R.M. (1997) Handbook of Microbiological Media, 2nd ed., CRC Press, Boca Raton, FL, p. 891.

Beun, J.J., Verhoef, E.V., M. Van Loosdrecht, C.M., and J. J. Heijnen (2000) Stoichiometry and Kinetics of Poly-β-Hydroxybutyrate Metabolism in Aerobic, Slow Growing, Activated Sludge Cultures. Biotechnology and Bioengineering, 67(4): p. 379-389.

Beun, J.J., Dircks, K., Van Loosdrecht, M.C.M., and J.J. Heijnen (2002) Poly-β-hydroxybutyrate metabolism in dynamically fed mixed microbial cultures. Water Research, 36(5): p. 1167-1180.

Bormann, E.J., M. Leissner, and B. Beer (1997) Growth and Formation of PoIy(hydroxybutyric acid) by Methylobacterium rhodesianum at Methanol Concentrations of above 25 g/l. Acta Biotechnologica, 17(4): p. 279-289.

Bourque, D., B. Ouellette, G. Andre, and D. Groleau (1992) Production of poly- β-hydroxybutyrate from methanol: Characterization of a new isolate of Methylobacterium extorquens. Applied Microbiology and Biotechnology, 37(1): p. 7-12.

Braunegg, G., Bona, R., and M. Koller (2004) Sustainable Polymer Production. Polymer-Plastics Technology and Engineering, 43(6): p. 1779-1793.

Braunegg, G., Lefebvre G., and K.F. Genser (1998) Polyhydroxyalkanoates, biopolyesters from renewable resources: Physiological and engineering aspects. Journal of Biotechnology, 65(2-3): p. 127-161.

Braunegg, G., B. Sonnleitner, and R.M. Lafferty (1978) A rapid gas chromatographic method for the determination of poly- ß-hydroxybutyric acid in microbial biomass. European Journal of Applied Microbiology and Biotechnology, 6(1): p. 29-37.

Carta, F., Beun, J.J., Loosdrecht, M.C.M.v., and J.J. Heijnen (2001) Simultaneous storage and degradation of phb and glycogen in activated sludge cultures. Water Research, 35(11): p. 2693-2701.

Chua, H., P.H.F. Yu, and C.K. Ma (1999) Accumulation of Biopolymers in Activated Sludge Biomass. Applied Biochemistry and Biotechnology, 77-79(1-3): p. 389-399.

Daniel, M., Choi, J.H., Kim, J.H., and Lebeault J.M. (1992) Effect of nutrient deficiency on accumulation and relative molecular weight of poly- β-hydroxybutyric acid by methylotrophic bacterium, Pseudomonas 135. Applied Microbiology and Biotechnology, 37(6): p. 702-706.

Dionisi, D., M. Majone, V. Papa, and M. Beccari (2004a) Biodegradable Polymers From Organic Acids by Using Activated Sludge Enriched by Aerobic Periodic Feeding. Biotechnology and Bioengineering, 85(6): p. 569-579.

Dionisi, D., Renzi, V., Majone, M., Beccari, M., and R. Ramadori (2004b) Storage of substrate mixtures by activated sludges under dynamic conditions in anoxic or aerobic environments. Water Research, 38(8): p. 2196-2206.

Dircks, K., Henze, M., Loosdrecht, M.C.M.v., Mosbæk, H., and H. Aspegren (2001) Storage and degradation of poly-β-hydroxybutyrate in activated sludge under aerobic conditions. Water Research, 35(9): p. 2277-2285.

Dufresne, R., A. Liard, and M.S. Blum (2001) Anaerobic Treatment of Condensates: Trial at a Kraft Pulp and Paper Mill. Water Environment Research 73(1): p. 103-109.

Khanna, S. and A.K. Srivastava (2005) Recent advances in microbial polyhydroxyalkanoates. Process Biochemistry, 40(2): p. 607-619.

Kim, S.W., P. Kim, Hyun S. Lee, and Jung H. Kim (1996) High Production of Poly- ß-hydroxybutyrate (PHB) from Methylobacterium organophilum under Potassium Limitation. Biotechnology Letters, 18(1): p. 25-30.

Lee, S.Y. (1996) Bacterial Polyhydroxyalkanoates. Biotechnology and Bioengineering, 1996. 49(1): p. 1-14.

Lee, S.Y., J.-i. Choi, and H.H. Wong (1999) Recent advances in polyhydroxyalkanoate production by bacterial fermentation: mini-review. International Journal of Biological Macromolecules, 25(1-3): p. 31-36.

Lenz, R.W. and R.H. Marchessault (2005) Bacterial Polyesters: Biosynthesis, Biodegradable Plastics and Biotechnology. Biomacromolecules, 6(1): p.1-8.

Loosdrecht, M.C.M.v., Pot, M.A., and J.J. Heijnen (1997) Importance of bacterial storage polymers in bioprocesses. Water Science & Technology, 35(1): p. 41-47.

Ma, C.K., H. Chua, P.H.F. Yu, and K. Hong (2000) Optimal Production of Polyhydroxyalkanoates in Activated Sludge Biomass. Applied Biochemistry and Biotechnology, 84(1-9): p. 981-990.

Madison, L.L. and G.W. Huisman (1999) Metabolic Engineering of Poly(3-hydroxyalkanoates): From DNA to Plastic. Microbiology and Molecular Biology Reviews, 63(1): p. 21-53.

Miller, M., M. Justiniano, and S. McQueen (2005) Energy and Environmental Profile of the U.S. Pulp and Paper Industry. U.S. Department of Energy, Office of Energy Efficiency and Renewable Energy, Industrial Technologies Program, Washington, DC.

Mockos, G.R., Loge, F.J., Smith, W.A., and D.N. Thompson. Selective enrichment of a methanol-utilizing consortium using pulp & paper mill waste streams. Applied Biochemistry and Biotechnology, in press (April 2008).

Reis, M.A.M., L.S. Serafim, P.C. Lemos, A.M. Ramos, F.R. Aguiar, and M.C.M. Van Loosdrecht (2003) Production of polyhydroxyalkanoates by mixed microbial cultures. Bioprocess and Biosystems Engineering, 25(6): 377-385.

Salehizadeh, H. and M.C.M.v. Loosdrecht (2004) Production of polyhydroxyalkanoates by mixed culture: recent trends and biotechnological importance. Biotechnology Advances, 22(3): p. 261-279.

Serafim, L.S., P.C. Lemos, R. Oliveira, and M.A.M. Reis (2004) Optimization of Polyhydroxybutyrate Production by Mixed Cultures Submitted to Aerobic Dynamic Feeding Conditions. Biotechnology and Bioengineering, 87(2): p. 145-160.

Springer, A.M. (2000) Industrial Environmental Control Pulp and Paper Industry, 3rd ed., Tappi Press, Atlanta, GA, p. 238-239.

Suzuki, T., T. Yamane, and S. Shimizu (1986a) Mass production of poly-β-hydroxybutyric acid by fully automatic fed-batch culture of methylotroph. Applied Microbiology and Biotechnology, 23(5): p. 322-329.

Suzuki, T., Yamane,T., and S. Shimizu (1986b) Mass production of poly-β-hydroxybutyric acid by fed-batch culture with controlled carbon/nitrogen feeding. Applied Microbiology and Biotechnology, 24: p. 370-374.

Weiss, R.F. (1970) The solubility of nitrogen, oxygen, and argon in water and seawater: Deep Sea Research, 17(4): p. 721-735

Figures

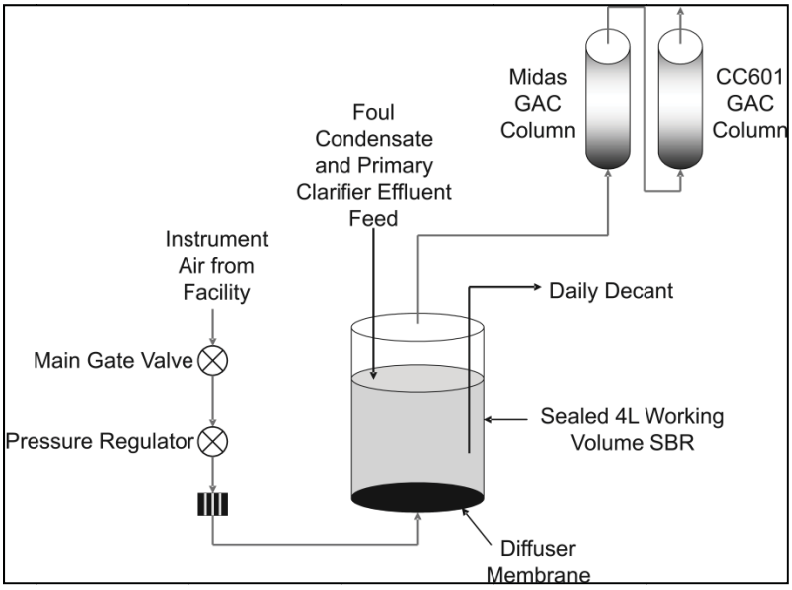

Figure 7. Experimental setup of sequencing batch reactors

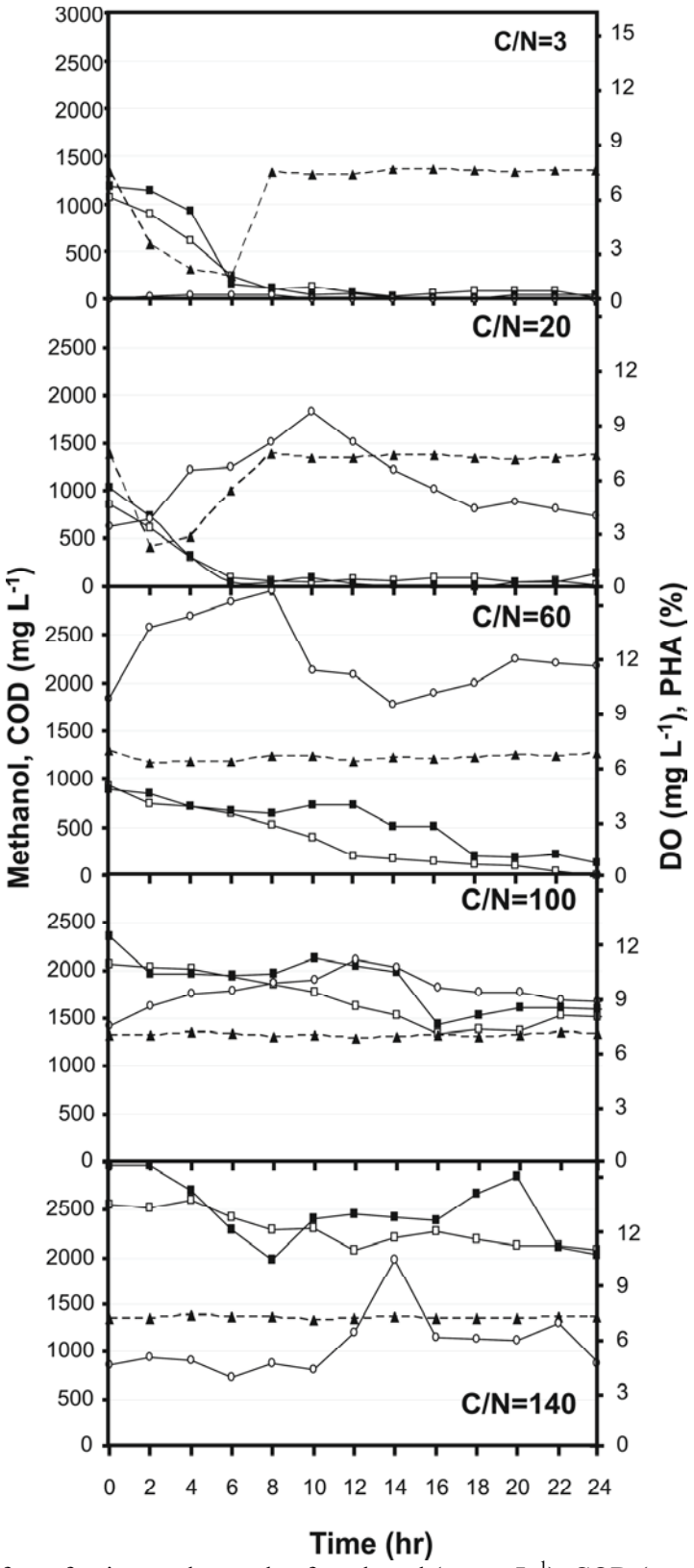

Figure 8. 24-hour feast-famine cycle trends of methanol (■, mg L^{-1}), COD (□, mg L^{-1}), DO (▲, mg L^{-1}), and PHA (○, %) in the methanol-only C:N reactors .

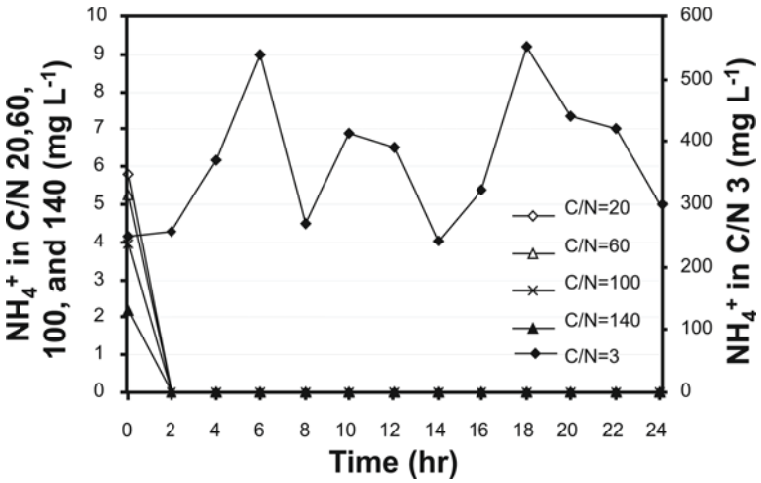

Figure 9. 24-hour feast-famine cycle ammonium concentrations in the C:N of 20, 60, 100, and 140 (primary y axis) and C:N of 3 (secondary y axis) methanol-only reactors

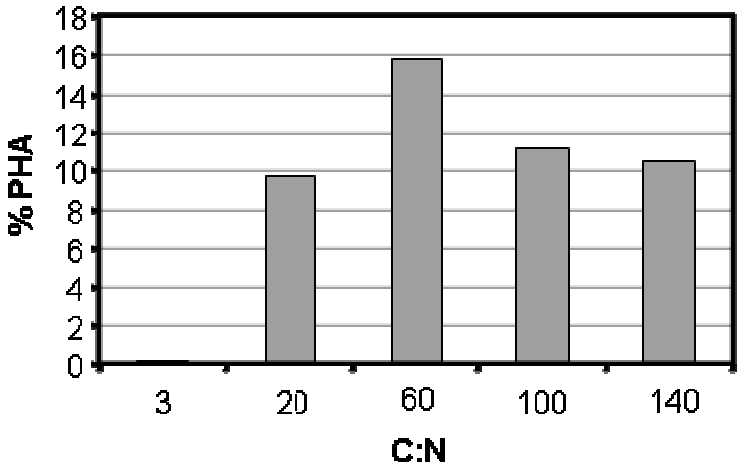

Figure 10. Peak PHA % versus C:N for the methanol-only reactors

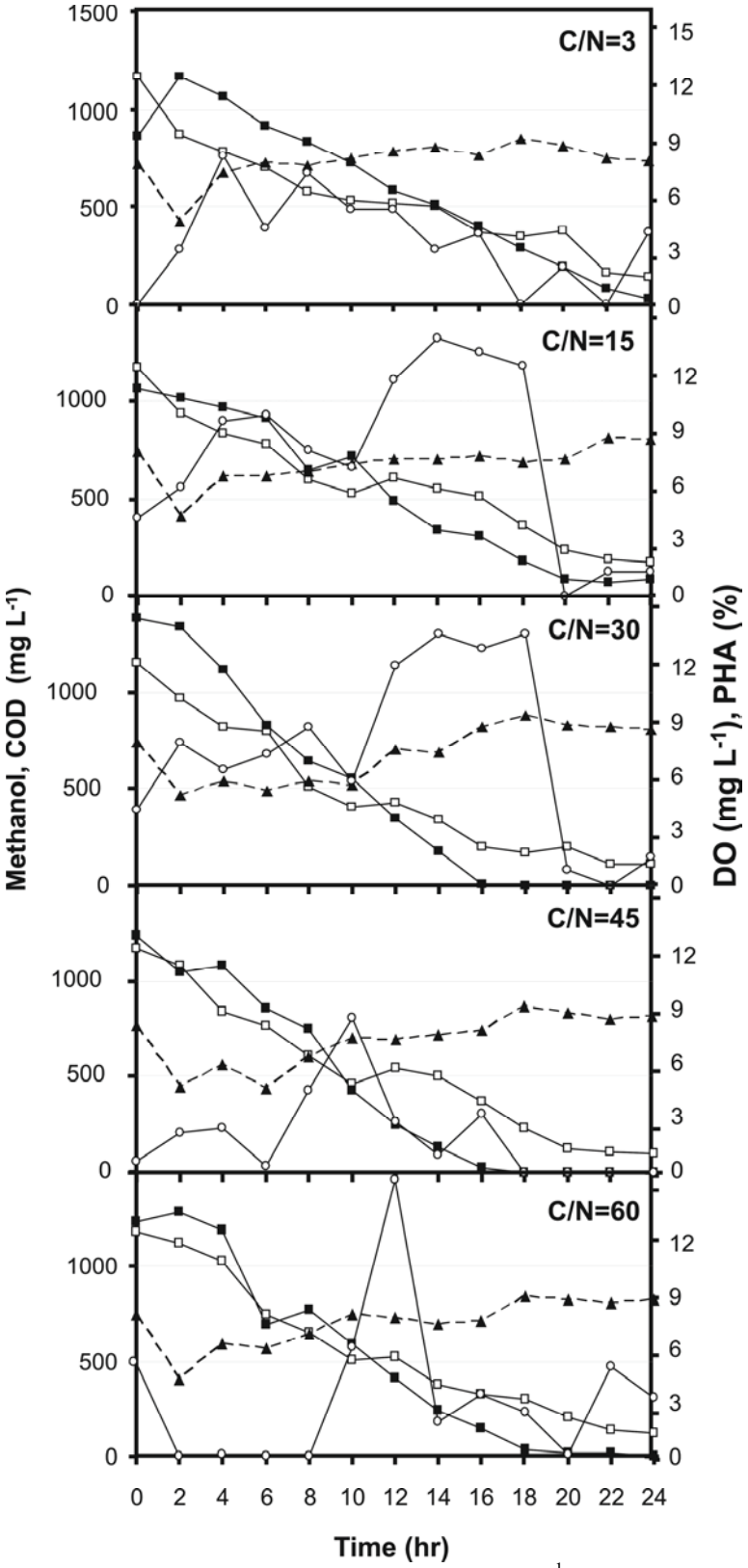

Figure 11. 24-hour feast-famine cycle trends of methanol (■, mg L^{-1}), COD (□, mg L^{-1}), DO (▲, mg L^{-1}), and PHA (○, %) in the diluted foul condensate C:N reactors .

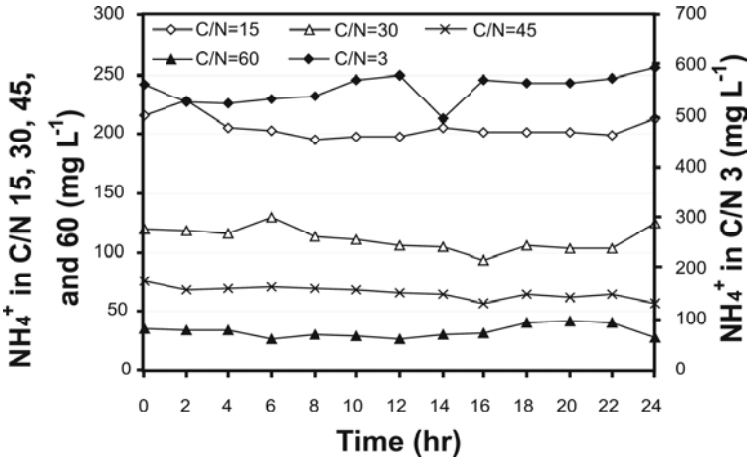

Figure 12. 24-hour feast-famine cycle ammonium concentrations in the C:N of 15, 30, 45, and 60 (primary y axis) and C:N of 3 (secondary y axis) diluted foul condensate reactors

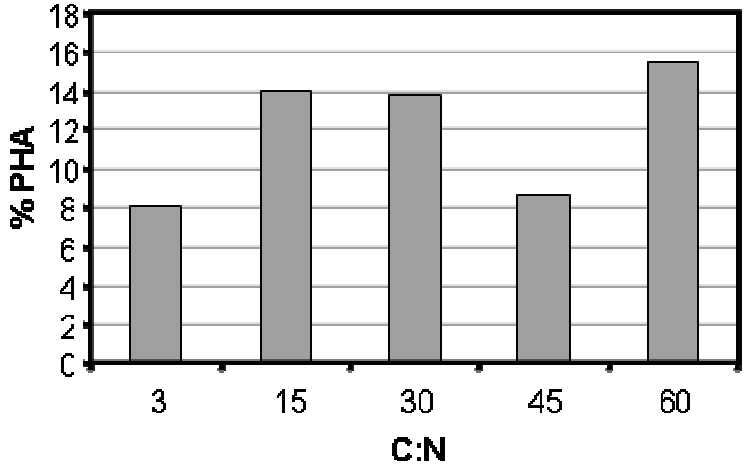

Figure 13. Peak PHA % versus C:N for the diluted foul condensate reactors

Tables

Table 2. Compositions of the foul condensate and primary clarifier effluent as received from the mill.

Component	Foul Condensate	Primary Clarifier Effluent
Total COD (g L^{-1})	61.0 ± 14.3	451 ± 89
Methanol COD (g L^{-1})	37.9 ± 8.2	nd*
Methanol (g L^{-1})	25.2 ± 5.4	nd*
NH_4^+ (mg L^{-1})	1626 ± 319	6.2 ± 1.1

* nd, not detected

Table 3. COD degradation and MLVSS observed prior to starting the feed and decant cycles for the methanol-only reactors.

Reactor ID	%COD Deg.	MLVSS (mg/L)
C/N=3	87	520
C/N=20	89	680
C/N=60	92	560
C/N=100	-86	190
C/N=140	-140	220

Table 4. Comparison of the observed nitrogen, DO, methanol and PHA concentrations within methanol-only reactors.

C/N	Nitrogen limitation	DO drop	Methanol Depletion	Feast-famine conditions	PHA production	PHA carry-over
3	-	+	+	+	-	-
20	+	+	+	+	+	+
60	+	-	+	+/-	+	+
100	+	-	-	-	+	+
140	+	-	-	-	+	+

Table 5. COD degradation and MLVSS observed prior to starting the feed and decant cycles for the diluted foul condensate reactors.

Reactor ID	%COD Deg.	MLVSS (mg/L)
C/N=3	56	500
C/N=15	43	460
C/N=30	56	500
C/N=45	43	540
C/N=60	51	460

Table 6. Distribution of COD in the foul condensate reactors by source.

COD Source	Percentage (%) of total COD in Reactor				
	C/N 3	C/N 15	C/N 30	C/N 45	C/N 60
Non-Methanol[a]					
Foul Condensate	35.5	35.5	25.4	16.4	12.0
Primary Out	5.8	5.8	6.0	6.2	6.3
Methanol[b]	58.7	58.7	68.6	77.4	81.7
Total	100	100	100	100	100

a Includes only non-methanol sources of COD originating from the pulp mill effluents.
b Includes methanol from all sources (foul condensates and exogenous methanol added to adjust the C/N).

Table 7. Comparison of the observed nitrogen, DO, methanol and PHA concentrations within diluted foul condensate reactors.

C/N	Nitrogen limitation	DO drop	Methanol Depletion	Feast-famine conditions	PHA production	PHA carry-over
3	-	+	-	-	+	-
15	-	+	-	-	+	+
30	-	+	+	+	+	+
45	-	+	+	+	+	+
60	-	+	+	+	+	+

Table 8. Relative amount of primary clarifier effluent and foul condensate in the diluted foul condensate reactors.

Feed Source	Percentage (%) of Feed Source in Reactor				
	C/N 3	C/N 15	C/N 30	C/N 45	C/N 60
Primary Out	83	83	87	92	94
Foul Condensate	17	17	13	8	6

Effect of Selected Reactor Conditions on Polyhydroxyalkanoate Production from Pulp Mill Activated Sludge using Foul Condensates

Summary

Biological treatment of foul condensates, methanol-rich kraft pulp mill effluents, offers the opportunity to capture lost carbon and convert it into renewable products such as polyhydroxyalkanoates (PHAs). Polyhydroxyalkanoates are microbially-synthesized intracellular polyesters that serve as carbon and energy storage reservoirs in bacteria. Sixteen laboratory-scale sequencing batch reactors (SBRs) were used with enriched inocula originating from pulp mill activated sludge to produce PHAs from foul condensate. The sixteen SBRs were operated under different environmental conditions by varying solids retention time (SRT, at 4, 8, and 12 days), hydraulic retention time (HRT, at 1, 2, and 4 days), and food to microorganism ratio (F:M, at 1, 3, and 5). Within the range of conditions tested, peak PHA % (40%) and PHA concentration (0.11 g L^{-1}) were achieved in an SBR operated at SRT=12 days, HRT=2 days, and F:M=3. PHA %, PHA concentration, and carbon degradation were predominantly influenced by the F:M ratio. The interaction between SRT and HRT affected total biomass concentrations and the interaction of SRT and F:M affected ammonium consumption**.** Since the SRT, HRT, and F:M are closely tied parameters, the central composite design was used as a tool to model the effects on PHA production, carbon and nitrogen source degradation, and biomass concentrations.

Introduction

For the forest products sector to remain profitable and sustainable, it must continuously strive to increase the diversity of its products while decreasing its energy use and environmental impact (Miller 2005). Presently, there are effluent waste streams within the kraft mill condensate system of pulp and paper mills that offer the opportunity to reduce emissions while creating an added value product. One such effluent stream is "foul condensate," a malodorous condensed high carbon strength waste stream recovered from kraft pulping (Dufresne 2001). Foul condensates contain varying concentrations of methanol (Springer 2000) and are commonly recycled within the pulp mill or incinerated. Incineration results in the emissions of volatile organic compounds (VOCs), SO_x, NO_x, and particulates (Smook 1992). However, by using foul condensates as a carbon source for biological synthesis of polyhydroxyalkanoates (PHAs), pulp mills could reduce emissions while producing a renewable and saleable product.

Polyhydroxyalkanoates are polymers of various hydroxyalkanoic acids, which are synthesized by a wide range of bacteria as an energy and carbon reserve material (Braunegg 1998; Lenz 2005). PHAs possess physical properties similar to conventional petroleum-based thermoplastics with the added benefit of being entirely biodegradable (Lee 1996). Bacteria produce such polymers when subjected to unbalanced growth conditions caused by a macronutrient limitation in the presence of excess carbon; electron donor/acceptor variability (e.g., aerobic/anaerobic cycling); or a feast-famine regime (transient carbon availability) (Salehizadeh 2004). Whereas these three environmental conditions will generally induce PHA storage in a given biological system, PHA production can be further controlled by modifying three environmental parameters: hydraulic residence time (HRT), solids retention time (SRT), and food to microorganism ratio (F:M) (Dionisi 2004a; Buen 2002; Dionisi 2006).

The HRT represents the average period of time the liquid fraction of a sequencing batch reactor (SBR) remains in the system, which governs the dilution rate and the extent of the feast-famine regime. When HRT is increased, the net carbon mass flux into the system is decreased resulting in conditions where the consortium lacks substrate for a more extended period of time (Yu 2001). As a result of the increased severity of the feast-famine regime, microbial PHA storage increases to the detriment of cell growth (Braunegg 1998). Conversely, when the HRT is decreased, a larger quantity of substrate enters the system over time resulting in the lack of a famine period because the consortium is incapable of entirely

degrading the substrate in the allotted amount of time (Yu 2001). Therefore, biological PHA storage is favored at longer HRTs (Beun 2000).

The food to microorganism ratio (F:M ratio) is the ratio of substrate to biomass concentration. The F:M ratio, in conjunction with the HRT, governs the relative lengths of the feast and famine phases within a SBR feed cycle. Low F:M ratios result in a short feast period followed by a long famine period. Increasing F:M ratios increases the feast period with respect to the famine period over the course of a feed cycle. PHA storage increases as F:M is increased until reaching a threshold value at which the conditions in the system favor growth rather than PHA storage (Dionisi 2006; Dionisi 2004a). The switch from a PHA storage to a microbial growth response occurs at relatively high F:M ratios because the microorganisms are incapable of degrading the entire carbon source within the time constraints of the feed cycle. Hence, a famine period never occurs resulting in a consortium which is not induced to accumulate PHA (Dionisi 2005).

The SRT is the average period of time solids (including biomass) remain in a biological reactor (Tchobanoglous 2003). The SRT influences the average biomass growth rate (Beun 2000), and in turn, the biomass concentration in a SBR. In addition, SRT has been documented to affect PHA storage within a biological reactor by selecting organisms capable of accumulating large quantities of PHA at longer SRTs (Barr 1996; Chua 2003; Leeuwen 1997).

Based on the literature reviewed above, the majority of work associated with PHA production has focused separately on either SRT, HRT, or F:M and their independent effects on PHA storage. In addition, none of the existing research in the literature has addressed the influence of SRT, HRT, and F:M on PHA production from carbon in kraft mill foul condensates. Since SRT, HRT, and F:M are closely tied with respect to their effect on PHA storage and biomass growth, our research group believed it was necessary to simultaneously evaluate their effect on PHA storage and biomass growth over a range of values that had practical operational relevance in wastewater treatment systems designed to treat foul condensates in pulp and paper mill wastewater. Therefore, the goal of this study was to simultaneously calculate the effects of F:M, HRT, and SRT, within a wastewater treatment system fed foul condensate, on three response variables: PHA % ((g PHA/g total organic matter)x100), PHA concentration (g PHA/reactor volume), and total biomass (g). To better understand the results obtained for these three response variables, SRT, HRT, and F:M were also evaluated for their effect on ammonium, chemical oxygen demand (COD), and methanol consumption. The influence of F:M, SRT, and HRT on PHA and biomass production was evaluated using a microbial consortium, originating from the P.H. Glatfelter (Chillicothe, OH) pulp mill activated sludge basin, which had been enriched using foul condensate diluted with primary clarifier effluent from the same wastewater facility. A face-centered central composite experimental design using 16 independently run SBRs was performed to simultaneously evaluate the effects of F:M, HRT, and SRT at three levels. F:M ratios of 1, 3, and 5 were tested with HRTs of 1, 2, and 4 days and SRTs of 4, 8, and 12 days. The information from this study will be used for the design of a pilot-scale PHA production facility at the P.H. Glatfelter pulp mill.

Materials and Methods

Laboratory-Scale Sequencing Batch Reactor Construction

Sixteen laboratory-scale SBRs were constructed from an 8 inch tall by 8 inch diameter clear acrylic cylinder with ½ inch wall thickness. The acrylic cylinder was mounted on an 8 inch diameter Sanitaire® Silver Series II fine bubble disc diffuser membrane (ITT Industries, Brown Deer, WI). Each reactor had a working volume of four liters, which was oxygenated and mixed by air, supplied at 1,500 mL min^{-1} (0.375 vvm). The reactor effluent gases were circulated through two granular activated carbon columns (CC601 and Midas OCM; USFilter, Los Angeles, CA) to remove the primary contaminants of concern: methanol, hydrogen sulfide and methyl mercaptan (present in the foul condensates). The experimental setup is illustrated in Figure 14.

Source of Microorganisms

The microbial consortium used to inoculate the SBRs was obtained from a previous study which assessed the effect of carbon to nitrogen (C:N) ratio on PHA storage in four liter SBRs fed a mixture of foul condensate diluted with primary clarifier effluent (Mockos 2008b). The C:N experimental SBRs were operated aerobically with an HRT and SRT of 4 days and a dilution ratio of 0.25 (a quarter of the reactor volume was replaced daily with 1 L of new feed). The daily decant from the C:N experimental SBR operated at a C:N of 30 was then stored at -80°C in 40% (v/v) glycerol (Fisher Scientific, Fair Lawn, NJ) for use in this study as inoculum. When enough inoculum had been stored, the frozen stocks were thawed, mixed, rinsed and re-suspended in phosphate-buffered saline at neutral pH containing 10mM phosphate and 150mM sodium chloride (Fisher Scientific, Fair Lawn, NJ).

Reactor Operation

The sixteen SBRs were inoculated by re-suspending 2 L of the thawed frozen stocks into 2 L of the desired feed. The reactors were operated at a 0.5 dilution ratio (half of the reactor volume was replaced with 2 L of new feed every feed cycle). The SBRs were fed a mixture of two waste streams from the P.H. Glatfelter pulp and paper mill facility (Chillicothe, OH). The first waste stream, foul condensate, was obtained from the kraft chemical recovery process. The second waste stream was obtained from the effluent of the primary clarifier in the facility's wastewater treatment system. The foul condensate had an average COD concentration of 61.0 ± 14.3 g L^{-1} and contained an average 1626 ± 319 mg L^{-1} of ammonium nitrogen. The primary clarifier effluent had an average COD and ammonium concentration of 451 ± 108.4 mg L^{-1} and 6.74 ± 5.02 mg L^{-1}, respectively. Both waste streams are described in detail in Mockos et al. (2008a). The feed mixture was prepared by diluting foul condensate with the primary clarifier effluent to attain F:M ratios of 1, 3, and 5 at a fixed C:N of 30. The dilution ratio of foul condensate to primary clarifier effluent was calculated based on their respective COD and ammonium concentrations. When the COD concentration of the foul condensate and primary clarifier effluent mixture was insufficient to support the higher F:M ratios of 3 and 5, the feed mixture was amended with pure methanol (99.99% methanol, Fisher Scientific, Fair Lawn, NJ).

Volatile compounds, including the feedstock methanol, were stripped from the medium to some degree because the reactors were aerated. The amount of methanol stripped (26 %) was estimated as previously described (Mockos 2008) and the feed concentrations were adjusted by adding reagent grade methanol (99.9%; Fisher Scientific, Fair Lawn, NJ) at the time of each feeding to account for this loss. The amount of methanol added to the feed mixture to account for loss due to stripping was included in the overall COD concentration when calculating the different C/N ratios.

The F:M ratio was calculated by dividing the total soluble COD concentration by the mixed liquor volatile suspended solids (MLVSS) concentration in each reactor. Each SBR had a starting MLVSS of 500 mg L^{-1}. The total amount of soluble COD to be added was calculated based on the different F:M ratios. Hence, the feed mixtures for the F:M of 1, 3, and 5 reactors were prepared with initial total COD concentrations of 500, 1500, and 2500 mg L^{-1} respectively. After a one SRT period, the reactor feed mixtures were adjusted to compensate for the change in MLVSS that had occurred over time. Thereafter, the SBRs were allowed to stabilize. Reactor stability was arbitrarily defined as the point at which the MLVSS concentrations and COD degradation values were within ±10% for three consecutive SRTs. F:M ratios were kept within ±10% of the experimental design values (0.9-1.1 for an F:M of 1; 2.7-3.3 for an F:M of 3; and 4.5-5.5 for an F:M of 5) for the final three SRTs of operation.

Sampling and Analyses

Reactor performance over the four SRT acclimation periods was monitored by sampling at the beginning and end of the last 24-hour feed cycle of each SRT. The samples were analyzed for MLVSS, mixed liquor suspended solids (MLSS), and COD. MLVSS and MLSS were measured according to ASTM Standard Method 2540 A-G (APHA 2005) using Millipore TCLP AP40 glass fiber filters. MLSS was used to track the amount of total suspended solids present in the reactors, while MLVSS was used as a surrogate measure of the fraction of suspended solids that was biomass. COD was measured according

to ASTM Standard Method 5220 AD (APHA 20051992) using Hach high–range ampoules with a Hach DRB 200 digestion block and Hach DR 2010 portable data logging spectrophotometer (Hach Company, Loveland, CO) set at a 620 nm wavelength. COD measurements were used as a direct indication of total COD degradation, as well as a surrogate measure of methanol consumption in the reactors over time.

When the reactors had been acclimatized by the conclusion of their respective fourth SRT, samples were taken every 2 hours over a 24-hour period immediately following the addition of the daily feed. Prior to the addition of the daily feed, a single 48 mL aliquot was withdrawn from each reactor for measurement of the total biomass. The 48 mL aliquot was mixed with 2 mL of commercial grade bleach (5% NaClO) (Clorox, Oakland, CA) and centrifuged at 4300 × *g* for 15 minutes. The pellets were dried at 60°C for 24 hours, weighed to determine the total suspended solids, then ashed at 550°C and reweighed to differentiate between the non-volatile and volatile fractions. The organic fraction, which includes cellular biomass and short cellulose fibers present in the primary clarifier effluent, was calculated as the difference between the non-ashed and ashed weights. The organic fraction was used to calculate total biomass (g) by multiplying the total suspended solids concentration in a reactor by the organic fraction and the total reactor volume (four liters).

The samples from the 24-hour sampling of the reactors were analyzed for pH, temperature, dissolved oxygen (DO), COD, methanol, ammonium, and PHA. The samples were filtered through a Millex GP 0.22 μm Express PES Membrane filter unit (Millipore Corporation, Billerica, MA) prior to COD and methanol analyses. Temperature, pH, and DO were measured directly in the reactors. Dissolved oxygen and temperature were measured using an Orion® 1230 DO Meter with an Orion® 083010 DO Probe (Orion Research, Beverly, MA), while pH was measured using an Accumet® AP61 Portable pH Meter with an Accumet® Gel-Filled Pencil-Thin pH electrode (Fisher Scientific, Fair Lawn, NJ).

Methanol was analyzed by high performance liquid chromatography (HPLC) using a Hitachi HPLC D-6000 Series HPLC system (Tokyo, Japan) consisting of a Hewlett Packard 1047A RI Detector (Agilent Technologies, Palo Alto, CA), a Hitachi L6200A Gradient Pump, and a Hitachi AS-4000 autosampler. The mobile phase consisted of 0.01% H_2SO_4 at 0.6 ml min^{-1}. Twenty microliter samples were prepared at 1:1 dilution and injected into a Bio Rad Aminex HPX-87H (300mm x 7.8mm ID) column (Hercules, CA) with a Bio Rad Micro-Guard cartridge (Cat. No. 125-0131). Methanol standards were prepared at 0.01 – 0.1% by volume using 99.99% methanol. Samples were run at 60°C, with the detector set at 50°C. The method detection limit (MDL) for the methanol analysis was 100 mg L^{-1}.

Ammonium, the only source of nitrogen tracked in this work, was measured by ion chromatography using a Dionex ED40 conductivity detector with a GP50 gradient pump, an AS50 autosampler, an AD20 absorbance detector, and an EG40 eluent generator (Dionex Corporation, Sunnyvale, CA). Samples were analyzed using 5 μL injections at a flow rate of 1 mL min^{-1}. Analytes were separated using a Dionex IonPac CS12A (250mm x 4mm ID) with a Dionex ECG-MSA eluent generator cartridge. Data were collected and analyzed using Peaknet v. 5.21 (Dionex Corporation, Sunnyvale, CA). Ammonium standards were prepared using the Dionex 6 Cation Standard II #46070. A seven-level cation standardization was performed (DI water, 5 standards, and the non-dilute Cation Standard II solution). The MDL for the ammonium analysis was 0.5 mg L^{-1} NH_4^+.

Analysis of PHAs was conducted following the procedure described by Braunegg et al. (1978) with the following modifications. Unfiltered 48 mL biomass samples were mixed with 2 mL of commercial grade bleach (5% NaClO) (Clorox, Oakland, CA) and centrifuged at 4300 ×*g* for 15 minutes to harvest the solids. The pellet was then dried at 60°C for 24 hours. Between 10-50 mg of the dried reactor solids were suspended in a mixture of 2 mL acidified methanol (3% H_2SO_4, v/v) and 2 mL chloroform. The mixture contained 0.25 mg mL^{-1} benzoic acid as an internal standard to estimate digestion and recovery efficiency. The mixture was then digested at 100°C for 4 hours in a Hach DRB 200 digestion block (Hach Company, Loveland, CO). Once the digestion was completed, 1 mL of deionized water was added and the mixture was vortexed for 30 seconds. The organic phase was removed, using a Pasteur pipette after phase separation, and was filtered through a Pasteur pipette packed with a cotton plug and 1 g of sodium sulfate (Fisher Scientific, Fair Lawn, NJ) to remove any remaining

water. The organic phase, that contained the esterified monomers from the depolymerized PHA molecules, was then analyzed by gas chromatography using a Hewlett Packard 5890 Series II GC System with a Flame Ionization Detector (Agilent Technologies, Palo Alto, CA). Samples were run at 40°C for 2 minutes at 1 ml min^{-1} with 1 µL injections using a Rtx-1 column (30m x 0.25µm x 0.25 stationary film thickness) (Restek, Bellefonte, PA). Injector temperature was 225°C and detector temperature was 250°C. Data were analyzed using GC Chemstation 1990-2000 Rev.A.08.01 software (Agilent Technologies, Palo Alto, CA). PHA % was quantified against standards of PHB and PHV (Poly(3-hydroxybutyric acid-co-3-hydroxyvaleric acid) standard) (Sigma-Aldrich, St. Louis, MO) as derivatized methyl esters and extraction efficiency was calculated based on the benzoic acid internal standard. PHA % values were then multiplied by the total suspended solids and divided by the organic fraction of the initial total suspended solids measured for each reactor to compensate for the inorganic portion of the harvested pellet. Whereas the PHA % response variable values used in this study were obtained directly from the GC analysis, the PHA concentration response variable values were calculated by multiplying the PHA % values by the total biomass (g) and then dividing by the reactor volume (4L).

Face-Centered Cube Central Composite Design

A regression model was used to evaluate the effects of the three parameters (HRT, SRT, and F:M) on PHA %, PHA concentration (g L^{-1}), total biomass (g), ammonium consumption (%), COD degradation (%), and methanol degradations (%). The three parameters were evaluated at three levels in a face-centered cube design which is a fractional factorial of the full 3^3 factorial requiring 27 experimental runs (Montgomery 2001; Hinkelmann 1994, 2005). The face-centered cube design matrix included 15 independent experimental runs with the design center-point being replicated to estimate the variance in the response surface. Center-point replication avoided the impractical necessity of repeating the entire design (Wu 2000). Certain information is lost due to parameter confounding in a face-centered cube design. However, the face-centered cube design does not confound main effects with each other and does not confound first order two-factor interactions with other two-factor interactions or main effects (Berthouex 2002). Since the face-centered cube design is a second order model by definition, it allows a quadratic model to be determined for each response variable (Mason 2003). The effects of HRT, SRT, and F:M and their interactions were modeled using the SAS (SAS 2004) and STATISTICA (StatSoft 2007) software packages. The resulting outputs were the coefficient estimate, t-value, and p-values for each factor and interaction. Overall significance of the models was based on an F-test. The smaller the p-value associated with the p-test, the more influence a factor had on the response. The interpretation of the p-values provided a comparison of the effect of HRT, SRT, F:M and their respective interactions on the response variables.

The quantitative statistical analyses were performed using the RSREG and REG procedures in SAS Version 9.1.3 (SAS 2004). The statistical analyses of the results began with the RSREG SAS procedure which used the linear and quadratic terms of all three parameter (F:M, HRT, SRT) and their first-order interactions in the regression model. This was done separately for each of the response variables. Then the SAS procedure REG was used to model the linear and quadratic relationships. The resulting models were the quadratic model for each response variable in terms of HRT, SRT, and F:M. Such models allowed predicted values to be computed for each response variable. The predicted values were then compared to the measured values obtained from experimental data. Thereafter, a regression analysis was performed for each response variable's predicted and measured values to determine the validity of the quadratic relationships describing the response variables. The statistical relevance of each response variable model was determined based on the R^2 value.

Results

At the conclusion of a three SRT acclimation period, the SBRs were sampled every 2 hours over a 24-hour period immediately following the addition of feed at the start of the fourth SRT. The samples collected over 24 hours were analyzed to assess trends of the following parameters: DO, COD, methanol, ammonium, and PHA (summarized in Table 9).

Dissolved oxygen concentrations dipped below saturation levels in all reactors upon addition of the carbon-rich feed mixture. DO concentrations gradually rebound to saturation or near-saturation concentrations by the end of the feed cycle regardless of whether the carbon source had been entirely consumed (data not shown). The DO dipped by an average of 24% in the reactors operated at an F:M of 1, by an average of 41% in the reactors operated at an F:M of 3, and by an average of 36% in the reactors operated at an F:M of 5. The reactor with the smallest drop in DO concentration (7%) was reactor #3 (F:M of 1, HRT of 4 days, and SRT of 4 days) (Table 9). In turn, the reactor with the largest drop in DO concentrations (47%) was reactor #13 (F:M of 3, HRT of 2 days, and SRT of 4 days).

Methanol degradation occurred in each SBR with methanol consumption ranging from 12 to 100% (Table 9). Methanol was entirely consumed by the end of the 24-hour sampling period in reactors #3, 7, and 9. The average methanol degradation was 89% in the reactors operated at an F:M of 1, 67% in the reactors operated at an F:M of 3, and 32% in the reactors operated at an F:M of 5 (Table 9). Methanol degradation improved as the F:M decreased. The trend in methanol concentration over the 24-hour sampling period varied according to the F:M ratio. Methanol concentrations in the reactors operated at an F:M of 1 rapidly declined within 4-6 hours to or near the MDL for methanol analysis (100 mg L^{-1}). In turn, the methanol concentrations in the reactors operated at an F:M ratios of 3 and 5 declined in an approximately linear fashion throughout the course of the 24-hour sampling period. The rate at which methanol was degraded in the F:M of 3 and F:M of 5 reactors was similar with the sole difference being the initial methanol concentration at the beginning of the feed cycle (data not shown).

COD degradation occurred in each SBR with COD degradation ranging from 26 to 87% (Table 9). The average COD degradation was 65% in the reactors operated at an F:M of 1, 63% in the reactors operated at an F:M of 3, and 38% in the reactors operated at an F:M of 5 (Table 9).The primary carbon source that contributed to the COD concentration in the reactors was methanol (Mockos 2008a), hence the profile of COD concentration over the course of the 24-hour sampling period resembled the aforementioned trends seen for methanol. However, the difference between the methanol and COD data was the presence of recalcitrant COD in the foul condensate (Dufresne 2001) at the end of the 24-hour feed cycle in each reactor (Table 9).

Ammonium consumption in the 16 SBRs ranged from 5% to 100% by the end of the 24-hour sampling period. The average ammonium degradation was 37% in the reactors operated at an F:M of 1, 26% in the reactors operated at an F:M of 3, and 13% in the reactors operated at an F:M of 5 (Table 9).Ammonium was entirely consumed prior to the end of the 24-hour sampling period only in reactor #7 (F:M of 1, HRT of 4 days, and SRT of 12 days), making this reactor the only nitrogen-deficient reactor in this study. The remainder of the reactors had ammonium degradation ranging from between 5 and 53% with ammonium consumption decreasing as F:M increased and ammonium consumption increasing as both HRT and SRT were increased.

A regression analysis was used to evaluate the effects of the three parameters (HRT, SRT, and F:M) on PHA %, PHA concentration (g L^{-1}), total biomass (g), ammonium consumption (%), COD degradation (%), and methanol degradation (%). The three parameters were evaluated at three levels in a face-centered cube design which included 15 independent experimental runs with the design center-point (reactors 15 and 16) being replicated. Center-point replication provided the ability to calculate the pure error associated with each response while avoiding the impractical necessity of repeating the entire design. The pure error, calculated based on the standard deviation of the replicated design center point, was ±7.3% for PHA %, ±0.008 g L^{-1} for PHA concentration, and ±0.14 g for total biomass. The progression through the analyses with regression results is presented below.

Effect of SRT, HRT, and F:M on PHA %

The maximum percentage of total dry organic matter that was PHA in the reactors was achieved at an F:M of 3, an SRT of 12 days, and an HRT of 2 days (Table 9). The quantitative statistical analyses performed using the RSREG and REG procedures in SAS Version 9.1.3 (SAS 2004) on the measured

PHA % values generated the coefficient estimates, t-values, and p-values in Table 10A and produced Equation 1:

$$\text{PHA (\%)} = 6.389 + 17.39\bullet(\text{F:M}) + 10.92\bullet(\text{HRT}) - 6.266\bullet(\text{SRT}) - 2.557\bullet(\text{F:M})^2 + 0.3253\bullet(\text{HRT x F:M}) - 3.352\bullet(\text{HRT})^2 + 0.04174\bullet(\text{SRT x F:M}) + 0.3720\bullet(\text{SRT x HRT}) + 0.3441\bullet(\text{SRT})^2 \quad (1)$$

Equation 1 is the statistical model describing the influence of HRT, SRT, and F:M on PHA %. Equation 1 was used to estimate predicted PHA % values based on the range of values used for SRT, HRT, and F:M. A regression model was then applied to the measured PHA % values and the predicted PHA % values. The resulting regression had an R^2 value of 0.7224 (Figure 15). Equation 1 is a system-specific model intended as a tool to predict the PHA % that can be produced in an SBR inoculated with consortia enriched from pulp mill activated sludge, fed a mixture of pulp mill foul condensate and primary clarifier effluent, and operated within the range of HRT, SRT, and F:M parameters used in this study. The p-values obtained as part of the statistical analysis provide an indication of the statistical relevance of each factor in the central composite design. The lowest p-values achieved in the PHA% model were the F:M and the F:M quadratic terms indicating that PHA% was mostly influenced by the F:M ratio, however the effect was not linear.

Effect of SRT, HRT, and F:M on Total Biomass

The highest total biomass concentrations in the reactors were achieved at an F:M of 1, an SRT of 12 days, and an HRT of 1 day (Table 9). Analyses of the measured total biomass values generated the coefficient estimates, t-values, and p-values in Table 10B and produced Equation 2:

$$\text{Total biomass (g)} = -0.4630 - 0.2143\bullet(\text{F:M}) - 1.121\bullet(\text{HRT}) + 0.6703\bullet(\text{SRT}) + 0.01790\bullet(\text{F:M})^2 + 0.1481\bullet(\text{HRT x F:M}) + 0.2922\bullet(\text{HRT})^2 - 0.03213\bullet(\text{SRT x F:M}) - 0.1173\bullet(\text{SRT x HRT}) - 0.009280\bullet(\text{SRT})^2 \quad (2)$$

Equation 2 is the statistical model describing the influence of HRT, SRT, and F:M on total biomass and was used to estimate predicted total biomass based on the range of SRT, HRT, and F:M. The regression model was then applied to the measured and predicted total biomass values. The resulting regression had an R^2 value of 0.7180 (See Figure 16). The lowest p-values obtained as part of the regression analysis for total biomass were associated with the HRT and SRT interaction factor. Thus, HRT and SRT had a combined effect on the total biomass in the reactors. This was evident as total biomass increased as HRT increased at both low and intermediate SRTs. In turn, this trend reversed at high SRT, with a decrease in biomass with increased HRT (Table 9).

Effect of SRT, HRT, and F:M on PHA Concentration

The maximum PHA concentration in the reactors was achieved at an F:M of 3, an SRT of 12 days, and an HRT of 2 days (Table 9). Analyses of the PHA concentrations generated the coefficient estimates, t-values, and p-values in Table 10C and produced Equation 3:

$$\text{PHA concentration (g L}^{-1}) = -0.03154 + 0.04493\bullet(\text{F:M}) + 0.000001000\bullet(\text{HRT}) - 0.002091\bullet(\text{SRT}) - 0.007219\bullet(\text{F:M})^2 + 0.003290\bullet(\text{HRT x F:M}) + 0.001018\bullet(\text{HRT})^2 - 0.0001410\bullet(\text{SRT x F:M}) - 0.002345\bullet(\text{HRT x SRT}) + 0.0008430\bullet(\text{SRT})^2 \quad (3)$$

Equation 3 is the model describing the influence of HRT, SRT, and F:M on PHA concentration and was used to estimate the predicted PHA concentration based on the range of SRT, HRT, and F:M. A regression model was then applied to the measured and predicted PHA concentrations. The resulting regression had an R^2 value of 0.7791 (See Figure 17). The lowest p-values obtained as part of the

regression analysis for PHA concentration were associated with F:M and F:M quadratic terms. Hence, F:M was deemed to have had the most impact on PHA concentration.

Effect of SRT, HRT, and F:M on Ammonium, COD, and Methanol Degradation

Ammonium Degradation

Ammonium degradation in the reactors peaked as F:M was at its lowest level and as SRT was at its highest. The lowest ammonium degradation occurred at the other end of the spectrum, where F:M was at its highest level and SRT was at its lowest. The full model results indicated that ammonium degradation was strongly influenced by the interaction of SRT and F:M, which had a p-value of 0.07 (Table 10D). Analyses generated the coefficient estimates, t-values, and p-values in Table 10D and produced Equation 4:

$$\text{Ammonium Degradation (\%)} = 0.9796 + 14.70\bullet(\text{F:M}) - 12.33\bullet(\text{HRT}) + 0.1873\bullet(\text{SRT}) - 1.046\bullet(\text{F:M})^2 - 1.203\bullet(\text{HRT x F:M}) + 2.276\bullet(\text{HRT})^2 - 1.613\bullet(\text{SRT x F:M}) + 1.254\bullet(\text{HRT x SRT}) + 0.3306\bullet(\text{SRT})^2 \quad (4)$$

Equation 4 is the statistical model describing the influence of HRT, SRT, and F:M on ammonium degradation and was used to estimate predicted ammonium degradation in the reactors based on the range of values used for SRT, HRT, and F:M. The regression model was then applied to the measured and predicted ammonium degradation percentages. The resulting regression had an R^2 value of 0.8047 (See Figure 18).

COD and Methanol Degradation

The best COD and methanol degradation occurred in the intermediate F:M range. The least amount of COD and methanol degradation occurred when F:M reached its highest level in the intermediate HRT range (Table 9). Analyses of COD and methanol degradation generated the coefficient estimates, t-values, and p-values in Table 10E and F and produced Equations 5 and 6:

$$\text{COD Degradation (\%)} = 83.44 + 10.07\bullet(\text{F:M}) - 30.53\bullet(\text{HRT}) + 4.018\bullet(\text{SRT}) - 4.256\bullet(\text{F:M})^2 + 3.046\bullet(\text{HRT x F:M}) + 6.775\bullet(\text{HRT})^2 + 0.1686\bullet(\text{SRT x F:M}) - 1.297\bullet(\text{HRT x SRT}) - 0.2395\bullet(\text{SRT})^2 \quad (5)$$

$$\text{Methanol Degradation (\%)} = 49.49 + 13.19\bullet(\text{F:M}) - 32.84\bullet(\text{HRT}) + 14.85\bullet(\text{SRT}) - 4.497\bullet(\text{F:M})^2 + 0.3645\bullet(\text{HRT x F:M}) + 9.331\bullet(\text{HRT})^2 - 0.1802\bullet(\text{SRT x F:M}) - 0.9739\bullet(\text{HRT x SRT}) - 0.7863\bullet(\text{SRT})^2 \quad (6)$$

Equations 5 and 6 are the statistical models describing the influence of HRT, SRT, and F:M on COD and methanol degradation, respectively and were used to estimate predicted COD and methanol degradation based on the tested ranges of SRT, HRT, and F:M. The regression models were then applied to the measured versus predicted values, with the resulting regressions having R^2 values of 0.7734 and 0.8428, respectively (See Figure 19 and Figure 20).

Discussion

The ultimate goals of this research were to identify which factors or interaction of factors had the most significant impact on the various response variables tested. Additionally, the statistical analyses were to be used as tools to empirically model the relationship between SRT, HRT, and F:M with the different response variables chosen. Previous work involving PHA production within waste streams has evaluated the influence of single factors affecting microbial PHA storage (Anderson 1990; Madison 1999). PHA production research has primarily focused on: (i) inducing a micro- or macro-nutrient limitation (Hong 2000; Daniel 1992; Kim 1996; Wang 2007; Suzuki 1986); (ii) inducing a feast-famine state (Frigon 2006; Salehizadeh 2004; Reis 2003); (iii) oxic/anoxic cycling (Serafim 2004; Dionisi

2004a); (iv) varying F:M (Dionisi 2004b, 2005, 2006); and (v) modifying SRT (Chua 2003). Such factors have been considered independently. To achieve the successful integration of PHA production and pulp mill wastewater treatment, biological reactor operation will need to be optimized by simultaneously varying SRT, HRT, and F:M (Coats 2007). In the study reported here, we simultaneously investigated the effects of SRT, HRT, and F:M on PHA production and biomass concentrations in sixteen reactors. Furthermore, the impacts of SRT, HRT, and F:M on carbon and nitrogen source degradation was investigated to gain insight into the metabolic state of the consortia in the reactors. The values of SRT, HRT, and F:M were selected to represent a range of values that, in our view, had practical operational relevance in wastewater treatment systems. This approach provided information necessary to evaluate interactions between factors that otherwise would have been lost if the factors affecting PHA storage and biomass concentrations had been evaluated independently.

PHA %

The F:M ratio had the largest effect on PHA % with SRT and HRT not being statistically significant within the range of parameter values tested , as evident by the p-values summarized in Table 10. PHA % increased as F:M increased from 1 to 3. Below an F:M of 3, PHA storage increased as F:M increased from 1 to 3, likely a result of more substrate entering the system. Above an F:M of 3 (Table 9). Beyond an F:M of 3, however, PHA storage declined as F:M was increased to 5, likely a result of a lack of famine conditions resulting from carbon carryover from feed cycle to feed cycle (Dionisi 2006; Dionisi 2004a).

Hydraulic retention time did not have a statistically significant impact on PHA % as p-values associated with HRT were above 0.10 in the full model (Table 10). HRT governs the amount of substrate entering the system (Yu et al. 2001) and ultimately the duration of feast and famine periods. When HRT is prolonged, the amount of substrate entering the system decreases resulting in feed cycles dominated by a longer famine period with respect to a feast period. PHA storage was expected to have been favored at longer HRTs because bacteria are induced to produce more PHA as the severity of the feast-famine regime is increased (Beun et al. 2000). However, as the length of the famine period is lengthened with longer HRTs the bacteria are forced to rely upon the stored PHA as a carbon source because exogenous carbon is no longer available. Hence, when the famine period is extended for a long enough period, the PHA % in the bacteria decreases. This is a possible explanation for which PHA % decreased as HRT increased above the two days. PHA % did not increase as HRT increased because the reactors operated above an F:M of 1 did not have a famine phase during the 24-hour sampling period. Hence, the relationship of HRT and PHA% did not follow the trends found in previous work (Salehizadeh 2004; Beun 2000; Yu 2001).

Solids retention time did not have a statistical impact on PHA %, as p-values associated with the SRT factor were above 0.10 (Table 10). SRT has been documented to affect PHA % by selecting for PHA-accumulating bacteria at longer SRTs (Barr 1996; Chua 2003). However, the increase in SRT did not translate into an increase in PHA %. A primary difference between results of previous work and the results in this study is that the effect of SRT on PHA % in this work was not evaluated independently of F:M. The only noticeable trend in PHA % with respect to SRT was an apparent “saddle” effect with the minimum PHA % occurring in the mid-SRT range at an intermediate F:M ratio. The reactors (described in Table 9) that were operated at the intermediate F:M of 3 and SRT of 8 days were able to degrade more carbon and nitrogen over the course of the 24-hour sampling period than the reactors operated at an SRT of 8 days and F:M ratios of 1 and 5 (Table 9). This would imply that the conditions in the F:M of 3 and SRT of 8 reactors selected for bacteria who had an advantage based on their ability to consume the nitrogen source and carbon source efficiently rather than to store intracellular polymer.

Estimates of PHA % were based on total dry organic matter rather than total dry biomass because of the presence of short cellulose fibers in the primary clarifier effluent fed to the reactors. The incineration method used in this work was incapable of differentiating between cellular biomass and non-cellular cellulose fibers in the harvested biomass pellets. The average organic fraction (cellular biomass and cellulose fibers) of the harvested pellets was 57%, with a range 36% to 71% (Table 9). The ability to

gravimetrically discern between the cellular biomass and the short cellulose fibers in the harvested pellets used for PHA analysis would have allowed for the PHA % results to be presented on a total dry cell weight basis rather than a total dry organic matter basis. This improvement would have inherently increased the PHA % values obtained in this study.

Total Biomass

There was evidence of microbial respiration in each of the central composite design SBRs as DO concentrations decreased immediately after carbon substrate addition followed by a rebound to saturation levels by the end of the feed cycle. DO returned to saturation or near-saturation levels by the end of the feed cycle despite incomplete carbon substrate consumption in the F:M 3 and 5 reactors (data not shown). Because the MLVSS remained stable after acclimatization, some portion of the carbon source was used for cellular growth. However, COD degradation occurred after DO returned to saturation, which may be an indication of continued low-level microbial activity between feedings.

The results from this study indicate that the conditions in the 16 SBRs selected for consortia that were predominantly composed of slow-growing cells. At low SRTs, the total biomass in the reactors increased with increasing HRT. Alternatively, at high SRT, the total biomass in the reactors increased as the HRT length decreased (Table 9). This interaction suggested that the consortia growth rate increased as the SRT length was reduced and as less substrate entered the system at long HRTs. In turn, the consortia growth rate decreased at longer SRTs and as more substrate entered the system at low HRTs. These trends conform to previous work in which short SRTs favored faster growing cells and long SRTs favored slower growing cells (Buen 2000). Accordingly, the slow-growing members of the mixed consortia in the reactors were less disadvantaged with respect to the fast-growing bacteria at the longer SRTs because the consortia were allowed to grow for a longer period of time (Kaewpipat 2002; Reis 2003). Therefore, since the highest biomass concentrations were achieved at the long SRT values, the consortia in the central composite reactors may have been composed of predominantly slow-growing cells. From an operational perspective this finding is relevant as it will affect the range of design parameters used in a PHA-producing biological system treating pulp mill waste streams with mixed consortia. If PHA storage is to be achieved in a consortium also capable of growth using pulp mill effluents such as foul condensate, the ranges of SBR operational parameters (SRT, HRT, and F:M) must be selected to favor slow-growing bacteria that are capable of accumulating PHA and degrading methanol.

Ammonium Degradation

The ammonium consumption in the 16 SBRs was primarily affected by the interaction of SRT and F:M, as evident by the p-values (Table 10). Ammonium consumption reached a maximum in the high SRT and low F:M ranges and a minimum in the low SRT and high F:M ranges. Ammonium consumption increased proportionally to SRT perhaps because of a shift in the composition of the microbial consortium to organisms capable of nitrification. Nitrification is a commonly recognized activated sludge process that is functionally dependent on SRT. Due to the lower specific growth rates of nitrifying bacteria, longer SRTs are required (4 to 7 days at 20˚C) for ammonium consumption to occur. Ammonium consumption decreased as F:M increased likely because more ammonium was fed to the reactors operated at higher F:M ratios. The ammonium supplied to the consortia originated entirely from the foul condensate in the daily feed. Since foul condensate was both the major source of carbon and ammonium, attaining high F:M ratios was achieved by increasing the foul condensate fraction in the daily feed. To maximize ammonium consumption in the reactors it was necessary to operate the reactors at SRTs above 8 days and at F:M ratios below 3.

Carbon Source Degradation

Carbon source degradation in the 16 SBRs was primarily affected by the F:M ratio with SRT and HRT having no statistically significant effect, as evident by the p-values (Table 10). COD and methanol degradation mirrored each other closely as methanol was the predominant component of total COD. Complete COD degradation never occurred in any of the central composite design reactors as a fraction of

the COD was non-biodegradable (Dufresne 2001; Mockos 2008). The optimum COD and methanol degradation occurred below an F:M of 3, while COD and methanol degradation decreased above an F:M of 3. Carbon source consumption decreased as the F:M was increased from 3 to 5 because the carbon loading at an F:M of 5 was in excess of what the consortia were capable of degrading during the feed cycle. In turn, optimum carbon source degradation occurred below an F:M 3 as in these reactors the consortia were capable of degrading the majority of the carbon by the end of the feed cycle. Therefore, the trends in carbon source degradation in this study suggest that operating reactors above an F:M of 3 would result in excessive and underutilized carbon substrate in the system.

PHA Concentration

The ultimate goal of this study was to determine the relationship between HRT, SRT, and F:M and PHA production from pulp mill effluents. Therefore, PHA concentration was the response variable of most importance. PHA concentration was calculated by multiplying PHA % by total biomass and then dividing by the SBR volume (four liters). Hence, achieving high PHA percentages in reactors that could not support high biomass concentrations would have resulted in relatively low PHA concentrations. It was, therefore, necessary to create environmental conditions within a biological system that could simultaneously promote PHA storage (on a percentage basis) and cellular growth.

PHA concentration was affected by F:M with SRT and HRT not being statistically relevant, as evident by the p-values (Table 10). PHA concentration increased as F:M increased from 1 to 3. PHA concentration then declined beyond an F:M of 3 as PHA storage was no longer favored due to the lack of famine conditions resulting from carbon substrate carryover (Dionisi et al. 2006; Dionisi et al. 2004b). Therefore, the reactors operated at F:M ratios above 3 were not induced to produce as much PHA as the reactors operated at an F:M of 3.

HRT and SRT did not have a statistical impact on PHA concentration. However, PHA concentration may have changed over the range of HRT and SRT values tested (Table 9). PHA concentration increased as HRT decreased. This trend contradicted trends found in the literature that showed increased PHA storage at longer HRTs due to an increase in the carbon substrate flux into the system (Yu et al. 2001). This phenomenon could only be explained if consortia capable of quickly converting carbon substrate to PHA were present in the 16 SBRs. Accordingly, PHA storage increased as SRT was increased. This finding conforms to findings in the literature where longer SRTs increased PHA concentrations by selecting for PHA-accumulating bacteria (Leeuwen 1997). Hence, the environmental conditions present in the reactors operated at the longer SRTs and the shorter HRTs favored bacteria capable of converting the utilizable carbon source into PHA.

The maximum PHA concentration achieved in this study was at an F:M of 3, an HRT of 2 days, and an SRT of 12 days (reactor 14, Table 9). The optimal PHA concentration was reached under environmental conditions in the reactors that favored the growth of slow-growing cells capable of quickly assimilating the carbon substrate and converting it to PHA. The most influential factors that created the optimal PHA-producing conditions in the reactors were two fold. Firstly, PHA concentration was optimized when the consortia were allowed to grow for longer periods of time (long SRTs). Secondly, PHA concentrations increased when the carbon flux into the system was sufficiently low as to allow the cells to degrade the carbon source by the end of the feed cycle (HRT in the range of 2 days, and an F:M of 3). The findings from this study, which only apply to SBRs that are operated similarly to the reactors used in this study, conclude that a maximum PHA concentration of 0.11 g L^{-1} can be obtained from a PHA-producing reactor fed pulp mill effluents operated at an F:M of 3, at an HRT of approximately 2 days, and at an SRT of approximately 12 days.

Conclusion and Future Work

The goal of this study was to evaluate the relationship between F:M, SRT, and HRT and PHA production in SBRs inoculated with mixed consortia enriched from pulp mill activated sludge and fed pulp mill effluents. A face-centered cube central composite design experiment was used as a tool to simultaneously assess the effects of SRT, HRT, and F:M on PHA %, PHA concentration, total biomass,

methanol and COD degradation, and ammonium degradation. The ability of the consortia to produce PHA, whether on a concentration basis or on a fraction of the total dry organic matter basis (PHA%), was predominantly affected by the F:M ratio. In addition, F:M overwhelmingly affected the amount of carbon source degradation that occurred in each reactor. Therefore, the amount of carbon entering the system ultimately played the dominant role in determining how much PHA the consortia were able to store and how much of the carbon source the consortia were able to degrade. The ability to support cell growth in the reactors was mainly affected by the combined effects of SRT and HRT. Biomass concentrations improved when the conditions in the reactors gave a selective advantage to slower growing cells. In parallel with the biomass concentrations, ammonium degradation was also affected by SRT. However, F:M also played a role in ammonium degradation as the nitrogen source used in this work was also the carbon source (foul condensate).To maximize PHA production using pulp mill effluents and consortia enriched from pulp mill activated sludge a PHA-producing SBR system must be operated at an intermediate F:M of 3, at the high SRT value of 12 days, and at the intermediate HRT value of 2 days. If a PHA-producing SBR is operated under these conditions, a maximum PHA concentration of 0.11 g L^{-1} can be achieved.

References

Anderson, A.J. and E.A. Dawes (1990) Occurrence, Metabolism, Metabolic Role, and Industrial Uses of Bacterial Polyhydroxyalkanoates. Microbiological Reviews, 54(4): 450-472.

APHA (2005) Standard Methods for the Examination of Water and Wastewater, 21st ed., American Public Health Association, Washington D.C.

Barr, T.A., J.M. Taylor, and S.J.B. Duff (1996) Effect of HRT, SRT and temperature on the performance of activated sludge reactors treating bleached kraft mill effluent. Water Research, 30(4): p. 799-810.

Berthouex, P.M., and Brown, L.C. (2002) Statistics for Environmental Engineers, 2nd ed., CRC Press, Baton Rouge, FL. p. 261-270.

Beun, J.J., Paletta, F., Loosdrecht M.C.M., and J.J. Heijnen (2000) Stoichiometry and Kinetics of Poly-b-Hydroxybutyrate Metabolism in Aerobic, Slow Growing, Activated Sludge Cultures. Biotechnology and Bioengineering, 67(4): p. 379-389.

Beun, J.J., Dircks, K., Loosdrecht, M.C.M., and J.J. Heijnen (2002) Poly-β-hydroxybutyrate metabolism in dynamically fed mixed microbial cultures. Water Research, 36(5): p. 1167-1180.

Braunegg, G., B. Sonnleitner, and R.M. Lafferty (1978) A rapid gas chromatographic method for the determination of poly-β-hydroxybutyric acid in microbial biomass. European Journal of Applied Microbiology and Biotechnology, 6(1): 29-37.

Braunegg, G., G. Lefebvre, and K.F. Genser (1998) Polyhydroxyalkanoates, biopolyesters from renewable resources: Physiological and engineering aspects. Journal of Biotechnology, 65(2-3): 127-161.

Chua, A.S.M., Takabatake, H., Satoh, H., and T. Mino (2003) Production of polyhydroxyalkanoates (PHA) by activated sludge treating municipal wastewater: effect of pH, sludge retention time (SRT), and acetate concentration in influent. Water Research, 37(15): p. 3602-3611.

Coats E.R., Loge, F.J., Smith, W.A., Thompson, D.N., and M.P. Wolcott (2007) Functional stability of a mixed microbial consortium producing PHA from waste carbon sources. Applied Biochemistry and Biotechnology, 136-140: p. 1-18.

Daniel, M., Choi, J.H., Kim, J.H., and Lebeault J.M. (1992) Effect of nutrient deficiency on accumulation and relative molecular weight of poly-β-hydroxybutyric acid by methylotrophic bacterium, *Pseudomonas 135*. Applied Microbiology and Biotechnology, 37(6): p. 702-706.

Dionisi, D., Majone, M., Miccheli, A., Puccetti, C., and C. Sinisi (2004a) Glutamic Acid Removal and PHB Storage in the Activated Sludge Process Under Dynamic Conditions. Biotechnology and Bioengineering, 86(7): p. 842-851.

Dionisi, D., M. Majone, V. Papa, and M. Beccari (2004b) Biodegradable Polymers From Organic Acids by Using Activated Sludge Enriched by Aerobic Periodic Feeding. Biotechnology and Bioengineering, 85(6): 569-579.

Dionisi, D., Beccari, M., DiGregorio, S., Majone, M., Papini, M.P., and G. Vallini (2005) Storage of biodegradable polymers by an enriched microbial community in a sequencing batch reactor operated at high organic load rate. Journal of Chemical Technology and Biotechnology, 80: p. 1306-1318.

Dionisi, D., Majone, M., Vallini, G., DiGregorio, S., and M. Beccari (2006) Effect of the Applied Organic Load Rate on Biodegradable Polymer Production by Mixed Microbial Cultures in a Sequencing Batch Reactor. Biotechnology and Bioengineering, 93(1): p. 76-88.

Dufresne, R., A. Liard, and M.S. Blum (2001) Anaerobic Treatment of Condensates: Trial at a Kraft Pulp and Paper Mill. Water Environment Research 73(1): 103-109.

Frigon, D., Muyzer, G., Loosdrecht, M.C.M., and L. Raskin (2006) rRNA and Poly-β-hydroxybutyrate dynamics in bioreactors subjected to feast and famine cycles. Applied and Environmental Microbiology, 72(4): p. 2322-2330.

Hinkelmann, K., and Kempthorne, O. (1994) Design and Analysis of Experiments, Volume I: Introduction to Experimental Design, John Wiley & Sons, New York, NY p. 409.

Hinkelmann, K., and Kempthorne, O. (2005) Design and Analysis of Experiments, Volume II: Advanced Experimental Design, John Wiley & Sons, New York, NY p. 507-563.

Hong, K., Chen, G.Q., Yu, P.H.F., Zhang, G., Liu, Y., and H. Chua (2000) Effect of C:N molar ratio on monomer composition of Polyhydroxyalkanoates produced by *Pseudomonas mendocina* 0806 and *Pseudomonas pseudoalkaligenus* YS1. Applied Biochemistry and Biotechnology, 84-86: p. 971-980.

Kaewpipat K., and C.P.L. Grady Jr. (2002) Microbial population dynamics in laboratory-scale activated sludge reactors. Water Science and Technology, 46(1-2): p. 19-27.

Kim, S.W., P. Kim, Hyun S. Lee, and Jung H. Kim (1996) High Production of Poly-β-hydroxybutyrate (PHB) from *Methylobacterium organophilum* under Potassium Limitation. Biotechnology Letters, 18(1): p. 25-30.

Lee, S.Y. (1996) Plastic bacteria? Progress and prospects for polyhydroxyalkanoate production in bacteria. Trends in Biotechnology, 14(11): p. 431-438.

Leeuwen, M.A.v.A., Pot, M.A., Loosdrecht, M.C.M., and J.J. Heijnen (1997) Kinetic Modeling of Poly-β-hydroxybutyrate Production and Consumption by *Paracoccus pantotrophus* under Dynamic Substrate Supply. Biotechnology and Bioengineering, 55(5): p. 773-782.

Lenz, R.W. and R.H. Marchessault (2005) Bacterial Polyesters: Biosynthesis, Biodegradable Plastics and Biotechnology. Biomacromolecules, 6(1): p. 1-8.

Ma, C.K., H. Chua, P.H.F. Yu, and K. Hong (2000) Optimal Production of Polyhydroxyalkanoates in Activated Sludge Biomass. Applied Biochemistry and Biotechnology, 84(1-9): p. 981-990.

Madison, L.L. and G.W. Huisman (1999) Metabolic Engineering of Poly(3-hydroxyalkanoates): From DNA to Plastic. Microbiology and Molecular Biology Reviews, 63(1): p. 21-53.

Mason, R.L., Gunst, R. F., and Hess, J. L. (2003) Statistical Design and Analysis of Experiments, 2nd ed., John Wiley & Sons, New York, NY p.598-613

Miller, M., M. Justiniano, and S. McQueen (2005) Energy and Environmental Profile of the U.S. Pulp and Paper Industry. U.S. Department of Energy, Office of Energy Efficiency and Renewable Energy, Industrial Technologies Program, Washington, DC.

Mockos, G.R., Loge, F.J., Smith, W.A., and D.N. Thompson (2008a) Selective enrichment of a methanol-utilizing consortium using pulp & paper mill waste streams. Applied Biochemistry and Biotechnology, pending publication, April 2008.

Mockos, G.R., Loge, F.J., Smith, W.A., and D.N. Thompson (2008b). Effect of carbon to nitrogen ratio on polyhydroxyalkanoate production by pulp mill activated sludge. Submitted to Biotechnology and Bioengineering.

Montgomery, D.C. (2001) Design and Analysis of Experiments, 5th ed., John Wiley & Sons, New York, NY p. 367-372.

Reis, M.A.M., L.S. Serafim, P.C. Lemos, A.M. Ramos, F.R. Aguiar, and M.C.M. Van Loosdrecht (2003) Production of polyhydroxyalkanoates by mixed microbial cultures. Bioprocess and Biosystems Engineering, 25(6): 377-385.

Salehizadeh, H. and M.C.M.V. Loosdrecht (2004) Production of polyhydroxyalkanoates by mixed culture: recent trends and biotechnological importance. Biotechnology Advances, 22(3): 261-279.

SAS Institute Inc. (2004) SAS OnlineDoc® 9.1.3. Cary, NC.

Serafim, L.S., P.C. Lemos, R. Oliveira, and M.A.M. Reis (2004) Optimization of Polyhydroxybutyrate Production by Mixed Cultures Submitted to Aerobic Dynamic Feeding Conditions. Biotechnology and Bioengineering, 87(2): 145-160.

Smook, G.A. (1992) Handbook for Pulp & Paper Technologists, 2nd ed., Angus Wilde Publications, Bellingham, WA, p. 382.

Springer, A.M. (2000) Industrial Environmental Control Pulp and Paper Industry, 3rd ed., Tappi Press, Atlanta, GA, pp. 238-239.

StatSoft, Inc. (2007) STATISTICA (data analysis software system), version 8.0.

Suzuki, T., Yamane,T., and S. Shimizu (1986) Mass production of poly-ß-hydroxybutyric acid by fed-batch culture with controlled carbon/nitrogen feeding. Applied Microbiology and Biotechnology, 24: p. 370-374.

Tchobanoglous, G., Burton, F.L., and Stensel H.D. (2003) Metcalf and Eddy Wastewater Engineering Treatment and Reuse, 4th ed., McGraw Hill , New York, NY, p. 222 and p. 676-681.

Wang, Y.J., Hua, F.L., Tsang, Y.F., Chan, S.Y., Sin, S.N., Chua, H., Yu, P.H.P., and N.Q. Ren (2007) Synthesis of PHAs from waste under various C:N ratios. Bioresource Technology, 98: p. 1690-1693.

Wu, C.F.J., and Hamada, M. (2000) Experiments Planning, Analysis, and Parameter Design Optimization, John Wiley & Sons, New York, NY p. 209-226.

Yu, J. and Y. Si (2001) A Dynamic Study and Modeling of the Formation of Polyhydroxyalkanoates Combined with Treatment of High Strength Wastewater. Environmental Science and Technology, 35(17): p. 3584-3588.

Figures

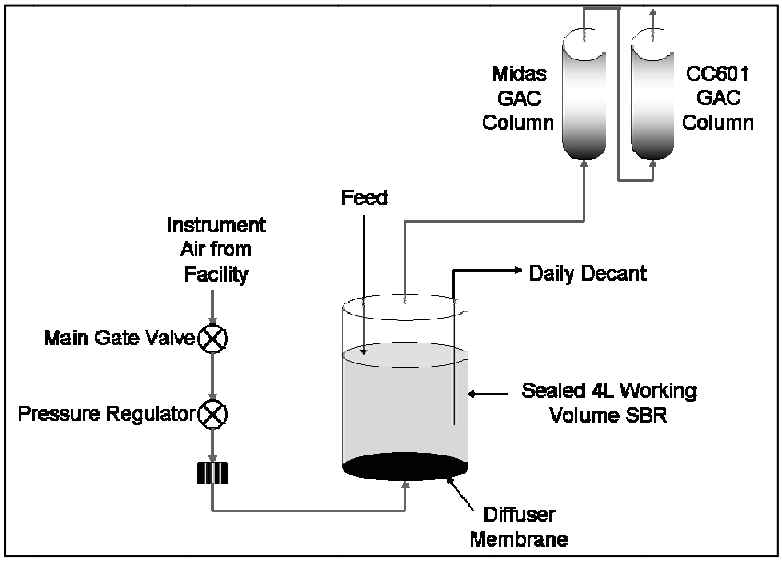

Figure 14. Experimental setup of sequencing batch reactors

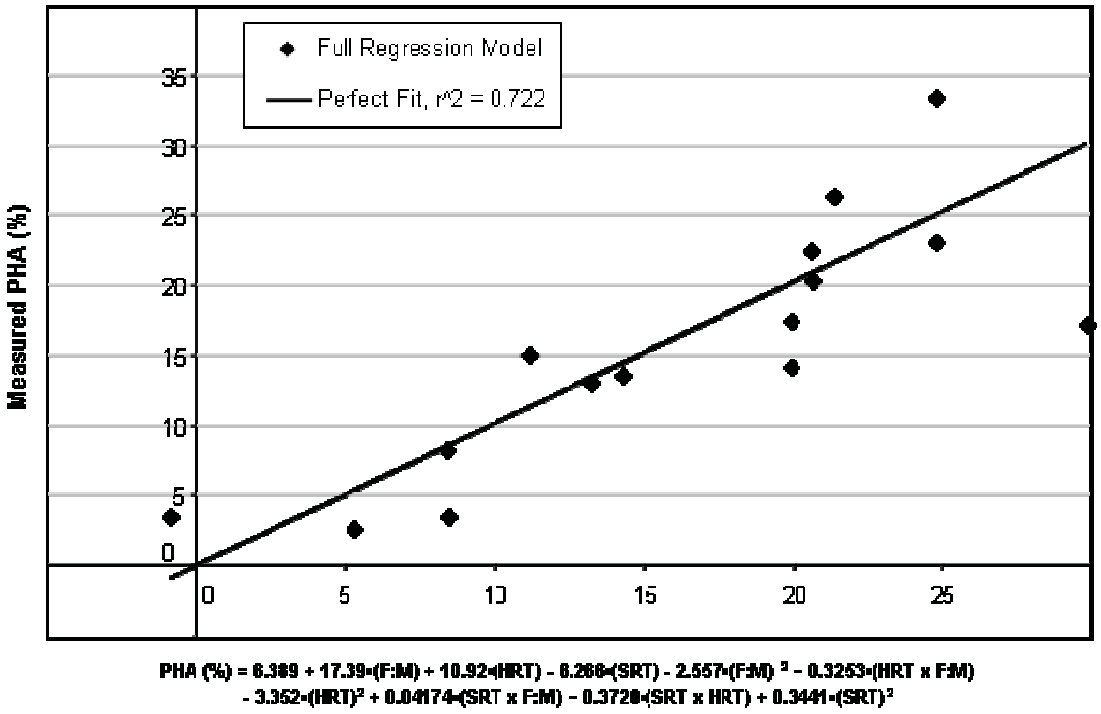

Figure 15. Regression Model of Predicted PHA % versus Measured PHA %

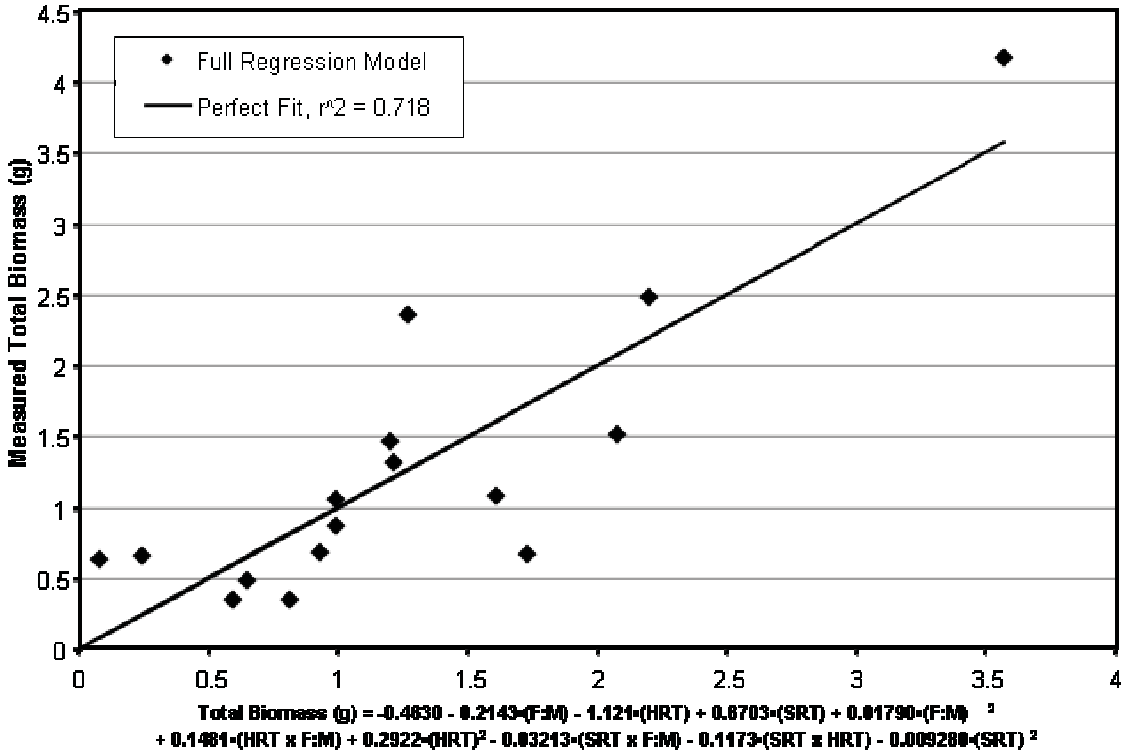

Figure 16. Regression Model of Total Biomass (g) versus Measured Total Biomass (g)

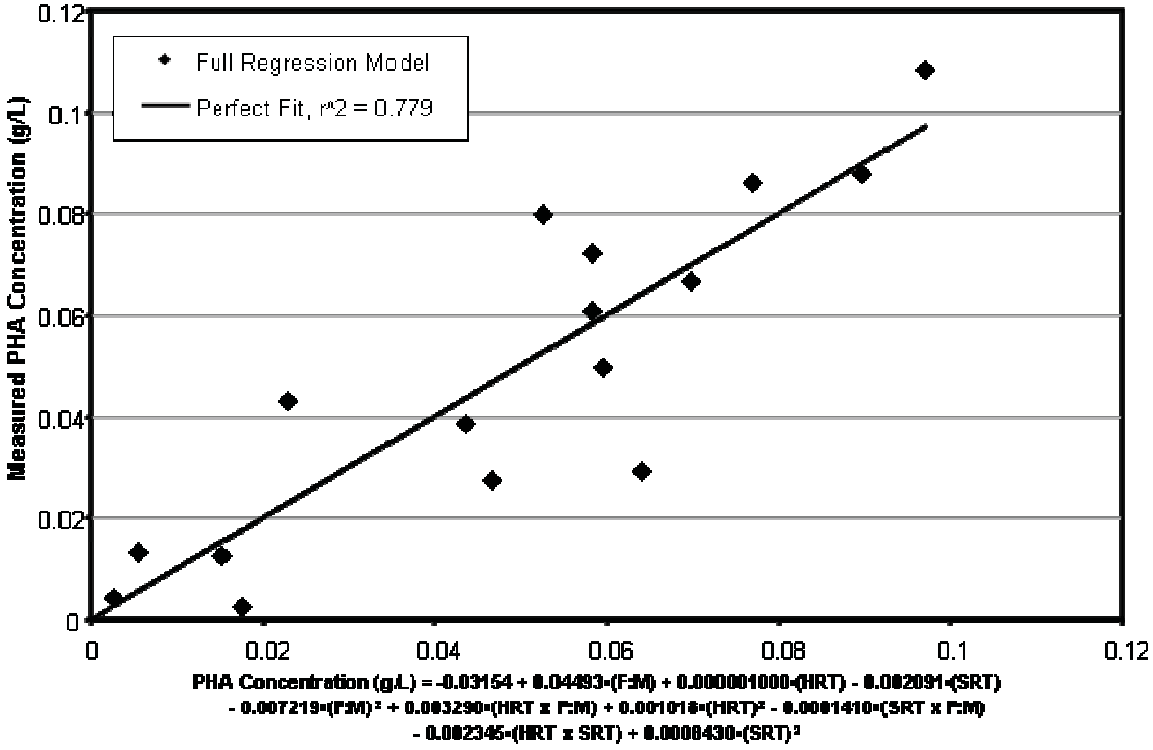

Figure 17. Regression Model of Predicted PHA Concentration (g L^{-1}) versus Measured PHA Concentration (g L^{-1})

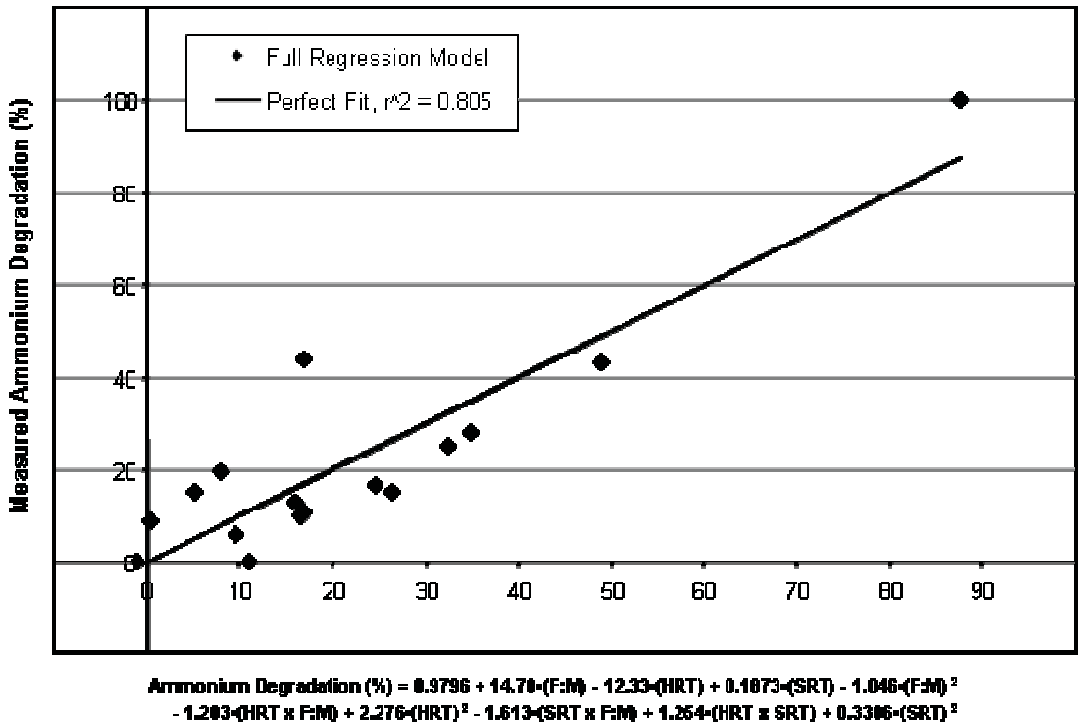

Figure 18. Regression Model of Predicted Ammonium Degradation (%) versus Measured Ammonium Degradation (%)

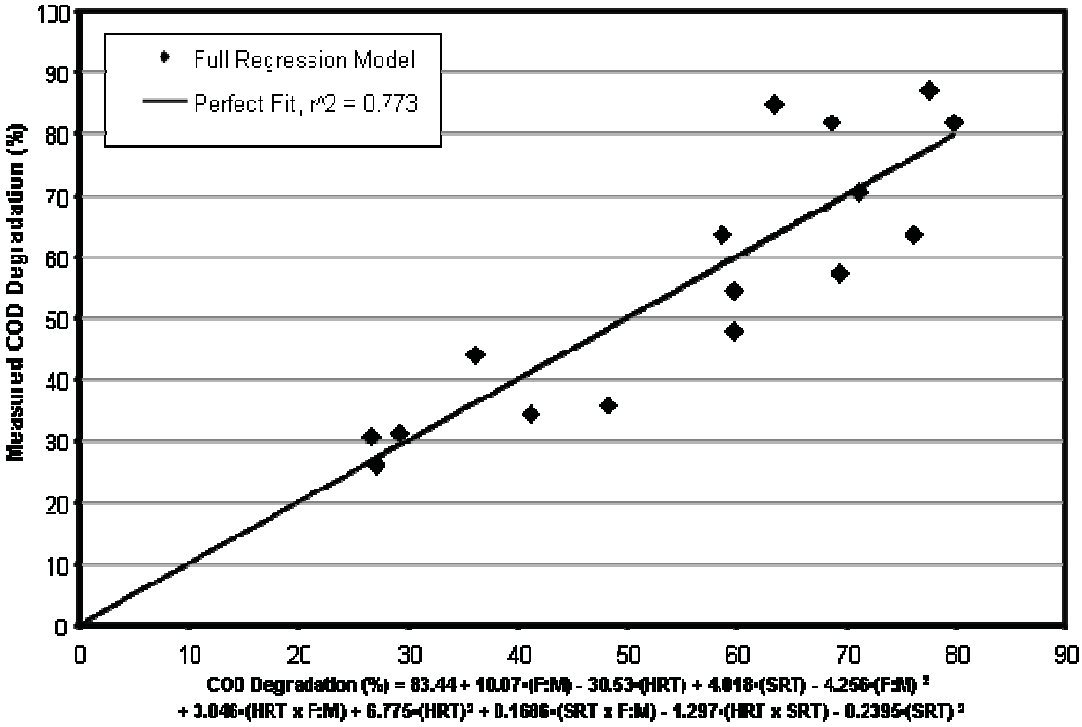

Figure 19. Regression Model of Predicted COD Degradation (%) versus Measured COD Degradation (%)

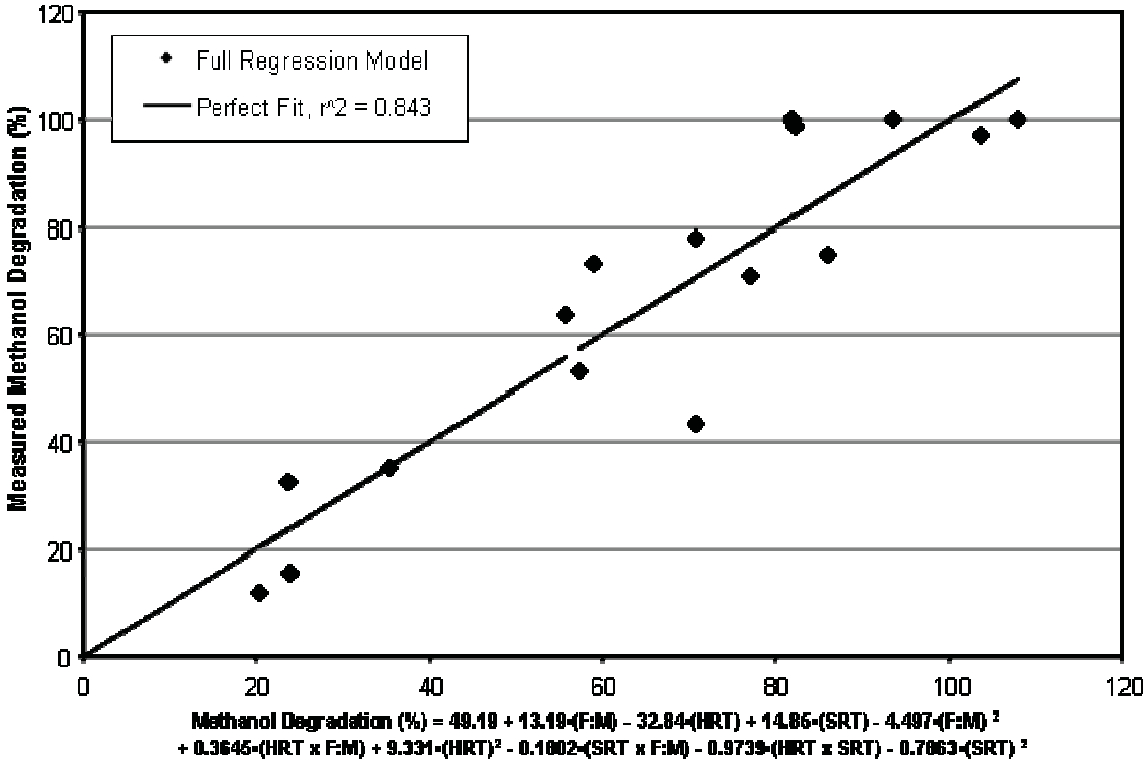

Figure 20. Regression Model of Predicted Methanol Degradation (%) versus Measured Methanol (Degradation (%)

Tables

Table 9. Face-centered cube central composite design results

Reactor #	F:M	HRT (d)	SRT (d)	Biomass fraction of Total Solids	PHA (%)	Total Biomass (g)	PHA (g/L)	COD Deg. (%)	Methanol Deg. (%)	Ammonium Deg. (%)	Max DO Drop (%)
1	1	1	4	0.69	15	0.35	0.013	63	71	5	29
4	1	1	12	0.41	8	4.18	0.086	82	75	53	33
9	1	2	8	0.70	3	1.47	0.012	64	100	15	32
3	1	4	4	0.58	3	0.49	0.004	82	100	10	7
7	1	4	12	0.58	3	0.35	0.002	34	100	100	20
11	3	1	8	0.59	17	0.67	0.029	70	99	13	40
13	3	2	4	0.71	17	0.64	0.027	85	73	6	47
15	**3**	**2**	**8**	**0.52**	**33**	**0.86**	**0.072**	**54**	**43**	**40**	**42**
16	**3**	**2**	**8**	**0.68**	**23**	**1.06**	**0.061**	**48**	**38**	**44**	**44**
14	3	2	12	0.55	40	1.08	0.108	36	53	28	58
12	3	4	8	0.67	13	2.36	0.08	87	97	25	18
2	5	1	4	0.52	26	0.66	0.043	31	12	5	41
6	5	1	12	0.50	14	2.49	0.088	26	33	12	31
10	5	2	8	0.36	22	0.69	0.039	31	15	17	40
5	5	4	4	0.54	13	1.52	0.05	57	64	15	27
8	5	4	12	0.59	20	1.32	0.067	44	35	16	41

Table 10. Statistical Model Results

A. PHA % Model (R^2 = 0.7224)				B. Total Biomass Model (R^2 = 0.7180)				C. PHA Conc. Model (R^2 = 0.7791)			
Factor	**Coefficient estimate**	**t-value**	**p-value**	**Factor**	**Coefficient estimate**	**t-value**	**p-value**	**Factor**	**Coefficient estimate**	**t-value**	**p-value**
Intercept	6.39	0.27	0.8	Intercept	-0.46	-0.2	0.85	Intercept	-0.0315	-0.47	0.65
F:M	17.39	1.91	0.1	F:M	-0.21	-0.24	0.82	F:M	0.0449	1.77	0.12
HRT	10.92	0.73	0.49	HRT	-1.12	-0.77	0.47	HRT	0	0	1
SRT	-6.27	-1.1	0.31	SRT	0.67	1.22	0.27	SRT	-0.0021	-0.13	0.89
F:M quadratic	-2.56	-1.9	0.1	F:M quadratic	0.02	0.14	0.9	F:M quadratic	-0.0072	-1.92	0.1
HRT × F:M	0.33	0.32	0.76	HRT × F:M	0.15	1.5	0.18	HRT × F:M	0.0033	1.16	0.29
HRT quadratic	-3.35	-1.23	0.23	HRT quadratic	0.29	1.11	0.31	HRT quadratic	0.001	0.13	0.89
SRT × F:M	0.04	0.11	0.92	SRT × F:M	-0.03	-0.86	0.42	SRT × F:M	-0.0001	-0.13	0.89
SRT × HRT	0.37	0.73	0.49	SRT × HRT	-0.12	-2.38	0.05	SRT × HRT	-0.0023	-1.65	0.15
SRT quadratic	0.34	1.02	0.35	SRT quadratic	-0.01	-0.28	0.78	SRT quadratic	0.0008	0.9	0.4
D. Ammonium Deg. Model (R^2 = 0.8047)				**E. COD Degradation Model (R^2 = 0.7734)**				**F. Methanol Degradation Model (R^2 = 0.8428)**			
Factor	**Coefficient estimate**	**t-value**	**p-value**	**Factor**	**Coefficient estimate**	**t-value**	**p-value**	**Factor**	**Coefficient estimate**	**t-value**	**p-value**
Intercept	0.98	0.02	0.98	Intercept	83.44	1.9	0.0157	Intercept	49.19	0.93	0.3875
F:M	14.7	0.83	0.44	F:M	10.07	0.61	0.56	F:M	13.19	0.66	0.53
HRT	-12.33	-0.42	0.69	HRT	-30.53	-1.12	0.31	HRT	-32.84	-1	0.36
SRT	0.18	0.02	0.99	SRT	4.02	0.39	0.71	SRT	14.85	1.19	0.28
F:M quadratic	-1.05	-0.4	0.7	F:M quadratic	-4.25	-1.74	0.13	F:M quadratic	-4.49	-1.52	0.18
HRT × F:M	-1.2	-0.61	0.57	HRT × F:M	-2.305	1.64	0.15	HRT × F:M	0.36	0.16	0.88
HRT quadratic	2.27	0.43	0.68	HRT quadratic	6.77	1.36	0.22	HRT quadratic	9.33	1.56	0.17
SRT × F:M	-1.61	-2.14	0.08	SRT × F:M	0.17	0.24	0.82	SRT × F:M	-0.18	-0.21	0.84
SRT × HRT	1.25	1.26	0.25	SRT × HRT	-1.29	-1.4	0.21	SRT × HRT	-0.97	-0.87	0.42
SRT quadratic	0.33	0.5	0.63	SRT quadratic	-0.24	-0.39	0.71	SRT quadratic	-0.78	-1.07	0.33

Results – Composite Processing & Material Properties of WFRTCs Utilizing PHA

Task 1 – Purified PHA ± Cell Debris Composite Processing & Material Properties

Investigators: Michael P. Wolcott[1], Karl R. Englund[1], Jinwen Zhang[1], Scott Anderson[1]

Performing Institutions: [1]Washington State University

Effect of Interfacial Modifiers on Mechanical and Physical Properties on PHB/WF and Their Effect on Composite Morphology

Abstract

As the social costs for fossil fuels are increasing and environmental concerns regarding climate change and sustainability are growing, the need for truly biodegradable and environmentally friendly consumer products has increased. Polyhydroxybutyrate (PHB) has received considerable attention as a bacterially derived biopolymer with attractive mechanical properties. Processing PHB with wood fiber (WF) reduces cost and improves mechanical properties. To explore the commercial viability of PHB/WF composites, systems were produced at industry-standard levels of fiber loading. Further, four interfacial modifiers were selected to improve upon the mechanical properties of PHB/WF composites. The composites were processed by injection molding of pre-compounded and palletized formulations. Interfacial modifiers studied include maleated PHB (MA-PHB), a low molecular weight epoxy, D.E.R., a low molecular weight polyester, Uralac, and polymethylene-diphenyl-diisocyante (pMDI). Mechanical properties were characterized through tensile testing (ASTM D638), notched impact testing (ASTM D256), and water absorption tests. Results show improvements in strength properties with the use of all the modifiers studied, however, pMDI showed the highest improvements. With the addition of 4% pMDI, PHB/WF composites displayed an increase in strength of 57%, and an increase in Young's modulus of 21%. The pMDI modifier also improved water uptake of the composites. Studies of the fracture interface showed signs of improved fiber bonding, as do morphological studies by dynamic mechanical analysis (DMA), and differential scanning calorimetry (DSC). Interpretation of the DSC and DMA results indicate possible reaction with lubricant, and interaction between PHB and wood fibers with the addition of pMDI.

Introduction

For some time now, natural fibers have received considerable attention as a reinforcing material for commercial thermoplastics. Wood fibers (WF) are attractive because of their low cost and high specific properties. Commercial wood plastic composites (WPCs) have been successfully developed utilizing polyolefins such as polypropylene and polyethylene (Clemons, 2002). While composite manufacturers use varying degrees of recycled polypropylene or polyethylene, many manufacturers still use 100% virgin polyolefin for the manufacturing of WPCs.

In an effort to reduce societies dependence on fossil fuels, biopolymers have been proposed as a viable alternative to polyolefins as matrix material in WPCs. Polymers such as polylactic acid (PLA) and polyhydroxyalkanoates (PHA) have been identified as possible alternatives to petrochemically derived polymers (Manju, 2005; Gatenholm, 1992).

PHAs are a class of polymers synthesized and grown by a wide range of bacteria through fermentation of sugars and lipids. In addition to being produced by bacteria, PHAs are also biodegradable through enzymatic degradation. Of the PHAs, considerable attention has been focused on

polyhydroxybutyrate (PHB) and poly(3-hydroxybutyrate-co-3-hydroxyvalerate) (PHBV). With tensile strength and tensile modulus reported to be from 20-25 MPa, and 600-800 MPa, respectively, PHB is comparable to polypropylene for many applications (Zhang, 2004).

While various PHB-based natural fiber composites have been evaluated in the literature, as of yet, no studies have studied the composite produced with industry-standard levels of fiber loading (Reinsch and Kelley, 1997; Gatenholm, 1992). Four interfacial modifiers have been selected to encourage PHB/WF interaction. Maleated systems have been well recognized for their potential in WPCs and have been developed for use in both PP and PE composites (Sombatsompop, 2005; Lu, 2005). Maleic anhydride has even been coupled with neat PHB to improve properties such as thermal stability (cold crystallization temperature, decomposition temperature, Chen, 2003). In this study, maleic anhydride grafted PHB (MA-PHB) was produced for use in a PHB/WF composite. In addition, two novel interfacial modifiers are used in this study. D.E.R. is a low molecular weight solid epoxy resin and Uralac is a low molecular weight polyester with carboxyl end groups. In both situations, it is hypothesized that the reactive end groups will chemically bond with the wood fibers and facilitate compatibility with the PHB matrix, forming a superior bond. Finally, polymeric isocyanates have long been used as adhesives for wood. First used in wood-strand composites, isocyanates are now considered for their application in WPCs (Zhang, 2005; Geng, 2005). Isocyanates have even been shown to be effective on PHB-based natural fiber composites. Qian (2006) showed that 3% polymethylene-diphenyl-diisocyante (pMDI) can be used to improve the strength of PHB/Bamboo fiber composites from 40 MPa to 50 MPa, and the stiffness from 5 GPa to 9 GPa. Illustrated in Table 11 is the chemical structure for each modifying agent and the anticipated reaction at the hydroxyl-functioned wood fiber surface. With MA-PHB, D.E.R., and Uralac, it is expected that the modifier becomes entangled with the PHB matrix thus forming a matrix-fiber linkage. In the case of pMDI it is possible that the pMDI may react to form a polyurethane which may entangle and hydrogen bond with the PHB matrix.

The focus of this study is to develop viable formulations for PHB/WF composites. The objectives of this study are to 1) investigate the effects of interfacial modifier type on improving mechanical and physical properties of the resultant composites, 2) to evaluate the modifying efficiency at the interface, and 3) to determine the morphological effects of the most promising interfacial modifier on PHB/WF morphology.

Materials

The WPC composites were composed primarily of PHB (Tianan Biologic Material Co., Ltd., Ningbo, China) and 60-mesh ponderosa pine wood fiber (American Wood Fibers, Schofield, WI). Because of the slow crystallizing nature of PHB, boron nitride (BN) in platelet form (Carbotherm PCTF5, obtained from Saint Gobain Advanced Ceramics Corporation, Amherst, NY) was included to promote homogeneous nucleation (Qian, 2007). Previous research has shown that the use of Glycolube WP2200 (provided by Lonza Inc., Allendale, NJ) may serve as an effective lubricant and produce composites with improved mechanical properties (Anderson, 2007a). Talc (Nicron 403 obtained from RioTinto of Centennial, CO) was used to improve processing and water uptake of the highly filled composites. Multiple interfacial modifiers were evaluated in the study. The pMDI (Mondur G541), supplied by Bayer MaterialScience (Pittsburgh, PA), contained 31.5 mass % NCO. Uralac P5142, a low molecular weight polyester was supplied by DSM Resins US, Inc (Augusta, GA). D.E.R. 662E, a low molecular weight solid epoxy resin was supplied by DOW (Midland, MI). Finally, to produce the maleated-PHB, dicumyl peroxide (98% purity) and maleic anhydride (95% purity) were obtained from Aldrich (St. Louis, MO).

Methods

Preparation of composites

PHB-WF compounds containing different interfacial modifiers were prepared by dry blending and then melt mixing in a twin screw extruder and granulated for use in injection molding in preparation for mixing, PHB was first dried in an oven at 100°C for 12 hours. Pine wood flour was dried by steam

tube to a moisture content of 2.8 mass %. Blends were prepared with 35 parts PHB, 57 parts WF, 8 parts Talc, 0.2 parts BN, 3 parts WP2200, and either 0, 1, 2 or 4 parts interfacial modifier. To produce the interfacial modifier MA-PHB, 95 parts PHB, 5 parts maleic anhydride, and 0.5 parts dicumyl peroxide (used as an initiator) were processed in a torque rheometer (Haake Polylab 3000P) at 180°C and 50 rpm for 40 minutes. The ungrafted maleic anhydride was removed by vacuum oven in 100 °C for 12 hours.

Except in the case of blends containing pMDI, all formulations were premixed by manually tumbling the components in a plastic bag for 5 minutes. In the case of blends containing pMDI, the liquid modifier was added to the PHB powder and dispersed using a standard kitchen blender for 1 minute. Melt mixing and pre-compounding were accomplished through a co-rotating twin screw extruder (Leistritz ZSE-18) fed by a volumetric feeder. The screw diameter was 17.8 mm and the L/D ratio was 40.

Extrusion temperatures for pre-compounding were independently controlled on eight zones along the extruder barrel. A declining temperature profile was chosen to reduce thermal degradation and improve melt strength (Zhang, 2004). From the feed throat to the die adapter, the temperatures were set as follows; 170°C, 175°C, 170°C, 165°C, 164°C, 163°C, 162°C, and 160°C. The formulations were introduced into the extruder throat with a screw-driven starve feeder. The extruder screw was maintained at a speed of 125 rpm. The resulting residence time was estimated be approximately 1.5 minutes. After exiting the die, the extrudate was air cooled and granulated.

Preparation of test specimens

Standard ASTM D638, type I tensile specimens and 12 x 3 x 127-mm flexure bars were produced by injection molding (Sumitomo SE 50D). Temperature zones were independently controlled at 175°C, 180°C, 175°C, 165°C from the feeding end to the nozzle. The mold temperature was held constant at 60°C. The filling pressure was set for 1700-kgf/cm^2 and the packing pressures were set to 1275-kgf/cm^2 and 1360-kgf/cm^2 for the 1st and 2nd stage, respectively. Residence times were consistently measured around 5 minutes.

Test specimens for impact testing were cut from the center (length-wise) of the flexure specimens and notched using a XQZ-I Specimen Notch Cutter (Chengde Jinjian Testing Instrument Co., Ltd.). Specimens for water absorption tests and DMA tests requiring specimen sizes differing from those produced through injection molding were milled on a manual milling machine to dimensions of 11 x 2.5 x 125-mm and 2 x 12 x 52-mm, respectively.

Mechanical and physical property testing

Tensile tests were performed in accordance with ASTM D638 using a screw driven Instron 4466 Standard with a 10-kN electronic load cell. Tests were performed at a crosshead speed of 5-mm/min and strain was measured with a clip-extensometer with a 25 mm gage length (MTS model # 634.12E-24). Sample geometry was measured on all samples prior to testing and density was calculated from the resulting volume (length x width x thickness) and the sample mass. Fractured tensile specimens were sputter coated with gold for observation by scanning electron microscopy (SEM) on a Hitachi S-570.

Notched impact testing was performed according to ASTM D256, method A. The test frame was configured with a load head corresponding to a maximum impact of 2.7-J. Water absorption tests were performed in a temperature controlled, distilled water bath held at room temperature. The surface moisture was blot-dried with a towel, and the specimens were allowed to air dry for 10 minutes prior to measurement. Moisture content was calculated on a mass percent basis using the following equation:

$$MC = \frac{(M - M_o) \times 100}{M_o} \quad (1)$$

Where MC is the moisture content (mass %), M is the mass of the specimen at time t, and M_o is the initial (dry) weight of the specimen.

Statistical Analysis

The influence of various formulations variables on the physical and mechanical properties of the composite was assessed using an analysis of variance (ANOVA). When the influence of density on mechanical properties was significant, density was accounted for as a covariate. This changed the analysis to an analysis of covariance (ANCOVA). All analyses were conducted using statistical software (SAS, Version 6.9.1, SAS Institute Inc., Cary, NC). Since data sets were unbalanced, the general linear model was employed. Significance was set for the $\alpha = 0.01$ level.

Testing of thermal properties

Dynamic mechanical properties of the modified systems were analyzed with a Rheometric Scientific RSA II using three-point-bending configuration. Before the temperature ramp tests were conducted, the linear viscoelastic range was determined through a strain sweep. Further experiments were conducted under a constant frequency of 1 Hz and a strain amplitude of 0.03% for dynamic temperature sweep tests from -30°C to 125°C.

The melting and crystallization behavior of the modified systems were examined using a differential scanning calorimeter (DSC) (Mettler Toledo, DSC 822e). Samples were taken from an exact location on the tensile-bar specimens and weighed from 3-6 mg. Aluminum crucibles (40-µl) were hermetically sealed to contain the specimens. Each sample was heated from 30°C to 180°C at 20°C/min, held for 2 minutes to erase the previous thermal history, and cooled at 20°C/min to -30°C. Following the cool down, samples are re-heated to 180°C at 20°C/min to collect the final DSC trace used to determine melt behavior.

Results and Discussion

Statistical analysis of mechanical and physical properties

Density has been shown by others to have a very large influence on mechanical properties in wood plastic composites. Micromechanical models that have been verified for natural fiber reinforced composites predict that composite stiffness may be increased by increasing the density of the composite (Facca, 2006). In wood-plastic composites, increases densities may be the result of better dispersion of fiber bundles, polymer penetration of the hollow fibers, or better bulk packing due to increased fiber alignment. Any of these conditions would manifest itself in improved stress transfer between fiber and polymer phases, resulting in the potential of improved mechanical properties. Because fiber alignment is largely influenced by the shear gradient in a die, it is likely that the various composites in this study have comparable fiber alignment. Therefore, changes in density would likely be a function of increased fiber dispersion or polymer penetration of the fibers.

Figure 21 presents the composite density when produced with various levels and types of modifier. For all systems, a step increase in density occurs from 0% to 1%, possibly resulting from improved fiber wetting leading to better polymer impregnation of the fiber lumens. An analysis of variance (ANOVA) was conducted to determine if the type of level of modifier produced a statistically significant affect on the composite density:

$$Y_{ij} = \beta_0 + \mu_i m_i + \lambda_j l_j + \varepsilon_{ij} \quad (2)$$

Where:

Y_{ij} = response value (density)

β_0 = model intercept

μ_i = coefficient of the main effect for the i^{th} interfacial modifier (i = MA-PHB, DER, Uralac, pMDI)

m_i = the Boolean variable for the main effect of the i^{th} interfacial modifier (i = MA-PHB, DER, Uralac, pMDI)

λ_j = coefficient of the main effect for the level of modifier (j = 0, 1, 2, or 4%)
l_j = the Boolean variable for the main effect of the level of modifier (j = 0, 1, 2, or 4%)
ε_{ij} = error associated with response value

Interpretation of the ANOVA results (Table 12) suggests significant differences in the composite density when incorporating different modifier types and levels. Using the Duncan groupings, it becomes apparent that these differences are largest between 0% and 1% modifier level, and between the composites produced with the Uralac and MA-PHB modifier types.

Given the differences in density and its potential to influence mechanical properties, it is appropriate that we look at the mechanical properties normalized to a mean density, so as to remove any variation in properties due to changes in density. To standardize mechanical properties for a mean density, an analysis of co-variance (ANCOVA) model was utilized. The main effects of both the type and level of modifier was considered, and density will be used as a covariate. The model statement will thus be composed as follows:

$$Y_{ij} = \beta_0 + \mu_i m_i + \lambda_j l_j + \tau\left(\rho_{ij} - \bar{\rho}_{..}\right) + \varepsilon_{ij} \quad (3)$$

Where:
Y_{ij} = response value (E or σ_{max})
β_0 = model intercept
μ_i = coefficient of the main effect for the i^{th} interfacial modifier (i = MA-PHB, DER, Uralac, pMDI)
m_i = the Boolean variable for the main effect of the i^{th} interfacial modifier (i = MA-PHB, DER, Uralac, pMDI)
λ_j = coefficient of the main effect for the level of modifier (j = 0, 1, 2, or 4%)
l_j = the Boolean variable for the main effect of the level of modifier (j = 0, 1, 2, or 4%)
τ = coefficient for the effect of covariate density
ρ_{ij} = the variable density corresponding to Y_{ij}
$\bar{\rho}_{..}$ = grand mean of density

Because density is a continuous and uncontrolled property in this experiment, the density coefficient (τ) reflects an assumed linear relation between changes in density and the response value (i.e. either E or σ_{max}). Using this linear relationship, each individual modulus or strength measurement may be adjusted by its deviation from the mean density.

Stiffness of modified composites

The adjusted values for Young's modulus as a function of modifier type and level are represented in Figure 22. Interpretation of the results indicates that pMDI as a modifier is highly effective at improving stiffness. Even at levels of 1% pMDI added on total, the modulus shows an increase 13% over that of the control. The performance improvement with the addition of pMDI appears to be a near linear trend through to 4% pMDI added on total. With 4% pMDI added to the composite, stiffness is increased to 9.9-GPa (or 21% over the control). The low molecular weight polyester Uralac showed mild signs of improvement over the control, while the low molecular weight epoxy, D.E.R., and maleated PHB showed no practical improvements in stiffness at any level.

The results from the ANCOVA of Young's modulus (Table 13) lead us to determine that both modifier type and level of modifier has a significantly different effect on stiffness. By examining the Duncan's grouping of modifiers, we can see that the stiffness of pMDI-modified systems is significantly higher than that of Uralac, which is higher than D.E.R. and MA-PHB. The Duncan's grouping also suggests that all levels of modifiers show a significantly different effect on stiffness.

The significant interaction of the type and level of modifier most likely results from the different slopes depicted in Figure 22 for each modifier. With increasing levels, pMDI has a much more pronounced effect than Uralac, and D.E.R. and MA-PHB have no effect.

Comparisons of the control composite to other PHB/natural fiber composites may be made if the effect of increased fiber percentages are taken into account. Gatenholm (1992) studied composites with 40% cellulose fiber processed through injection molding with various polymeric matrices. In tensile testing of PP/cellulose composites, the Gatenholm (1992) reported a Young's modulus of 3.7-GPa, polystyrene/cellulose composites had a modulus of 6.3-GPa, and PHB/cellulose composites had a modulus of 6.2-GPa. Previous studies by the authors on the effect of wood fiber loading on PHB also agree with trends noted in stiffness (Anderson, 2007b). Unmodified, and filled with only 40% fiber, the PHB/cellulose composite exhibited much higher stiffness than the PP/cellulose composite. This is consistent with results reported by Beg and Pickering (2006) who studied injection molded PP/WF composites with 60% WF. The PP/WF composites were tested in accordance with ASTM D638, and exhibited a modulus of 2.2-GPa. When coupled with 2% maleated PP (MAPP), the modulus was increased to 5.2-GPa. Alternatively, this study has shown that when PHB/WF is coupled with 2% pMDI, the stiffness may be increased to 9.4-GPa.

Strength of modified composites

The effect of modifier type and level on the tensile strength of the composite is depicted in Figure 23. Unlike the varying effect of modifiers on stiffness, their addition appears to have a positive influence on strength. However, yet again pMDI shows the most drastic of improvements; reaching a maximum strength of 34.5-MPa with 4%, followed by Uralac. D.E.R. and MA-PHB both show modest improvements over the unmodified composite; reaching 28.2-MPa and 25.2-MPa, respectively.

Looking at Table 14 for the results of the ANCOVA on tensile strength it can be seen that again, both modifier type and level has a significant effect on strength. The corresponding Duncan groupings show us that all types of modifiers and levels of modifiers are significantly different from each other with the pMDI producing the highest properties followed by Uralac, D.E.R and MA-PHB.

With respect to strength, PHB/WF composites without interfacial modifier performed comparably to PP/WF composites. In this study, a maximum strength of 22-MPa for the control formulation was achieved. Similarly, Beg and Pickering (2006) reported a tensile strength of 19.9-MPa. Now, a direct comparison cannot be made, because Beg and Pickering used wood fibers treated with a NAOH solution, and used no talc or lubricant. However, as an estimate, this comparison suggests that strength properties may not be significantly different. Once modified with 2% MAPP, the PP/WF composite shows drastic improvements in strength to 45.5-MPa. In contrast, 2% of pMDI added to PHB/WF composites improved the strength to 27.8-MPa. It must be noted, however that in this study, the full potential of pMDI has not been realized. For both stiffness and strength, with the addition of pMDI, each further percent increment of pMDI has only resulted in further improvements. The point at which higher levels of pMDI starts to decrease mechanical properties has not been realized.

Failure strain and impact properties of modified composites

The failure strain of modified composites was recorded as a measure of ductility. Because of the originally brittle nature of PHB and the addition of high wood fiber levels, all recorded failure strains were low for any practical purpose. The control formulation fractured at 0.37% strain and addition of MA-PHB, D.E.R., and Uralac did little to change the failure strain of the composites. While still low, pMDI did exhibit a slight effect on failure strain, increasing it from 0.37% to 0.47% strain with 4% pMDI added on total. Impact properties were also measured. The type and level of modifiers did not significantly affect the notched impact energy of the composites, which ranged from 3.2 to 3.7-kJ/m^2.

Water uptake of modified composites

Because of the hydrophilic nature of wood fibers and the environmental conditions WPCs are often exposed to in application, understanding of the water uptake behavior in WPCs is beneficial. The transport of liquids and gases through a solid medium is often described by Fickian diffusion. Fick's second law describes the transport of molecules through a medium in which the diffusion flux and concentration gradient at a particular point change with time. Under conditions of non-steady state diffusion, the apparent diffusion constant, D_A may be described by:

$$D_A = \pi \left[\frac{h}{4M_{sat}}\right]^2 \left[\frac{\partial M_t}{\partial \sqrt{t}}\right]^2 \quad (4)$$

Where h is the thickness of the sample, M_{sat} is the moisture uptake at saturation, and $\partial M_t/\partial\sqrt{t}$ is the slope of the moisture uptake versus square root of time (Chowdhury and Wolcott, 2007). Water absorption plots exhibit Fickian behavior when $M_t/\sqrt{t}$ exhibits a linear relationship. Deviation from Fickian behavior can occur when approaching saturation, or when composite defects (such as cracks) are present (Roy and Xu, 2001). Formation of micro-cracks may be caused by induced stresses arising from hygrothermal swelling. It is also possible that the presence of these cracks to increase the moisture content at saturation by the addition of surface area or facilitating capillary uptake of moisture.

The percentage of water uptake as a function of the square root of time is plotted in Figure 24 for the 4% level of modified composites. During testing, cracking was visually observed and recorded for each specimen (as shown in Figure 25). The time recorded for the onset of cracking coincided with the inflection in the water absorption slope and increased with the addition of interfacial modifiers. Because of the damage to the composites, the realistic calculation of diffusion coefficients is difficult, as the saturated moisture content and the moisture uptake rate are likely increased.

The point of deviation from Fickian behavior was estimated for each formulation. The inflection point for the control was around 400-$s^{1/2}$, 4% MA-PHB, D.E.R., and Uralac were estimated to change in slope around 500-$s^{1/2}$, and the water uptake slope for 4% pMDI inflected around 725-$s^{1/2}$. Since the cracking is most likely due to hygrothermal expansion of the fibers resulting in a residual stress on the composite, it is reasonable that the pMDI modified composites took the longest to crack. Further, prior to cracking, the slope of the water uptake curve is lowest for the composites modified with 4% pMDI. It is possible that pMDI helps to reduce moisture transport under Fickian conditions as well. The water uptake behavior was also recorded for composite modified with 1% and 2% pMDI. While not shown, the effect of increasing pMDI content from the control composite to the 4% pMDI had the effect of reducing the initial water uptake slope, and increasing the time before cracking and deviation from fickian behavior occur. Similar results were noted in the study of the effect of pMDI on polyethylene/WF composites. The addition of pMDI has been shown to reduce the water uptake rate and saturated moisture content of polyethylene/WF composites (Zhang, 2005).

Influence of modifiers on fracture morphology

After tensile testing, the fracture surface of the composites was imaged. Micrographs of representative fibers for each composite modified at the 4% level are shown in Figure 26. In the first image, the control formulation displays a fiber drawn clean from the matrix with no signs of polymer adhesion. When comparing this to the composites modified with 4% MA-PHB, 4% D.E.R., and 4% Uralac, it can be seen that these composites again show signs of fiber pull-out, but upon close examination, the fibers reveal some degree of polymer adhesion as is evidenced by the irregular surface of the standing fibers. Images of the fiber surface for a composite modified with 4% pMDI do not show fiber pull-out, but rather a clean fracture that likely propagated from the matrix straight through the fiber. For these pMDI modified composites, it appears that the adhesion between the PHB and the fiber is strong enough fracture the fiber and matrix before failing at the interphase.

Examining the macroscopic scale of the composites reveals the same trends. Taken at 300x, Figure 27 displays micrographs of the composites produced with, and without 4% interfacial modifier. Consistent with the microscale view of the control surface, Figure 27a shows a micrograph of the unmodified composite with many examples of fiber pull-out and clean, exposed fibers. Composites modified with 4% MA-PHB, 4% D.E.R., and 4% Uralac all display fiber pull-out, however it is important to note that as the images progress from MA-PHB to D.E.R. to Uralac, the exposed fibers become shorter and the fiber and matrix domains become more difficult to distinguish from one another. In contrast, in micrographs of the 4% pMDI modified composite, no fibers are visible, and the domains between fiber and PHB are indistinguishable, suggesting crack propagation through PHB and fiber and not through the interphase.

With the addition of pMDI to PHB/WF composites mechanical testing has shown a 17% increase in Young's modulus and a 53% increase in tensile strength. Water absorption tests show decreased water uptake and suggest increased resistance to cracking through residual stresses. Observations of the fracture surface also indicated great improvements in adhesion. While the other modifiers (MA-PHB, D.E.R., and Uralac) showed improvements in physical and mechanical properties, for practical purposes and for the purposes of this research, continued investigation will be focused upon pMDI as a modifier.

Effect of pMDI on polymer morphology

While the PHB/WF composites are primarily composed of WF, much can be gained from the understanding of the polymer crystal morphology. The modifying agent pMDI may be serving to chemically or physically bond the PHB to the fiber, crosslink the PHB, or both. The polymer crystalline structure may be assessed through the use of DSC which may yield insight into changes in the polymer crystal perfection (through Tm measurements) or the degree of crystallization.

Displayed in Figure 28 is a representative DSC trace for the unmodified PHB/WF composite. On the initial heating scan, a double melt-peak is evident where crystals with a low degree of perfection melt, anneal, and then melt again. However, this feature is not evident in the second heating scan where the cooling rate is likely slow enough to yield a more homogeneous and ordered crystal structure. This double melting phenomena has been recorded through other literature (Qian, 2007) and through the use of a faster heating rate (20°C/min) it is possible to further minimize the effect of recrystallization. Further, by focusing further interpretation on the second heating and first cooling trace, variability in measurements due to differences in thermal history of the samples can be minimized.

The PHB/WF composites are produced from multiple polymeric components, with each manifesting their unique thermal transitions. To fully understand the different features evident in the scans of the composite material, the behavior of the individual components were examined. Figure 29 and Figure 30 show DSC thermograms for wood fiber, lubricant (WP2200), and the PHB (with boron nitride). Included at 3%, the lubricant displays a melting temperature (T_m) of 148°C, and a crystallization temperature (T_c) of 141°C. The wood fibers show a very broad thermal transition when cooling at ca. 145°C, while the PHB shows a melt temperature of 166°C and a crystallization temperature of 106°C. The thermal signatures of each component can be distinguished in the DSC trace of the composite material (Figure 28). Shown in Figure 29 is an illustration of how the heat of fusion was measured through this study the measurements for all composites were standardized by the mass of PHB within the specimen. The heat of crystallization was similarly measured.

When comparing the melt temperatures of the PHB/BN (Figure 29) with that of the control PHB/WF composite (Figure 28) it can be seen that the incorporation of wood fibers has the effect of decreasing the melt temperature of the PHB by 10°C. Research by Reinsch and Kelley (1997) on PHB/cellulose composites show that the reduction in T_m is due to the reduced crystalline perfection of crystals nucleated on the fiber surface. Studies by Harper (2003) correlate decreases in T_m with the onset of a transcrystalline layer (TCL), or a distinct crystalline structure that forms the fiber surface.

Because the possibility exists that pMDI may react with both the lubricant and the PHB, two additional composites were produced for analysis by DSC. One composite was a control produced

without lubricant, and the other was a composite modified with 4% pMDI and without lubricant. The properties obtained through DSC traces for composites without lubricant are displayed in Table 15. The addition of 4% pMDI increases T_m from 159.9°C to 163.0°C, while the T_c decreases from 106.4°C to 104.9°C and no considerable changes in either the heat of fusion or the heat of crystallization were noted. If pMDI reacts with PHB to form a crosslinked network, the degree of crystallization would likely decrease. Because no changes were noted in ΔH_f or ΔH_c between the modified and unmodified composite, the addition of pMDI had no effect on the degree of crystallization. However, the T_m and T_c did change with the addition of pMDI. Increases in T_m suggest that the perfection of the polymer crystals through the entire composite is increasing. Further, decreases in T_c suggest a decreased ability of the polymer to crystallize. If pMDI is acting at the interface in a manner similar to that of MAPP (Hristov and Vasileva, 2003), it is possible that strong interaction between the pMDI-PHB grafted polymer and the wood fiber is inhibiting the PHB from nucleating on the wood fiber surface. Because crystallites grown from fiber are energetically less stable than spherulitic crystal structures, a macro-scale decrease in the crystallization on the fiber surface would result in an increase in the crystal perfection and the T_m. Similarly, increased interaction between the fiber and the polymer matrix could reduce the mobility of the polymer surrounding the fiber, decreasing the ability of the fiber to act as a nucleation site. Hristov and Vasileva (2003) reported similar findings with PP/WF and rubber-toughened PP/WF composites with the addition of MAPP. The addition of MAPP to PP/WF was shown in this study to prohibit heterogeneous nucleation on the fiber, and thus allow for more spherulitic growth.

However, the composites examined through tensile testing, water absorption, and fracture morphology were all processed with 3% lubricant included in the formulation. With crosslinked polymers, the glass transition temperature (T_g) increases with increased crosslink density due to the restriction of polymer mobility within, and surrounding the crosslinked network. In addition to assessing the melting and crystallization behavior by DSC, DMA was used to assess changes in the T_g. The thermal behavior of these composites modified with 0, 1, 2, and 4% pMDI is illustrated in Figure 31 and Figure 32 for the heating and cooling traces, respectively. Scans of the same composites through DMA are shown in Figure 33. The DMA traces indicate increases in T_g as measured by the onset of the plateau (around 20°C) in the dampening (tan(δ)) trace. Further, an increase in storage modulus (E'), and decreases in both loss modulus (E") and dampening levels can be seen with increases in pMDI content. As seen in Figure 31 and Figure 32, the addition of pMDI to the composite increases T_m and T_c, and decreases ΔH_m and ΔH_c.

Increases in storage modulus reflect the trends observed for tensile testing of the same composites; stiffness increases with increased levels of pMDI. Decreases in dampening levels may indicate increased interfacial adhesion of polymer-WF composites (Correa, 2007). In situations where fiber adhesion is limited, the dampening of a composite should be comparable to that of just the polymer. If fiber adhesion is high, the ability of the polymeric phase to accommodate deformation is limited, and the mechanical dampening of the composite is reduced. Similarly, if adhesion is high, the mobility of polymer chains is limited and the temperature at which the glass transition occurs should increase. The same logic holds for increases in matrix crosslinking as well. If crosslinked networks are present, the ability of the polymeric phase to accommodate deformation is limited, and the mechanical dampening of the composite is reduced. While results indicate increased T_g and dampening, the effects of crosslinking and increased fiber adhesion cannot be distinguished from each other with the given information.

Increases in T_m are possibly the same reflection of increased fiber adhesion discussed for composites without lubricant. Changes in crosslinking should result in an decreased percentage of polymer crystals this would have an effect on the heat of fusion and the heat of crystallization, as there would be fewer crystals to melt, or less polymer available for crystallization. First, the effects of just lubricant on crystallization should be examined. Table 15 also gives the thermal properties for composites processed with lubricant. If the composites processed with and without lubricant are compared, it can be seen that the addition of lubricant decreases the ΔH_m and ΔH_c slightly. However, if pMDI is added to the composite with lubricant, both ΔH_m and ΔH_c show further signs of decreasing (Table 16). This suggests

that the matrix system of pMDI, lubricant, and PHB are crosslinking in some manner, reducing the degree of crystallinity in the composite. It is apparent that the inclusion of lubricant allows for crosslinking of the PHB-pMDI system, but without information on the proprietary structure of the lubricant, no further speculation as to the mechanism of crosslinking may be made at this time.

The T_c also shows a significant increasing trend with the addition of pMDI. Other studies have reported increases in crosslinking, with increases in T_c in the use of isocyanate based interfacial modifiers, but have attributed the phenomena to an increased nucleation effect of the isocyanate (Lee and Wang, 2006). This justification does not fit with the results presented here because a decreased nucleation effect was noted in the composites with no lubricant and pMDI. Based on the results currently available, no viable explanation can be made at this time to fit this phenomena.

Conclusion

Biopolymers have been limited in use to packaging applications since their introduction into consumer products. In an effort to develop PHB for competition in the wood plastics industry with applications such as decking, siding, and fencing, composites of PHB and WF were produced with wood levels comparable to those used for WPC applications. The composites were processed through injection molding to conserve raw materials and produce uniform test specimens. Tensile testing of the unmodified PHB/WF composites resulted in an average Young's modulus of 8.1-GPa, and Ultimate strength of 21.9-MPa. Interpretation of results suggests that PHB/WF composites have high stiffness compared to PP/WF composites, and are more comparable in stiffness with PS/WF composites. The strength of PHB/WF composites was suggested to be comparable with that of PP/WF.

The addition of interfacial modifiers was found to have a positive influence on both stiffness and strength. The most promising interfacial modifier was pMDI. At levels of 0, 1, 2, and 4%, pMDI improved tensile properties more effectively than Uralac, D.E.R., and MA-PHB. The addition of 4% pMDI coincided with a 57% increase in ultimate strength, and a 21% increase in Young's modulus. Similarly, water absorption tests indicate increased resistance to water uptake with the addition of interfacial modifiers with pMDI showing the greatest improvements.

Improved fiber adhesion was suggested with the addition of pMDI, and observed through SEM micrographs. Micrographs of the control showed a large degree of fiber pull-out, and fully exposed fibers. Composites modified with D.E.R. and Uralac showed signs of improved fiber adhesion, and pMDI exhibited complete fiber-matrix coherency.

Investigations into the effect of pMDI on the polymer morphology of PHB/WF composites Showed signs of increased Tm, Tg, and decreased ΔH_m and ΔH_c in the control composite (which included lubricant). Interpretation of these results suggests improved fiber adhesion and possible crosslinking within the PHB-lubricant-pMDI system.

References

Anderson, S.P. 2007a. Effect of Interfacial Modifiers on Mechanical and Physical Properties on PHB/WF and Their Effect on Composite Morphology – Appendix A - Study of Various Lubricants on PHB/WF Composites. Master Thesis, Washington State University, Pullman, WA.

Anderson, S.P. 2007b. Effect of Interfacial Modifiers on Mechanical and Physical Properties on PHB/WF and Their Effect on Composite Morphology – Appendix B - Varied Wood Fiber Levels and HV Content on PHB/WF Composites. Master Thesis, Washington State University, Pullman, WA.

Beg, M.D.H. and K.L. Pickering. 2006. Fiber Pretreatment and Its Effects on Wood Fiber Reinforced Polypropylene Composites. Materials and Manufacturing Processes, 21(3):303-307.

Chen, C., S. Peng, B. Fei, Y. Zhuang, L. Dong, Z. Feng, S. Chen and H. Xia. 2003. Synthesis and Characterization of Maleated Poly(3-hydroxybutyrate). Journal of Applied Polymer Science, 88(3):659-668.

Chowdhury, M.J.A. and M.P. Wolcott. 2007. Compatibilizer Selection to Improve Mechanical and Moisture Properties of Extruded Wood-HDPE Composites. Forest Products Journal, 57(9):46-53.

Clemons, C. 2002. Wood-Plastic Composites in the United States: The Interfacing of Two Industries. Forest Products Journal, 52(6):10-18.

Correa, C.A., C.A. Razzino, and E. Hage. 2007. Role of Maleated Coupling Agents on the Interface Adhesion of Polypropylene-Wood Composites." Journal of Thermoplastic Composite Materials, 20(3):323-338.

Facca, A.G., M.T. Kortschot, and N. Yan. 2006. Predicting the Elastic Modulus of Natural Fibre Reinforced Thermoplastics. Composites Part A: Applied Science & Manufacturing, 37(10):1660-1671.

Gatenholm, P., J. Kubat, and A. Mathiasson. 1992. Biodegradable Natural Composites. I. Processing and Properties. Journal of Applied Polymer Science, 45(9):1667-1677.

Geng, Y., K. Li, and J. Simonsen. 2005. A Combination of Poly(diphenylmethane diisocyanate) and Stearic Anhydride as a Novel Compatibilizer for Wood-Polyethylene Composites. Journal of Adhesion Science and Technology, 19(11):987-1001.

Harper, D.P. 2003. A Thermodynamic, Spectroscopic, and Mechanical Characterization of the Wood Polypropylene Interphase. Doctoral Dissertation, Washington State University, Pullman, WA.

Hristov, V. and S. Vasileve. 2003. Dynamic Mechanical and Thermal Properties of Modified Poly(propylene) Wood Fiber Composites. Macromolecular Materials and Engineering, 288(10):798-806.

Lee, S-H. and S. Wang 2006. Biodegradable Polymers/Bamboo Fiber Biocomposite with Bio-Based Coupling Agent. Composites Part A: Applied Science & Manufacturing, 37(1):80-91.

Lu, J.Z., Q. Wu, and L.I. Negulescu. 2005. Wood-fiber/high-density-polyethylene composites: Coupling agent performance. Journal of Applied Polymer Science, 96(1):93-102.

Manju, M., H. Masud, L.T. Drzal, and A.K. Mohanty. 2005. Studies on Wood and Other Natural Fiber Reinforced Poly(lactic acid) Composites. AIChE Annual Meeting, Conference Proceedings, p. 9477, Oct. 30-Nov. 4.

Qian, J. 2006. Investigation of Crystallization of Poly(3-hydroxybutyrate co-3-hydroxyvalerates) and their Bamboo Fiber Reinforced Composites. Master Thesis, Washington State University, Pullman, WA.

Qian, J., L. Zhu, J. Zhang, and R.S. Whitehouse. 2007. Comparison of Different Nucleating Agents on Crystallization of Poly(3-hydroxybutyrate-co-3-hydroxyvalerates). Journal of Polymer Science: Part B: Polymer Physics, 45(13):1564-1577.

Reinsch, V. and S.S. Kelley. 1997. Crystallization of Poly(hydroxybutyrate-co-hydroxyvalerate) in Wood Fiber-Reinforced Composites. Journal of Applied Polymer Science, 64(9):1785-1796.

Roy, S. and W. Xu. 2001. Modeling of Diffusion in the Presence of Damage in Polymer Matrix Composites. International Journal of Solids and Structures, 38(1):115-125.

Sombatsompop, N., C. Yotinwattanakurntorn, and C. Thongpin. 2005. Influence of Type and Concentration of Maleic Anhydride Grafted Polypropylene and Impact Modifiers on Mechanical Properties of PP/Wood Sawdust Composites. Journal of Applied Polymer Science, 97(2):475-484.

Zhang, C., K. Li, and J. Simonsen. 2005. Improvement of Interfacial Adhesion Between Wood and Polypropylene in Wood-Polypropylene Composites. Journal of Adhesion Science and Technology, 18(14):1603-1612.

Zhang, J., S. McCarthy, and R.J. Whitehouse. 2004. Reverse Temperature Injection Molding of Biopol and its Effect on Properties. Journal of Applied Polymer Science, 94(2):483-491.

Figures

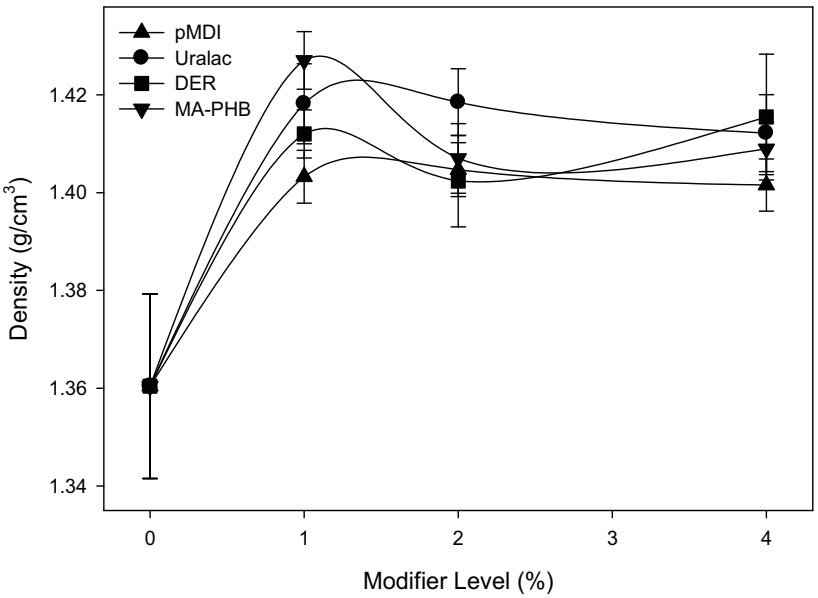

Figure 21. Effect of modifiers on density.

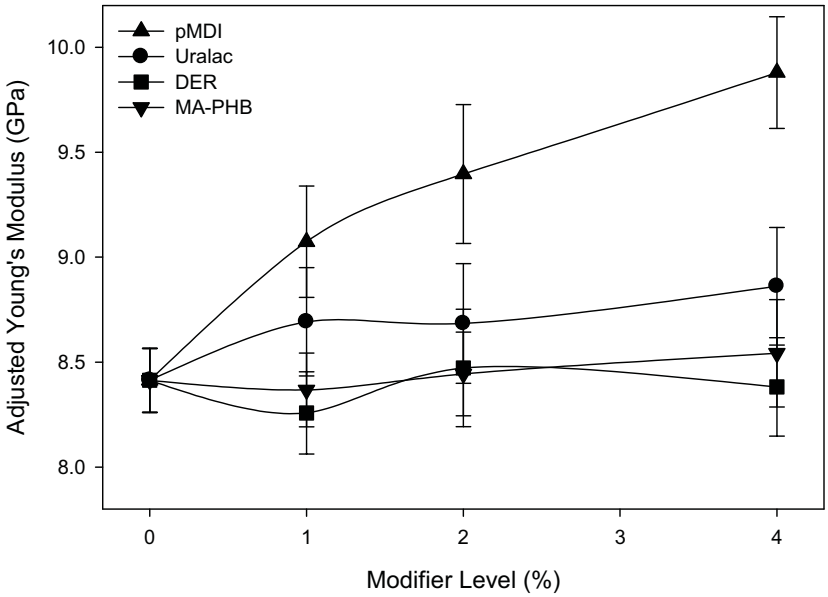

Figure 22. Tensile modulus of PHB/WF and PHB/WF modified composites.

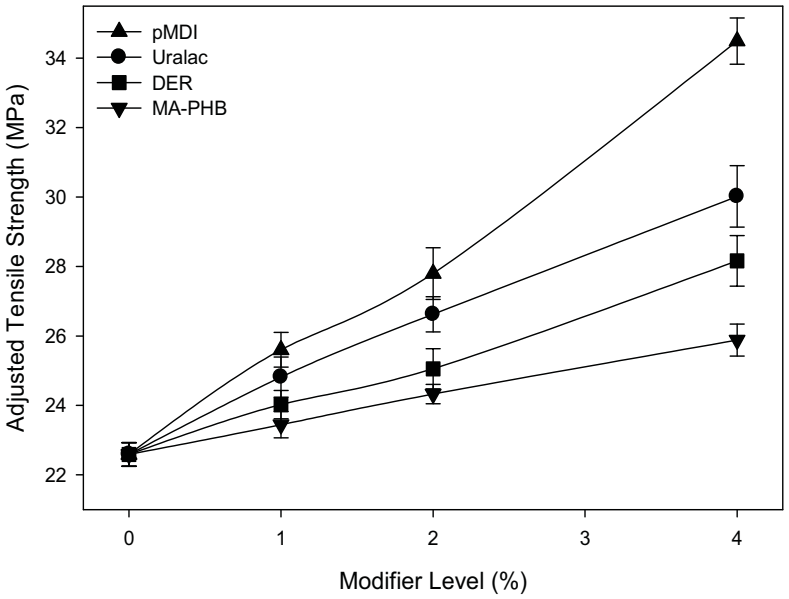

Figure 23. Tensile strength of PHB/WF and PHB/WF modified composites.

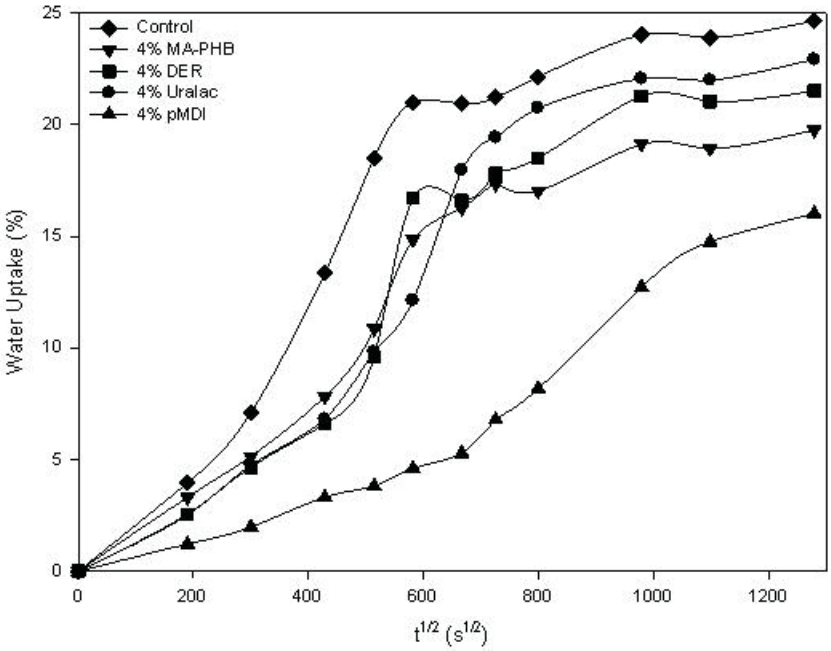

Figure 24. Water absorption of PHB/WF and PHB/WF modified composites at 4% on total, plotted against the square root of time.

Figure 25. Specimen photograph of PHB/WF composite depicting cracking damage occurring during water absorption experiments. All specimens experiencing such damage were noted.

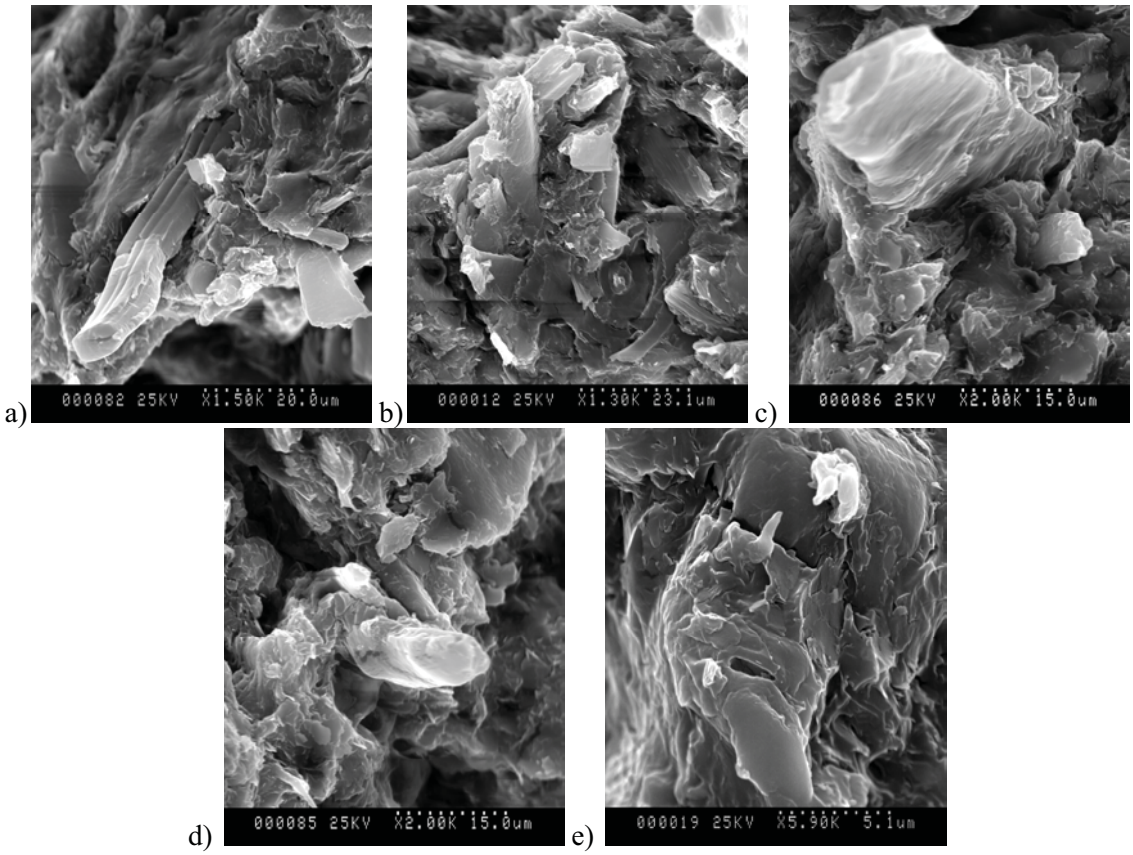

Figure 26. SEM micrograph of tensile-fractured PHB/WF: a) Unmodified, and modified with b) 4% MA-PHB, c) 4% D.E.R., d) 4% Uralac, and e) 4% pMDI.

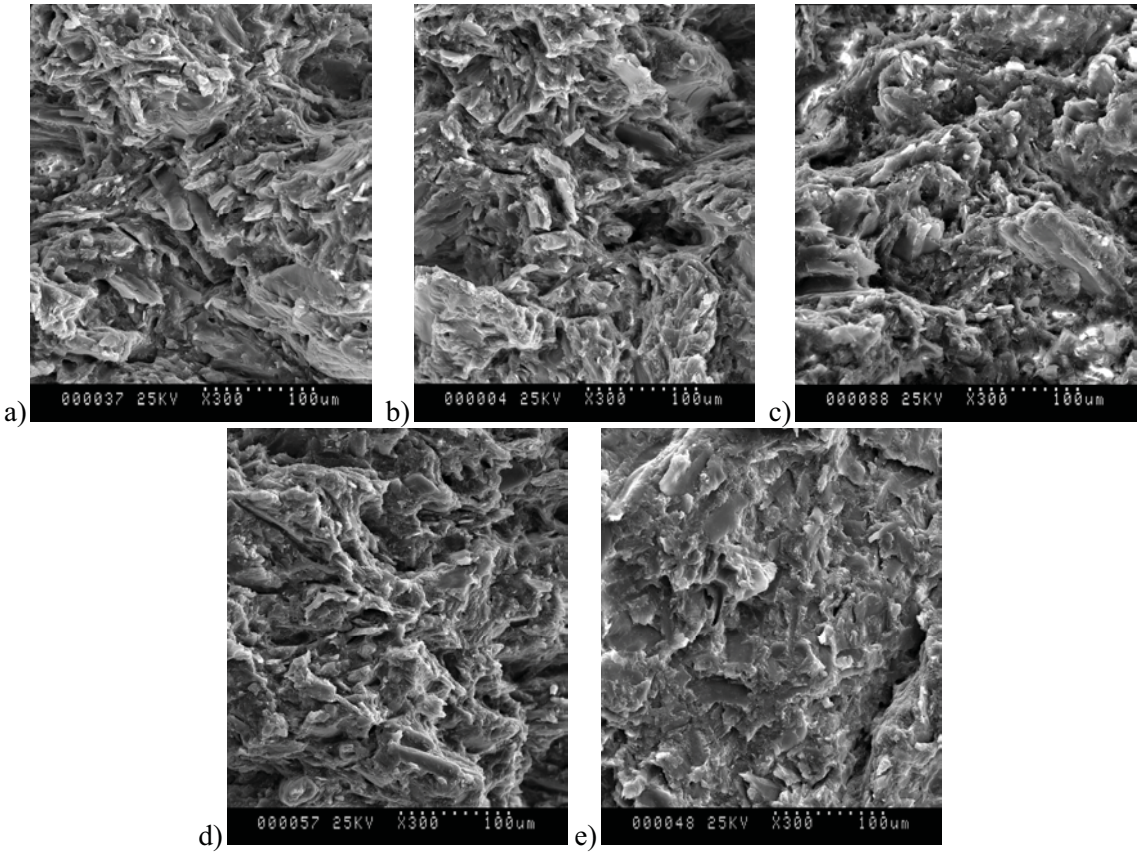

Figure 27. SEM micrograph of tensile-fractured PHB/WF, taken at 300x. The composites are; a) Unmodified, and modified with b) 4% MA-PHB, c) 4% D.E.R., d) 4% Uralac, and e) 4% pMDI.

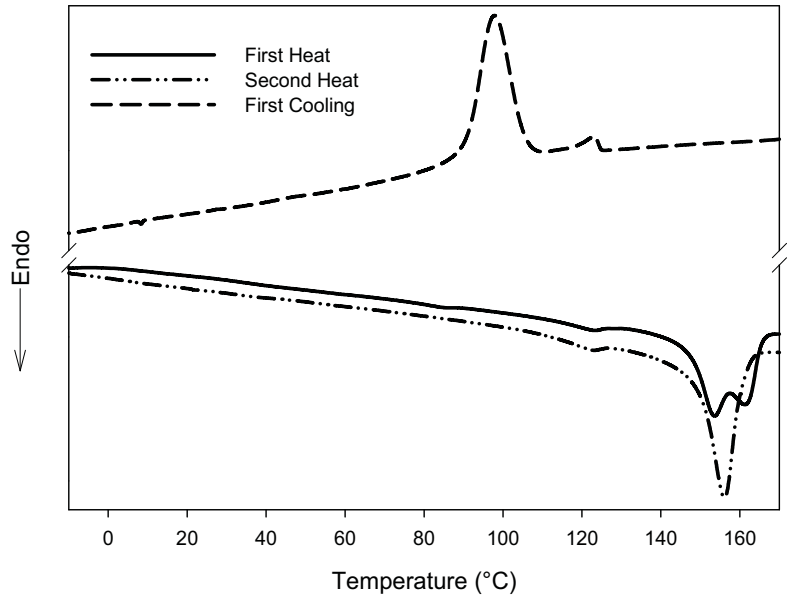

Figure 28. DSC thermogram of one full heat treatment of PHB/WF. Includes 1st heat, cooling, and 2nd heat.

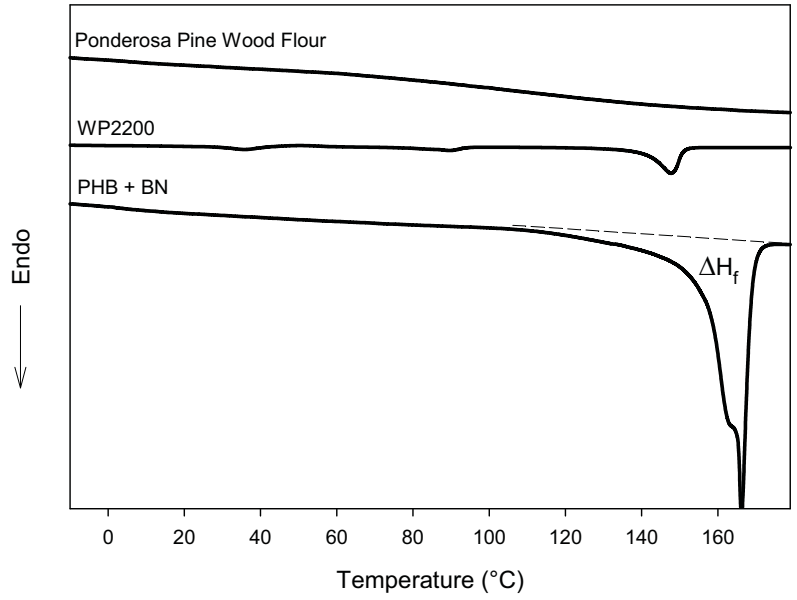

Figure 29. Example DSC thermograms of the neat polymeric components used to produce the various composites.The area used to measure values for ΔH_f is indicated.

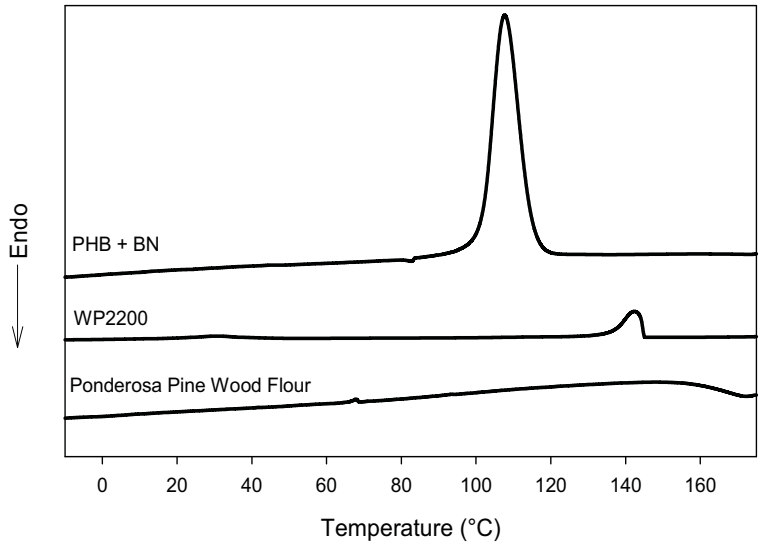

Figure 30. Example DSC thermogram of the cooling of neat polymeric components used to produce the various composites after 2 min at 180°C.

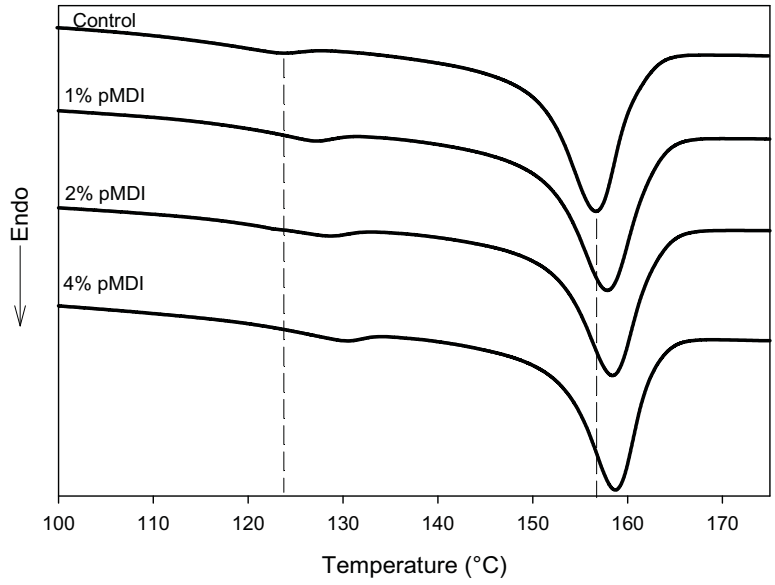

Figure 31. DSC thermogram of PHB/WF systems modified with pMDI including lubricant. Heat is measured in J/g of PHB.

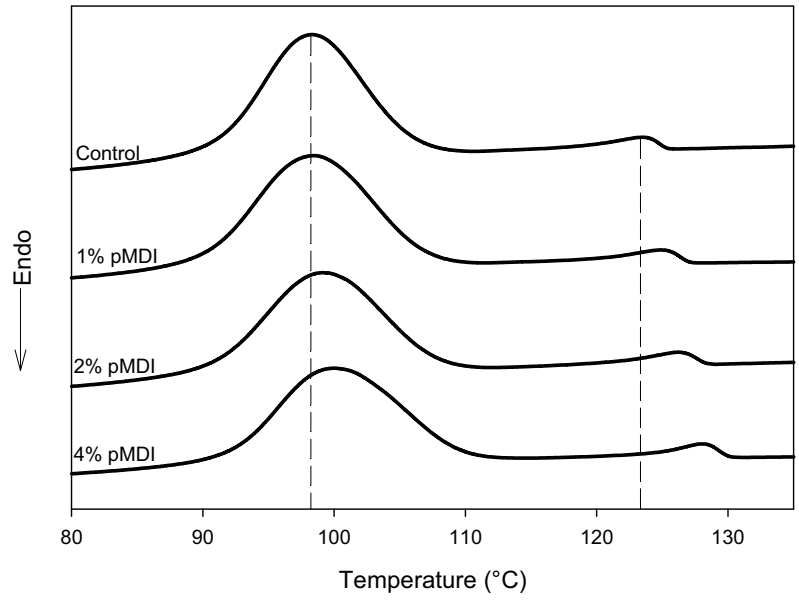

Figure 32. DSC thermogram of PHB/WF systems modified with pMDI including lubricant, cooling after 2 min at 180°C. Heat is measured in J/g of PHB.

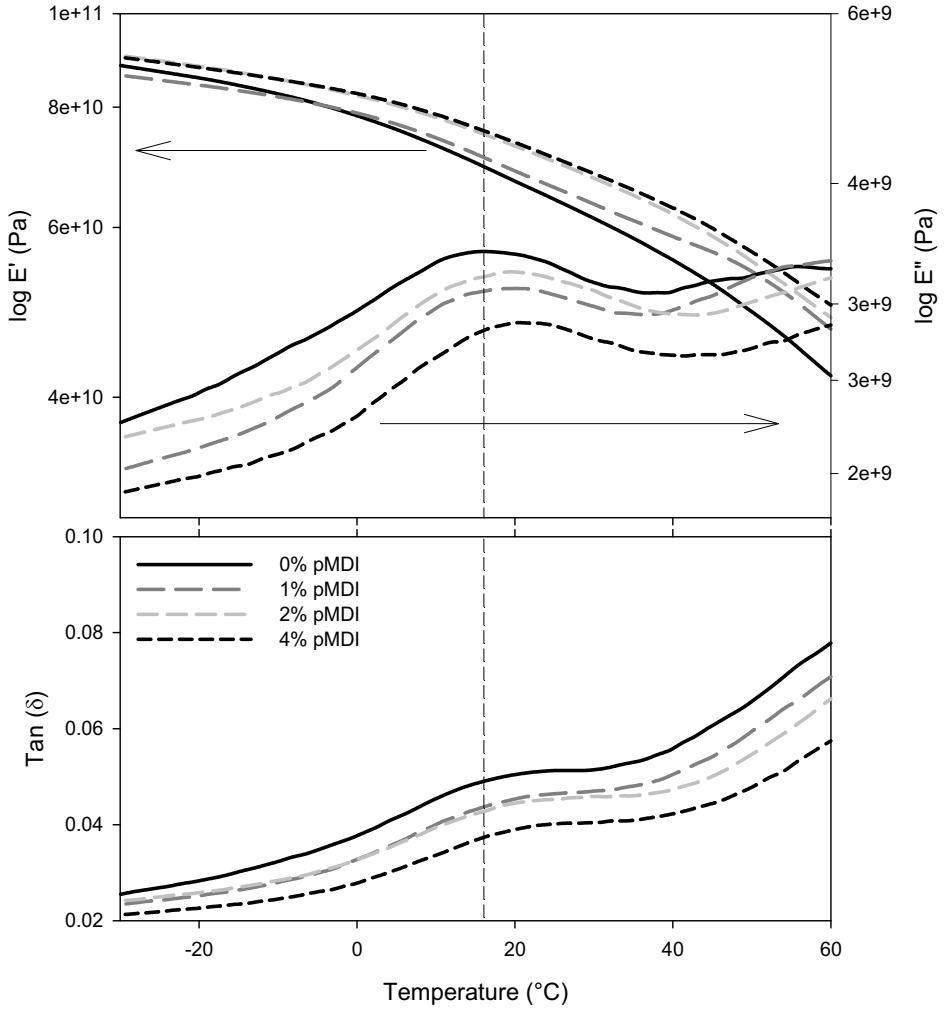

Figure 33. DMA scan of PHB/WF systems modified with pMDI (including WP2200).

Tables

Table 11. Structure of interfacial modifiers and possible reactions with the wood fiber surface.

Modifier	Structure	WF Interaction
MA-PHB	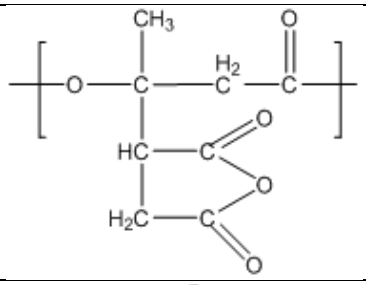	Esterification
D.E.R.	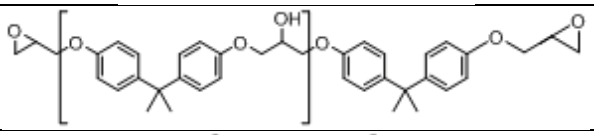	Etherification
Uralac	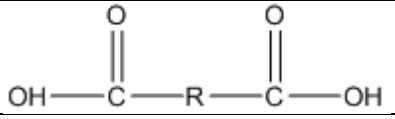	Esterification
pMDI	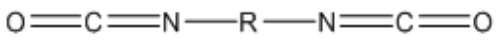	Urethane linkage

Table 12. Type III ANOVA and Duncan grouping for effect of modifiers and levels of modifiers on density (R2 = 78.8%).

Source	DF	Type III SS	Mean Square	F Value	Pr > F
Modifier	3	0.0045	0.0015	10.09	<0.0001
Level	3	0.1568	0.0523	352.05	<0.0001
Modifier*Level	9	0.0067	0.0007	5.01	<0.0001

Modifier	Uralac	pMDI	DER	MA-PHB
Duncan Grouping	A	A B	B	C
Mean (g/cm^3)	1.402	1.400	1.398	1.392

Level	1	4	2	0
Duncan Grouping	A	B	B	C
Mean (g/cm^3)	1.415	1.410	1.408	1.36

Table 13. Type III ANCOVA and Duncan grouping for effect of modifiers and levels of modifiers on tensile modulus (R2 = 79.3%).

Source	DF	Type III SS	Mean Square	F Value	Pr > F
Modifier	3	1.01	0.34	5.40	0.0012
Level	1	7.26	7.26	116.17	<0.0001
Modifier*Level	3	12.58	4.19	67.10	<0.0001
Density	1	4.82	4.82	77.08	<0.0001

Modifier	pMDI	Uralac	MA-PHB	DER
Duncan Grouping	A	B	C	C
Mean (GPa)	9.15	8.63	8.36	8.33

Level	4	2	1	0
Duncan Grouping	A	B	C	D
Mean (GPa)	8.93	8.76	8.64	8.14

Table 14. Type III ANCOVA and Duncan grouping for effect of modifiers and levels of modifiers on tensile strength (R2 = 97.3%).

Source	DF	Type III SS	Mean Square	F Value	Pr > F
Modifier	3	531.43	177.14	625.36	<0.0001
Level	1	1457.24	485.75	1714.80	<0.0001
Modifier*Level	3	422.15	46.91	165.59	<0.0001
Density	1	2.70	2.70	9.53	0.0022

Modifier	pMDI	Uralac	MA-PHB	DER
Duncan Grouping	A	B	C	D
Mean (MPa)	27.53	25.95	24.83	23.78

Level	4	2	1	0
Duncan Grouping	A	B	C	D
Mean (MPa)	29.82	25.99	24.58	21.95

Table 15. Effects of 4% pMDI on and lubricant thermal properties of composites. Heat is measured in J/g of PHB.

% Lubricant	% pMDI	Melt		Crystallization	
		T_m (°C)	ΔH_m (J/g)	T_c (°C)	ΔH_c (J/g)
0	0	159.9	9.96	106.4	8.72
0	4	163.0	10.04	104.9	8.45
3	0	157.3	9.02	97.7	7.90

Table 16. Effects of pMDI on thermal properties of PHB/WF including lubricant. Heat is measured in J/g of PHB.

% pMDI	Melt		Crystallization	
	T_m (°C)	ΔH_m (J/g)	T_c (°C)	ΔH_c (J/g)
0	157.3	9.02	97.7	7.90
1	158.2	8.46	98.2	7.59
2	158.4	7.98	98.9	7.39
4	159.0	7.15	100.2	6.69

Effect of Processing on Physical and Mechanical Properties of PHB/WF Composites

Abstract

Composites made from polyhydroxybutyrate (PHB) and wood fiber (WF) have been shown to exhibit excellent mechanical properties. Unfortunately no studies have, as of yet investigated PHB/WF composites as processed through extrusion processes. This is significant because extrusion is preferred processing method for wood plastic composite (WPC) products such as decking and siding. This study utilizes parallel formulations of composites to investigate the influence of interfacial modifiers and processing method. Mechanical and physical properties were investigated through tensile, impact, density, and water absorption tests. It was found that injection molding produced composites of a higher density, and that differences in density produced a direct effect on stiffness and strength of the composites. The stiffness and strength of injection molded formulations was higher than that of the same formulations processed through extrusion. Both processing methods displayed similar trends in mechanical properties with the increasing effectiveness of incorporated interfacial modifiers. Water absorption tests showed similar trends across modifying agents from injection molding to extrusion. However, hygrothermal strains within the higher density injection molded samples resulted in surface cracking and increased water uptake of specimens. Changes in all of the physical and mechanical properties investigated suggest better dispersion of the injection molded specimens when compared to the same formulations processed with extrusion. The difference in dispersion may result from the pre-compounding step prior to injection molding, and density differences from the high packing pressures used during injection molding. Microtomed surfaces of the composites were viewed through scanning electron microscopy (SEM), and show further evidence of improved fiber dispersion from injection molding. Differential scanning calorimetry (DSC) was used to investigate differences in crystallization. While results indicate that extrusion processing resulted in a greater degree of crystal perfection from that of injection molding, no correlations may be made regarding the implications on mechanical properties at this time.

Introduction

Polymer/natural fiber composites have increasingly been utilized for consumer products (Smith and Wolcott, 2006). Most predominantly, wood plastic composites have made their way into the home construction industry. Used in products such as decking, siding, window framing, and fencing, WPCs have proven to be cost-effective, environmentally friendly, and durable alternatives to wood lumber (Smith and Wolcott, 2006). For most of these products, extrusion processes are employed (Clemons, 2002). Due to growing environmental concerns, however, the use of natural fiber composites is rapidly expanding into other markets. Non-structural automotive parts, food storage/utensils, and packaging for consumer products have started to emerge as natural fiber composite products (Bledzki and Gassan, 1999). Such new applications for natural fiber composites require the ability to manufacture complex, three dimensional shapes. While extrusion processes can produce components with constant cross section, injection molding may be used to produce many complicated shapes. Much experimental development on composite material properties has been undertaken through both means of processing. Studies employing the extrusion process are commonly conducted at fiber loading levels of at least 50%, and more commonly 60-70% (Chowdhury and Wolcott, 2007). Conversely, fiber composite formulations designed for injection molding commonly contain at most 50% fiber, and more commonly 10-40% fiber (Singh and Mohanty, 2007). With injection molding, lower fiber loading levels are preferred to achieve good flow and surface properties through the mold (Kato, 1999).

Often, studies aimed at improving composite properties for materials destined for specific applications utilize processing methods used commercially to create the consumer product. For example, a study investigating the use of a compatibilizer system to improve the mechanical properties of polyethylene/wood fiber (PE/WF) composites used a compression molding machine to produce test

specimens (Geng, 2006). The same study was aimed at improving the properties of wood plastic composites (WPCs) that have applications in decking and siding. Because processing methods such as injection molding and compression molding are a semi-continuous processing method from which test coupons may directly be formed, such processing methods are often preferred for laboratory scale research.

While basic research on compatibilizers and interfacial modifiers is necessary, it is possible for variation in processing methods to have a tremendous effect on physical and mechanical properties (Chambers, 2001; Stark, 2004). Further, the effect of the interfacial modifier may alter the rheology or wetting of fibers which, depending on processing conditions may, or may not have an influence on composite properties of the test coupon.

In their early stage of commercial development, PHB and other PHAs are relatively expensive, but with advances in production technology, the price is anticipated to continuously decrease (Esposito, 2005). Owing to their easier crystallization and relatively higher crystallinity than that of PLA, PHB and some PHBVs show higher heat distortion temperatures (HDT) and higher resistance to diffusion. In recent years, PHAs and their composites have received extensive study from both academia and industry for cost effectiveness and performance enhancement (Esposito, 2005; Chen, 2003). Thus far, all studies published involving PHB and natural fibers have employed either injection molding, or compression molding for processing of composites (Singh and Mohanty, 2007; Fernandes, 2004). For the laboratory setting, these processes are particularly useful because only limited quantities of raw material are necessary to produce a suitable number of processed coupons for testing. Nevertheless, information lacks on the properties of extruded PHB or other PHA/natural fiber composites.

Previous research (Anderson, 2007) has found that interfacial modifiers have a positive influence on composite mechanical and physical properties. Inclusion of all interfacial modifiers at levels of 4% on the total mass of the composite resulted in higher strength, decreased moisture transport, and in one case, improved stiffness. While high levels of wood fiber were used for these studies, a practical comparison of mechanical and physical properties with wood composites similar to those used in WPC applications still cannot be made. In this study, the mechanical and physical properties of extruded PHB/WF composites will be presented, and the properties of parallel formulations, as processed through injection molding will be compared.

Objectives

The focus of this study is to determine the effects of scale-up in the processing of PHB/WF composites and to determine the viability of commercial PHB based WPCs. The objectives of this study are to:

1. Improve the mechanical and physical properties of extruded PHB/WF composites using interfacial modifiers.
2. Compare mechanical and physical properties of PHB/WF composites, as processed through injection molding and extrusion.
3. Isolate possible differences between injection molding and extrusion that may influence interpretation for studies intended to be scaled up.

Approach

Formulations of PHB/WF composites were produced with, and without interfacial modifiers through both injection molding and extrusion processes. Composites were modified with maleated PHB (MA-PHB), low molecular weight epoxy resin, D.E.R., low molecular weight polyester, Uralac, and polymethylene diphenyl diisocyanate (pMDI). Previous studies (Anderson, 2007) showed improvements in mechanical and physical properties with the addition of these interfacial modifiers. The authors of this study wanted to compare not only the properties of PHB/WF through different processes, but to determine differences as PHB/WF composites are modified as well. Composites were processed at comparable temperatures and standard cooling methods were used for each processing method.

Mechanical properties were investigated through tensile and flexural testing, notched impact testing, and water absorption tests.

Materials

PHB (Tianan Biologic Material Co., Ltd, Ningbo, China) and 60-mesh ponderosa pine wood flour (American Wood Fibers, Schofield, WI) were used to form the basis of the wood composites. To improve processing by both injection molding and extrusion, lubricant in the form of Glycolube WP2200 (Lonza, Inc., Allendale, NJ) and talc (Nicron 403 obtained from RioTinto of Centennial, CO) were used as additives. Further, because PHB has been known to crystallize slowly, nucleating agent was employed to speed up nucleation and reduce secondary crystallization (Qian, 2007). Based results reported by Qian (2007), fine boron nitride (BN) in platelet form was chosen as a nucleating agent (Carbotherm PCTF5, obtained from Saint Gobain Advanced Ceramics Corporation, Amherst, NY). Interfacial modifiers shown previously (Anderson, 2007) to improve mechanical properties were incorporated at the 0, or 4% level. The use of interfacial modifiers allowed the authors to investigate differences in processing due to differences in fiber wettability and/or melt viscosity. The modifiers include pMDI (Mondur G541, supplied by Bayer MaterialScience, Pittsburgh, PA), MA-PHB, D.E.R. 662E (DOW, Midland, MI), and Uralac P5142 (DSM Resins US, Inc, Augusta, GA). Finally in order to produce MA-PHB, maleic anhydride (95% purity) and dicumyl peroxide (98% purity) were obtained from Aldrich (St. Louis, MO).

Methods

Grafting of MA-PHB

Qian (2006) described production of MA-PHB through reactive extrusion. Based on this report, MA-PHB was produced through reactive grafting in a torque rheometer (Haake Polylab 3000P). The raw components consisted of 95 parts PHB, 5 parts maleic anhydride, and 0.5 parts dicumyl peroxide. These were mixed in a torque rheometer at 180°C and 50 rpm for 40 minutes. Following reactive processing, a vacuum oven (100°C for 12 hours) was used to remove the residual maleic anhydride not grafted to the PHB.

Premixing

Composites of wood fiber reinforced PHB were produced with ca. 60% wood fiber in order to reflect industry standard levels of reinforcement for products such as WPC decking. Higher levels of reinforcement increase melt pressures in extrusion such that the composites may retain their shape after exiting the die. To remove moisture prior to processing, PHB was dried for 12 hours at 100°C, and the wood flour was dried by steam tube to a moisture content of 2.8-mass % (based on oven dry weight). Composite compositions were as follows: 35 parts PHB, 57 parts WF, 8 parts Talc, 0.2 parts BN, 3 parts WP2200, and 4 parts interfacial modifier.

The raw components were assembled and dry blended by tumbling the mixture in a plastic bag (for injection molded quantities), or by tumbling in a drum mixer for 10 minutes (for extrusion on the Cincinatti Milicron CM 35). Prior to dry blending, pMDI was dispersed in small quantities of PHB using a standard kitchen blender for 1 minute. The pMDI-rich PHB was then dispersed back into the bulk PHB for use in the WF composites modified with pMDI.

Processing by injection molding

Preparing samples through injection molding is a two step process. It is often desirable to compound composites using a twin screw extruder in order to ensure good distribution and mixing of composite components. For compounding, a co-rotating twin screw extruder equipped with a volumetric feeder was utilized (Leistritz ZSE-18). The screw diameter was 17.8-mm, and the L/D ratio was 40. Extrusion temperatures were independently controlled on eight zones along the extruder barrel. A reverse temperature profile was chosen in order to reduce thermal degradation and improve melt strength (Zhang, 2004). From the feeding throat to the die adapter, the temperatures were set as follows; 170°C, 175°C,

170°C, 165°C, 164°C, 163°C, 162°C, and 160°C. The screw speed was maintained at 125 rpm, and the resulting residence time was measured to be around 1.5 minutes. After exiting the die, the extrudate was discharged into air and cooled naturally. Finally, the extrudate was ground into granules using a granulator fitted with a 6 mm pore-size screen (Nelmor, G810M1).

Standard tensile (ASTM D638, type I) specimens and flexure bars (12 x 3 x 127 mm) were produced by injection molding (Sumitomo SE 50D). The temperature zones of the injection molding machine were independently controlled at 175°C, 180°C, 175°C and 165°C from the feeding end to the nozzle. The mold temperature was held constant at 60°C, and the average cycle time was 50 seconds. The filling pressure was set for 1700-kgf/cm^2 and packing pressures were set to 1275-kgf/cm^2 and 1360-kgf/cm^2 for the 1st and 2nd stage, respectively. Residence times were consistently measured around 5 minutes.

Processing by extrusion

After dry blending in a drum mixer for 10 minutes, composite blends were fed through a conical co-rotating twin screw extruder (Cincinnati Milicron CM 35). The screw diameter is tapered from 35-mm at the feeding throat to the die, and the length-to-diameter ratio of the extruder was 22. A slit die with cross section dimensions of 3.7 x 0.95-cm was used to produce rectangular bars. The temperature zones were independently controlled through 3 barrel zones, 2 die zones, and through the screw at 170, 175, 163, 162, 160, and 160°C, respectively. Melt pressures ranged from 4.5 to 7.5-MPa, and residence times averaged around 5 minutes. Upon exiting the die, the extrudate was cooled through a cold water bath.

Preparation of test specimens

For tensile testing, the injection molded bars were used as received (type I geometry). Extruded samples were trimmed by a shaper to match the geometry for type III tensile tests. Flexure tests were also conducted using the rectangular specimens as received from injection molding, and the as received profile extrusion specimens (cut to 20 cm in length). For impact testing, the test specimens were prepared in accordance with ASTM D256. The straight bars produced through injection molding were cut to 62 mm lengths from both ends of the bar (and were labeled accordingly). The specimens were notched using a V-shaped specimen notch cutter with a 0.25-mm notch radius (XQZ-I, Chengde Jinjian Testing Instrument Co., Ltd.). The extruded samples were milled down to the core such that the long axis of the impact specimen matched that of the extrusion direction with dimensions of 62 x 12.5 x 3-mm (to match the size of the injection molded specimens). Extruded samples were similarly notched.

Specimens for water absorption tests were milled on a manual milling machine to dimensions of 11 x 2.5 x 125-mm. Both the injection molded and extruded specimens were milled from the exterior skins towards the core. It was necessary to mill the injection molded specimens in order to remove any polymer-rich cap, and it was necessary to mill the extruded specimens such that the process of moisture transport happened on the same scale as with the injection molded specimens.

Mechanical and physical properties

Tensile tests were performed on all composites in accordance with ASTM D638. Specimens were of type I and type III geometry for injection molded specimens, and extruded specimens, respectively. All specimens were conditioned 48 hours prior to testing. Testing was performed using a screw driven Instron 4466 Standard with a 10-kN electronic load cell. The crosshead speed was 5-mm/min, and the initial strain was measured with a clip-extensometer with a 25-mm gage length (MTS model # 634.12E-24). The geometry (length, width, and thickness) and weight were measured on all samples and density was calculated on a weight/volume basis. Flexural testing was executed in accordance with ASTM D790. The support span was set to be equal to 16 times the specimen depth.

To investigate the fiber dispersion and/or fiber breakdown of the composites, cross sections of the composite surface were cut using Reichert Ultramicrotome fitted with a glass knife. Water was used to facilitate smooth cuts to the composite surface. After removing the surface moisture under a hot light the

specimens were placed in a desicator to further reduce the surface moisture content. The dried specimens were then sputter coated with gold for observation by scanning electron microscope (SEM) on a Hitachi S-570.

Because improvements in interfacial modification in polymer-fiber composites may reveal improved toughness and resistance to crack propagation, notched impact tests were performed to assess differences in interfacial adhesion, or processing method. Notched impact tests were performed in accordance with ASTM D256, method A. The Izod pendulum impact test frame was configured for a maximum impact energy of 2.7-J.

Immersion test ASTM D570 was in part, adopted to measure the water absorption of the composites. Specimens were soaked in a bath of distilled water held at room temperature. Prior to taking measurements, specimens were blot-dried with a towel and allowed to naturally dry in air for 10 minutes. The moisture content (MC) was calculated on a mass percent basis using the following equation:

$$MC = \frac{(M - M_o) \times 100}{M_o} \quad (1)$$

Where M is the weight of the specimen at time t, and M_o is the initial (dry) weight of the specimen.

Statistical Analysis

To help sort the influence of processing vs. interfacial modifiers, mechanical properties were assessed using an analysis of variance (ANOVA). When significant, the influence of density was accounted for as a covariate. The resulting analysis of covariance (ANCOVA) helped to account for the variability in mechanical properties due to variance in density. A general linear model with significance, $\alpha = 0.01$ was employed through SAS statistical software (SAS Version 6.9.1, SAS Institute Inc., Cary, NC).

Thermal Properties

Properties of the polymer melt and crystallization for the composites were examined using a differential scanning calorimeter (DSC) (Mettler Toledo, DSC 822e). Injection molded samples were taken from tensile specimens in a specific location in the center of the specimen. Extruded DSC samples were taken from the bulk of the cross section (2-mm from the edges). All tested specimens weighed from 3-6-mg and were hermetically sealed in 40-µl aluminum crucibles. Each sample was heated from -30°C to 180°C at 20°C/min in order to obtain information for the polymer crystal morphology post processing. All samples were aged similarly, post processing.

Results and Discussion

Effect of processing on density

In the processing of materials through injection molding, most systems employ two stages for applying pressure to force the molten material into the mold cavity. Initial injection of the material is controlled by the injection pressure. This stage is used to force a set volume of material (as determined by the injection shot size) into the mold cavity (Osswald, 2006). Once the mold cavity has been filled, additional material is forced into the cavity to compensate for shrinkage of the material as it cools on contact with the cool mold wall. This excess pressure to compensate for material contraction is specified by the packing pressure (Kamal, 1977).

Conversely, extrusion processes rely on normal stresses developed due to the pressure of the melt being forced into smaller volumes by the screw. This normal stress forces the extruded material to take the shape of the die (White, 1977). Depending on the formulation, the melt pressures of the PHB/WF composites through extrusion ranged from 5.1-MPa to 7.2-MPa. In contrast, the filling pressure for injection molding was held constant at 167-MPa, and the packing pressure was held at ca. 128-MPa.

Given the differences in processing pressures, it would be apparent that these two methods would lead to differences in composite density.

As is depicted in Figure 34, the two processing methods do result in differing densities. For the unmodified PHB/WF composite the results show a jump in density from 1.29-g/cm^3 to 1.36-g/cm^3 for the extruded and injection molded composites, respectively. These differences in density are within reasonable limits, as HDPE/WF composites processed by injection molding and extrusion have exhibited densities of 1.40-g/cm^3 and 1.26-g/cm^3, respectively (Stark, 2004).

Statistical analysis of stiffness and strength

Previous studies have shown that the influence of density on mechanical properties is very strong (Facca, 2006). An analysis of covariance (ANCOVA) is a general linear model with which the power of an analysis of variance (ANOVA) is combined with the features of a linear regression. The ANCOVA describes main effects after removing the variance in the response variable due to the variance in the continuous covariate. If the effect of the covariate is found to be significant, then equal regression slopes are assumed. This assumption allows for a single regression relationship to be estimated between the covariate and the response variable. Using either Young's modulus or tensile strength (E, or σ_{max}, respectively) the ANCOVA model statement was constructed as follows:

$$Y_{ij} = \beta_0 + \varphi_i p_i + \mu_j m_j + \tau\left(\rho_{ij} - \bar{\rho}_{..}\right) + \varepsilon_{ij} \quad (2)$$

Where:
Y_{ij} = response value (E or σ_{max})
β_0 = model intercept
φ_i = coefficient of the main effect for processing method (i = Injection Molded, Extruded)
p_i = the Boolean variable for the main effect for processing method (i = Injection Molded, Extruded)
μ_j = coefficient of the main effect for the ith interfacial modifier (i = MA-PHB, DER, Uralac, pMDI)
m_j = the Boolean variable for the main effect of the ith interfacial modifier (i = MA-PHB, DER, Uralac, pMDI)
τ = coefficient for the effect of covariate density
ρ_{ij} = the variable density corresponding to Y_{ij}
$\bar{\rho}_{..}$ = grand mean of density

Using τ, subsequent adjustments may be made to the original response variable in order to express them at a common density. Since the extruded specimens all exhibited lower density than the injection molded specimens, the general effect of adjusting to a mean density is that the stiffness and strength for the extruded specimens is raised relative to the injection molded specimens.

The high packing pressures applied on the part while solidifying in the mold helps the densification of the materials and wetting of fiber by the polymer. With extrusion, the increases in fiber affinity with more effective modifiers may allow for better fiber disintegration. As fiber bundles are broken down, the interfacial area across which stress may be transmitted is increased. As is shown in Figure 35, this has the effect of increasing the composite stiffness of the extruded specimens from that of the unmodified composite.

In contrast, composites produced through injection molding display comparable modulii, with the exception of the composite modified with pMDI. Where different modifiers improved stiffness of composites processed through extrusion, the same composites show little difference in stiffness processed through injection molding. It is possible that the effects of increased fiber wetting have no benefit in light

of the high-shear pre-compounding process, and the high pressures of the injection molding process. However, the high stiffness of the pMDI is no fluke, as was shown previously (Anderson, 2007) increasing amounts of pMDI added to PHB/WF composites consistently resulted in higher composite stiffness. It is likely that in addition to better wetting of the wood fibers, pMDI is helping to physically or chemically improve the PHB-fiber adhesion.

Interpretation of the ANCOVA results (Table 18) for stiffness suggests that all factors have a significant effect on stiffness. Examination of the Duncan groupings does not indicate differences between the Uralac and the MA-PHB, as well as the D.E.R. from the control. However, the mean value separation of the Duncan groupings are taking into account the mean from both injection molding and extrusion processes. Similarly, in averaging the effect of different modifiers, the Duncan grouping also suggests a significant difference between injection molding and extrusion.

The results from the ANCOVA lead us to conclude that all effects for tensile strength are significant. The effect of processing is still highly significant, but less so than with stiffness because of the convergence in strength properties with the addition of more effective modifiers. The Duncan groupings also support the notion of significant differences in strength between all modifiers and between both injection molding and extrusion processes.

The adjusted values for tensile strength as a function of processing method and modifier type are represented in Figure 36. Interpretation of the results suggests that the tensile strength of composites processed by injection molding is generally higher than that of composites processed by extrusion. However, as the modifiers increase in effectiveness, the differences between composites processed by different methods decreases. This behavior suggests two competing effects; the first is that the addition of the interfacial modifier improves fiber wetting and as a result facilitates fiber dispersion through the composite, the second effect is that the high shear rate involved in pre-compounding (a twin screw speed of 125-rpm) followed by the high shearing of the composite during injection molding facilitates better mixing and fiber dispersion. With the control formulation a large difference in strength can be seen between the extruded and the injection molded samples, here injection molding is likely dispersing fibers more thoroughly through the composite allowing for stress to be shared equally among the fibers. With the addition of 4% pMDI, no practical difference in strength is present between the composites processed by both methods.

While no other studies have used PHAs in composites reinforced with wood fiber at levels of 60% WF, data from other fiber composites, or differing wood levels can help to gauge reasonable levels for mechanical properties. Gatenholm (1992) studied PHB, PP, and polystyrene (PS) composites reinforced with 40% cellulose fiber, processed through injection molding. Stiffness was measured for each system in terms of Young's modulus and was found to be 3.7-GPa, 6.3-GPa, and 6.2-GPa, for the PP, PS, and PHB composite systems, respectively. While the reported values in this study seem high for tensile modulus, they seem to be consistent in that PHB composites yield much higher stiffness than those of PP. Summarized in Table 20 are tensile stiffness and strength for composites modified with 60% WF, produced through injection molding. The results indicate that in comparison with unmodified PP/WF composites, PHB/WF composites exhibit much higher stiffness, and comparable strength. When modified with equal levels of MAPP, or pMDI, the strength of the PP/WF composites exceeds that of the PHB/WF composites, and PP/WF is exceeded by PHB/WF in stiffness.

Through extrusion the differences in flexural properties are not as drastic as those just described for injection molded composites. Shown in Table 20 are values for PP, PE, and PHB/WF composites produced through extrusion with ca. 60% WF. The values suggest that strength values of PP and PHB/WF composites are relatively comparable for both modified and unmodified composites. Further, the stiffness of PHB/WF composites is higher than that of PP/WF for both the modified and unmodified composites. Finally, both the stiffness and the strength are higher than those values reported for PE/WF composites. However, because these composites were produced with different additives, and through different extruders these comparisons should be made lightly, as results may differ for a contiguous study conducted on PP/WF, PE/WF, PHB/WF composites.

Composite toughness

As measures of ductility and resistance to crack propagation, both failure strain (under tensile loading) and the impact energy (by notched Izod tests) were recorded for both processing methods and interfacial modifiers. Because of the brittle nature of the composites, no differences were noted in fracture energy as a function of either processing method or modifier type. All composites indicated fracture energies ranging from 3.0 to 3.5-kJ/m^2. Similarly, the failure strain of all the composites was low. Values for failure strain by tensile testing ranged from 0.3 to 0.6%. An ANCOVA similar to the model described for stiffness and strength was analyzed. The effect of the covariate density was not found to be significant. As a result, tensile strain has not been adjusted to a mean density and is displayed in its raw form in Figure 37. The results pictured in Figure 37suggest no overall difference in failure strain between injection molding and extrusion processes. However, the extruded samples seem to have a larger spread of failure strains as function of modifier type than that of the injection molded samples. This is most likely due to the varying effect of wetting due to modifier type, was earlier suggested to have a strong influence on properties through extrusion.

Effect of processing on water uptake of composites

PHB/WF composites of similar size were tested for water uptake when fully immersed. Water uptake is often described non-steady state diffusion (or Fickian behavior). Under conditions of non-steady state diffusion, the concentration gradient of a molecule diffusing through a medium changes with respect to time and results in a net accumulation in mass. A direct solution to Fick's second law by which an apparent diffusion coefficient D_A may be calculated is described by the following equation:

$$D_A = \pi \left[\frac{h}{4M_{sat}}\right]^2 \left[\frac{\partial M_t}{\partial \sqrt{t}}\right]^2 \quad (3)$$

Where h is the thickness of the sample, M_{sat} is the water uptake percentage at saturation, and $\partial M_t/\partial \sqrt{t}$ is the slope of the water uptake versus square root of time (Chowdhury and Wolcott, 2007). Fickian diffusion may then be described by a linear relationship of $\partial Mt/\partial \sqrt{t}$. When the composites immersed in water approach saturation, deviation from Fickian diffusion will occur. Further, if composite defects are present or form, fast diffusion paths are created within the composite that also result in deviation from steady state diffusion (Roy and Xu, 2001).

Depicted in Figure 38 and Figure 39, the water uptake behavior is plotted as a function of time$^{1/2}$ for both extruded and injection molded specimens respectively. It can be seen through Figure 39, that modified and unmodified composites exhibit an inflection point in the slope of the curves. Further, with increasing modifier effectiveness, this inflection point occurs later in testing. It was observed that the inflection in the plots coincided with the visual observation (Figure 40) of the injection molded composites cracking. As a result, it may be determined that steady state diffusion occurs until the inflection point (due to composite damage).

In contrast, the extruded samples exhibited steady state behavior until saturation. It is possible that this difference in behavior is due to the higher average density of the injection molded specimens. With larger quantities of fiber and matrix enclosed within the same volume, it would be expected that the hygrothermal strains due to fiber swelling would be greater in the composite with a higher density. The increase in hygrothermal strains due to an increase in density may cause debonding, which may lead to cracking of the composite.

To calculate representative diffusion coefficients, Rao (1988) proposed a correction that considers edge the edge effects of diffusion through a specimen. The apparent diffusion coefficient may be adjusted as follows to calculate the true diffusion coefficient (D):

$$D = \frac{D_A}{\left(1+\frac{h}{L}+\frac{h}{W}\right)^2} \quad (4)$$

Where W is the specimen width and L is the specimen length. The average diffusion coefficients were calculated for the control, 4% MA-PHB, 4% D.E.R., 4% Uralac, and 4% pMDI, and were found to be 3.94e-6, 2.44e-6, 2.96e-6, 2.23e-6, and 8.86e-7 mm^2/sec, respectively. It was found that incorporation of more effective modifiers reduced the diffusion coefficient of the PHB/WF composites. The diffusion coefficients calculated for PHB/WF are higher than results reported for PE/WF (60%) extruded composites, which ranged from 6.29e-7 to 8.07e-7 mm^2/sec (Chowdhury and Wolcott, 2007).

Effect of processing on composite morphology

Since we are only able to view a 2-d slice of the composite, it is not easy to get a global image of the fiber bundles, however, looking at the two extreme cases (of 4% pMDI modified composites vs. the control) will give us the best estimation of the bulk differences. Figure 41 displays SEM micrographs of the microtomed surface of the control and 4% pMDI composite, processed through both methods. With the control composites a large discrepancy in the fiber morphology is present across processing methods. The extruded control specimen displays fiber bundles that are fully in-tact. Conversely, the injection molded control shows little evidence of fiber bundles, and fibers are evenly dispersed through the matrix. When looking at composites modified with 4% pMDI, little differences in fiber morphology between processing methods are visible. Both injection molded and extruded composites display fibers that are dispersed and collapsed. This processing/modifier effect on fiber morphology supports results described from tensile testing. The stronger fiber affinity of the pMDI modified composites has the effect of dispersing fibers in extrusion similar to that in injection molding. Conversely, the hydrophobic PHB matrix in the control composite does not wet the fiber bundles adequately. As a result, when processed through extrusion, fiber bundles remain in-tact, and when processed with high pressure in injection molding, fiber bundles are broken down by the high shear forces.

Effect of processing on polymer crystalline structure

The mechanical properties of PHB have been shown to be greatly influenced by aging time, and thermal treatment, or annealing (de Koening and Lemstra, 1993; Biddlestone, 1996). Since crystallization kinetics are greatly influenced by cooling parameters from the melt, and aging has been shown to be a mechanism of secondary crystallization (de Koening and Lemstra, 1993), differences in crystallinity are likely to arise when looking at the composite from the as-processed state. Because PHB is prone to recrystallization effects resulting in bimodal melting, (Qian, 2007), a rapid heating rate was used to minimize this effect.

Figure 42 illustrates representative DSC heating thermograms of unmodified composites processed and cooled through injection molding (with a mold temperature of 60°C), and through extrusion (cooled by a water bath). In order to avoid differences in polymer content, DSC samples were taken from the core of the extruded profile instead of the polymer-rich skin. The injection molded specimen displays a bimodal melting system, while the extruded specimen does not. Because of the larger cross-section size of the extruded bars, and the fact that DSC specimens were taken from the bulk material, it is likely that the tested material underwent cooling at a rate so slow enough to allow for a higher degree of crystallization which allowed for less secondary crystallization. This resulted in a more homogeneous crystal structure, unlike the injection molded specimens which were cooled relatively rapidly. Further, Table 21 indicates no significant difference in crystallinity by cooling method as is measured by the heat of fusion.

These differences in crystallization are likely to have an effect on mechanical and physical properties. However, given the multitude of other variables taking effect on these properties, the direct effect of crystallization cannot be isolated through these studies.

Conclusion

To further investigate the viability of PHB/WF composites for use in commercial WPC applications, PHB/WF composites have been extruded with modifiers previously shown to significantly improve mechanical properties. Further, the effects of processing PHB/WF composites through injection molding and extrusion processes have been compared. Raw formulations have been prepared similarly for both processes with various interfacial modifiers, and resulting mechanical and physical differences examined. Tensile testing of composites showed higher values of Young's modulus and ultimate tensile strength for injection molded specimens over extruded specimens. Similar composite specimens showed higher density from injection molding processes than from extrusion processing. The variation in mechanical properties was accounted for through statistical analysis of density as a covariate in an ANCOVA using processing methods and interfacial modifier types as main effects. Further differences in mechanical properties were attributed to fiber dispersion within the matrix. Micrographs of the composite surfaces from SEM suggested decreased size in fiber bundles with injection molded composites. Regardless of processing method, the type of interfacial modifier added to the composite formulations was suspected to have an influence on fiber dispersion, likely through better fiber wetting.

Mechanical properties of PHB/WF composites processed through extrusion were shown to be competitive with coupled PP/WF composites. PHB/WF composites modified with pMDI indicated higher stiffness, and comparable strength to MAPP coupled PP/WF composites at the same percentage of modifiers.

Water absorption of the composites processed by different methods displayed considerable differences in behavior. Cracking of the injection molded specimens was observed and suggested to be a result of the higher composite density. Extruded specimens displayed characteristics only of water uptake and saturation. Prior to cracking, moisture transport was more limited in injection molded specimens than that in extruded specimens.

Interpretation of DSC traces suggested differences in crystal perfection between injection molded and extruded specimens. The degree of crystallization, as measured through the heat of fusion and the heat of crystallization was unchanged respective to processing method.

References

Anderson, S.P. 2007. Effect of Interfacial Modifiers on Mechanical and Physical Properties on PHB/WF and Their Effect on Composite Morphology. Chapter 2. Master Thesis, Washington State University, Pullman, WA.

Beg, M.D.H. and K.L. Pickering. 2006. Fiber Pretreatment and Its Effects on Wood Fiber Reinforced Polypropylene Composites. Materials and Manufacturing Processes, 21(3):303-307.

Biddlestone, F., A. Harris, and J.N. Hay. 1996. The Physical Ageing of Amorphous Poly(hydroxybutyrate). Polymer International, 39:221-229.

Bledzki, A.K., and J. Gassan. 1999. Composites Reinforced With Cellulose Based Fibers. Progress in Polymer Science, 24:221-274.

Chambers, R., D. Hayward, and J.J. Liggat. 2001. The Effect of Processing on the Properties of Poly(3hydroxybutyrate-co-3-hydroxyvalerate) Copolymers. Journal of Materials Science, 36:3785-3792.

Chen, C., S. Peng, B. Fei, Y. Zhuang, L. Dong, Z. Feng, S. Chen and H. Xia. 2003. Synthesis and Characterization of Maleated Poly(3-hydroxybutyrate). Journal of Applied Polymer Science, 88(3):659-668.

Chowdhury, M.J.A. and M.P. Wolcott. 2007. Compatibilizer Selection to Improve Mechanical and Moisture Properties of Extruded Wood-HDPE Composites. Forest Products Journal, 57(9):46-53.

Clemons, C. 2002. Wood-Plastic Composites in the United States: The Interfacing of Two Industries. Forest Products Journal, 52(6):10-18.

Esposito, F. 2005. More Bio-Resins Become Commercially Available. Plastics News, Nov. 21.

Facca, A.G., M.T. Kortschot, and N. Yan. 2006. Predicting the Elastic Modulus of Natural Fibre Reinforced Thermoplastics. Composites Part A: Applied Science & Manufacturing, 37(10):1660-1671.

Fernandes, E.G., M. Pietrini, and E. Chiellinim. 2004. Bio-Based Polymeric Composites Comprising Wood Flour as Filler. Biomacromolecules, 5:1200-1205.

Gardner, D.J., J. Son, S. O'Neill, and W.T. Tze. 2004. Study of the Crystallization Behavior and Material Properties of Extruded Polyolefin Wood-Plastic Composite Lumber as a Function of Post Die Process Conditions. Conference Proceedings for Progess in Woodfibre-Plastic Composites, May 10-11.

Gatenholm, P., J. Kubat, and A. Mathiasson. 1992. Biodegradable Natural Composites. I. Processing and Properties. Journal of Applied Polymer Science, 45(9):1667-1677.

Geng, Y. and L.J. Simonsen. 2006. Further Investigation of Polyaminoamide-Epichlorohydrin/Stearic Anhydride Compatibilizer System for Wood-Polyethylene Composites." Journal of Applied Polymer Science, 99:712-718.

Kamal, M.R., V. Tan, and M.F. Ryan. 1977. Injection Molding: A Critical Profile. Science and Technology of Polymer Processing, MIT Press, Cambridge, MA.

Kato, K., Y. Zhang, and N. Otake. 1999. Numerical Analysis of Flow and Fiber Orientation in Slit Channel Flow of Short Fiber-Polymer Melt Mixture. JSME International Journal, Series C, 42(4):1061-1067.

de Koning, G.J.M. and P.J. Lemstra. 1993. Crystallization Phenomena in Bacterial Poly[(R)-3 hydroxybutyrate]: 2. Embrittlement and rejuvenation. Polymer, 34(19):4089-4094.

Osswald, T. and J.P. Hernandez-Oritz. 2006. Polymer Processing: Modeling and Simulation. Hanser Publishers, Munich, Germany.

Qian, J. 2006. Investigation of Crystallization of Poly(3-hydroxybutyrate co-3-hydroxyvalerates) and their Bamboo Fiber Reinforced Composites. Master Thesis, Washington State University, Pullman, WA.

Qian, J., L. Zhu, J. Zhang, and R.S. Whitehouse. 2007. Comparison of Different Nucleating Agents on Crystallization of Poly(3-hydroxybutyrate-co-3-hydroxyvalerates). Journal of Polymer Science: Part B: Polymer Physics, 45(13):1564-1577.

Rao, R.M., N. Balasubramanian, and M. Chanda. 1988. Factors Affecting Moisture Absorption in Polymer Composites, Part I: Influence of Internal Factors. Environmental Effects on Composites Materials, 3:75-87.

Roy, S. and W. Xu. 2001. Modeling of Diffusion in the Presence of Damage in Polymer Matrix Composites. International Journal of Solids and Structures, 38(1):115-125.

Singh, S. and A.K. Mohanty. 2007. Wood Fiber Reinforced Bacterial Bioplastic Composites: Fabrication and Performance Evaluation. Composites Science and Technology, 67:1753-1763.

Smith, P.M. and M.P. Wolcott. 2006. Opportunities for Wood/Natural Fiber-Plastic Composites in Residential and Industrial Applications. Forest Products Journal, 56(3):4-11.

Stark, N.M., L.M. Matuana, and C.M. Clemons. 2004. Effect of Processing Method on Surface and Weathering Characteristics of Wood-Flour/HDPE Composites. Journal of Applied Polymer Science, 93:1021-1030.

White, J.L. 1977. Extrusion of Polymer Melt Systems Through Dies. Science and Technology of Polymer Processing, MIT Press, Cambridge, MA.

Zhang, J., S. McCarthy, and R.J. Whitehouse. 2004. Reverse Temperature Injection Molding of Biopol and its Effect on Properties. Journal of Applied Polymer Science, 94(2):483-491.

Figures

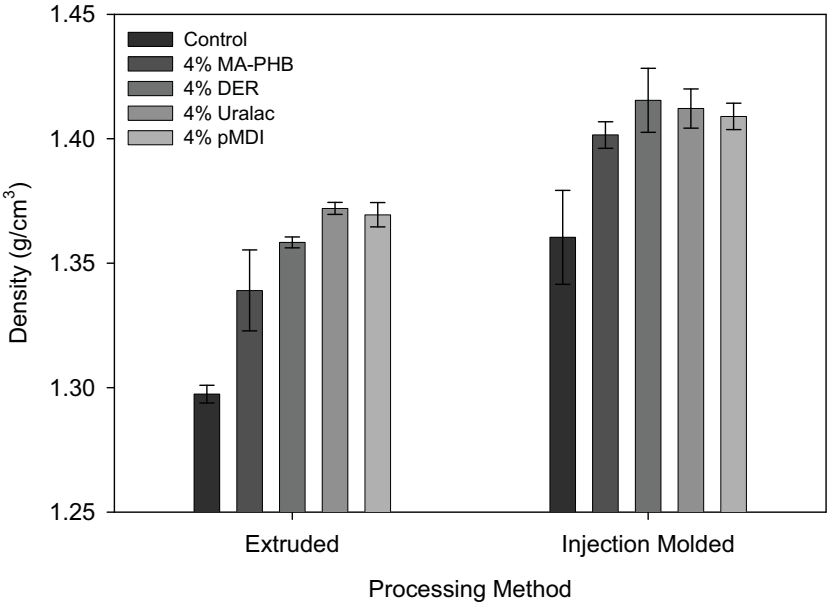

Figure 34. Density of PHB/WF modified composites processed through extrusion and injection molding.

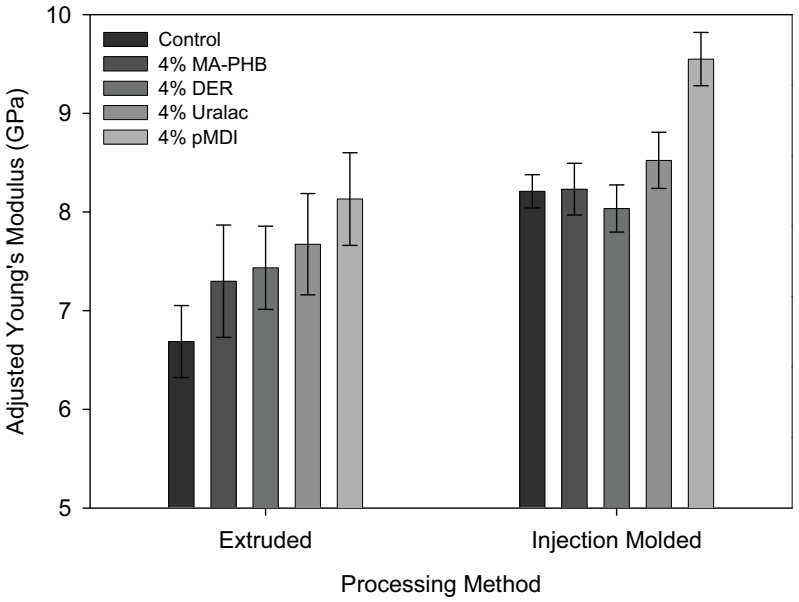

Figure 35. Tensile modulus of PHB/WF and PHB/WF modified composites processed through extrusion and injection molding.

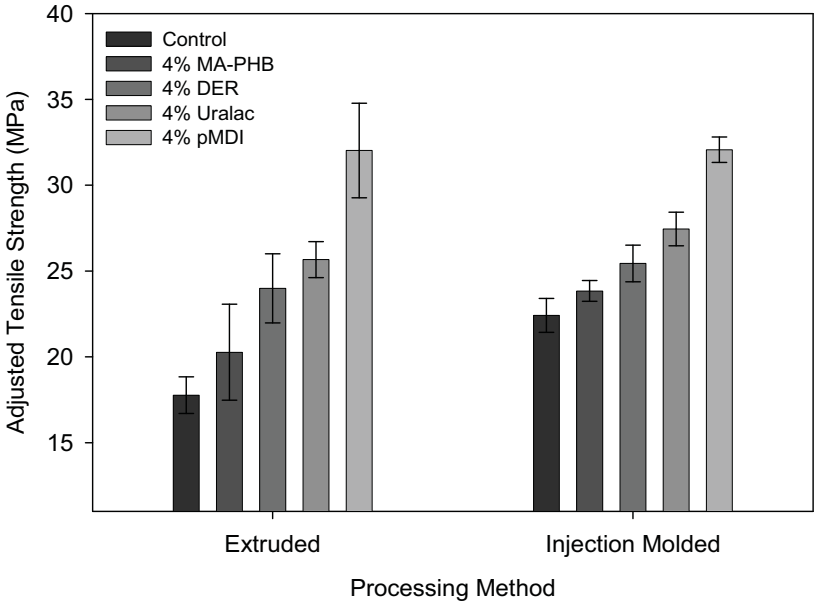

Figure 36. Tensile strength of PHB/WF and PHB/WF modified composites processed through extrusion and injection molding.

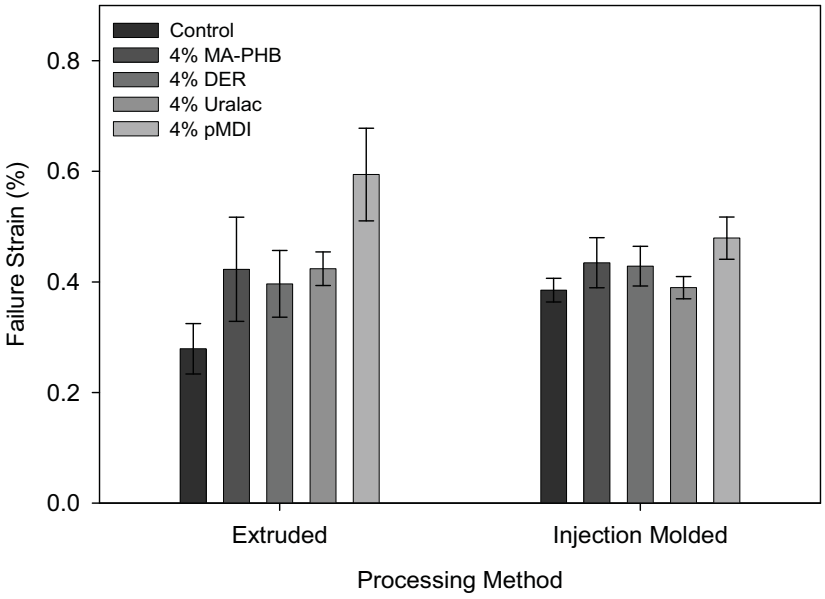

Figure 37. Failure strain of PHB/WF and PHB/WF modified composites processed through extrusion and injection molding.

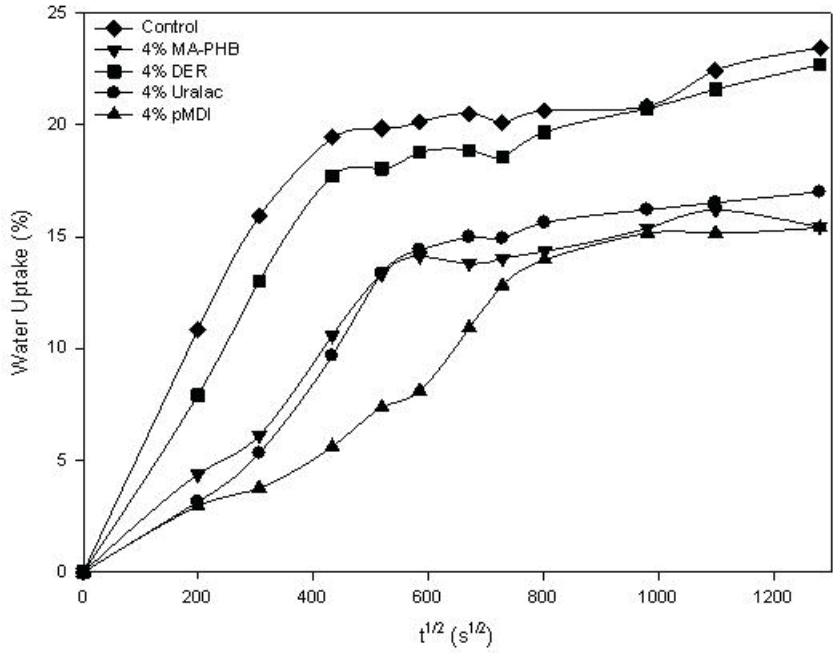

Figure 38. Water absorption of PHB/WF and PHB/WF modified composites processed through extrusion.

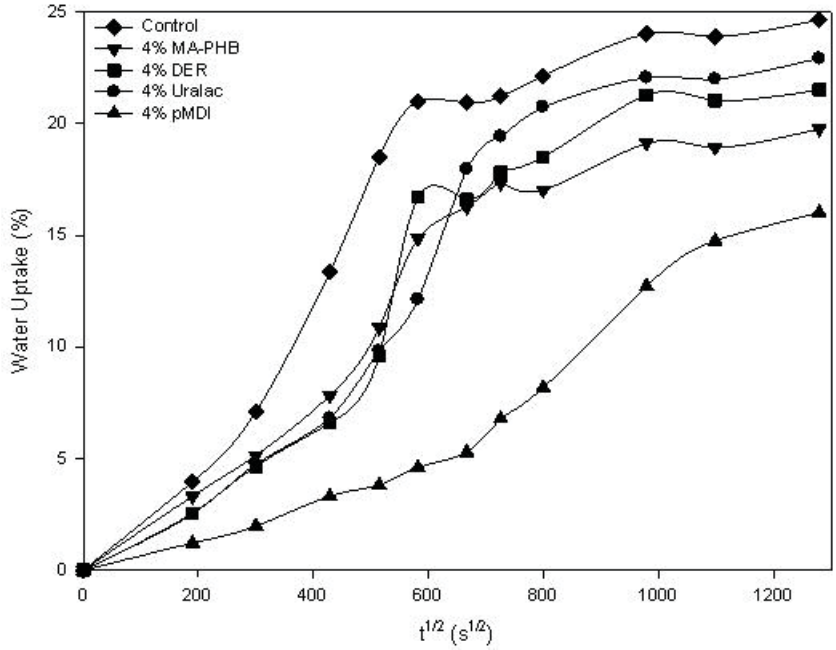

Figure 39. Water absorption of PHB/WF and PHB/WF modified composites processed through injection molding (Anderson, 2007).

Figure 40. Photograph of an injection molded PHB/WF composite (control formulation, immersed for 4 days) (Anderson, 2007).

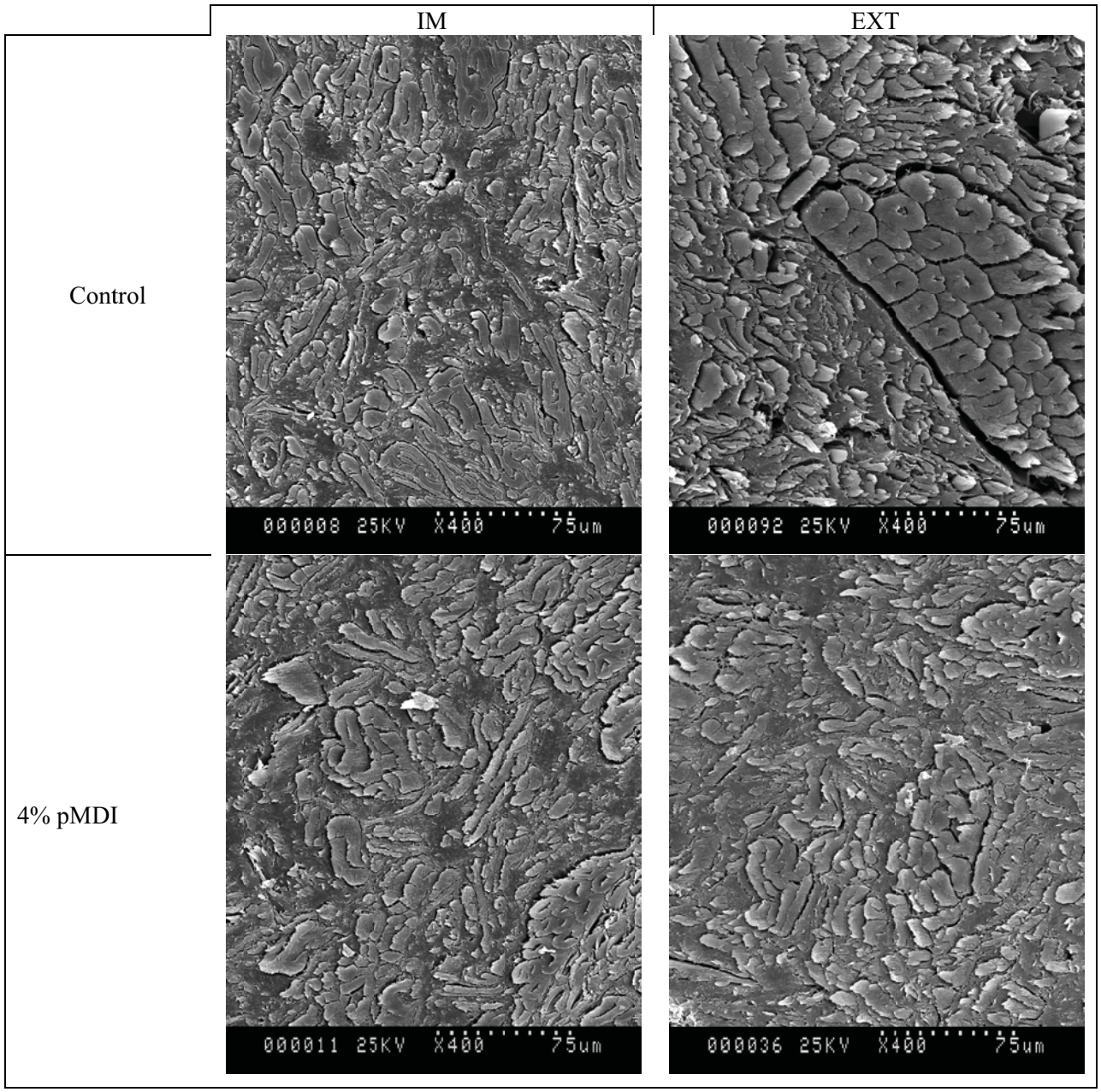

Figure 41. SEM micrograph of microtomed PHB/WF, processed through injection molding and extrusion.

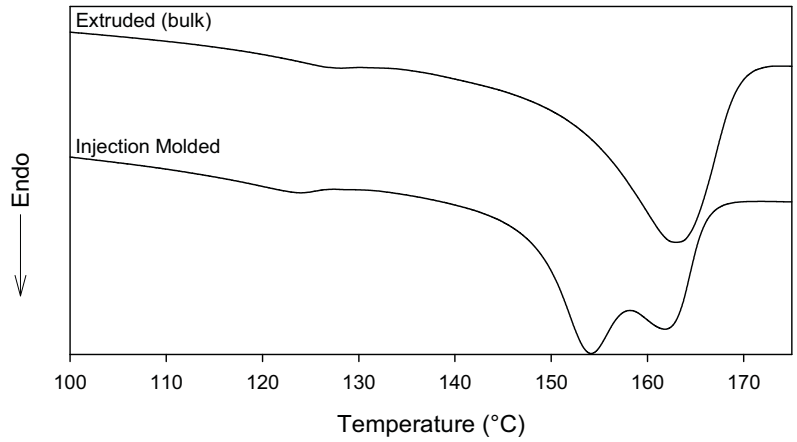

Figure 42. DSC thermogram of the first heating after processing of PHB/WF (control formulation) processed through injection molding and extrusion.

Tables

Table 17. Type III ANOVA and duncan grouping for effect of processing and modifiers on density (R^2 = 91.6%).

Source	DF	Type III SS	Mean Square	F Value	Pr > F
Processing	1	0.233	0.233	1338.00	<0.0001
Modifier	4	0.075	0.019	107.85	<0.0001
Processing*Modifier	4	0.004	0.001	6.42	<0.0001

Processing	Injection Molding	Extrusion
Duncan Grouping	A	B
Mean (g/cm^3)	1.40	1.33

Modifier	4%Uralac	4% pMDI	4% DER	4% MA-PHB	Control
Duncan Grouping	A	A	A	B	C
Mean (g/cm^3)	1.39	1.38	1.38	1.37	1.33

Table 18. Type III ANCOVA and duncan grouping for effect of modifiers and processing method on tensile modulus (R^2 = 89.8%).

Source	DF	Type III SS	Mean Square	F Value	Pr > F
Processing	1	4.938	4.938	38.41	<0.0001
Modifier	4	24.591	6.148	47.83	<0.0001
Processing*Modifier	4	4.658	1.165	9.06	<0.0001
Density	1	1.913	1.913	14.88	0.0002

Processing	Injection Molding	Extrusion
Duncan Grouping	A	B
Mean (GPa)	8.77	7.13

Modifier	4% pMDI	4% Uralac	4% MA-PHB	4% DER	Control
Duncan Grouping	A	B	C	C	D
Mean (GPa)	9.06	8.32	7.90	7.84	7.33

Table 19. Type III ANCOVA and duncan grouping for effect of modifiers and processing method on tensile strength (R^2 = 94.7%).

Source	DF	Type III SS	Mean Square	F Value	Pr > F
Processing	1	23.167	23.167	10.03	0.0019
Modifier	4	1542.548	385.637	166.94	<0.0001
Processing*Modifier	4	105.646	26.411	11.43	<0.0001
Density	1	98.475	98.475	42.63	<0.0001

Processing	Injection Molding	Extrusion
Duncan Grouping	A	B
Mean (MPa)	28.20	21.30

Modifier	4% pMDI	4% Uralac	4% DER	4% MA-PHB	Control
Duncan Grouping	A	B	C	D	E
Mean (MPa)	33.00	27.77	25.59	21.86	18.13

Table 20. Tensile properties of WPCs injection molded with ca. 60% WF (*Reference: Beg and Pickering, 2004).

Matrix	Modifier	Extruded, 60% WF		Injection Molded, 40% WF	
		MOE (GPa)	MOR (MPa)	E (GPa)	σ_{max} (MPa)
PHB	-----	5.3	28	2.2	19.9
PHB	2% pMDI	7.0	42	5.2	45.5
PP	-----	4.1*	33*	8.1†	22.0†
PP	2% MAPP	4.3*	48*	9.4†	27.8†
PE	-----	2.9*	18*	-----	-----
PE	2% MAPE	2.6*	39*	-----	-----

Table 21. Effects of processing on thermal properties of PHB/WF (control formulation).

Processing Method	Melt Crystallization		Melting				
			1st Scan			2nd Scan	
	T_c (°C)	ΔH_m (J/g)	T_{m1} (°C)	T_{m2} (°C)	ΔH_m (J/g)	T_m (°C)	ΔH_m (J/g)
Ext	100.4	22.3	NA	163.1	-23.8	160.1	-24.7
IM	98.3	23.3	154.2	162.1	-24.9	156.8	-26.6

Task 4 – Waste Effluents PHA Composite Processing & Material Properties

Investigators: Michael P. Wolcott[1], Karl R. Englund[1], Jinwen Zhang[1], Long Jiang[1], Meng-Hsin Tsai[1]

Performing Institutions: [1]Washington State University

Developing PHB/Wood Four/Cell Debris Ternary Composites through Injection Molding

Abstract

Wood plastic composites traditionally depend on thermoplastics derived from fossil fuels, which increases their overall energy costs by over 230% compared to traditional engineered wood products. Utilizing biobased thermoplastics for WPCs can lower the overall energy costs of these products and reduce our dependence on foreign oil. Poly-3-hydroxybutyrate (PHB) is a biodegradable microbial polyester and can be produced by microbes in waste effluents. Using unpurified PHB (i.e. PHB with microbe cells) in WPCs can significantly lower their material and energy costs. In this study, purified PHB and PHB-free cell debris were used to simulate PHB laden microbes in producing PHB/wood flour/cell debris ternary composites with various wood flour/cell debris ratios. The composites were prepared using twin screw compounding followed by injection molding. Polymeric (methylene-diphnenyl-diisocynate) (pMDI) was used as a coupling agent to increase the interfacial bonding between the PHB matrix and the wood four/cell debris. Morphology, mechanical properties, and water adsorption of the composites were investigated. Interpretation of morphological studies indicates that wood flour had stronger interfacial bonding to the PHB matrix than did the cell debris. This phenomenon led to decreasing mechanical properties and water resistance of the composites with increasing cell debris contents. At the cell debris/wood flour ratio of 3:2, the ternary composites exhibited 55 to 65% of the tensile and flexural properties of the PHB/wood flour binary composite.

Introduction

Wood plastic composites (WPCs) are a rapidly growing product area, averaging a 38% growth rate since 1997. WPCs are traditionally depend on petroleum based thermoplastics, i.e. polyethylene(PE), polypropylene(PP), polystyrene(PS) etc., increasing their overall energy costs by over 230% when compared to traditional engineered wood products (EWP). Renewable microbial polyesters are not currently used in WPCs primarily because their production costs are about 2 ~ 3 times higher than those of conventional petrochemical-derived plastics. One possible solution for economically producing WPCs using microbial polyesters might be realized by reducing or eliminating the most costly and energy intensive step in the microbial plastic production - purification of the polymer from the cell debris. This goal can be achieved by producing the PHB using wastewater effluents from industrial sectors. After production, the plastic-laden biosolids will be dried and used directly to replace petroleum-derived plastics and the cell debris will be used as fillers in WPCs. Using this strategy, the cost of producing and utilizing these renewable plastics in WPCs can be greatly reduced.

It is estimated that annual energy savings of over 42-trillion BTU by 2020 can be achieved by using the proposed technology. If it deploys across the building/construction industry, the potential for 310 trillion BTU can be saved annually. Significant environmental benefits will also be realized by the wastewater treatment industry in the municipal, industrial (pulp mill), and agricultural sectors through incorporation of waste biosolids into composites. Improved economic competitiveness of the domestic forest products industry is expected, as the plastic in WPCs comprises on average 52% of formulation costs and 30% of total product costs.

It has been found from previous studies that the coupling agent polymeric diphenylmethane diisocyanate (pMDI) could significantly increase the mechanical properties and water resistance of PHB/wood flour composites (Anderson 2007). This was attributed to the reactions of pMDI with both the

wood fiber and the PHB matrix, which substantially improved the interfacial bonding between the two phases and improved the dispersion of the wood flour.

In this study, purified microbial polyester poly (3-hydroxybutyrate) (PHB) and PHB-free biosolid (cell debris) were used to simulate the PHB-laden biosolid. The objective of this research was to determine the phase morphology, mechanical properties, and moisture resistance of PHB/wood flour/cell debris (PWC) composites. Specifically, our goal is to evaluate the influence of the material composition on these resulting performance variables.

Materials & Methods

Materials

The purified PHB powder (Tianan Biologic Material Co., Ltd, Ningbo, China) and wood flour (60-mesh ponderosa pine, American Wood Fibers, Schofield, WI) were commercially obtained for composite production. The cell debris was produced from wastewater effluents and provided by collaborators at UC-Davis. In preparation for composite manufacture, the material was ground to a nominal 60-mesh particle size using impact milling and the particle distribution was characterized using sieve analysis (Table 22), Boron nitride (BN) (Carbotherm PCTF5, Saint Gobain Advanced Ceramics Co., Amherst, NY) was used as a nucleating agent to promote PHB crystallization. Glycolube WP2200 (Lonza Inc., Allendale, NJ) was included as a lubricant to improve processability. Talc (Nicron 403) was provided by Riotinto of Centennial and was used for processability and water resistance improvements. Liquid form pMDI (Mondur 541, Bayer MaterialScience, Pittsburgh, PA) containing 31.5 mass % NCO was used as the coupling agent between hydrophobic PHB and hydrophilic wood flour and cell debris.

Methods

Preparation of composites

60-mech pine wood flour was dried in a rotary steam tube drier to 3% moisture content. The ground cell debris was dried at 100^{o}C for 24 hours in a convection oven. The PHB, BN, WP2200, and talc components were used as received. While preparing the mixture for extrusion, the PMDI was mixed with PHB powder in a physical blender. The PHB/pMDI mixture was subsequently combined with the other components in a plastic container and manually mixed by vigorous shaking and tumbling for 5-minutes. The mass ratios of the various formulations studied are presented in Table 23. The contents of the PHB and the cell debris/wood flour mixture were maintained at 35 and 57 parts, respectively, for all the formulations. The mixtures were then compounded using a co-rotating twin screw extruder (Leistriz ZSE-18) with a screw diameter of 18 mm and length/diameter (L/D) ratio of 40 equipped with a volumetric feeder. To improve melt strength and reduce thermal degradation, a declining temperature profile of the extruder was applied during the extrusion process. The temperatures of the barrel zones were set to be 170 ^{o}C, 175 ^{o}C, 170 ^{o}C, 165 ^{o}C, 164 ^{o}C, 163 ^{o}C, 162 ^{o}C, and 160^{o}C, from the feed throat to the die adapter. The screw speed was maintained at 125 rpm. Under this speed, the residence time of the materials in the barrel was estimated to be about 1.5 minutes. The extrudate exiting the die was air cooled and pelletized for injection molding.

Preparation of testing specimens

Flexural test specimens (12 x 3 x 127-mm) and tensile specimens (ASTM standard D638 type III) were produced using an injection-molding machine (Sumitomo SE 50D). Injection temperatures were controlled at 175 ^{o}C, 180 ^{o}C, 175 ^{o}C, and 170 ^{o}C from the feeding zone to the nozzle with the mold temperature set to 60 ^{o}C. A filling pressure of 1700 kgf/cm^2 was established along with packing pressures of 1250 kgf/cm^2 and 1360 kgf/cm^2 for the 1st and 2nd stage, respectively. At these conditions, the injection molding cycling time was approximately 75 seconds.

Impact test specimens (12 x 3 x 60-mm) were prepared following ASTM D256. All the specimens were notched by a XQZ-I specimen Notch Cutter. The specimens for water absorption test were cut by a milling machine to the size of 11x 2.5 x 125-mm.

Thermal degradation analysis of raw materials

Thermal gravimetric analysis (TGA) of PHB, wood flour, and cell debris was performed using a Rheometric Scientific STA. 8 to 10 mg of each of the materials was heated from room temperature to 600 ^{o}C at 10 ^{o}C/min. Sample weight was monitored continuously during the process.

Mechanical properties and density

A screw driven Instron 4466 equipped with a 10-KN load cell and a pair of mechanical grips was used for tensile and flexural tests. The tensile tests were conducted at a crosshead speed of 5-mm/min, with the sample strain measured by an extensometer (MTS model # 634.12E-24). The flexural tests (three point bending) were performed with a crosshead speed of 1.40-mm/min. Impact tests were conducted using a Dynisco Basic Pendulum Impact tester. ASTM standard D638, D256 (mode A), and D790 were followed in the tensile, impact, and flexural tests, respectively. Five replicates were tested for each formulation to obtain a mean value. Sample density was calculated by dividing sample mass by sample volume. All the samples (for both mechanical and density testing) were conditioned at 23 ^{o}C and 50% relative humidity (RH) for 7-days prior to the tests.

Phase Morphology

To investigate wood flour and cell debris distribution in the PHB matrix and particle-polymer interfacial bonding, tensile fracture surfaces of the composites were sputter coated with gold and observed using a Hitachi S-570 scanning electronic microscope (SEM). The sizes and shapes of the neat cell debris and pine wood flour were also studied by SEM.

Moisture resistance

Water absorption of the composites was performed following ASTM D 570. Samples were immersed in distilled water at room temperature. The weight and thickness of the samples were measured after different periods of immersion time. Moisture content (MC) and thickness swelling (TS) were calculated by the following equations:

$$MC(\%) = \frac{(M - M_o)}{M_o} \cdot 100 \quad (1)$$

$$TS(\%) = \frac{(T - T_o)}{T_o} \cdot 100 \quad (2)$$

where M is the mass of the specimens at time t, and M_o is the initial mass of the specimens; T is the thickness of the specimens at time t, and T_o is the initial thickness of the specimens.

Results and Discussion

Thermal degradation

TGA is used to assess the thermal sensitivity of materials by continuously monitoring the sample weight while the sample is heated at a constant ramp rate. The thermal degradation temperature of each component in the sample can be obtained from the weight-temperature curve. Figure 43 presents the relationships of percentage of weight remaining after thermal exposure for neat wood flour, ground cell debris and neat PHB powder. It was clear from this figure that PHB degraded rapidly within a short temperature range (between 250 and 280 ^{o}C). The wood flour started to decompose at a lower

temperature (ca. 200°C) but the entire degradation occurred within a larger temperature range (lower degradation rate) and through a two step degradation process. Finally, the cell debris displayed the lowest degradation start temperature (ca. 100 °C), the widest degradation temperature range (the lowest degradation rate), and the highest sample residual at the end of the test (about 40% at 600 °C). The wide degradation temperature range and high sample residual of the cell debris was believed to be due to its complex constituents including primarily various types of proteins, polysaccharides, and triglycerides, while a high inorganic content is likely to account for the residuals.

Mechanical properties and density

The density of the composites manufactured from the six different formulations is shown in Table 24. Little change in density was noted with the various cell debris/wood flour ratios ranging from 1:4 to 5:0. These results indicate that the cell debris and wood flour possessed similar densities after the high pressure injection molding where PHB melt penetrated into the cell lumen of the wood flour.

Table 24 also shows the tensile and flexural strength and modulus of the six composites. Their trends were plotted in Figure 44 and Figure 45. Both strength and modulus were shown to decrease with increasing content of the cell debris. At the cell debris/wood flour ratio of 3:2, the composites exhibited 55 to 65 % of the tensile and flexural properties of the control sample PW (39.7 MPa and 10.2 GPa in tensile strength and modulus; 69.4 MPa and 7.43 GPa in MOR and MOE). Impact strength of the composites also showed a declining trend: the higher the cell debris content, the lower the impact strength (Figure 46). The reason of this tread is believed to be poor interfacial bonding between the cell debris and PHB (discussed later in phase morphology) and degradation (starting at 100°C) of the cell debris during processing. The degradation of the cell debris produced gaseous substance which could cause voids and other sample defects in the composites. Moreover the cell debris had a cubic shape which was unfavorable to the mechanical properties of the composites compared to the fiber- shaped wood flour.

Phase Morphology

The microstructure of the cell debris and wood flour within the composite matrix is shown in Figure 47. The cell debris displayed wide particle size distribution with large particles measuring at ca. 300 microns (Figure 47a). These particles exhibited irregular shapes with low length/diameter (L/D) ratio or cubic-like shape. In contrast, the wood flour particles are composed of bundles of wood fibers (Figure 47b). The intensive shear during extrusion could break some of these bundles and increase their L/D ratios, which further enhanced their reinforcing effect. After extrusion and injection molding, the biomass powder and wood flour were found to be homogenously distributed in the polymer matrix (Figure 48). On the fracture surface of the PHB/wood flour composite, no interfacial debonding between the wood fibers and the PHB matrix was observed, an indication of strong interaction between the two phases (Figure 48b). In contrast, the interaction between the cell debris and PHB was poor as debonding at their interfaces can be clearly seen (indicated by the arrows in Figure 48c). The difference in the interfacial properties can be distinguished more easily under higher magnification (Figure 49). The high interfacial adhesion between the PHB matrix and wood fiber, indicated by the arrows in Figure 49b, is due to pMDI, which is highly reactive with both hydroxyl and carboxyl groups, and is able to chemically link the two phases. The cell debris is a complicated system, comprising mainly protein, polysaccharides, triglycerides, and inorganic impurities. The cell debris pre-treatment during its production, impurities of the cell debris, and the cell debris degradation during processing might limit the access of pMDI to the reactive sites of the cell debris and therefore reduce its compatibilization effects, which eventually resulted in poor interfacial bonding between the cell debris and the PHB matrix (Figure 49c).

Figure 50a and b show the sectioned surfaces of the PHB/wood flour/cell debris composites. Due to the high pressure occurred in injection molding, many wood cells were crushed or severely deformed (Figure 50b, deformation indicated by arrows). The high pressure also forced PHB melt into some of the cells. From Figure 51 it was clear that the polymer melt was forced into the cells through longitudinal and transverse lumens. The penetration of polymer into the wood cells generated a mechanical interlock

between the polymer and the wood fiber, which substantially improved stress transfer between the two phases. In contrast, biomass particles seemed to be solid and cannot be deformed or penetrated (Figure 50a). As a result, they formed poor interfacial bonding with the polymer and resulted in deteriorated properties.

Moisture behavior

As shown in Figure 52, water absorption increased with increasing cell debris concentration in the 12-week test period. Water absorption rate (initial slope of the curve) also increased with rising cell debris concentration. The samples with higher cell debris concentrations took less time to reach moisture saturation. For example, the sample with 100% cell debris concentration (PC) reached moisture saturation content (M_{sat}, ca. 28%) in three days. In comparison, the control sample (PW) reached the saturation content (ca. 17%) in six weeks. Following exactly the same trend of water absorption, sample thickness increased to a larger extent and at a higher rate at higher cell debris concentration (Figure 53). Therefore, it can be concluded that the addition of cell debris increased water absorption of the composites. This was most probably due to high hydrophility of cell debris. The PC composite had much higher moisture saturation content (28% vs. 17%) compared to the PW composites. Moreover, poor interfacial bonding between cell debris and PHB allowed faster moisture penetration.

Cracks formed on the sample surfaces during water immersion due to sample swelling. Surface cracks appeared on the third, second, and first day of immersion on the PWC60, PWC80, and PC composites, respectively. The samples with lower cell debris concentration showed cracks after the 4-week period of immersion.

Liquid or gas transportation through a solid material is often modeled by Fickian diffusion equation. In Fickian diffusion, plotting the amount of uptake (moisture in this case) at a given time period against the square root of the time period produces a linear region followed by a non-linear approach to M_{sat}. The apparent diffusion constant (D_A) can be calculated by:

$$D_A = \pi \left[\frac{h}{4M_{sat}} \right]^2 \left[\frac{dM_t}{d\sqrt{t}} \right]^2 \tag{3}$$

where h is the thickness of the specimens and $dMt/d\sqrt{t}$ is the slop of the weight gain versus square root of time.

For calculating 3-dimensional diffusion, a geometric edge correction factor is used to calculate the true diffusion constant (D):

$$D = \frac{D_A}{(1 + h/L + h/W)^2} \tag{4}$$

where L and W are the length and width of the specimens respectively.

As shown in Table 25, the composite of PC had the highest true diffusion coefficient (4.09E-6 mm^2/sec) among the six formulations, which indicates that the composite had the highest moisture penetrating rate or the lowest water resistance. The degree of sample swelling was defined by a swelling coefficient, $\beta = TS_{\max} / MC_{\max}$.

Table **25** shows that increased levels of cell debris results in a higher swelling coefficient of the composites (ranging from 0.716 to 1.102). This could be due to higher hydrophility and larger moisture absorption rate of the cell debris.

Conclusions

Purified PHB and PHB-free cell debris were successfully compounded with wood flour by twin screw extrusion and molded into test samples by injection molding. Because of the cell debris' large size,

irregular shape, poor interfacial bonding, and thermal degradation during processing, the mechanical properties and water resistance of the composites were found to decrease with increasing cell debris content. Improving interfacial bonding between PHB and cell debris and sizing down cell debris particle are expected to improve composite properties due to better bonding and larger contact area. Therefore, the Plastic-laden cell debris could be successfully applied on WPCs.

Acknowledgements

The authors gratefully acknowledge the financial support provided by the U.S. Department of Energy, under the grant of *Development of Renewable Microbial Polyesters for Cost Effective and Energy-Efficient Wood-Plastic Composites*.

References

Anderson, S.P. 2007. Wood Fiber Reinforced Bacterial Biocomposites: Effects of Interfacial Modifiers and Processing on Mechanical and Physical Properties." Master Thesis, Washington State University, Pullman, WA.

American Society for Testing and Materials. 2004. Standard test method for tensile properties of plastics. ASTM D 638-03. ASTM. Philadelphia, PA.

American Society for Testing and Materials. 2005. Standard test methods for flexural properties of unreinforced and reinforced plastics and electrical insulating materials. ASTM D 790-03. ASTM. Philadelphia, PA.

American Society for Testing and Materials. 2005. Standard test methods for determining the izod pendulum impact resistance of plastics. ASTM D 256-05. ASTM. Philadelphia, PA.

American Society for Testing and Materials. 2006. Standard test method for water absorption of plastics. ASTM D 570-98. ASTM. Philadelphia, PA.

Figures

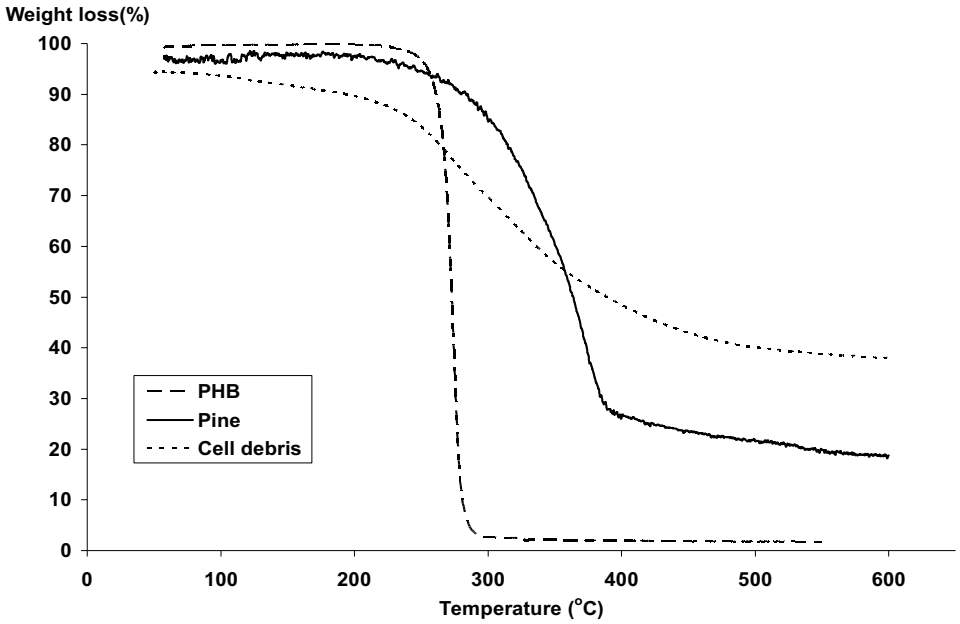

Figure 43. Thermogravimetric curves of neat pine wood flour, neat cell debris, and neat PHB.

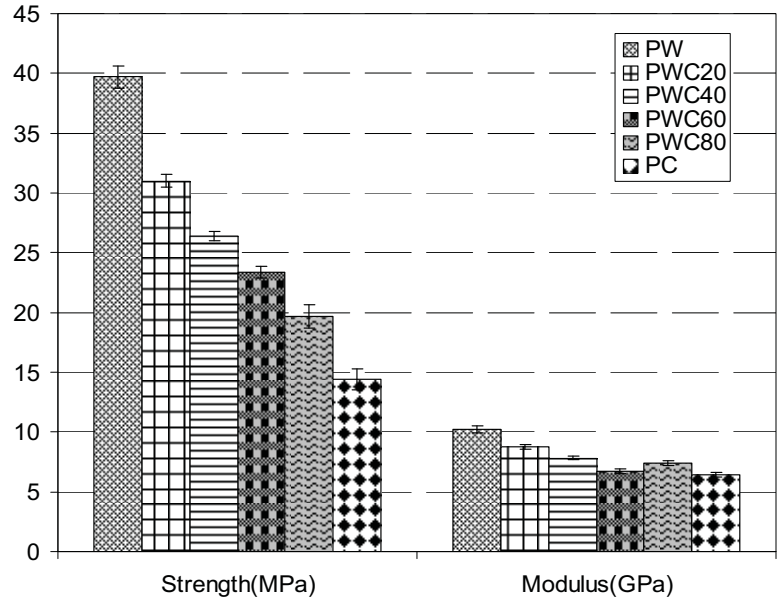

Figure 44. Tensile properties of the six composites.

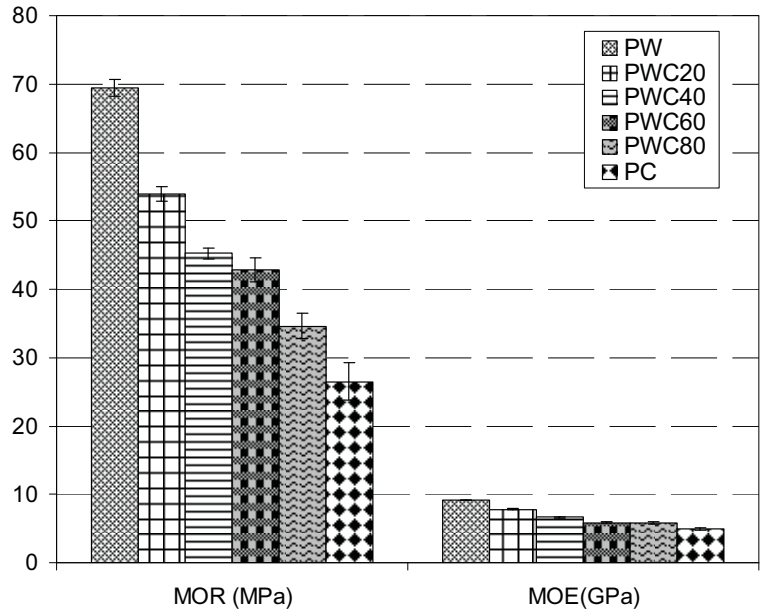

Figure 45. Flexural properties of the six composites.

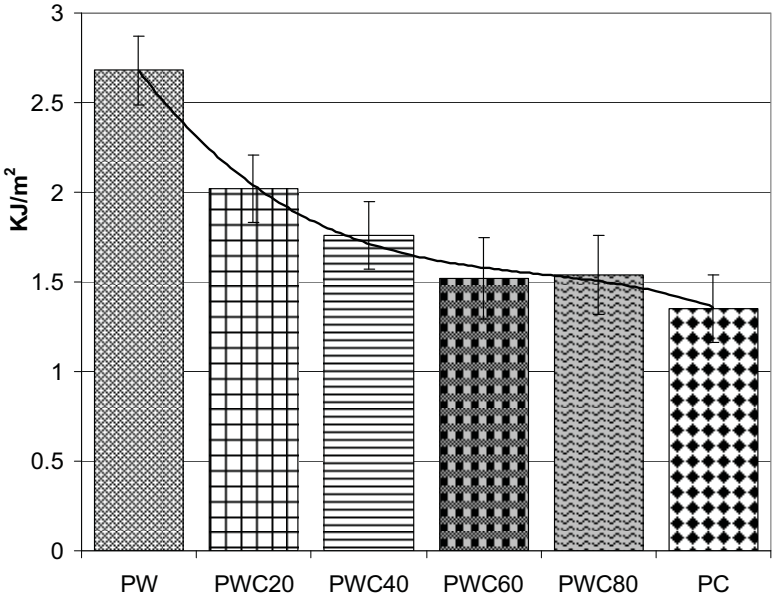

Figure 46. Impact strength of the six composites.

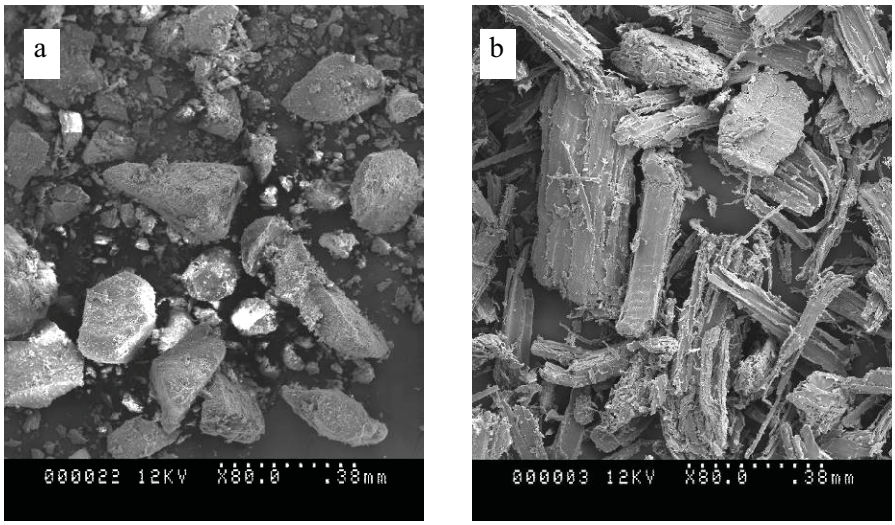

Figure 47. SEM micrographs of cell debris (a) and pine wood flour (b).

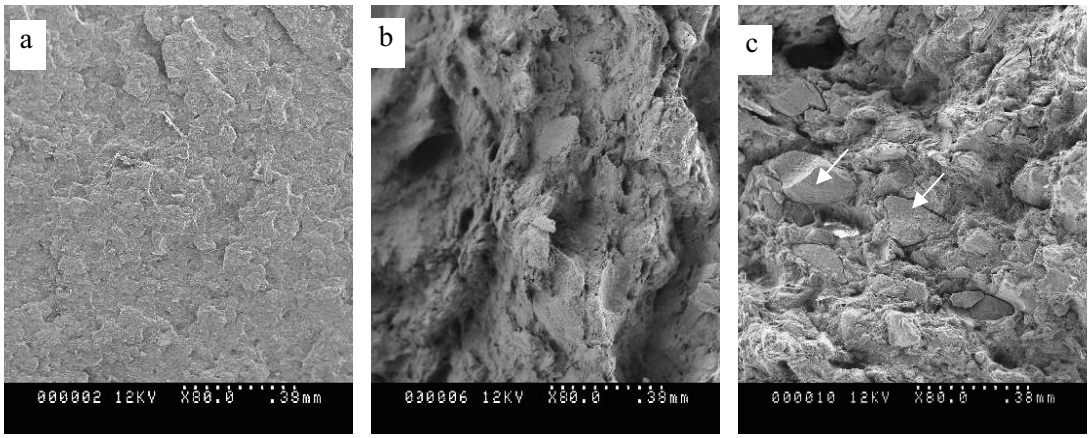

Figure 48. Fracture surfaces of neat PHB (a), PHB/Wood flour composite (b), and PHB/Wood flour/cell debris composite (c). Magnification: X80.

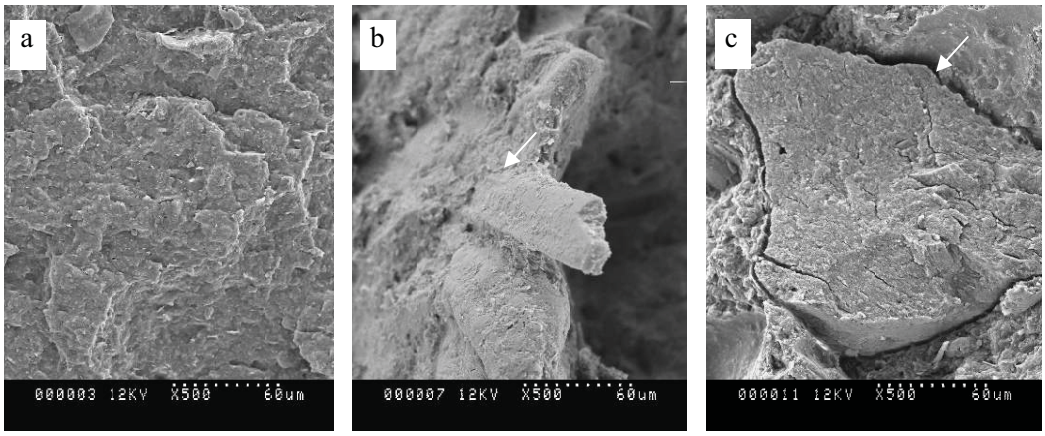

Figure 49. Fracture surfaces of neat PHB (a), PHB/Wood flour composite (b), and PHB/Wood flour/cell debris composite (c). Magnification: X500.

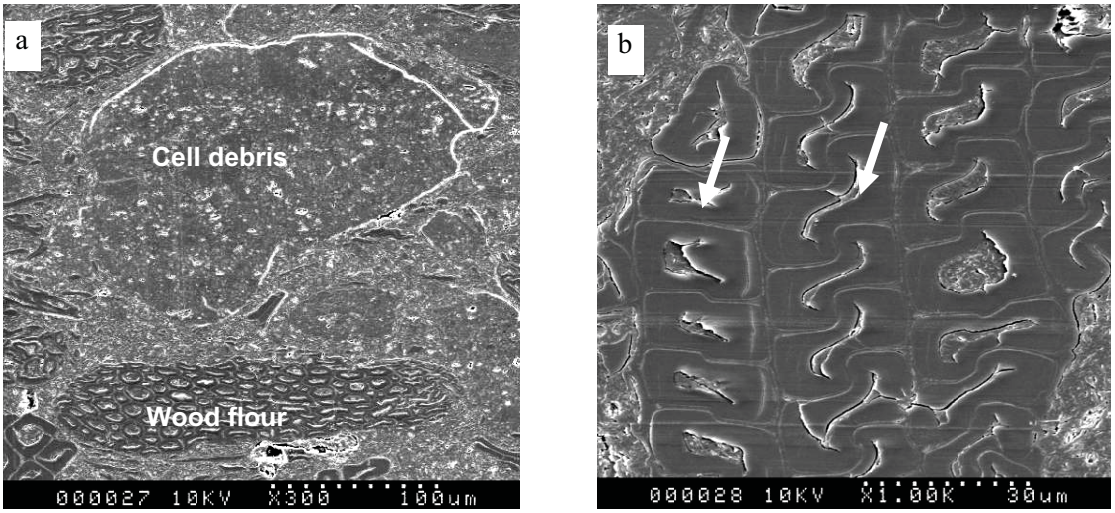

Figure 50. Sectioned surface (c and d) of PHB/Wood flour/Cell debris composites.

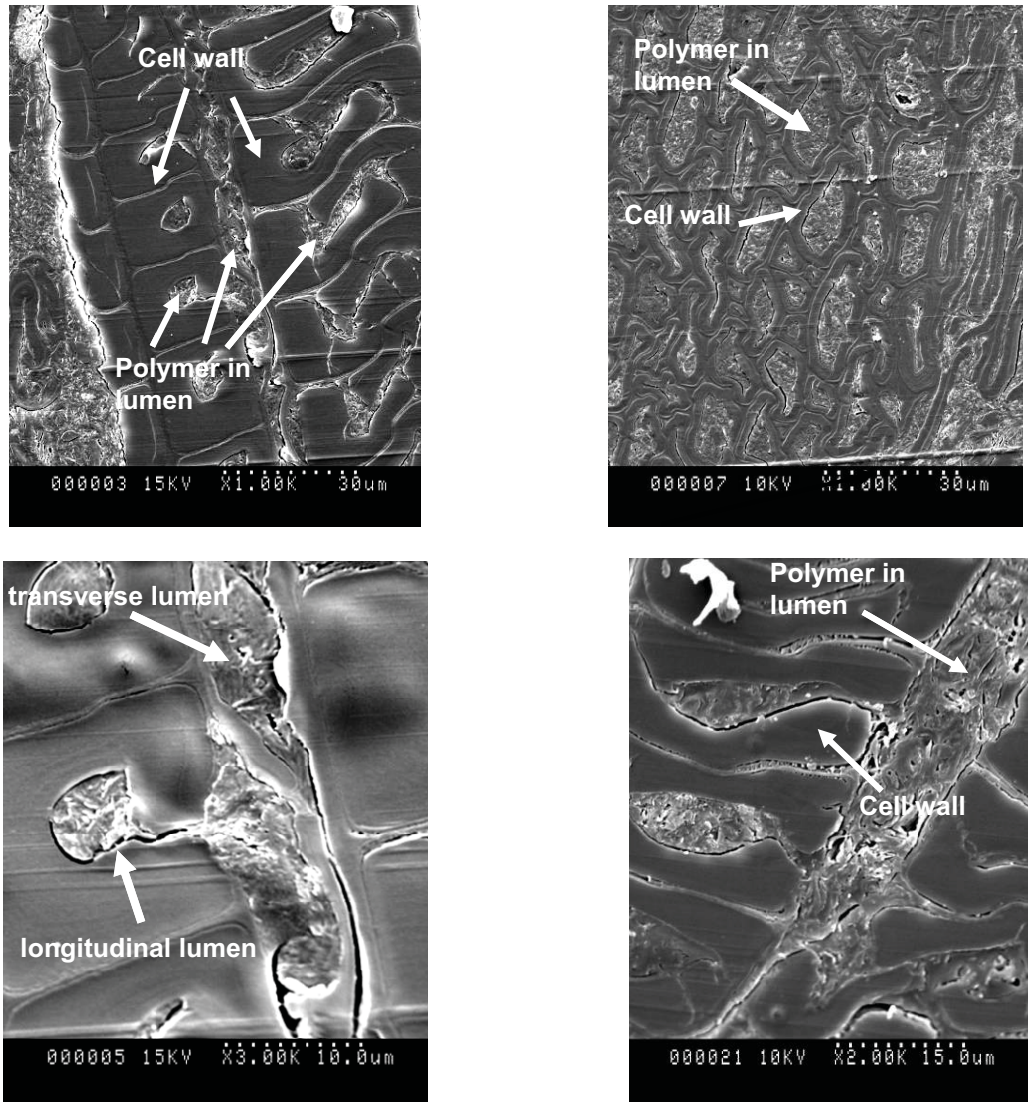

Figure 51. Wood lumens and cells filled with polymer.

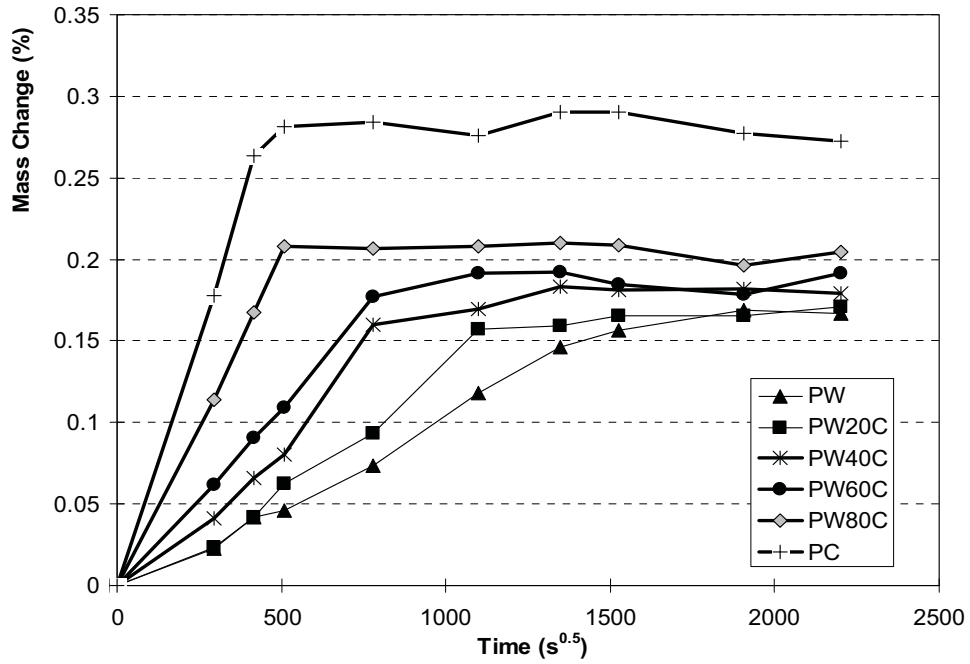

Figure 52. Mass change of the six formulations within 12 weeks period.

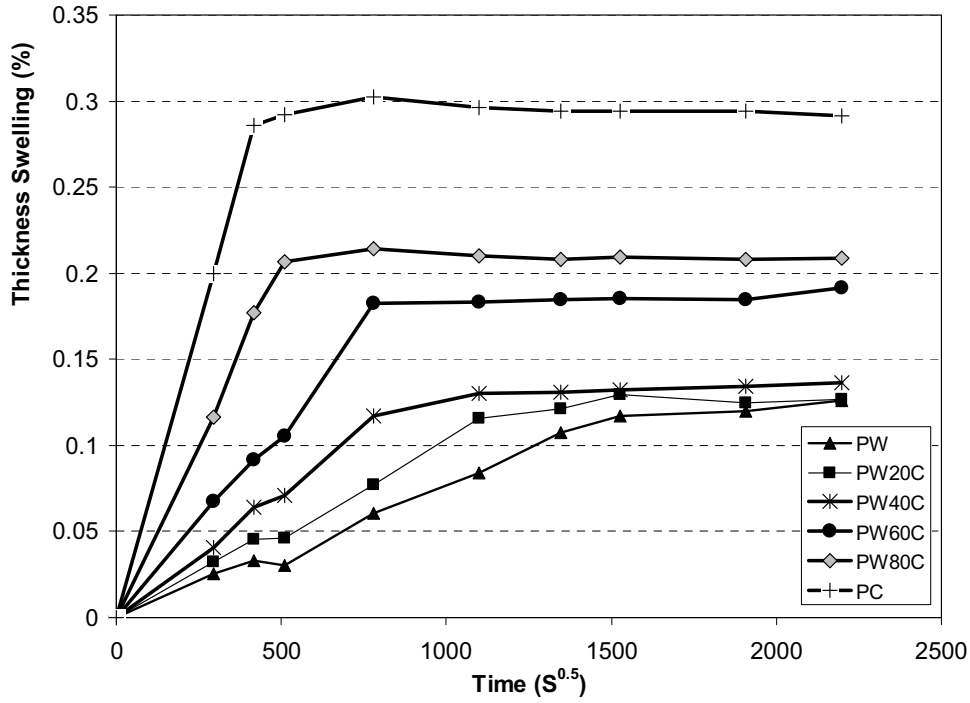

Figure 53. Thickness change of the six formulations within 12 weeks period.

Tables

Table 22. Particle size distribution of the ground cell debris.

Particle size (μm)	<125μm	125~150μm	150~177μm	177~250μm	250~420μm	420~833μm	> 833μm
Weight Percentage (%)	38.6%	5.6%	12.8%	38.7%	4.1%	0.0%	0.2%

Table 23. Formulations of PHB/WF (PW) control and PHB/WF/cell debris (PWC) composites.

Formulation / Components	PW	PWC20	PWC40	PWC60	PWC80	PC
Cell debris*	0	11.4	22.8	34.2	45.6	57
Wood Flour (pine)*	57	45.6	34.2	22.8	11.4	0
PHB	35	35	35	35	35	35
Talc-Nicron 403	8	8	8	8	8	8
pMDI	4	4	4	4	4	4
Lubricant (WP2200)	3	3	3	3	3	3
Nucleating agent (Boron Nitride)	0.2	0.2	0.2	0.2	0.2	0.2

*: 60 mesh particle size. WF: Wood Flour. All units are in parts

Table 24. Densities and mechanical properties with standard deviation of four formulations

		Tensile Properties		Flexural Properties	
Formulation	Density*	Strength (MPa)	Modulus (GPa)	MOR (MPa)	MOE (GPa)
PW	1.396	39.7(0.94)	10.2(0.30)	69.4(1.25)	9.18(0.06)
PWC20	1.388	31.0(0.54)	8.76(0.18)	53.9(1.07)	7.80(0.07)
PWC40	1.388	26.4(0.36)	7.83(0.13)	45.2(0.85)	6.66(0.07)
PWC60	1.390	23.4(0.51)	6.74(0.17)	42.8(1.73)	5.88(0.09)
PWC80	1.368	19.7(0.99)	7.40(0.22)	34.6(1.83)	5.85(0.21)
PC	1.365	14.4(0.86)	6.43(0.15)	26.5(2.68)	4.92(0.22)

* standard deviation less than 0.01
( ) Standard deviation

Table 25. Apparent (D_A) and true (D) diffusion constants for the six formulations.

	PW	PWC20	PWC40	PWC60	PWC80	PC
Slope*	1.08E-04	1.45E-04	2.03E-04	2.27E-04	4.06E-04	5.77E-04
TS_{max}	12.93 %	13.66 %	15.43 %	20.12 %	20.81 %	29.41 %
MC_{max}	17.68 %	19.09 %	20.32 %	22.16 %	20.82 %	29.05 %
D_A	6.56E-07	1.22E-06	1.96E-06	2.24E-06	6.11E-06	6.73E-06
D	4.02E-07	7.49E-07	1.19E-06	1.36E-06	3.27E-06	4.09E-06
β	0.731	0.716	0.759	0.908	0.993	1.102

*: $dMt/d\sqrt{t}$

Developing PHB/Wood Four/Cell Debris Ternary Composites through Extrusion

Abstract

Poly-3-hydroxybutyrate (PHB) is a biodegradable microbial polyester which can be produced by microbes in waste effluents. Using unpurified PHB (i.e. PHB with microbe cells) in WPCs can significantly lower their material and energy costs. In this study, purified PHB and PHB-free cell debris were used to simulate PHB laden microbes in extruding PHB/wood flour/cell debris products with various wood flour/cell debris ratios. A high density polyethylene/wood flour composite with a formulation similar to a commercial WPC was also extruded for comparison. All the WPCs were extruded using a 35-mm twin screw extruder. Polymeric methylene-diphnenyl-diisocynate(pMDI) was used as a coupling agent to increase the interfacial bonding between the PHB matrix and the wood four/cell debris. Mechanical properties and water adsorption of the composites were investigated. It was found that the mechanical properties and moisture resistance of the WPCs decreased with the increasing content of the cell debris, same to the trend found in the injection molded WPCs (first paper). The cell debris laden PHB WPCs (cell debris/wood flour ratio 3:2) showed mechanical properties and water resistance comparable to the commercial HDPE WPC. They could potentially replace some of the petroleum derived WPCs in current markets

Introduction

In our first report for Task 4, PHB/wood flour/cell debris WPCs were developed by melt compounding and injection molding. The injection molded WPCs showed high mechanical properties and water resistance when compared to commercial polyethylene-based WPCs like the current extruded WPC products such as deck floors, sidings, railings, etc. But the packing pressure provided by a typical commercial extrusion process is much lower than those that develop in an injection molding process. These lower process pressures and longer processing times of the typical extrusion process may result in lower product density, product defects, and thermal degradation of the thermally unstable cell debris. The goal of the research presented here is to determine the optimal extrusion conditions for WPCs produced with cell debris laden PHB with varying levels of cell debris content. The extruded products were compared with a commercial polyethylene-based WPC with respect to mechanical performance and water resistance.

Materials & Methods

Materials

The purified PHB powder (Tianan Biologic Material Co., Ltd, Ningbo, China), and wood flour (60-mesh ponderosa pine, American Wood Fibers, Schofield, WI) were obtained commercially for the composite production. Cell debris produced from wastewater by cooperators at UC Davis was impacted milled to a nominal 60-mesh particle size. Boron nitride (BN) (Carbotherm PCTF5, Saint Gobain Advanced Ceramics Co., Amherst, NY) was used as a nucleating agent to promote PHB crystallization. Glycolube WP2200 (Lonza Inc., Allendale, NJ) was included as a lubricant to improve processability. Talc (Nicron 403) was provided by Riotinto of Centennial and was used for processability and water resistance improvements. Liquid form pMDI (Mondur 541, Bayer MaterialScience, Pittsburgh, PA) contained 31.5 mass % NCO and functioned as the coupling agent between hydrophobic PHB and hydrophilic wood flour and cell debris.

To compare the properties of the WPCs extruded with PHB and cell debris with commercial versions, a polyethylene-based WPC was extruded as a control. Its formulation was composed of high density polyethylene (HDPE, Petrothene® LB010000 from Equistar), wood flour, talc, zinc stearate, and ethylene bis staramide (EBS) wax.

Methods

Particle size distribution analysis of ground cell debris

A hammer mill with a screen size of 0.0312-inch was used to grind the cell debris as-received. Particle size distribution analysis of the ground cell debris was conducted using a Ro-Tap sieve analyzer with a series of stacked screens with the screen size ranging from 20 to 120 mesh (top to bottom). The instrument was allowed to run for about 10 minutes to separate the cell debris. The distribution of particle sizes was determined using sieve analysis and is reported in Table 26.

Torque rheometry

The mixing torque of different formulations was evaluated using a Haake Rheomix 600p equipped with a 69 ml mixing chamber. 70 vol% of the chamber was filled with each formulation. The materials were mixed by a pair of roller blades at 20 rpm under different temperatures for 10 minutes. The torque was continuously monitored during the mixing process. The torque values obtained under different mixing conditions were used to optimize the conditions of extrusion process. The formulations used for torque rheometry were shown in Table 26, which were the same as the ones in the first paper, except that no lubricants, talc, and nucleation agent were used. These components were excluded from this experiment because they did not markedly alter the viscosity of the formulations.

Preparation of composites

The 60-mesh pine wood flour was dried by a rotary steam tube drier to a nominal moisture content of ca 3%. Ground cell debris powder was dried at 100^{o}C in a convection oven for 24 hours. Purified PHB, BN, WP2200, and talc were used as-received. Liquid pMDI resin was first dispersed in PHB powder and then blended with all the other components in a drum blender for 5-minutes. The formulations of all the mixtures were shown in Table 28. Melt compounding was accomplished using a conical co-rotating twin screw extruder (Cincinnati Milicron CM 35) with a screw diameter of 35-mm (the small end) and a length/diameter (L/D) ratio of 22. To improve melt strength and reduce material thermal degradation, a declining temperature profile of the extruder was applied during the extrusion process. The temperature profiles for all formulations, which had been optimized based on the torque data of torque rheometry, were shown in Table 27. The screw speed was maintained at 20-rpm. Extrusion residence time was about 1 minute. Each formulation was extruded through a slit die (cross-section 38 x 9.8-mm), and was cooled by spray water upon exiting. Melting pressure was monitored as an indicator of the melt viscosity of the composites before the materials entered the first die zone. Six formulations of PHB/wood flour/cell debris WPCs and one commercial WPC were prepared (Table 28). The former formulations were the same as the ones detailed in the first paper.

Preparation of testing specimens

The extrudate for each formulation were cut into 205-mm long sections for flexural testing. The testing span was 20-times of the sample thickness (9.8-mm), meeting ASTM standard D 790 requirements. Impact test specimens were prepared following ASTM standard D256. The dimensions of the specimens were 12 x 9.8 x 60-mm and the specimens were notched by a XQZ-I specimen Notch Cutter. Specimens for water absorption were surfaced by a planer and cut into 11 x 8 x 100-mm panels.

Mechanical properties and sample density

A screw driven Instron 4466 equipped with a 10-kN load cell and a three point bending test fixture was used for flexural test. The flexural tests were performed with a crosshead speed of 3.80-mm/min. Impact tests were conducted using a Dynisco BPI tester. ASTM standard D256 (mode A), and D790 were followed in the impact and flexural tests, respectively. Five replicates were tested for each formulation to obtain a mean value. Sample density was calculated by dividing sample mass by sample volume. All the samples (for both mechanical and density testing) were conditioned at 23 ^{o}C and 50% relative humidity (RH) for 7 days prior to the tests.

Moisture resistance

Water absorption of the composites was performed following ASTM D 570. Samples were immersed in distilled water at room temperature. The weight and thickness of the samples were measured after different periods of immersion time. Moisture content (MC) and thickness swelling (TS) were calculated by the following equations:

$$MC(\%) = \frac{(M - M_o)}{M_o} \cdot 100 \quad (1)$$

$$TS(\%) = \frac{(T - T_o)}{T_o} \cdot 100 \quad (2)$$

where M is the mass of the specimens at time t, and M_o is the initial mass of the specimens; T is the thickness of the specimens at time t, and T_o is the initial thickness of the specimens.

Results and Discussion

Cell debris particle size distribution

The size distribution of the ground cell debris is shown in Table 29. About 88% by mass of the cell debris particles were sized down to less than 250 μm (60-mesh). The ground cell debris was comprised of higher content (68 wt%) of fine particles (<150μm) compared to the cell debris particles (45 wt%) used for injection molding (the first paper). This was because the hammer mill was more effective than the coffee grinder (used to grind the cell debris in the first paper) in reducing particle size. Finer particles were expected to be beneficial to composite properties.

Torque rheometry

Torque rheometry was used to optimize extrusion temperature profiles for different formulations. Due to cell debris's low aspect ratio (ca. 1.0) and poor interaction with the PHB matrix, the viscosity of the PHB/wood flour/cell debris melt with high cell debris content was low. This led to the lack of high die pressure which was essential for the packing of the extrudate. Insufficient packing of the extrudate resulted in low-density products with high void content.

In this study, the control formulation (PW) was first mixed in the torque rheometer at different temperatures (160, 165, 170, 175, and 180°C) using a constant roller speed (20 rpm). After 8 minutes of mixing in the rheometer, the control formulation showed similar torque (2.5 Nm) at the temperatures equal to or higher than 170 °C (Figure 54). At 160 °C, PHB did not melt at all after 8 minutes of mixing (PHB melting point ca. 165 °C). The material was still in dry powder form and therefore the torque was low. At 165 °C, the polymer became molten and the wood flour was wetted by the polymer. The viscosity of the material was high under this condition and therefore this mixing process showed the highest torque (ca. 3.5 Nm).

Next all six formulations were examined for their viscosities at 165 °C using the torque rheometer. PHB in all the formulations was well melted and wood flour was completely wetted by the molten polymer after six minutes of mixing at this temperature. However, Figure 55 shows that at 6 minutes the formulations with high cell debris contents (e.g., PBW60, PBW80, and PBW100) exhibited lower torque (ca. 2 Nm) compared to the other three formulations (ca. 3.5Nm). This was due to the low aspect ratio of the cell debris and its poor interaction with the polymer matrix. The materials after the mixing also appeared loose for formulations PBW80 and PBW100. To increase the torques for the three low-torque formulations, the mixing temperature was further decreased to 160 °C

By reducing the mixing temperature from 165 to 160 °C for the formulations PBW60, PBW80, and PBW100, the torques increased to about 3 Nm, which was comparable to those of the other three low

cell debris content formulations at 165 °C (Figure 56). Moreover, the materials after the mixing were as dense as the other formulations at 165 °C. Therefore, 160 °C could be used as the extrusion temperature for the three high cell debris content formulations and 165 °C for the low cell debris content formulations. The extrusion temperature profiles for all the formulations were shown in Table 27.

Mechanical properties and sample density

The densities of the six extruded PHB formulations were shown in Table 30. The values ranged from 1.27 to 1.35 g/cm^3, which indicated that due to the increased die pressure for high cell debris content formulations (Table 31), the materials were more densely packed and their densities were similar to the formulations containing less cell debris. Furthermore, compared to the densities of the injection molded samples (see the first paper), the extruded composites exhibited only slightly lower values (average 1.33 as opposed to 1.38 g/cm^3 by injection molding). This was due to the higher pressure (ca. 18,000 psi) in injection molding, which could crush wood cells and force the polymer into the porous structure of wood flour. The commercial formulation (HW) had the lowest density among all the samples. This was because the density of HDPE (ca.0.9 g/cm^3) was substantially lower than the density of PHB (ca. 1.2 g/cm^3).

Modulus of rupture (MOR) of the extruded composites decreased with increasing cell debris content (Figure 57). The same trend was found for the injection molded samples (see the first paper). Low aspect ratio of the cell debris particles and its poor interfacial bonding with the PHBV matrix were attributed to this property deterioration. MOR of PW and PBW20 were comparable to the injection molded samples. But at higher cell debris contents, the extruded samples showed moderately lower MOR compared to the injection molded samples. Modulus of elasticity (MOE) and the impact strength of the extruded samples also showed similar trends (Figure 58 and Figure 59). The impact strength of HW was lower than that of PW but substantially higher than those composites containing cell debris (Figure 59). On the other hand, the ternary PHB composites containing high cell debris contents (PWC60 and PWC80) exhibited MOR and MOE values comparable to HW.

Moisture behavior

Figure 60 and Figure 61 show water absorption and thickness swelling of all the seven formulations during a 8-week immersion test The commercial formulation HW showed the highest moisture saturation content (M_{sat}, ca. 22%) after ca. 1000 hrs. However, HW did not exhibit the highest thickness change. The PHB composites with high content of cell debris, i.e. PC and PWC 80, showed larger thickness change. The results indicated that with pMDI to improve interfacial bonding and suppress the hydrophility of wood flour and cell debris, the water resistance of the cell debris laden PHB/wood flour composites could be higher than the commercial WPC. The larger thickness change of the high content biomass composites (PC and PWC 80) might be due to the large expansion of the cell debris after water absorption. Overall, the composite of PWC 60 exhibited better water absorption properties than HW.

Liquid or gas transportation through a solid material is often modeled by Fickian diffusion equation. In Fickian diffusion, plotting the amount of uptake (moisture in this case) at a given time period against the square root of the time period produces a linear region followed by a non-linear approach to M_{sat}. The apparent diffusion constant (D_A) can be calculated by:

$$D_A = \pi \left[\frac{h}{4M_{sat}} \right]^2 \left[\frac{dM_t}{d\sqrt{t}} \right]^2 \quad (3)$$

where h is the thickness of the specimens and dMt/d√t is the slop of the weight gain versus square root of time.

For calculating 3-dimensional diffusion, a geometric edge correction factor can be used to calculate the true diffusion constant (D):

$$D = \frac{D_A}{(1 + h/L + h/W)^2} \tag{4}$$

where L and W are the length and width of the specimens respectively.

As shown in Table 32, formulation PC had the highest true diffusion constant (1.04E-05 mm^2/sec) among the seven formulations, which indicated that this composite had the highest moisture penetrating rate or the poorest water resistance. The degree of sample swelling was defined by a swelling coefficient:

$$\beta = TS_{\max} / MC_{\max} \tag{5}$$

Table 29 shows that higher cell debris content results in higher swelling coefficient of the composites (ranging from 0.502 to 1.261). This was believed to be due to the higher hydrophility and larger moisture absorption rate of the cell debris.

Conclusions

In this paper we successfully developed extruded PHB/wood flour/cell debris products. Torque rheometer was used to determine extrusion temperature profiles for the formulations with different cell debris contents. A suitable temperature profile was set for each formulation so that a high packing pressure in the die occurred. All the products extruded at high die pressure were free of sample defects even at high cell debris contents. The composites prepared by direct extrusion showed a property trend similar to those prepared by extrusion compounding and injection molding, i.e. the mechanical properties and water resistance of the composites decreased with the increasing content of the cell debris. The PHB/wood flour/cell debris composites with a cell debris/wood flour ratio of 3:2 showed mechanical properties and water resistance similar to the commercial HDPE WPC. Therefore, the cell debris laden biodegradable PHB/wood flour composites could potentially replace some of current fossil oil derived WPCs.

Acknowledgements

The authors gratefully acknowledge the financial support provided by the U.S. Department of Energy, under the grant of *Development of Renewable Microbial Polyesters for Cost Effective and Energy-Efficient Wood-Plastic Composites*.

References

American Society for Testing and Materials. 2005. Standard test methods for flexural properties of unreinforced and reinforced plastics and electrical insulating materials. ASTM D 790-03. ASTM. Philadelphia, PA.

American Society for Testing and Materials. 2005. Standard test methods for determining the izod pendulum impact resistance of plastics. ASTM D 256-05. ASTM. Philadelphia, PA.

American Society for Testing and Materials. 2006. Standard test method for water absorption of plastics. ASTM D 570-98. ASTM. Philadelphia, PA.

Figures

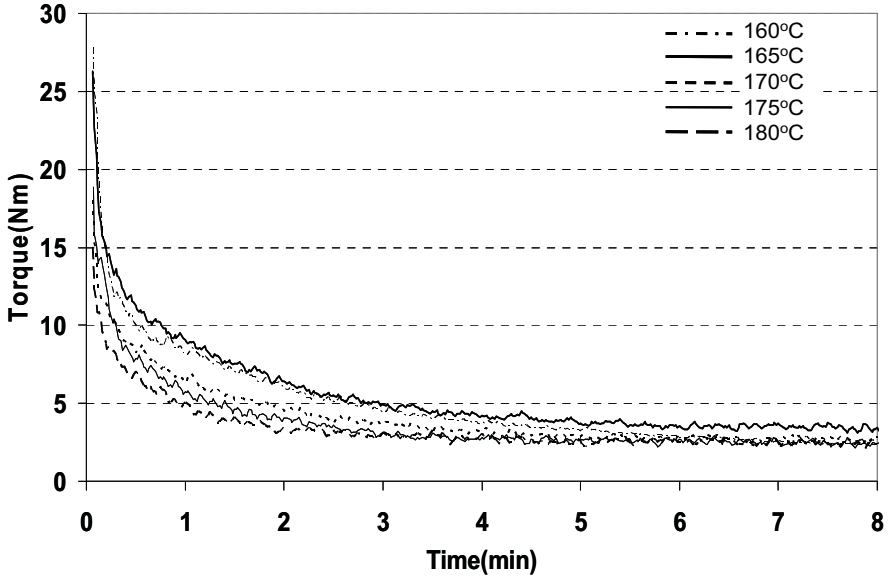

Figure 54. Torque vs. time at different temperatures for the control formulation (PW).

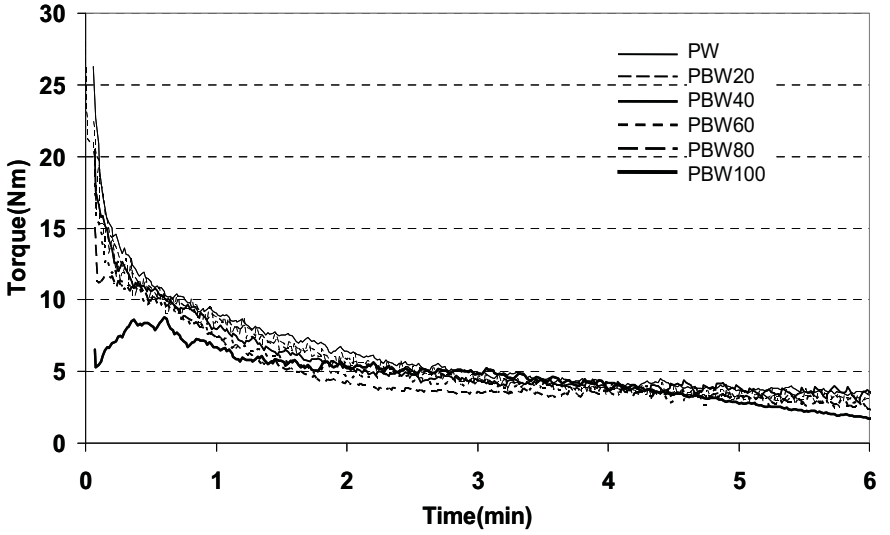

Figure 55. Torque vs. time at 165^{o}C for all six formulations.

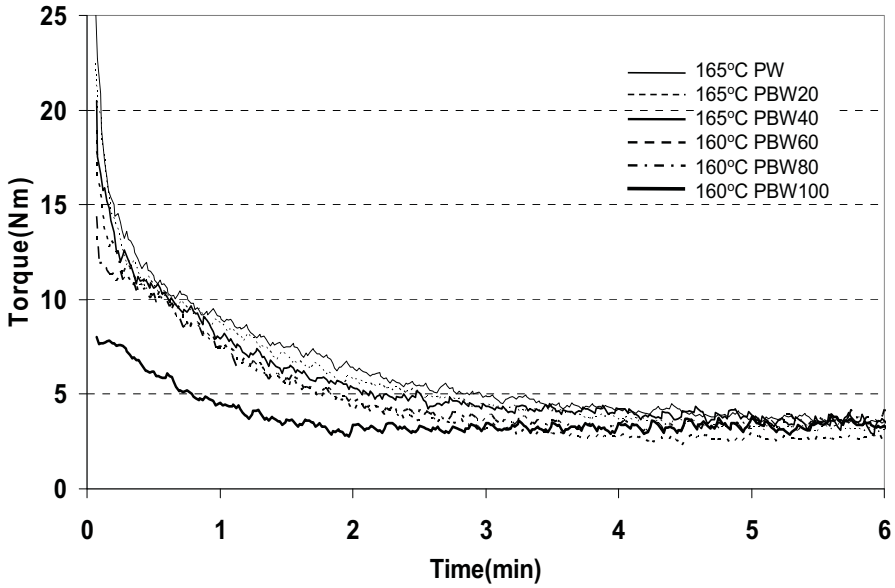

Figure 56. Comparison of the torque vs. time curves at 165 °C (for PW, PBW20, and PBW40) and 160 °C (for PBW60, PBW80, and PBW100).

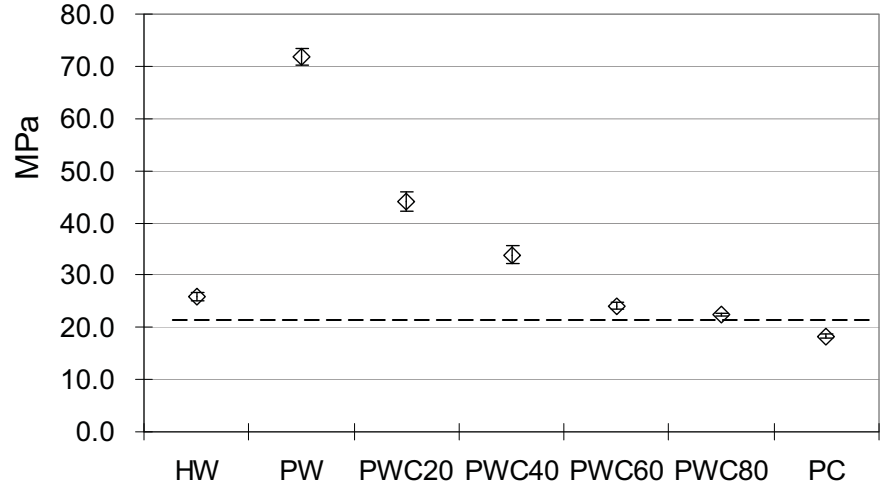

Figure 57. Modulus of rupture (MOR) of the seven composites.

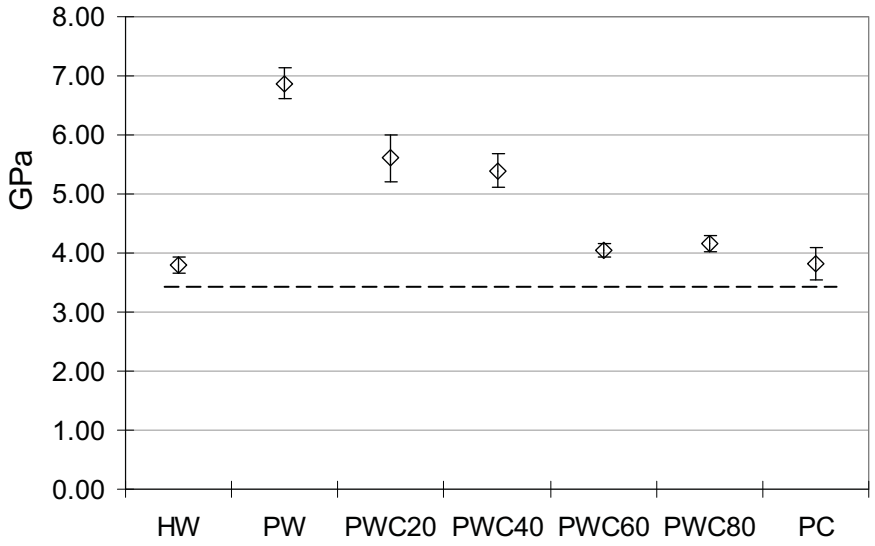

Figure 58. Modulus of elasticity of the seven composites.

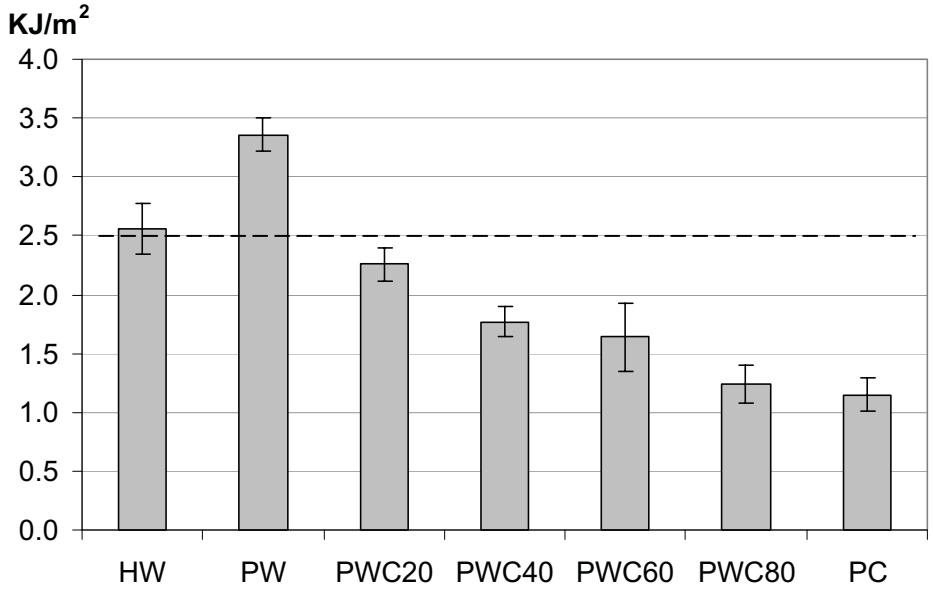

Figure 59. Impact strength of seven different formulations of composites.

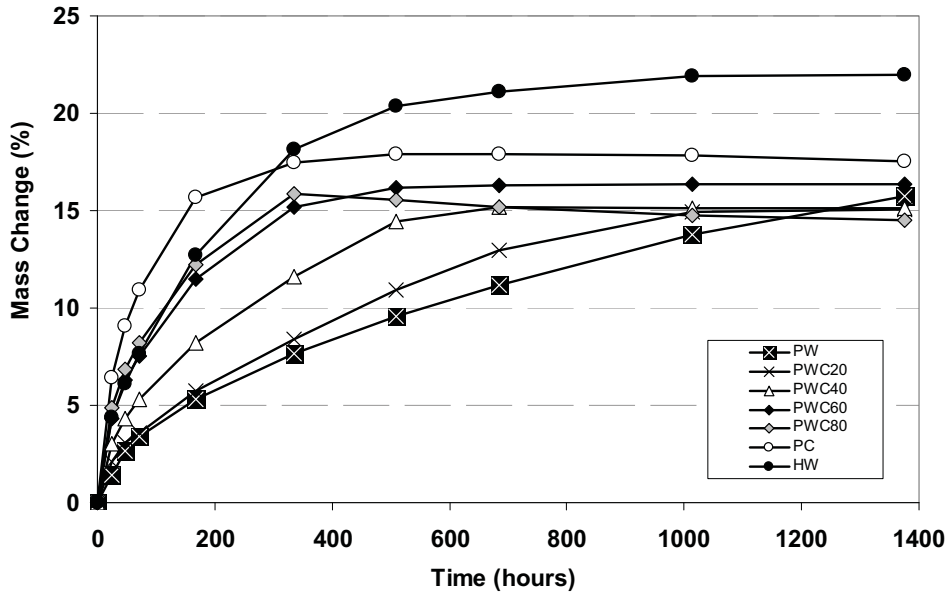

Figure 60. Mass change of the seven formulations within an 8 week immersion period.

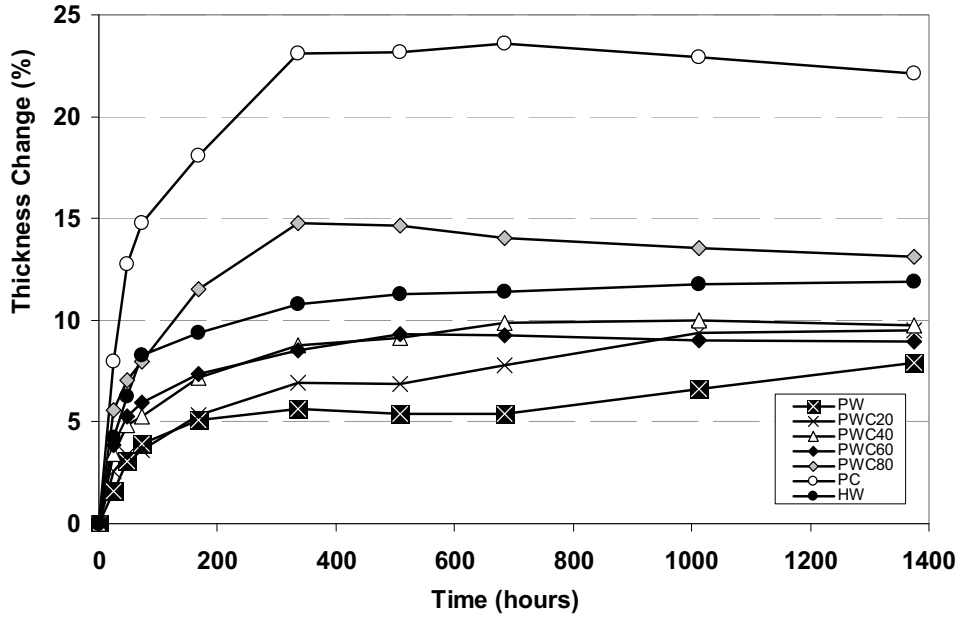

Figure 61. Thickness change of the seven formulations within an 8 week immersion period.

Tables

Table 26. Formulations of the PHB/WF control and the PHB/WF/Cell debris mixtures for torque rheometry study.

Formulation / Components	PHB/WF (PW)	PHB/WF/ 20% Cell debris (PBW 20)	PHB/WF/ 40% Cell debris (PBW 40)	PHB/WF/ 60% Cell debris (PBW 60)	PHB/WF/ 80% Cell debris (PBW 80)	PHB/Cell debris (PBW100)
Cellmass*	0	11.4	22.8	34.2	45.6	57
Wood Flour (pine)*	57	45.6	34.2	22.8	11.4	0
PHB	35	35	35	35	35	35
pMDI	4	4	4	4	4	4

*: 60-mesh particle size.
WF: Wood Flour.
All units are in parts.

Table 27. Temperature profiles used for the extrusions of the seven formulations.

^{o}C	BZ1	BZ2	BZ3	Screw	DZ1	DZ2
HW	163	163	163	163	170	170
PW	170	175	165	163	163	160
PWC 20	170	175	165	163	163	160
PWC 40	170	170	165	160	160	160
PWC 60	165	170	165	155	155	155
PWC 80	160	165	160	150	150	150
PC	160	160	155	150	150	150

BZ: barrel zone DZ: die zone

Table 28. Formulations of HDPE/WF, PHB/WF control, and PHB/WF/cell debris composites.

Formulation / Components	HDPE/ WF (HW)	PHB/W F (PW)	PHB/WF/ 20% Cell debris (PWC 20)	PHB/WF/ 40% Cell debris (PWC 40)	PHB/WF/ 60% Cell debris (PWC 60)	PHB/WF/ 80% Cell debris (PWC 80)	PHB/ Cell debris (PC)
Cell debris*	0	0	11.4	22.8	34.2	45.6	57
Wood Flour (pine)*	58	57	45.6	34.2	22.8	11.4	0
Polymer	32	35	35	35	35	35	35
Talc-Nicron 403	7	8	8	8	8	8	8
pMDI	0	4	4	4	4	4	4
Lubricant	2	3	3	3	3	3	3
Wax (EBS)	1	0	0	0	0	0	0
Nucleating agent (Boron Nitride)	0	0.2	0.2	0.2	0.2	0.2	0.2

*: 60 mesh particle size.
WF: Wood Flour.
Lubricant: Zinc stearate for HW and WP2200 for the others.
All units are in parts.

Table 29. Particle size distribution of the cell debris after hammer milling.

Particle size (μm)	<125μm	125~150μm	150~177μm	177~250μm	250~420μm	420~833μm	> 833μm
Weight percentage (%)	59.1%	9.3%	7.7%	11.7%	8.9%	2.8%	0.4%

Table 30 Table 5. Densities of HDPE/wood flour, PHB/WF control and PHB/wood flour/Cell debris composites.

	HW	PW	PWC20	PWC40	PWC60	PWC80	PC
Density (g/cm^3)	1.18	1.31	1.33	1.32	1.27	1.34	1.35

*: standard deviation less than 0.01

Table 31. Extrusion parameters of the HDPE/wood flour, PHB/WF control and PHB/wood flour/Cell debris composites.

Parameters / Formulations	Die Temperature (^oC)	Die Pressure (psi)	Ampere (A)
HW	170	536	5
PW	163	910	7
PWC 20	166	842	6
PWC 40	164	618	5
PWC 60	160	530	5
PWC 80	156	850	5
PC	153	921	5

Table 32. True (D) diffusion constants and thickness swelling coefficient for the seven formulations.

	HW	PW	PWC20	PWC40	PWC60	PWC80	PC
Slope*	1.49E-04	6.63E-05	7.21E-05	1.04E-04	1.49E-04	1.63E-04	2.16E-04
TS_{max}	11.9%	7.9%	9.5%	9.8%	9.0%	13.1%	22.1%
MC_{max}	22.0%	15.7%	15.1%	15.1%	16.3%	14.5%	17.5%
D (mm^2/sec)	2.34E-06	2.48E-06	1.80E-06	3.34E-06	5.32E-06	8.25E-06	1.04E-05
β	0.541	0.502	0.632	0.645	0.549	0.901	1.261

*: $dMt/d\sqrt{t}$

Results – Pilot Testing of PHA Production and Composite Extrusion

Task 5 – Pilot-scale Extrusion Testing of Waste Effluents PHA Composites

Investigators: Michael P. Wolcott[1], David Bennet[2]; Alfred B. England[3], Karl R. Englund[1], James Flanders[4], Frank J. Loge[5], William A. Smith[6], David N. Thompson[6], James Waller[5], Katherine A. Wiedeman[4], Jinwen Zhang[1], Long Jiang[1], Meng-Hsin Tsai[1]

Performing Institutions: [1]Washington State University; [2]Eco:Logic Inc.; [3]Strandex, Inc.; [4]Glatfelter, Inc.; [5]The University of California-Davis; [6]Idaho National Laboratory

Developing PHB/Wood Four/Cell Debris Ternary Composites through Pilot-scale Extrusion

Abstract

In this study, PHB/wood flour/cell debris blend with the cell debris/wood flour ratio of 3:2 (PWC60) were extruded into deck boards on an industrial scale extrusion line. The flexural properties, density profile, and nail/screw withdrawal strength of the deck boards were investigated and compared with those of HDPE/wood flour (HW) and PHB/wood flour (PW) deck boards. Visual examination and density profiles of the boards showed that the PWC60 was prone to cell debris degradation which caused sample defects such as cracks, voids, and bubbles. The PWC60 samples free of defects exhibited flexural properties similar to HW and PW samples and higher density and screw withdrawal strength. However, the PWC60 boards were too hard for nailing using general purpose nails, due to its high density and modulus.

Introduction

It has been demonstrated in Task 4 that the PHB/wood flour/cell debris composites could be successfully prepared by both injection molding and extrusion. The composites with the cell debris/wood flour ratio of 3:2 (PWC60) exhibited properties comparable to commercial WPCs. In this study, PWC60 deck boards were prepared using an industrial scale extrusion line. Flexural properties, density profile, and nail/screw withdrawal strength of the deck boards were investigated. HDPE/wood flour and PHB/wood flour deck boards were also extruded and examined for comparison.

Materials & Methods

Materials

The purified PHB powder (Tianan Biologic Material Co., Ltd, Ningbo, China), waste effluents cell debris (provided by UC-Davis and hammer milled with a screen size of 0.0312 inch , see Table 33 for the particle distribution), and wood flour (60-mesh ponderosa pine, American Wood Fibers, Schofield, WI) were the three main components of the composites. Boron nitride (BN) (Carbotherm PCTF5, Saint Gobain Advanced Ceramics Co., Amherst, NY) was used as a crystallization agent to promote PHB crystallization. Glycolube WP2200 (Lonza Inc., Allendale, NJ) was included as a lubricant to improve processability. Talc (Nicron 403) was provided by Riotinto of Centennial and was used for processability and water resistance improvements. Liquid form pMDI (Mondur 541, Bayer MaterialScience, Pittsburgh, PA) contained 31.5 mass % NCO and functioned as the coupling agent between hydrophobic PHB and hydrophilic wood flour and cell debris.

For comparison, a commercial formulation of WPCs, which was comprised of high density polyethylene (HDPE, Petrothene® LB010000 from Equistar), wood flour, talc, zinc stearate (Chemical

Distributors, Inc. DLG20), and ethylene bis-staramide (EBS) wax (General Electric Specialty Chemicals), were also extruded for testing.

Methods

Hammer Milling

A hammer mill with a screen size of 0.0312-inch was used to grind the cell debris. All the cell debris was ground as-received. Particle size distribution analysis of the ground cell debris was conducted using a Ro-Tap sieve analyzer with a series of stacked screens with the screen size ranging from 20 to 120 mesh (top to bottom). The instrument was allowed to run for about 10-minutes to separate the cell debris.

Preparation of composites

The 60-mesh pine wood flour was dried by a rotary steam tube drier to a moisture content of about 3%. Ground cell debris powder was dried at 100^{o}C in a convection oven for 24-hours. Purified PHB, BN, WP2200, and talc were used as-received. PMDI was first dispersed in PHB powder, and then blended with all the other components in a drum blender for 10-minutes. Three formulations were prepared, including one HDPE/wood flour, one PHB/wood flour, and one PHB/wood flour/cell debris mixtures (Table 34). WPC deck boards (cross section 127 x 25-mm) were extruded using an industrial scale conical co-rotating twin screw extruder (Cincinnati Milacron TC- 86) with a screw diameter of 86-mm. To improve melt strength and reduce material thermal degradation, a declining temperature profile of the extruder was applied during the extrusion process (Table 35). The screw speed was maintained at 14 rpm throughout the extrusion process for all the three formulations. Melting pressure was monitored as an indicator of the melt viscosity of the composites before the materials entered the first die zone. Table 36 shows the die pressure, temperature and extruder ampere of the three extrusion processes. The extruded deck boards were cooled by water spray upon exiting the die.

Flexural properties testing

The extruded boards were cut into 508 mm long sections (20 times of the thickness of the boards following ASTM D6109) and used directly for flexural testing. A screw driven Instron 4400R equipped with a 150-KN load cell and a set of four point bending test fixtures was used for the tests. The span of the two supports was 406.4 mm, and the distance between the two loading noses was one third of the span (ca. 135.5 mm, Figure 62). The flexural tests were performed using a constant crosshead speed of 11.9mm/min. Mid-span deflection of the specimens was measured by a +/- 25.4 mm linear variable differential transformer (LVDT). Stress and strain were calculated according to ASTM D 6109 to obtain the modulus of rupture (MOR) and modulus of elasticity (MOE). Five replicates were tested for each formulation to obtain a mean value. All the specimens were conditioned at 23 ^{o}C and 50% relative humidity (RH) for 7 days prior to the tests.

Density profile testing

Density distribution of the extruded boards was investigated by an X-ray vertical density profiler (Model QDP-01X, Quintek Measurement Systems, Inc.). The boards were cut into 50.8 x 50.8 x 25.4-mm (length x width x depth) pieces for the investigation. Five replicates were tested for each formulation to obtain a mean value. All the specimens were conditioned at 23 ^{o}C and 50% relative humidity (RH) for 7 days prior to the tests.

Nail/screw withdrawal testing

Nail and screw withdrawal tests were performed to evaluate the nail withdrawal strength of the WPCs. The specimens were prepared by cutting the boards into 127 mm long sections following ASTM D1037 (in accordance with ASTM D7031). In order to eliminate the effects of material relaxation, the nail withdrawal tests were carried out immediately after the nails were driven into the specimens. The nails were 2.52 x 51.9-mm (diameter x length) steel nails. Screw withdrawal testing was performed on pre-drilled pilot through holes perpendicular to the board surface. The holes were drilled using a 2.39 mm

diameter drill bit (ca. 88% of root diameter of the screw). Test screws were all purpose wood screws (#8 Hillman) with yellow dichromate finish, measuring 2.70 x 51.3-mm (root diameter x length). The screw withdrawal tests were also performed immediately after the screws were driven into the pilot holes. A picture of the nail and screw used in the tests was shown in Figure 63. A screw driven Instron 4466 equipped with a 10-kN electronic load cell and a set of test fixtures was used to conduct the tests at a constant crosshead speed of 1.5 mm/min. The nail/screw withdrawal resistance was calculated by dividing the maximum load by nail/screw traveling distance. Five replicates were tested for each formulation to obtain a mean value. All the specimens were conditioned at 23 ^{o}C and 50% relative humidity (RH) for 7-days prior to the tests.

Results & Discussion

Particle size distribution of ground cell debris

The size distribution of the ground cell debris is shown in Table 33. About 88 wt% of the cell debris particles were smaller than 250-μm (60-mesh).

Density and flexural properties

The density and flexure properties are shown in Table 37. PWC showed the highest density among the three formulations probably due to the high density of the cell debris. The three deck boards had similar flexural properties (MOR around 20-MPa, and MOE around 4.2 to 4.6-GPa). Due to severe thermal degradation of the cell debris (see Task 4), the gases produced during extrusion could not be thoroughly removed by the vacuum vent of the extruder. Therefore, part s of the extruded boards of PCW60 showed internal and external defects such as cracks and bubbles. The specimens used for the density and flexural tests were chosen from the board sections free of defects. Similar defects were not found in the extruded products from the 35 mm extruder (Task 4). Therefore, the venting system of the 86mm extruder might need to be improved for higher venting efficiency. The flexural results indicated that PCW60 had mechanical strength comparable to ordinary commercial WPCs, and therefore it had the potential for product substitution.

Density profile

Extrusion process generally can produce a uniformed through-thickness density profile of the extrudate. This was demonstrated by the density profiles of HW and PW. For PWC60 board, the prolonged thermal degradation of cell debris in the core of the board (board surfaces were quickly cooled by water spray) caused voids and cracks in the board center. Therefore, PWC60 board showed a lower density in the core area than in the surface area (Figure 64).

Nail/Screw withdrawal strength

Nail and screw withdrawal strength of the three boards was shown in Table 38. HW and PW boards exhibited similar nail withdrawal strength of 0.153-kgf/mm. No data could be collected for the PWC60 board because nails could not be driven into the board due to high hardness of the board. Instead, all nails were bent by hammering before they could penetrate the board (Figure 65). This may complicate the construction process when using this board as a building material. On the other hand, PWC60 showed the highest screw withdrawal strength among the three boards (1.39 compared to 1.28 and 1.23-kgf/mm). However, the PWC60 board cracked or even broke after the screws were pulled out, whereas similar board failure did not occur on the HW and PW boards (Figure 66). Some board materials also stuck to the screws after they were pulled out. These findings indicated that the PWC60 boards were more brittle than the HW and PW boards, which meant that additional design considerations was required when the PWC60 boards were used as building materials.

Conclusions

Industrial scale extrusion of PWC60 deck boards was successfully performed. The boards were more prone to sample defects than the cell debris free boards (i.e. HW and PW boards) due to cell debris

thermal degradation. The PWC60 boards showed flexural properties comparable to the HW and PW boards and a screw withdrawal strength higher than the HW and PW boards (1.39 vs.1.23-kgf/mm). However, the PWC60 boards were too hard for nailing using general purpose nails. This could be solved by preparing pre-drilled holes before nailing or screwing.

Acknowledgements

The authors gratefully acknowledge the financial support provided by the U.S. Department of Energy, under the grant of *Development of Renewable Microbial Polyesters for Cost Effective and Energy-Efficient Wood-Plastic Composites*.

References

American Society for Testing and Materials. 2006. Standard test methods for evaluating properties of wood-based fiber and particle panel materials. ASTM D 1037-06a. ASTM. Philadelphia, PA.

American Society for Testing and Materials. 2005. Standard test methods for flexural properties of unreinforced and reinforced plastic lumber and related. ASTM D 6109-05. ASTM. Philadelphia, PA.

American Society for Testing and Materials. 2004. Standard guide for evaluating mechanical and physical properties of wood-plastic composites. ASTM D 7031-04. ASTM. Philadelphia, PA.

Figures

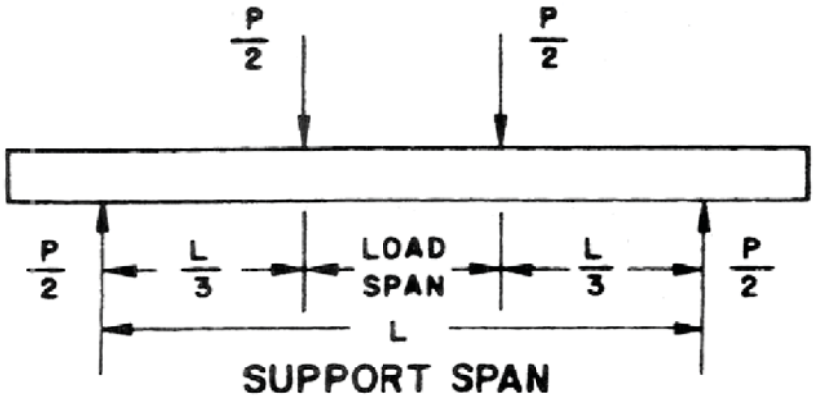

Figure 62. Displace of third point (4-point) flexural testing

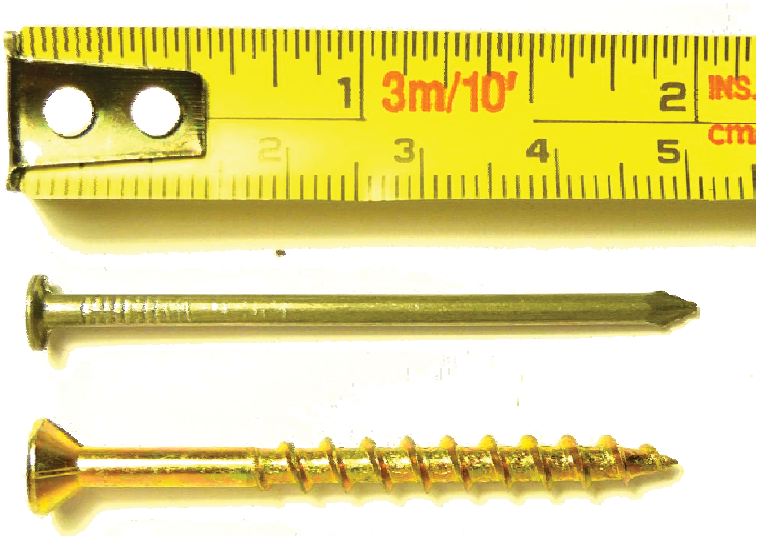

Figure 63. The nail and screw used for withdrawal testing.

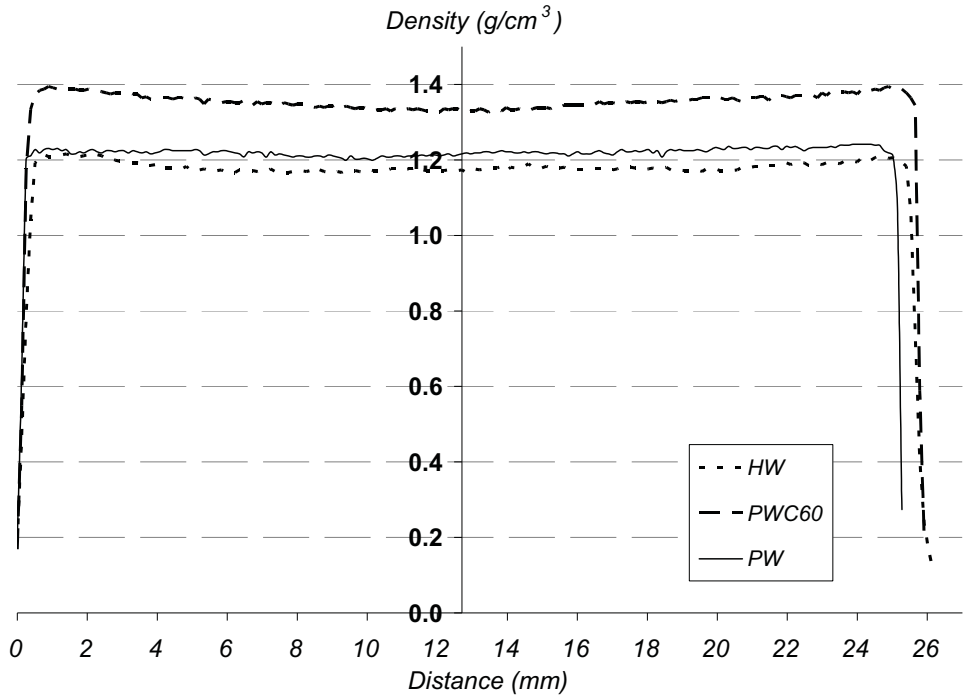

Figure 64. Density profile in the through-thickness direction for the three different deck boards.

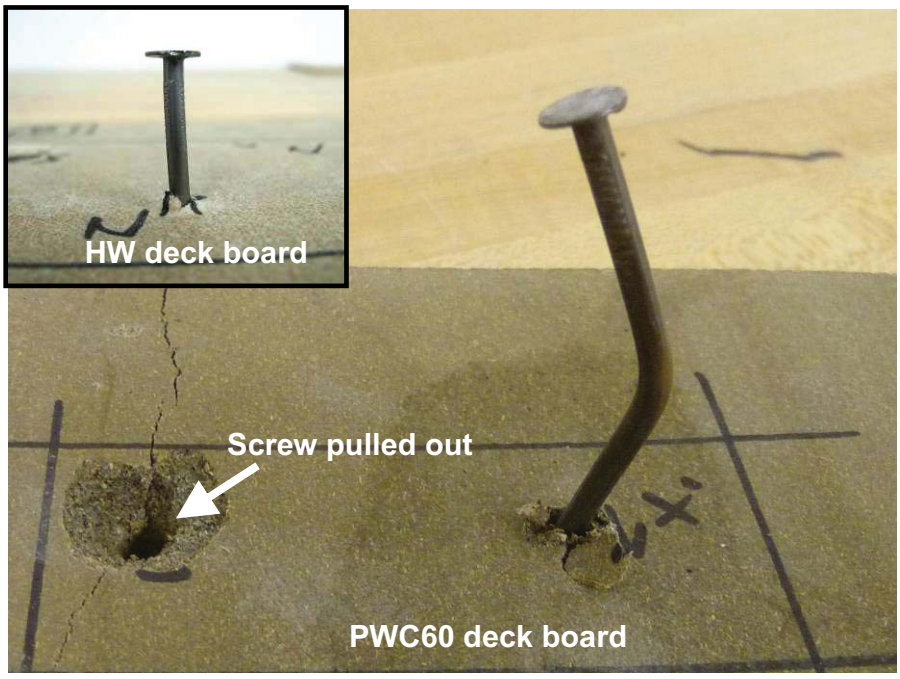

Figure 65. Nail was bent before being fully hammered into the PWC60 board.

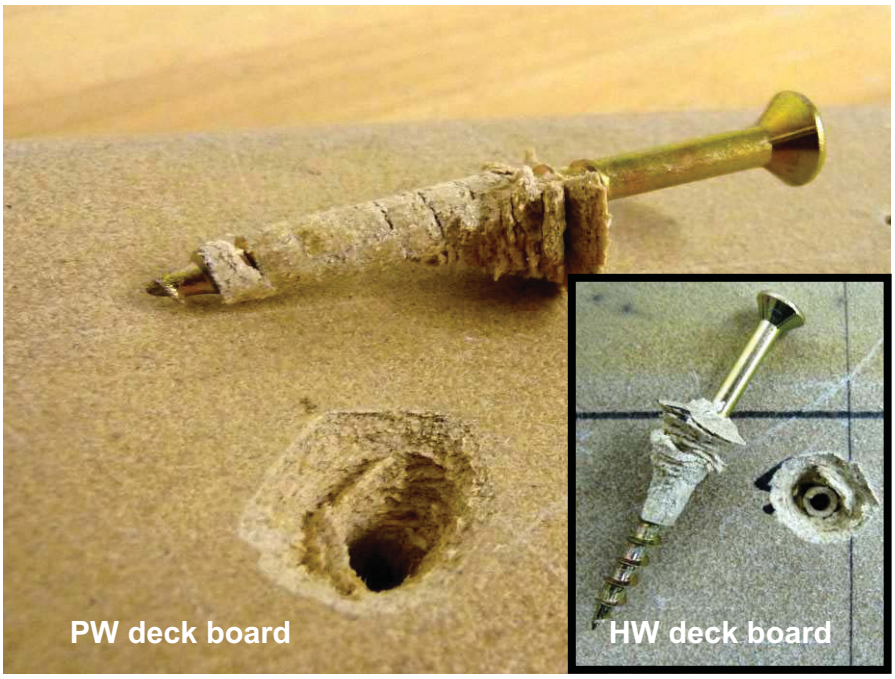

Figure 66. The PW and HW deck boards and screws after screw withdrawal tests.

Tables

Table 33. Particle size distribution of hammer mill ground cell debris.

Particle size (μm)	<125μm	125~150μm	150~177μm	177~250μm	250~420μm	420~833μm	> 833μm
Weight percentage (%)	59.1%	9.3%	7.7%	11.7%	8.9%	2.8%	0.4%

Table 34. Formulations of HDPE/wood flour, PHB/wood flour, and PHB/wood flour/cell debris composites.

Formulation / Components	HDPE/ WF (HW)	PHB/ WF (PW)	PHB/WF/60% Cell debris (PWC 60)
Cell debris*	0	0	34.2
Wood Flour (pine)*	58	57	22.8
Polymer	32	35	35
Talc-Nicron 403	7	8	8
pMDI	0	4	4
Lubricant	2	3	3
Wax (EBS)	1	0	0
Nucleating agent (Boron Nitride)	0	0.2	0.2

* : 60 mesh particle size.
WF: Wood Flour.
Lubricant: Zinc stearate for HW and WP2200 for the others.
All units are in parts.

Table 35. Temperature profiles used for the extrusions of the 3 formulations.

^{o}C	BZ1	BZ2	BZ3	Screw	DZ1	DZ2
HW	163	163	163	163	170	170
PW	170	175	165	163	163	160
PWC 60	165	170	165	155	155	155

BZ: barrel zone DZ: die zone

Table 36. Extrusion parameters for the three formulations.

Parameters / Formulations	Die Temperature (^{o}C)	Die Pressure (psi)	Ampere (A)
HW	173	755	23
PW	163	1088	20
PWC 60	160	1050	30

Table 37. Density and flexural properties of the 3 composites.

	HW	PW	PWC60
Density * (g/cm^3)	1.19	1.21 *	1.34 *
MOR (MPa)	20.6 (0.6)	20.9 (2.0)	19.8 (3.4)
MOE (GPa)	4.19 (0.09)	4.16 (0.26)	4.63 (0.98)

* The standard deviation is about 0.01

Table 38. Nail/Screw withdrawal strength of the 3 composites.

	HW	PWC60	PW
Nail withdrawal strength (kgf/mm)	0.154 (0.01)	-	0.153 (0.01)
Screw withdrawal strength (kgf/mm)	1.284 (0.03)	1.390 (0.29)	1.227 (0.03)

- Nail bent before hammer nailing in (see **Figure 65**)

A Feasibility Study of PHA Production Utilizing Mixed Cultures and Industrial Waste Streams at Pilot-Scale

Introduction

Increasing global demand for crude oil and concerns about greenhouse gas emissions has created an interest in discovering other production methods for thermoplastics. Current research has focused on finding new feedstocks for production that avoid the use of crude oil. Plant-based feedstocks, such as cornstarch, are used to make biodegradable plastics currently sold on the commercial market (EcoProducts, Boulder, CO). Another promising area of research is production of polyhydroxyalkanoate (PHA) thermoplastics by bacterial cultures. Bacteria have been found in the environment that uses a wide variety of carbon sources to produce these biodegradable polymers in their cells. The use of single bacterial strains, both wild and recombinant, has been the focus of many studies to maximize the efficiency of producing PHA in batch fermentations (Salehizadeh 2004). This method currently produces PHA for the commercial market, but it is not cost competitive with petroleum-based thermoplastics and requires significantly more energy; specifically the energy associated with feedstock production and the equipment necessary for sterile production (Reis 2003).

Producing PHA with mixed cultures using industrial waste stream feedstocks could significantly reduce costs and input energy. These waste streams traditionally require treatment to reduce soluble carbon concentrations before discharge. The process of producing PHA using industrial waste streams utilizes the soluble carbon as a feedstock, effectively producing a valuable plastic product from a carbon source that would otherwise be lost, while concurrently treating the industrial waste. Studies at the bench-scale have demonstrated that producing significant amounts of PHA from many different industrial wastes, such as brewery waste (Liu 2008), pulp and paper mill waste (Mockos 2008a), food scrapes (Rhu 2003), primary solids (Coats 2007), palm oil effluent (Din 2006) and sugar cane molasses (Albuquerque 2007) is possible under specific conditions.

PHA is a promising future source of thermoplastics for consumers but a safe, efficient method of utilizing the intracellular plastic is necessary for this process to be environmentally friendly. Natural fiber reinforced thermoplastic composites have been produced at the bench top scale in previous studies using PHA-laden biomass (Coats 2007). This production method avoids the use of toxic solvents typically needed to extract the plastic from the cells by incorporating both the cell mass and PHA directly into the final product. Additionally, these composite thermoplastics have similar physical properties to products produced with petroleum-based plastics.

The aim of this study was to produce PHA-laden biomass from industrial waste streams using mixed microbial cultures at the 200-gallon pilot-scale. Two pilot units were constructed and operated using brewery waste and pulp and paper mill waste as feedstocks under previously determined optimal operating conditions assessed at the bench-scale (Liu 2008; Mockos 2009). The pilot-scale unit was intended to assess the feasibility of scaling the existing bench-scale PHA production configurations. The specific objectives of this study were to:

1. Startup the pilot units and confirm the removal of soluble carbon measured as chemical oxygen demand;
2. Determine intracellular PHA content and consistency at the pilot-scale;
3. Produce significant quantities of PHA-laden biomass and dried cellular material, without PHA, for pilot-scale extrusions of natural fiber reinforced thermoplastic composites.

Methods and Materials

Brewery Waste Pilot Unit

Pilot Unit Construction

A 700 liter pilot unit was constructed to demonstrate PHA production using brewery waste. Figure 67 displays the process and flow-rates of the pilot unit system. The sequencing batch reactor (SBR) and the batch reactor were based around 700 liter high-density polypropylene tanks mounted on heavy-duty plastic pallets (Mcmaster, Robbinsville, NJ). Six 7" Sanitaire fine bubble disc diffusers (ITT Industries, Brown Deer, WI) were mounted at the bottom of the reactor and connected together with PVC piping. Air was continuously supplied to the diffusers by two Gast diaphragm type air pumps (Fisher Scientific, Pittsburg, PA) to ensure fully aerobic conditions in the reactors. A used 240V mixer motor was mounted on top of the reactor with a custom steel stand and connected to a stainless steel impeller built at UC Davis for mixing of the reactor. Water-tight bulkhead fittings (Grainger, West Sacramento, CA) were attached to the side of the reactor tank for connection of the feed and drain pumps. A 20 GPM flexible impeller motor (Grainger, West Sacramento, CA) was used to pump brewery waste into the reactor. Three 4 GPM flexible impeller pumps were employed for pumping to the batch reactor, the system drain, and the speed controlled basket centrifuge (AML Industries, Hatboro, PA). The centrifuge was used to collect the PHA-laden biomass from the batch reactor. Digital timers (Ace Hardware, Davis, CA), connected to medium amp mechanical relays (McMaster Carr, Robbinsville, NJ), controlled each pump independently. An AC speed controller (Dart Controls, Zionsville, IN) was hardwired to the flexible impeller pump that transferred PHA-laden biomass from the batch reactor to the centrifuge. This controller set the pump flow rate at 1 GPM to the centrifuge to increase biomass recovery. The electronic controls, relays, and speed controllers were mounted in a NEMA-4 steel enclosure with watertight electrical fittings (McMaster Carr, Robbinsville, NJ). Three 1200-L intermediate bulk containers (IBC) (McMaster Carr, Robbinsville, NJ) were used to transport and store brewery waste prior to feeding to the SBR and batch reactor. PHA-laden biomass collected from the centrifuge was dried in a commercial oven at 55°C in baking pans. Overall, this pilot system required a footprint of 8' by 12' and included three feed tanks and four pallets.

Feedstock Source

Brewery waste was collected from Sierra Nevada Brewing Company's wastewater treatment plant (Chico, CA). The characteristics of brewery waste are described in Liu et al., 2008. Primary influent was collected in the 1200L IBC tanks and transported on a 2-ton flatbed truck. A 5000-lb forklift was necessary for loading and unloading the tanks. Brewery waste was picked up on a weekly basis and the tanks were thoroughly cleaned out between refills to prevent excessive bacterial and fungal growth. Once the tanks had been refilled and delivered to UC Davis, they were allowed to sit undisturbed overnight. The suspended solids that settled overnight were removed from the tank the following morning by pumping 100L from the bottom of each tank. This prevented introduction of large solids to the reactors, which was previously shown to lower the percentage of PHA in the solids collected (Liu 2008). The feed tanks were stored outside for seven days between cleaning and refills, and were tightly capped to prevent excessive contamination and oxygen transfer that would promote bacterial and fungal growth.

Microbial Sources

Activated sludge from the Sierra Nevada wastewater treatment plant was acquired as a source of microorganisms for the initial inoculation of the pilot unit as outlined in Liu et al. (2008). The activated sludge was already conditioned to brewery waste and was therefore a perfect source of inoculum.

Operating Parameters

The brewery pilot unit operating parameters were based on the bench-scale experiments performed by Liu et al., 2008. The goal for the pilot unit was to remove a large portion of the COD and produce significant quantities of PHA. The pilot scale SBR was operated with a four-day SRT and four-day HRT with feed provided one cycle per day. At the bench scale, this reactor configuration removed 80% of the COD per cycle and produced a peak intracellular PHA content of 30%. At the bench-scale, other reactor configurations did produce higher intracellular PHA content with similar COD removal, but these alternative configurations required differing values of HRT and SRT. Operating the pilot unit with different HRT and SRT values would require additional steps, including either (1) turning off the aeration and mixing to settle the solids with differing points of controlled withdrawal of biomass and liquid or (2) employing a centrifuge to remove the solids with manual addition back to the reactor. These additional steps to separate SRT and HRT were deemed unnecessary at the pilot scale given the specified HRT and SRT of four days provided adequate COD removal and intracellular PHA content for production of natural fiber reinforced thermoplastic composites.

Startup and Stabilization Procedure

The brewery waste pilot unit was started in April 2008. Volumes of 350L of activated sludge and 350L of brewery waste were added to the SBR. The air pump and mixing motor were turned on to begin aeration and mixing, and continued for the duration of its operation. On the second day of operation, the first drain and feed cycle took place. The 4 GPM flexible impeller pump drained 175L from the SBR in 11.5 minutes. Five minutes after the drain cycle ended, the 20 GPM flexible impeller pump pumped 175L of brewery waste to the SBR in two minutes and twenty seconds. This process was controlled by the digital timers and supervised daily to ensure the flow rates were consistent and the reactor volumes were maintained.

PHA Production Procedure

Once the pilot unit removed a consistent percentage of COD per cycle, harvesting PHA biomass commenced utilizing the batch reactor. The batch reactor's carbon concentration was twice the level in the SBR based on previous work (Liu 2008). The following procedure was performed each day during pilot operation. A volume of 175L of liquid from the SBR was pumped by a 4 GPM flexible impeller pump to the batch reactor during the SBR drain cycle. At the same time, 175L of brewery waste feed was pumped by a 20 GPM flexible impeller pump to the batch reactor and 175L of brewery waste was pumped to the SBR by a second 20 GPM flexible impeller pump. When the batch reactor reached the period of peak PHA content (gPHA/gBiomass), the entire volume of the batch reactor was pumped at 1 gal/min by a 4 GPM flexible impeller pump, connected to the AC speed controller, to the centrifuge. Once all of the contents had passed through the centrifuge, the solids were collected from the centrifuge basket via the solids collection port and placed into a 4L plastic beaker. The 4L volume of concentrated biomass was typically collected from this process and 400mL of bleach was added to kill the bacteria and prevent PHA degradation. A 20mL sample was collected from the liquid and dried separately in an aluminum dish for PHA analysis. The rest of the liquid was placed into an 11" × 11" glass container and dried in the oven for one week at 60°C. Dried biomass was removed from the glass container and placed in a labeled plastic bag for long-term storage.

Pulp and Paper Mill Pilot Unit

Pilot Unit Construction

A 700L pilot unit was constructed to demonstrate PHA production using Foul Condensate 3200 and Primary Effluent. Figure 68 displays the process and flow-rates of the pilot unit system. The SBR was based around a 700L high-density polypropylene tank mounted on a heavy-duty plastic pallet (Mcmaster, Robbinsville, NJ). Six 7" Sanitaire fine bubble disc diffusers (ITT Industries, Brown Deer, WI) were mounted at the bottom of the reactor and connected together with galvanized steel tubing. Air

was continuously supplied to the diffusers by two Gast diaphragm-type air pumps (Fisher Scientific, Pittsburg, PA) to ensure fully aerobic conditions in the reactors. A used 240V mixer motor was mounted on top of the reactor with a custom steel stand and connected to a stainless steel impeller built at UC Davis for mixing of the reactor. Water-tight bulkhead fittings (Grainger) were attached to the side of the reactor tank for connection of the feed and drain pumps. A 20 GPM flexible impeller motor (Grainger, West Sacramento, CA) was used to pump Primary Effluent into the reactor. A peristaltic pump and Master-Flex tubing (Cole-Palmer, Vernon Hills, IL) was used to pump Foul Condensate into the reactor. A 4 GPM flexible impeller pump (Grainger, West Sacramento, CA) was employed for pumping to the system drain and the speed controlled basket centrifuge (AML Industries, Hatboro, PA). The centrifuge was used to collect PHA-laden biomass from the batch reactor. An AC speed controller (Dart Controls, Zionsville, IN) was hardwired to the flexible impeller pump that pumped PHA-laden biomass from the reactor to the centrifuge and with the flow-rate set to 1 L/min to increase the recovery of solids. The electronic controls, relays, and speed controllers were mounted in a NEMA-4 steel enclosure with watertight electrical fittings (McMaster Carr, Robbinsville, NJ). Two 1200L Intermediate Bulk Containers (IBC) (McMaster Carr, Robbinsville, NJ) tanks were used to transport and store foul condensate prior to feeding into the SBR. Primary Effluent was collected and stored in a 500L high-density polypropylene tank sourced from the Glatfelter Mill. PHA-laden biomass collected from the centrifuge was dried in a Commercial Oven at 60°C in glass containers. Overall, this pilot system required a footprint of 8' by 12' and included three feed tanks and three pallets.

The initial control system consisted of a Dell personal computer (Dell, Austin, TX), mounted in a metal housing, along with the liquid and air pumps, on a separate pallet. Labview software and a Labview relay board (National Instruments, Austin, TX) controlled solid state relays (McMaster Carr, Robbinsville, NJ) to switch the pumps on and off and prevent overloading the Labview relay board. The Labview program controlled the timing of the cycles to ensure proper feed and drain volumes were maintained. A NEMA-4 steel enclosure (McMaster Carr, Robbinsvile, NJ) mounted on the side of the metal enclosure housed the solid-state relays, power input, and breaker panels.

A reconstruction of the control system took place in June 2008 during a restart to address several issues. The PC had broken due to the harsh operating conditions and was replaced with digital timers (Ace Hardware, Davis, CA). Separate timers controlled each pump and could be easily replaced if damaged. Additionally, cold reactor temperatures were addressed with the addition of three temperature control units with temperature probes (Cole Palmer, Vernon Hills, IL) connected to three strips of 1000w Heat-Tape wrapped around the reactor. Insulation was also wrapped around the reactor to increase heat retention.

Feedstock Source and Pre-Treatment

The feedstocks were chosen based on previous work performed on the bench scale that identified pulp and paper mill waste streams appropriate as feedstocks for PHA production (Mockos, 2008). Foul Condensate was collected from a pipeline in the pulp digestion portion of the plant and consisted of the combined evaporator condensates as described in Mockos et al., 2008. The 1200L IBC tanks were filled and then pH adjusted with HCl to pH 7. Primary Effluent was collected from the wastewater treatment plant at Glatfelter (Chillicothe, OH) after the primary clarifier in the 500L HDPE tank.

Microbial Sources

Activated sludge from the Glatfelter wastewater treatment plant was used as a source of microorganisms for the initial startup in January 2008 and March 2008. This source was chosen based on the bench scale enrichment performed in Mockos et al. (2008).

Enriched cultures capable of utilizing methanol as a carbon source were used in the restarts of the pilot scale system in July 2008 and February 2009. These enriched cultures were collected from previous bench-scale experiments with pulp and paper mill waste. A 24L volume of decant from the sequencing batch reactors operated in Mockos et al. (2008) was collected and 40% glycerol (vol/vol) was added to

prevent cell lysis. The cultures were then stored at -80°C. A 12L volume of frozen material was thawed and centrifuged to concentrate the mixed culture into 500mL for direct inoculation into the pilot unit. Following the February 2008 restart, three separate 2L enriched, concentrated cultures were collected from the pilot unit decant with the basket centrifuge and shipped overnight to UC Davis at 0°C. Once received at UC Davis, the cultures were concentrated further with centrifugation to 1L and stored in 40% glycerol at -80°C.

Nutrient Media

Methanol-Utilizing Bacteria Medium B was used in the startup phase, based on the results of previous work with pulp and paper mill waste (Mockos 2008), in the restarts performed in July 2008 and February 2009. Media was not used in any other restarts. During the first three feed additions in these restarts, which brought the volume up from 100L to 700L, the required nutrient media was added to achieve concentrations described in Mockos et al. (2008). Media was then weighed out for each 175L feed addition and placed into individual plastic bags. One bag was added daily after the drain and feed cycles for the first 45 days to maintain media component concentrations in the reactors. During the first 30 days, the media concentration was maintained at 100%. For the following 15 days media was added at 50% strength and was discontinued thereafter. This media addition schedule aided the establishment of methanol-utilizing bacteria and was slowly removed to prevent shock.

Operating Parameters

The pulp and paper mill pilot unit operating parameters were based on the bench-scale experiments performed by Mockos et al. (2008). The pilot scale reactor was operated with a four-day SRT and four-day HRT with one feed and drain cycle per day. At the bench scale, this reactor configuration removed 95 percent of the COD per cycle and produced a peak intracellular PHA content of 16%. At the bench-scale, other reactor configurations did produce higher intracellular PHA content with similar COD removal, but these alternative configurations required differing values of HRT and SRT. Operating the pilot unit with different HRT and SRT values would require additional steps, including either (1) turning off the aeration and mixing to settle the solids with differing points of controlled withdrawal of biomass and liquid or (2) employing a centrifuge to remove the solids with manual addition back to the reactor. These additional steps to separate SRT and HRT were deemed unnecessary at the pilot scale given the specified HRT and SRT of four days provided adequate COD removal and intracellular PHA content for production of natural fiber reinforced thermoplastic composites.

January and March 2008 Startup Procedure

The sequencing batch reactor was inoculated with 350L of activated sludge and filled to a total volume of 700L with primary out effluent. Daily cycling commenced the day after startup.

July 2008 and February 2009 Startup Procedure

The enriched culture was added to 100L of water containing Methanol-Utilizing Bacteria Medium B and methanol. Once the culture had consumed over 50% of the methanol (based on COD readings), the volume was increased to 250L and additional media and methanol were added. The volume was then increased to the full working volume of 700L and additional media and methanol were added after significant COD removal. After removal of a large portion of the COD, the reactor was drained of 175L and water, media and methanol were added. The following day, the sequencing batch reactor began daily feeding of foul condensate and primary effluent. Daily cycling consisted of draining 175L followed by feeding 102.5L from the foul condensate tank and 72.5L from the primary effluent tank. The initial foul condensate tank fill consisted of 50% neutralized foul condensate and 50% water with methanol added to match the overall COD of pure foul condensate. The foul condensate tank was refilled every 12 days when the tank was ¼ full and neutralized afterwards. After four refills (48 days), the tote contained 97% foul condensate. On the 5th refill, the tote was completely drained and refilled

with 100% foul condensate. The primary effluent was also diluted 50% on the first fill up. On the next refill, the tank was fully drained and refilled with 100% primary effluent.

Analytical Methods

Mixed liquor suspended solids (MLSS) and mixed liquor volatile suspended solids (MLVSS) were determined gravimetrically in accordance with Standard Methods 2540-D (Eaton 2005).Soluble carbon was measured by the COD test in accordance with Standard Methods 5220-D (Andrew D. Eaton 2005) using Hach high-range ampoules (Hach Company, Loveland, Colorado, USA). Soluble ammonia nitrogen was measured in accordance with Standard Method 4500 D (Eaton 2005) using an ammonia-selective electrode and ammonia-gas permeable membrane.

Polyhydroxyalkanoates (PHA) were measured using Gas Chromatography (GC). Specifically, polyhydroxybutyrate (PHB) and polyhydroxyvalerate (PHV) were measured based on a modified procedure outlined in Brauness et al. (1978). A 45 mL aliquot was collected from the reactors and placed into 50mL centrifuge tubes containing 5mL bleach (Clorox, Oakland, CA) to prevent PHA degradation. The tubes were centrifuged at 3750 rpm for 10 minutes and the harvested pellets were dried at 60°C. A measured weight of the dry sample (between 10 and 40mg), 2mL of acidified methanol (3% Sulfuric acid vol/vol) and 2mL of HPLC-grade chloroform (containing 0.5 mg/mL benzoic acid as an internal standard) were added to each vial. The vials were then digested in a Hach heating block for four hours at 100°C to produce esterified monomer units. After heating, 1mL of de-ionized water was added to each vial and the mixture was vortexed for 30 seconds. The chloroform organic phase, containing the esterified monomer units, was then removed from the bottom of the tubes with 9" pastuer pipets and filtered through 5" pastuer pipets, containing 1g sodium sulfate and a cotton plug (to remove any solid particles), into 2mL GC vials. The esterified monomer units were then analyzed on an Agilent 4650 gas chromatograph equipped with an Agilent DB-WAXetr column (60 m, 0.32 mm diameter, 0.25 µm film thickness) and a thermal conductivity detector (TCD). The inlet and detector temperatures were set to 150°C and 200°C, respectively. A 2µL aliquot of each sample was injected into the system and the column temperature was held at 35°C for five minutes and then ramped up to 220°C at 15°C/min. Data was collected and analyzed with GC Chemstation 1990-2000 Rev.A.08.01 software (Agilent Technologies, Palo Alto, CA). Standards containing 88% PHB and 12% PHV (Sigma, St. Louis, MO) were also analyzed to determine sample concentrations based on linear regression.

Methanol was analyzed using GC. Reactor samples were filtered through a 0.22um syringe filter and 2mL of filtered sample was placed into 2mL GC vials. Methanol concentrations were then analyzed on an Agilent 4650 gas chromatograph equipped with an Agilent DB-WAXetr column (60 m, 0.32 mm diameter, 0.25 µm film thickness) and a thermal conductivity detector (TCD). The inlet and detector temperatures were set to 150°C and 200°C respectively. A 2µL aliquot of each sample was injected into the system and the column temperature was held at 35°C for one minute and then ramped up to 150°C at 5°C/min. Data was collected and analyzed with GC Chemstation 1990-2000 Rev.A.08.01 software (Agilent Technologies, Palo Alto, CA). Methanol standards were also analyzed to determine sample concentrations based on linear regression.

Results

Brewery *Waste Pilot Unit*

The brewery waste pilot unit was started in April 2008 and consistently removed COD during the first four weeks of operation. Samples taken from the beginning and end of three separate cycles over the first four weeks of operation displayed consistent removal of COD averaging 73% (data shown in Table 39). A full cycle sampling was performed four weeks after start up to determine the temporal concentrations of PHA and biomass over the course of a single feed cycle (data shown in Figure 69). A peak intracellular PHA content of 41%, with a MLVSS of 848 mg/L, was obtained eight hours into the feed cycle. This sampling confirmed the presence and production of significant quantities of PHA-laden biomass.

After the confirmation of PHA production and the stable removal of COD in the SBR, the single-stage batch reactor downstream from the SBR began production of PHA-laden biomass. Sampling of the batch reactor over the course of a single feed cycle on the first cycle confirmed a peak intracellular PHA content of 40% (data not shown). Daily harvesting commenced immediately afterwards, and the temporal concentration of PHA over the course of a feed cycle was no longer monitored. Cell mass was harvested successfully from the batch reactor forty-three times. A total of 5.1 kg of dried PHA-laden biomass was harvested from the batch reactor with an average PHA content of 19% and a standard deviation of 7%. The overall quantity of PHA in the dried biomass (19%) was significantly less than the peak quantity of 40% observed at startup of the batch reactor. The discrepancy in the PHA values between the single discrete sampling event (40%) and the average value obtained in the overall biomass likely reflects variations in feedstock composition and ambient temperature (discussed in further detail below). The dried PHA-laden biomass was shipped to Washington State University for pilot-scale extrusion of natural fiber reinforced thermoplastic composites.

Pulp *and Paper Mill Pilot Unit*

The pilot unit was shipped to Glatfelter in January 2008 and began operation immediately upon arrival. Weekly samples were taken by a Glatfelter employee and shipped back to UC Davis for analyses. Sample analyses determined the reactor was not reducing COD over each sampled cycle (Table 40) and therefore not operating properly. The foul condensate was not pH adjusted, as had taken place in bench-scale laboratory experiments (Mockos 2008a) and was the most likely cause of failure. Additionally, the toxic organic phase of the foul condensate may have been fed to the reactor. A restart was required to address these issues. A restart took place in March 2008 and the reactor again failed to start properly. Weekly sampling displayed no reduction in COD over each sampled cycle (see Table 41). Based on the results of the first two restarts, a different startup procedure was initiated.

A restart was successfully performed in July 2008 using an enriched culture obtained from previous laboratory experiments (Mockos, 2008). The culture successfully reduced the COD over each cycle during startup (Sampling Data displayed in Table 42). The reactor was allowed to completely stabilize after discontinuing Methanol-Utilizing Bacteria Medium B addition; weekly sampling confirmed that the reactor continued to removed methanol and COD (Table 43). During this stage, the reactor was operated at a carbon/nitrogen ratio that was not expected to produce PHA. In the Fall Quarter of 2008, funding for the project was put on hold and the reactor continued to operate under these parameters until November 2008 when the pilot unit was shutdown due to the reactor being drained by an unknown individual. The unit therefore required another restart.

A successful restart of the pilot unit was performed in February 2009. The restart was performed following the same procedure executed in the July 2008 restart. The reactor performed similarly to the previous restart (data shown in Table 44). The reactor consistently removed methanol and COD in subsequent weekly samplings (data shown in Table 45). Several enriched cultures were collected from the pilot unit effluent with the centrifuge and shipped back to UC Davis for storage as backup cultures. These were frozen at -80°C in 40% glycerol for future pilot unit restarts (if needed). Overall, this restart was a success and proved the startup procedure could be successfully reproduced.

The C/N ratio was modified to induce significant PHA production. The foul condensate was supplemented with methanol to achieve a C/N of 30. This change caused the reactor to become overloaded and no longer remove methanol or COD over each feed cycle (data not shown). The reactor was then drained of ¾ of its contents and refilled with water in an attempt to salvage the culture. Subsequent feedings did not remove COD or methanol and the reactor was shutdown.

Discussion

Brewery Waste Pilot Unit

The brewery waste pilot unit's removal of carbon was similar to the bench-scale reactor (Liu 2008). The unit successfully started and removed a significant percentage of the COD during the cycles sampled. COD removal in the pilot SBR averaged 73% and is close to the previously reported removal of 83% (Liu, 2008). COD removal was a critical objective for this study because it confirmed the activity of the biomass and the uptake of carbon necessary to produce PHA.

A second focus of this study was to determine the content and consistency of intracellular PHA in biomass produced at the pilot-scale. The batch reactor was employed to increase intracellular PHA content above the peak levels in the SBR. In this study on the pilot-scale, the peak PHA content, based on a single discrete sampling event temporally over a feed cycle at startup, in the batch reactor (40%) was similar to the SBR (41%). Over the entire course of pilot-scale operation, the average quantity of PHA in the dried biomass obtained from the batch reactor was 19% (with a standard deviation of 7%), a value significantly less than that observed (40%) over the single discrete sampling event at startup. This discrepancy in PHA content in the discrete sampling event at start up (40%) and the average value in the biomass collected over the nine weeks of pilot-scale operation (19%), can be attributed to two likely causes: (1) variability in reactor temperatures and (2) variability in brewery waste used as feedstock. The pilot unit was operated outdoors and subjected to varying ambient temperatures compared to the bench-scale experiments performed in a laboratory by Liu et al. (2008). Ambient outdoor temperatures varied between 7 and 40°C, whereas laboratory experiments were executed at a constant ambient temperature of 22°C. Temperatures above 25°C have been documented to negatively impact PHA production(H. Salehizadeh 2003). Variability in the ambient temperature could have influenced either the timing of peak PHA production in the pilot-scale batch reactor and/or the magnitude of this value. The consistency of the brewery waste collected from Sierra Nevada Brewing Company was also a likely cause of low PHA content in harvested biomass. A majority of the waste originates from the cleaning of fermentation tanks and washing of the grain extraction mash-tuns in the brewery (Redmond 2008). The waste's composition can change over the year with the production of different beers and fermentation methods. Additionally, the brewery waste feedstock was also stored outdoors and subjected to outdoor ambient temperatures. Collectively, variability in the brewery waste collected and its subjection to ambient atmospheric temperatures could have changed the COD of the feed significantly over the pilot-scale study, which in turn could have either influenced the timing of peak PHA production in the batch reactor and/or the magnitude of this value.

Despite lower than expected PHA content, the pilot unit produced significant quantities of PHA-laden biomass. This study successfully demonstrated the production of PHA-laden biomass from brewery waste at the 700L pilot-scale. Operation of the pilot unit and the successful harvesting of PHA-laden biomass also facilitated the pilot-scale production of natural fiber reinforced thermoplastic composites with PHA-laden biomass at Washington State University. Therefore, this study was successful in accomplishing the third stated objective.

Pulp and Paper Mill Pilot Unit

The two startups performed in July 2008 and February 2009 demonstrated how to start a pilot unit fed pulp and paper mill waste streams. The enriched culture used methanol immediately compared to the activated sludge used in the first two startups and illustrates the necessity of starting with microbes conditioned to the waste stream. The activated sludge was not conditioned to foul condensate or methanol and did not perform well. Additionally, this study demonstrated how small culture volumes can be grown up quickly to the full working volume as demonstrated by the July 2008 and February 2009 startups. Future pilot units fed harsh waste streams, such as foul condensate, should carefully examine startup procedures. Overall, this study demonstrated the feasibility of starting a pilot unit and removing COD at the 700L scale, satisfying the first objective of this study.

After stabilization, the pilot unit was changed to a C/N of 30 and became overloaded. This is in contrast to the bench-scale experiments of (Gregory R. Mockos 2008b) that performed well under the same conditions. Future restarts at the pilot-scale should examine slowly changing the C/N to 30 to prevent shock to the culture and over-loading. However, this C/N ratio of 30 may not be possible at pilot-scale and this deserves consideration in future work.

Conclusions and Future Work

The brewery waste pilot unit satisfied the objectives of this study and produced PHA-laden biomass at the 700L scale. The following conclusions can be drawn for this study:

1. PHA production at the 700L scale is feasible.
2. PHA content is variable between cycles and future work should investigate the causes.
3. Significant quantities of PHA laden biomass were produced, dried and stabilized for extrusion runs of natural fiber reinforced composite thermoplastics.

The pulp and paper mill pilot unit satisfied the first objective of this study. PHA-laden biomass was not produced because the SBR was not stable at the C/N of 30. The following conclusions can be drawn from this study:

1. The pilot-scale unit did not perform in a manner similar to the bench scale work of Mockos et al., 2008b under similar process conditions. Further optimization of this process at the pilot-scale will be necessary for process success.
2. The successful startups utilized an enriched culture and Methanol-Utilizing Bacteria Medium B. Future work should investigate the necessity of Methanol-Utilizing Bacteria Medium B.
3. The pilot unit became overloaded at a C/N of 30 and future work should investigate the causes of this failure.

References

Albuquerque MGE, E. M., Torres C, Nunes BR, Reis MAM (2007). "Strategies for the development of a side stream process for polyhydroxyalkanoate (PHA) production from sugar cane molasses." Journal of Biotechnology 130(4): 411-421.

Braunegg, G., B. Sonnleitner, and R.M. Lafferty (1978). "A rapid gas chromatographic method for the determination of poly-β-hydroxybutyric acid in microbial biomass." European Journal of Applied Microbiology and Biotechnology 6(1): 29-37.

D.H. Rhu, W. H. L., J.Y. Kim and E. Choir (2003). "Polyhydroxyalkanoate (PHA) production from waste." Water Science and Technology 48(8): 221-228.

Erik Coats, F. L., Michael Wolcott, Karl Englund, Armando McDonald (2007). "Synthesis of polyhydroxyalkanoates in municipal wastewater treatment." Water Environment Research 79(12): 2396-2403.

Erik R. Coats, F. J. L., Michael P. Wolcott, Karl Englund, Armando McDonald (2007). "Production of natural fiber reinforced thermoplastic composites through the use of polyhydroxybutyrate-rich biomass." Bioresource Technology 99: 2680-2686.

Gregory R. Mockos, W. A. S., Frank J. Loge, David N. Thompson (2009). "Effect of selected reactor conditions on polyhydroxyalkanoate production from pulp mill activated sludge using foul condensates." In Press.

H. Salehizadeh, M. C. M. V. L. (2003). "Production of polyhydroxyalkanoates by mixed culture: recent trends and biotechnological importance " Biotechnology Advances 22: 261-279.

Liu, H.-Y. (2008). Bioplastics Poly(hydroxyalkanoate) Production during Industrial Wastewater

Treatment. Civil and Environmental Engineering. Davis, CA, University of California.

M.F. Md Din, Z. U., M.C.M. van Loosdrecht, A. Ahmad and M.F. Sairanc (2006). "Optimization of nitrogen and phosphorus limitation for better biodegradable plastic production and organic removal using single fed-batch mixed cultures and renewable resources." Water Science and Technology 53(6): 15-20.

Mockos, G. R., Loge, F.J., Smith, W.A., and D.N. Thompson (2008). "Selective enrichment of a methanol-utilizing consortium using pulp & paper mill waste streams." Applied Biochemistry and Biotechnology in press.

Redmond, R. (2008). P. C. James Waller. Chico, CA, Sierra Nevada Brewing Company.

Reis, M. A. M., L.S. Serafim, P.C. Lemos, A.M. Ramos, F.R. Aguiar, and M.C.M. Van Loosdrecht (2003). "Production of polyhydroxyalkanoates by mixed microbial cultures." Bioprocess and Biosystems Engineering 25(6): 377-385.

Figures

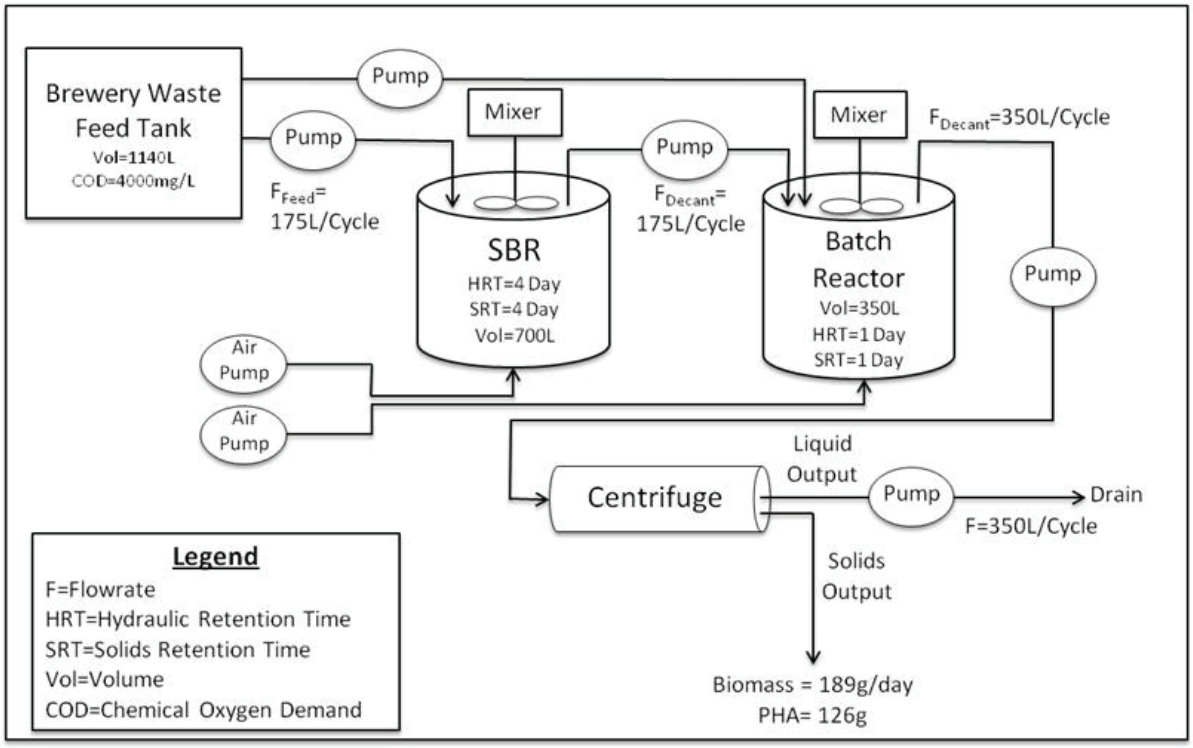

Figure 67. Brewery Waste Pilot Unit Flow-Chart

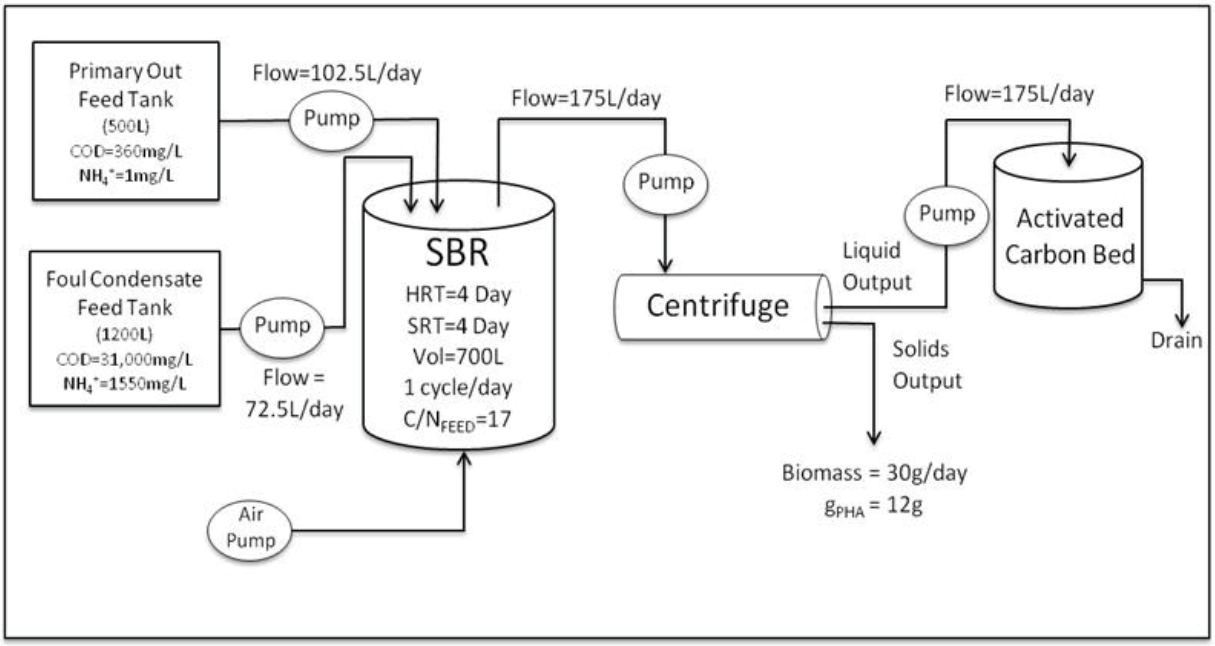

Figure 68. Pulp and Paper Mill Waste Pilot Plant

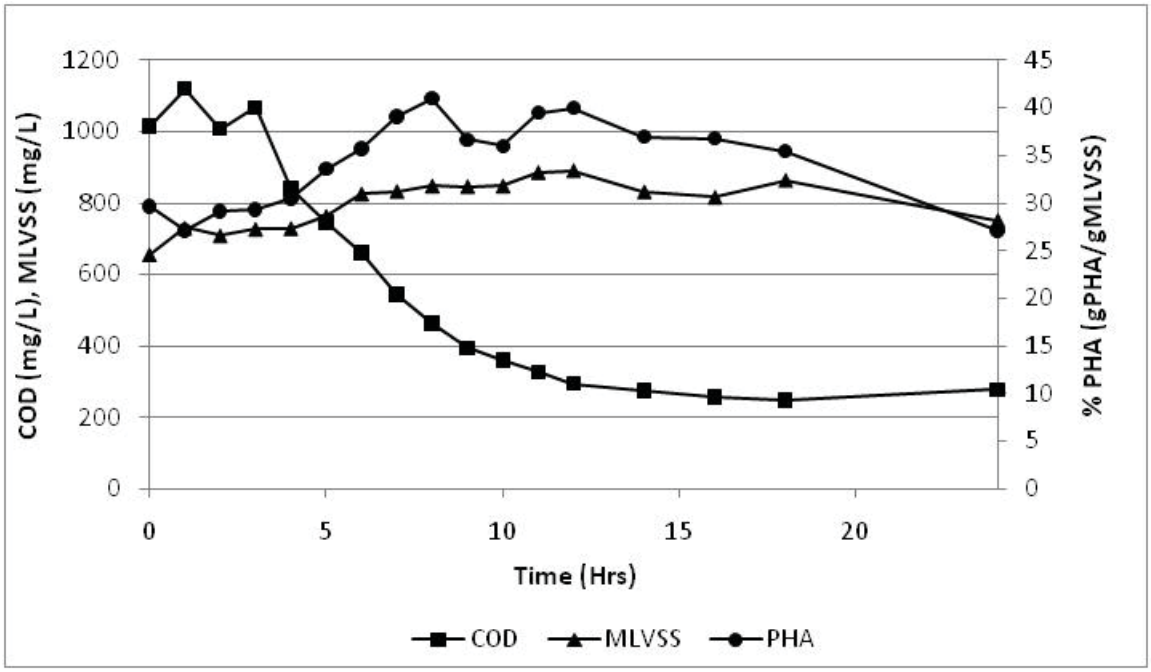

Figure 69. 24 Sampling Data – SBR Brewery Pilot Unit

Tables

Table 39. Removal of COD During Stabilization Period – Brewery Waste Pilot Unit

Sample Date	Beginning of Cycle COD (mg/L)	End of Cycle COD (mg/L)	% Removal of COD
5/13/08	1041	213	79.5%
5/29/08	909	293	67.7%
6/2/08	1016	279	72.5%

Table 40. Weekly COD Sampling – Pulp and Paper Mill Pilot Unit

Sample Date	Beginning of Cycle COD (mg/L)	End of Cycle COD (mg/L)
2/18/08	2388	2016
2/25/08	2580	2152
3/3/08	2416	2288

Table 41. Weekly COD Sampling – Pulp and Paper Mill Pilot Unit

Sample Date	Beginning of Cycle COD (mg/L)	End of Cycle COD (mg/L)
4/7/08	1384	1316
4/14/08	2028	1876
4/21/08	1216	1004

Table 42. July 2008 Restart Sampling Data – Pulp and Paper Mill Pilot Unit

Description	Volume (L)	Date	Time	COD (mg/L)	NH4 (mg/L)
Methanol Addition/Nutrient Media/No Inoculum	100	7/17/08	11:00AM	1796	900
Methanol, Nutrient Media, and Inoculum Added	100	7/17/08	11:20AM	2912	800
-	100	7/17/08	3:00AM	5500	390
-	100	7/18/08	10:20AM	2820	255
150L H2O, 850mL Methanol Added	250	7/18/08	1:40PM	5256	487.5
-	250	7/19/08	11:20AM	196	345
450L H2O, 2365mL Methanol Added	700	7/19/08	3:00PM	4024	480
-	700	7/19/08	7:15PM	2840	652.5
-	700	7/20/08	2:00AM	1148	750
-	700	7/20/08	9:00AM	109	360
-	700	7/20/08	2:30PM	128	535
Drained 175L; 2365mL Methanol and Nutrient Media Added	700	7/20/08	3:30PM	3824	390
	700	7/20/08	5:00PM	738	480
Drained 175L; 72.6L FC & 102.4L Effluent Added	700	7/21/08	6:30PM	3384	465
	700	7/22/08	9:30AM	2368	465
Drained 175L; 72.6L FC & 102.4L Effluent Added	700	7/22/08	2:00PM	4552	330

Table 43. Weekly Sample Analysis – Pulp and Paper Mill Pilot Unit

Sample #	COD (mg/L)	Methanol (mg/L)	MLVSS (mg/L)	PHA % (g PHA/g Biomass)
8-13-08 Beg Cycle	1466	455		
8-14-08 End Cycle	444	0 (below detection of 50mg/L)	291	2%

Table 44. February 2007 Restart Data – Pulp and Paper Mill Pilot Unit

Sample #	Description	Volume (L)	Date/Time	Time	COD (mg/L)	NH4 (mg/L)
1	Methanol, Nutrient Media, Added	100	2/10/09	3:30PM	2664	684
2	Inoculum Added	100	2/10/09	3:30PM	4240	648
3		100	2/11/09	8:15AM	3416	644
4	675mL Methanol, 150L H2O, Nutrient Media Added	250	2/11/09	1:30PM	4544	564
5		250	2/12/09	4:00PM	224	464
6	1875mL Methanol, 450L H2O, Nutrient Media Added	700	2/12/09	5:00PM	4253	540
7		700	2/13/09	1:30PM	472	464
8	Drain 175L; 72.4L FC, 102.6 L Primary Effluent Added	700	2/13/09	3:15PM	3208	480

Table 45. Weekly Sample Analysis – Pulp and Paper Mill Pilot Plant

Sample	COD (mg/L)	NH3 (mg/L)	Methanol (mg/L)	MLVSS (mg/L)
Beg 4-8-09	3856	350	1612.4274	768
End 4-9-09	1064	170	0 (below detection of 50mg/L)	628

Appendix A – Study of Various Lubricants on PHB/WF Composites

Introduction

As the viscosity of wood-plastic composites increases with higher wood content, the selection of a lubricant suitable for the polymer matrix becomes very important. The proper selection of lubricant can improve the surface quality of extruded products and allow for faster processing speeds. The following research includes an extensive study on lubricant packages was conducted to determine the most effective system for polyhydroxybutyrate/wood fiber (PHB/WF) composites.

Methods and Materials

Wood plastic composites (WPCs) based on PHB were produced with the same control formulations and materials reported previously (Anderson, 2007). No interfacial modifiers were used and a variety of lubricants in addition to Glycolube WP2200 (Lonza, Inc, Allendale, NJ) were tested; EBS (N,N'-ethylene-bisstearamide from GE Specialty Chemicals), Zinc Stearate (ZnSt) (DLG-20B from Ferro Corp., Cleveland, OH) in a blend of 2:1 ZnSt/EBS, Optipak 100 (OP100) (Honeywell, Morristown, NJ), oxidized polyethylene (OPE) (A-C 629 from Honeywell, Morristown, NJ), and Struktol 306 (Struktol Co. of America, Stow, OH) were included in PHB/WF composites at 3% on total. The formulations were mixed in a drum blender for 10 minutes and then processed through twin screw extrusion (Cincinnati Milicron CM 35). The temperatures for extrusion processing were controlled through 3 barrel zones, 2 die zones, and through the screw at 170, 175, 163, 162, 160, and 160°C, respectively. The extrudate was cooled through a cold water bath after exiting the die. Flexural testing was performed on the as-received rectangular specimens cut to 20-cm in length, in accordance with ASTM D790 on a screw driven Instron 4466 Standard.

Results and Discussion

Based on mechanical performance, Figure 70shows that composites processed with the lubricant Glycolube WP2200 performed exceptionally in both stiffness and strength when compared to the performance of the composites with other lubricant systems. The flexure strength of all of the composites except those with WP2200 fluctuates from 20-23-MPa, whereas using WP2200 resulted in a 36% increase to 30-MPa. Similarly, for flexural stiffness, the use of WP2200 instead of other lubricants resulted in an increase of roughly 21%. While visual observations are subjective, there was some variation in the quality of the surface of the extruded bars that coincided with the variation in lubricant packages, both Glycolube WP2200 and OPE appeared to perform well.

Conclusions

From these results it is apparent that Glycolube WP2200 helps to produce PHB/WF composites with superior mechanical properties. Both stiffness and strength displayed strong improvements over all other lubricant systems studied. All further investigations will make use of this investigation by utilizing WP2200 just as shown presently, at levels of 3% on total.

References

Anderson, S.P. 2007. Effect of Interfacial Modifiers on Mechanical and Physical Properties on PHB/WF and Their Effect on Composite Morphology. Chapter 2. Master Thesis, Washington State University, Pullman, WA.

Figures

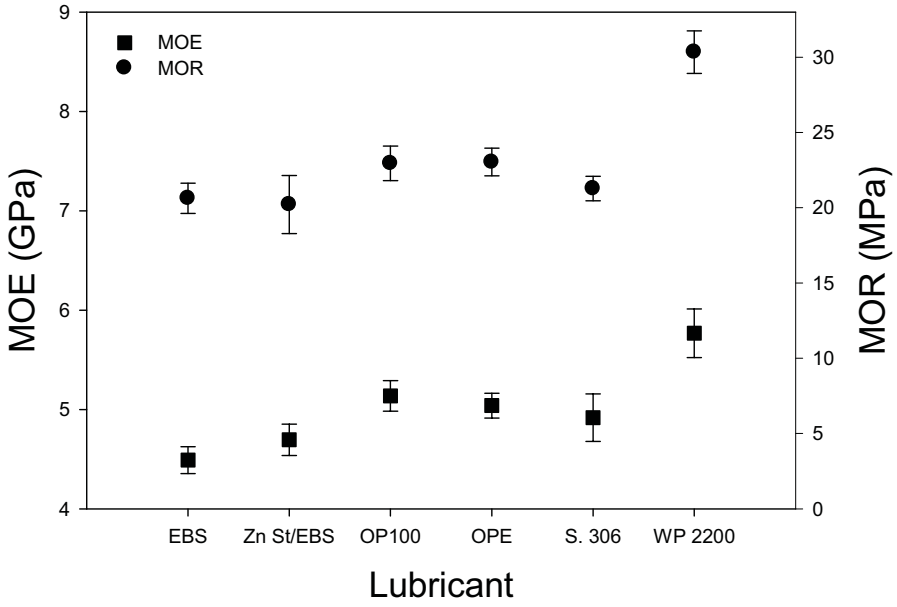

Figure 70. Comparison of lubricant systems in PHB/WF composites on flexural stiffness and strength.

Appendix B –Varied Wood Fiber Levels and HV Content on PHB/WF Composites

Introduction

In current literature, polyhydroxyalkanoate/wood fiber (PHA/WF) composites are produced with varying variables, making comparisons to other research difficult. Studies of PHA composites have utilized various wood contents (Coats, 2007), and various types PHAs (Gatenholm. 1992). As was shown by Facca (2006), variation in the fiber content on high density polyethylene (HDPE) can have a strong effect on both stiffness and strength. Gatenholm (1992) also showed that variation in hydroxyvalerate (HV) content on polyhydroxybutyrate-co-hydroxyvalerate (PHBV) can also have a strong effect on both the stiffness and strength of composites. In this study, the effects of both variation in wood flour content, and HV content on the mechanical properties of PHA/WF composites are investigated.

Methods and Materials

Polyhydroxybutyrate (PHB), and PHBV containing 8 and 12% HV in fine powder form were provided by Tianan Biologic Material Co. (Ningbo, China), and Metabolix Inc. (Cambridge, MA), respectively. Boron nitride (BN) powder (Carbotherm PCTF5, obtained from Saint Gobain Advanced Ceramics Corporation, Amherst, NY) was used as a nucleating agent at levels of 0.5% on total polymer weight. Ponderosa pine wood flour (60-mesh) was obtained from American Wood Fibers (Schofield, WI) and was dried by steam tube.

Prior to precompounding, the PHA/WF mixes were manually tumbled in a plastic bag for 5 minutes. Precompounding was performed through a Leistritz ZSE-18 twin screw extruder. The extrudate was cooled in a water bath and then pelletized and oven dried for injection molding.

Tensile specimens in accordance with ASTM D638 (type I) standards were produced through injection molding (Sumitomo SE 50D). The temperature zones of the injection molding machine were independently controlled at 180°C, 185°C, 175°C, and 165°C from the feeding end to the nozzle, respectively. The mold temperature was held constant at 60°C. Tensile specimens were tested on a screw driven Instron 4466 Standard with a 10-kN electronic load cell. The crosshead speed was 5-mm/min, and the initial strain was measured with a clip-extensometer with a 25 mm gage length (MTS model # 634.12E-24).

Results and Discussion

Produced with 40% wood flour, the effect of PHBV composites with varying HV content on mechanical properties is shown in Figure 71. An increased HV content in PHB yields a slight increase in strength a at 8% HV, and a subsequent decrease with 12% HV. As has been suggested from previous literature, the stiffness of the PHB/WF composite decreases with increasing HV content (Gatenholm, 1992). This may be due to the decrease in the degree of crystallization suggested by Qian (2007) with increases in HV content.

Composites utilizing PHB as the matrix material were also tested with varying wood content from 20-60% WF. It was found that increases in reinforcement resulted in a linear increase in Young's modulus (Figure B.2, R^2 = 97.3%). This linear trend in Young's modulus is consistent with results reported by Facca (2006) who studied the mechanical properties of HDPE/Oak Fiber (20 and 40-mesh) composites. This is also consistent with predictions from micromechanical models such as Rule of Mixtures (ROM) and Halpin-Tsai, which predict that composite stiffness is increased with increased fiber loading. Also represented in Figure 72 is the effect of fiber loading on the strength of PHB/WF composites. Composites display increases in strength with low fiber loadings, transitioning to decreases in strength at higher levels. This trend is also consistent with the findings of Facca (2006).

Conclusions

From this study we have a basis to compare PHB/WF composites produced at varying levels of wood fiber. This is important because no studies as of yet have produced PHB/WF composites at WF levels higher than 40%. Further, it has been identified that utilization of PHB in wood fiber composites displays good strength and stiffness when compared to PHBV8 and PHBV12. Further studies will involve the use of PHB because of its availability and respectable mechanical properties.

References

Coats, E.R., F.J. Loge, M.P. Wolcott, K. Englund, and A.G. McDonald. 2008. Production of natural fiber reinforced thermoplastic composites through the use of polyhydroxybutyrate-rich biomass. Bioresource Technology, 99(7):2680-2686.

Facca, A.G. 2006. Predicting the Tensile Modulus and Strength of Single and Hybrid Natural Fiber Reinforced Themoplastic Composites. Doctoral Dissertation, University of Toronto, Toronto, Canada.

Gatenholm, P., J. Kubat, and A. Mathiasson. 1992. Biodegradable Natural Composites. I. Processing and Properties. Journal of Applied Polymer Science, 45(9):1667-1677.

Qian, J., L. Zhu, J. Zhang, and R.S. Whitehouse. 2007. Comparison of Different Nucleating Agents on Crystallization of Poly(3-hydroxybutyrate-co-3-hydroxyvalerates). Journal of Polymer Science: Part B: Polymer Physics, 45(13):1564-1577.

Figures

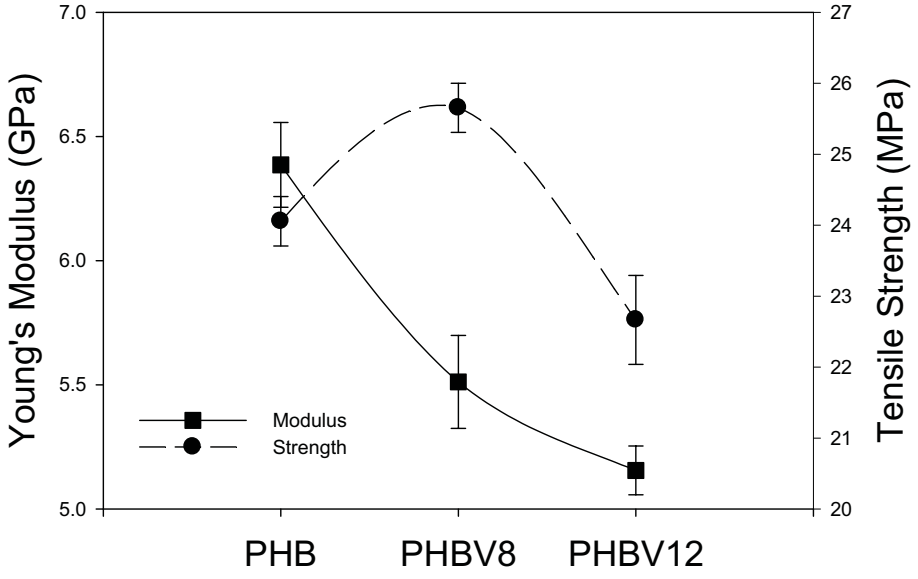

Figure 71. Effect of HV content in PHB compounded with WF on tensile stiffness and strength

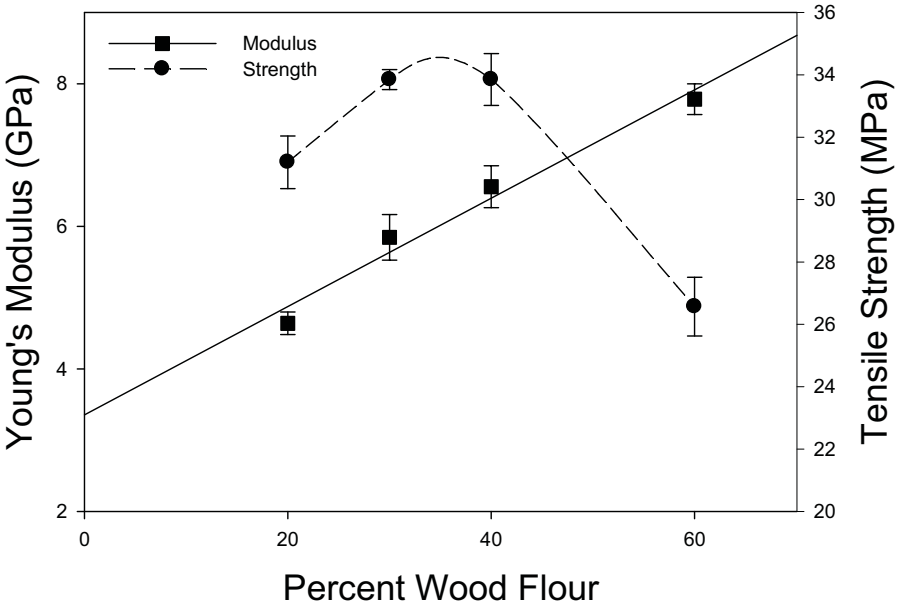

Figure 72. Influence of varied wood fiber loading in PHB/WF composites on tensile strength and stiffness